



**UNIWERSYTET  
MIKOŁAJA KOPERNIKA  
W TORUNIU**

Collegium Medicum  
im. Ludwika Rydygiera w Bydgoszczy

**Bydgoszcz 2025 r.**



**UNIWERSYTET  
MIKOŁAJA KOPERNIKA  
W TORUNIU**

Wydział Lekarski  
Collegium Medicum w Bydgoszczy

**Natalia Warmuzińska**

## **Analiza lipidomiczna w diagnostyce transplantacyjnej**

**Rozprawa na stopień doktora nauk medycznych i nauk o zdrowiu**

**Promotor:**

**Prof. dr hab. Barbara Bojko**

**Bydgoszcz, 2025 r.**

*Składam serdeczne podziękowania  
Pani prof. dr hab. Barbarze Bojko za okazane zaufanie,  
wspaniałe możliwości rozwoju i towarzyszenie mi w tej  
niezwykłej naukowej przygodzie.*

*Dziękuję za wiarę we mnie i wsparcie na każdym  
etapie realizowania niniejszej rozprawy.*

*Dziękuję Panu prof. Markusowi Selznerowi  
oraz jego zespołowi z Toronto General Hospital  
za współpracę i dostarczenie materiału do badań.*

*Serdeczne podziękowania kieruję  
do Pana prof. Zbigniewa Włodarczyka  
oraz zespołu Kliniki Transplantologii i Chirurgii Ogólnej  
Szpitala Uniwersyteckiego nr 1 w Bydgoszczy  
za współpracę oraz umożliwienie pozyskania materiału do badań.*

*Dziękuję Koleżankom i Kolegom  
z Katedry Farmakodynamiki i Farmakologii Molekularnej  
za pomoc, burze mózgów, wspólne pokonywanie przeciwności i świetną atmosferę.*

*Dziękuję mojej wspaniałej rodzinie - Rodzicom i Bratu-  
za wiarę we mnie na każdym etapie mojej życiowej drogi.  
Wasza obecność i troska są dla mnie nieocenionym źródłem siły i motywacji.*

*Dziękuję, że zawsze mogę na Was liczyć.*

*Dziękuję mojemu narzeczonemu Kamilowi  
za towarzyszenie mi w tej wymagającej podróży.*

*Bez Twojej pomocy realizacja tej pracy nie byłaby możliwa.*

*Dziękuję za pomoc w laboratorium, ale przede wszystkim dziękuję  
za bezwarunkowe wsparcie, cierpliwość i wiarę w moje możliwości.  
Jesteś moim najlepszym przyjacielem i najlepszym co mnie w życiu spotkało.*

Przedstawiona rozprawa doktorska została zrealizowana dzięki grantowi Narodowego Centrum Nauki – OPUS numer 2017/27/B/NZ5/01013 pt. *„Bezbiopsyjna analiza metabolomiczna i lipidomiczna nerek jako krok w kierunku lepszej oceny jakości narządów selekcjonowanych do transplantacji i uszkodzenia poreperfuzyjnego”*

## Spis treści

1. Wykaz skrótów .....	6
2. Wykaz publikacji stanowiących podstawę postępowania w sprawie o nadanie stopnia naukowego doktora .....	7
3. Streszczenie w języku polskim .....	9
4. Streszczenie w języku angielskim.....	11
5. Wstęp .....	13
5.1. Ocena jakości narządów do przeszczepu: współczesne metody i kierunki rozwoju w medycynie transplantacyjnej .....	13
5.2. Mikroekstrakcja do fazy stałej .....	49
6. Cel rozprawy doktorskiej.....	67
7. Wyniki badań .....	68
7.1. Zastosowanie biopsji chemicznej do oceny jakości przeszczepu. Analiza porównawcza profilu lipidomicznego nerki związanego z perfuzją u dawców po śmierci mózgowej oraz po zatrzymaniu krążenia – P.3. oraz P.4. ....	68
7.2. Wpływ normotermicznych i hipotermicznych metod konserwacji na lipidom nerek — badanie porównawcze z wykorzystaniem biopsji chemicznej – P.5.....	110
7.3. Profilowanie metabolomiczne i lipidomiczne w predykcji ryzyka opóźnionej funkcji przeszczepu z wykorzystaniem mikroekstrakcji do fazy stałej – P.6. ....	140
8. Wnioski .....	173
9. Bibliografia .....	174
10. Spis rycin .....	176
11. Wykaz osiągnięć.....	177
11.1. Publikacje naukowe.....	177
11.2. Rozdziały w monografii naukowej .....	179
11.3. Wystąpienia konferencyjne .....	179
11.4. Projekty naukowe.....	181
12. Opinia Komisji Bioetycznej .....	182
13. Oświadczenie autora rozprawy doktorskiej .....	187
14. Oświadczenia współautorów .....	189

## 1. Wykaz skrótów

**AUC** – pole pod krzywą (*ang. area under the curve*)

**CAR** – acylokarnityna (*ang. acylcarnitine*)

**DCD** – dawca po zatrzymaniu krążenia (*ang. donor after cardiac death*)

**DD** – dawcy zmarły (*ang. deceased donor*)

**DGF** – opóźniona funkcja przeszczepu (*ang. delayed graft function*)

**ECD** – dawca o rozszerzonych kryteriach (*ang. expanded criteria donor*)

**HBD** – dawca z bijącym sercem (*ang. heart beating donor*)

**HMP** – hipotermiczna perfuzja maszynowa (*ang. hypothermic machine perfusion*)

**IRI** – uszkodzenie niedokrwienno–reperfuzyjne (*ang. ischemia–reperfusion injury*)

**LPC** – lizofosfatydylocholina (*ang. lysophosphocholine*)

**LPE** – lizofosfatydyloetanolamina (*ang. lysophosphatidylethanolamine*)

**MS** – spektrometria mas (*ang. mass spectrometry*)

**NEVKP** – normotermiczna perfuzja nerek w warunkach ex vivo (*ang. normothermic ex vivo kidney perfusion*)

**PC** – fosfatydylocholina (*ang. phosphatidylcholine*)

**PCA** – analizy głównych składowych (*ang. principal component analysis*)

**PE** – fosfatydyloetanolamina (*ang. phosphoethanolamine*)

**PI** – fosfatydyloinozytol (*ang. phosphatidylinositol*)

**PNF** – pierwotna niewydolność przeszczepu (*ang. primary nonfunction*)

**ROC** – krzywa charakterystyki operacyjnej odbiornika (*ang. receiver operating characteristic curve*)

**SCD** – dawca o standardowych kryteriach (*ang. standard criteria donor*)

**SCS** – hipotermia prosta (*ang. static cold storage*)

**SPME** – mikroekstrakcja do fazy stałej (*ang. solid–phase microextraction*)

**TG** – trójgliceryd (*ang. triacylglycerol*)

**UHPLC** – ultrasprawa chromatografii cieczowa (*ang. ultra–high–performance liquid chromatography*)

## 2. Wykaz publikacji stanowiących podstawę postępowania w sprawie o nadanie stopnia naukowego doktora

P.1. N. Warmuzińska, K. Łuczykowski, B. Bojko: ***A review of current and emerging trends in donor graft-quality assessment techniques***. J. Clin. Med., 2022, 11, 487; punktacja MNiSW:140, IF: 3,900

P.2. K. Łuczykowski\*, N. Warmuzińska\*, B. Bojko: ***Solid phase microextraction – a promising tool for graft quality monitoring in solid organ transplantation***. Separations, 2023, 10, 153; punktacja MNiSW: 20, IF: 2,500

\* [Dwóch równorzędnych pierwszych autorów]

P.3. I. Stryjak\*, N. Warmuzińska\*, K. Łuczykowski, M. Hamar, P. Urbanellis, E. Wojtal, M. Masztalerz, M. Selzner, Z. Włodarczyk, B. Bojko: ***Using a chemical biopsy for graft quality assessment***. Jove-J. Vis. Exp, 2020, 160, e60946; punktacja MNiSW: 70, IF: 1,355

\* [Dwóch równorzędnych pierwszych autorów]

P.4. I. Stryjak\*, N. Warmuzińska\*, K. Łuczykowski, K. Jaroch, P. Urbanellis, M. Selzner, B. Bojko: ***Metabolomic and lipidomic landscape of porcine kidney associated with kidney perfusion in heart beating donors and donors after cardiac death***. Transl Res., 2024, 267:79-90; punktacja MNiSW: 140, IF: 6,400

\* [Dwóch równorzędnych pierwszych autorów]

P.5. N. Warmuzińska, K. Łuczykowski, I. Stryjak, H. Rosales-Solano, P. Urbanellis, J. Pawliszyn, M. Selzner, B. Bojko: ***The impact of normothermic and hypothermic preservation methods on kidney lipidome—comparative study using***

***chemical biopsy with microextraction probes.*** Front. Mol. Biosci., 2024, 11, 1341108; punktacja MNiSW: 140, IF: 3,900

**P.6.      N. Warmuzińska, K. Łuczykowski, I. Stryjak, E. Wojtal, A. Woderska-Jasińska, M. Masztalerz, Z. Włodarczyk, B. Bojko: *Metabolomic and lipidomic profiling for pre-transplant assessment of delayed graft function risk using chemical biopsy with microextraction probes.* Int. J. Mol. Sci., 2024, 25, 13502; punktacja MNiSW: 140, IF: 4,900**

Łączna wartość wskaźnika Impact Factor (IF) dla prac wchodzących w cykl: 22,955.  
Łączna wartość punktów Ministerstwa Nauki i Szkolnictwa Wyższego (MNiSW) dla prac wchodzących w cykl: 650.

### 3. Streszczenie w języku polskim

Liczba pacjentów umieszczanych na listach oczekujących na przeszczep nerki szybko rośnie, co prowadzi do coraz większej dysproporcji między zapotrzebowaniem na narządy a ich dostępnością. W związku z tym ośrodki transplantacyjne stają przed wyzwaniem maksymalnego wykorzystania dostępnych zasobów narządów oraz rozszerzenia puli dawców, aby zmniejszyć tę lukę. Dawcy spełniający standardowe kryteria są preferowani do przeszczepień nerek, ponieważ narządy od tych dawców zazwyczaj dają lepsze wyniki. Jednak, niedobór dostępnych nerek wymusza korzystanie z narządów marginalnych, pochodzących od dawców o rozszerzonych kryteriach w celu zwiększenia liczby przeszczepień i skrócenia czasu oczekiwania pacjentów. Wiadomo jednak, że jakość narządu dawcy ma wpływ na długoterminowe wyniki transplantacji, a przeszczepy od dawców o rozszerzonych kryteriach mają gorsze rokowania, zwiększone ryzyko opóźnionej funkcji przeszczepu oraz pierwotnej niewydolności przeszczepu. W związku z tym istnieje pilna potrzeba opracowania nowych strategii umożliwiających wczesną ocenę jakości narządu, predykcję wystąpienia powikłań oraz optymalizację postępowania z biorcami o wysokim ryzyku po przeszczepie. Dodatkowo niezbędne są skuteczne strategie ograniczania uszkodzeń podczas przechowywania narządów, które mogłyby poprawić ich jakość i zwiększyć szanse na udany przeszczep.

W odpowiedzi na te potrzeby, głównym celem niniejszej rozprawy było zaadresowanie problemu nieefektywnej diagnostyki okołotransplantacyjnej poprzez wykazanie potencjału mikroekstrakcji do fazy stałej (SPME, ang. solid-phase microextraction) w ocenie jakości nerek. Badania zakładały przetestowanie nowego podejścia analitycznego opartego na bezpośredniej analizie tkanki *in vivo* z wykorzystaniem biopsji chemicznej w połączeniu z profilowaniem lipidomicznym. W pierwszym etapie badań wykorzystano model zwierzęcy w celu oceny wpływu niedokrwienia na jakość narządu bazując na dwóch typach dawców oraz porównania różnych metod konserwacji narządu i określenia ich oddziaływania na profil lipidomiczny nerki. Następnie zastosowano SPME w warunkach klinicznych w celu predykcji ryzyka wystąpienia powikłań oraz wyodrębnienia panelu metabolitów i lipidów o potencjalnym znaczeniu diagnostycznym.

Dzięki zastosowaniu SPME, które nie wymaga fizycznego pobrania fragmentu tkanki oraz zapewnia małe rozmiary sondy ekstrakcyjnej (średnica ~200  $\mu\text{m}$ ), możliwe było

wielokrotne pobieranie próbek z tego samego narządu bez jego uszkodzenia. Pozwoliło to na monitorowanie zmian zachodzących w narządzie podczas całej procedury przeszczepienia - od pobrania narządu, przez jego przechowywanie, aż po reperfuzję oraz identyfikację licznych związków o zróżnicowanej polarności. Ponadto, porównanie różnych metod konserwacji narządu, wykazało, że temperatura przechowywania narządu ma większy wpływ na profil lipidomiczny nerki niż mechaniczny charakter metody konserwacji. Dodatkowo zastosowanie perfuzji normotermicznej powodowało mniejszą kumulację lipidów związanych z uszkodzeniem niedokrwienno-reperfuzyjnym, dysfunkcją mitochondrialną, działaniem prozapalnym i stresem oksydacyjnym, co wskazuje, że jej zastosowanie może korzystnie wpływać na funkcję narządu.

W kolejnym etapie zastosowano SPME w warunkach klinicznych przeprowadzając analizy metabolomiczne i lipidomiczne w wielu punktach czasowych, obejmujących zarówno tkankę nerkową od dawców, jak i osocze biorców, w celu wykrycia zmian związanych z opóźnioną funkcją przeszczepu. Zidentyfikowane związki o potencjalnej wartości predykcyjnej obejmowały głównie aminokwasy i ich pochodne, nukleotydy, kwasy organiczne, peptydy oraz lipidy, w szczególności fosfolipidy i trójglicerydy. Uzyskane wyniki wskazują na znaczący potencjał translacyjny biopsji chemicznej oraz analizy metabolitów osoczowych w ocenie ryzyka i nieinwazyjnym monitorowaniu wystąpienia powikłań. Zidentyfikowane metabolity stanowiąc będą podstawę do opracowania kompleksowej metody oceny i monitorowania opóźnionej funkcji przeszczepu oraz zarządzania pacjentami z wysokim ryzykiem. Zastosowanie biopsji chemicznej w warunkach klinicznych nie wydłuża czasu zimnego niedokrwienia ani nie zaburza przebiegu procedury przeszczepienia, co znacząco zwiększa jej potencjał translacyjny oraz może ułatwić wdrożenie do rutynowej diagnostyki.

Słowa kluczowe: mikroekstrakcja do fazy stałej (SPME); transplantacja nerki; lipidomika; ocena jakości narządu; opóźniona funkcja przeszczepu (DGF)

## 4. Streszczenie w języku angielskim

### Lipidomic analysis in transplant diagnostics

The number of patients placed on kidney transplant waiting lists continues to rise, resulting in a growing disproportion between organ demand and availability. Consequently, transplant centers are increasingly challenged to optimize the utilization of available organ resources and to expand the donor pool to mitigate this gap. Standard criteria donors are typically preferred in kidney transplantation, as grafts from these donors are associated with more favorable outcomes. However, the ongoing shortage of donor kidneys has necessitated the inclusion of marginal organs from expanded criteria donors to increase transplant rates and reduce patient wait times. It is well established that donor organ quality significantly influences long-term transplant outcomes, with expanded criteria donor kidneys being associated with poorer prognoses, an increased risk of delayed graft function, and a higher incidence of primary non-function. Accordingly, there is an urgent need for innovative strategies that enable early graft quality assessment, prediction of post-transplant complications, and improved management of high-risk recipients. Additionally, effective preservation strategies are required to minimize ischemic injury, enhance organ quality, and ultimately improve transplant success rates.

In response to these challenges, the primary aim of this study was to address the limitations of current peri-transplant diagnostics by demonstrating the potential of solid-phase microextraction (SPME) for kidney quality assessment. The study was designed to evaluate a novel analytical approach involving direct *in vivo* tissue analysis through chemical biopsy, combined with lipidomic profiling. In the initial phase, an animal model was used to assess the impact of ischemia on organ quality based on two donor types, and to compare different preservation techniques with respect to their effects on the kidney lipidome. Subsequently, the SPME technique was applied in a clinical setting to predict the risk of complications and to identify a panel of metabolites and lipids with potential diagnostic relevance.

The use of SPME—characterized by a minimally invasive sampling probe (~200 µm in diameter) that does not require tissue excision—enabled repeated, non-destructive sampling from the same organ. This facilitated monitoring of biochemical alterations

throughout the transplantation process, from organ retrieval and preservation to reperfusion, while also enabling the detection of a wide range of compounds with diverse polarities. Moreover, comparative analysis of different preservation methods revealed that storage temperature exerted a greater influence on the kidney's lipidomic profile than the mechanical nature of the preservation technique. Notably, normothermic perfusion was associated with reduced accumulation of lipids linked to ischemia-reperfusion injury, mitochondrial dysfunction, pro-inflammatory responses, and oxidative stress, suggesting a potential protective effect on graft function.

In the final stage of the study, SPME was implemented clinically to perform metabolomic and lipidomic analyses at multiple time points using both donor kidney tissue and recipient plasma samples, with the aim of detecting changes associated with delayed graft function. The identified compounds with potential predictive value included amino acids and their derivatives, nucleotides, organic acids, peptides, and lipids—particularly phospholipids and triacylglycerols. These findings highlight the translational potential of chemical biopsy and plasma metabolite profiling for non-invasive risk assessment and monitoring of post-transplant complications. The identified metabolites may form the basis for the development of a comprehensive tool for the evaluation and prediction of delayed graft function and for managing high-risk transplant recipients. Importantly, the application of chemical biopsy in a clinical setting did not prolong cold ischemia time or disrupt the transplantation workflow, thereby further supporting its clinical feasibility and potential for integration into routine diagnostic practice.

Keywords: solid-phase microextraction (SPME); kidney transplantation; lipidomics; graft quality assessment; delayed graft function (DGF)

## 5. Wstęp

### 5.1. Ocena jakości narządów do przeszczepu: współczesne metody i kierunki rozwoju w medycynie transplantacyjnej

W ciągu ostatnich kilku dekad transplantacja narządów litych stała się rutynową częścią opieki klinicznej na całym świecie, przyczyniając się do wyższych wskaźników przeżycia i lepszej jakości życia pacjentów. Postępy w technikach chirurgicznych, standardach opieki i immunosupresji znacząco poprawiły wyniki przeszczepów [1]. Niestety liczba pacjentów umieszczanych na listach oczekujących gwałtownie rośnie, co prowadzi do coraz większej dysproporcji między zapotrzebowaniem na narządy a dostępnością nerek do przeszczepienia. Według danych Eurotransplantu w 2024 roku przeszczepiono 3 223 nerki od zmarłych dawców. Jednak na koniec roku na liście oczekujących nadal znajdowało się 10 414 pacjentów czekających na przeszczep [2]. Ze względu na ograniczoną liczbę dostępnych narządów kluczowe jest wdrażanie strategii mających na celu zwiększenie puli dawców, skrócenie czasu oczekiwania pacjentów oraz zmniejszenie liczby odrzuconych narządów.

Powszechnie wiadomo, że zarówno typ jak i jakość narządu mają znaczący wpływ na wyniki przeszczepu. Nerki od żywych dawców zapewniają krótszy czas oczekiwania oraz lepsze wyniki zarówno w krótkim, jak i długim okresie w porównaniu z nerkami od dawców zmarłych. Ponadto zwiększają ogólną pulę dostępnych narządów, co przynosi korzyść wszystkim kandydatom do przeszczepu [3]. Jednakże chociaż nerki od żywych dawców są uznawane za najlepsze pod względem jakości, dawstwo żywe nie zawsze jest możliwe. Dlatego najczęstszym rodzajem przeszczepu nerki jest przeszczep od dawcy zmarłego (DD, ang. deceased donor). Preferowanymi dawcami nerek są osoby spełniające standardowe kryteria (SCD, ang. standard criteria donor), ponieważ ich narządy zazwyczaj prowadzą do bardziej korzystnych wyników w porównaniu do innych typów dawców. Jednak niedobór dostępnych nerek skłania do wykorzystywania narządów marginalnych, pochodzących od dawców o rozszerzonych kryteriach (ECD, ang. expanded criteria donor) w celu poszerzenia puli dawców i skrócenia czasu oczekiwania pacjentów [4]. Kryteria dawcy ECD to wiek powyżej 60 lat lub wiek powyżej 50 lat oraz dwa z spośród następujących kryteriów: obecne nadciśnienie tętnicze, przyczyna śmierci - naczyniowa mózgu, poziom kreatyniny powyżej 1,5 mg/dl [5].

Przeszczepy nerek od dawców ECD wiążą się ze zwiększonym ryzykiem opóźnionego podjęcia funkcji przeszczepu (DGF, ang. delayed graft function) oraz pierwotnej niewydolności przeszczepu (PNF, ang. primary nonfunction), co może prowadzić do gorszych rezultatów w porównaniu z przeszczepami od dawców o standardowych kryteriach [6]. Przewiduje się, że częstość występowania DGF i innych powikłań wzrośnie w nadchodzących latach ze względu na coraz częstsze stosowanie nerek od dawców o rozszerzonych kryteriach. Trend ten dodatkowo nasila zmieniająca się demografia starzejącego się społeczeństwa, prowadząca do wzrostu liczby starszych dawców i biorców, co może potęgować ryzyko związane z jakością przeszczepu i wynikami po transplantacji [7]. W związku z tym istnieje pilna potrzeba opracowania nowych strategii umożliwiających wczesną ocenę jakości narządu, predykcję wystąpienia powikłań oraz optymalizację postępowania z biorcami o wysokim ryzyku po przeszczepie. Dodatkowo niezbędne są skuteczne strategie ograniczania uszkodzeń podczas przechowywania narządów, które mogłyby poprawić ich jakość i zwiększyć szanse na udany przeszczep. Konwencjonalne metody oceny przeszczepów nerkowych, takie jak analiza historii medycznej dawcy, ocena wizualna oraz rutynowe badania laboratoryjne, często nie mają wystarczającej specyficzności do przewidywania ryzyka powikłań i dokładnego diagnozowania. Biopsja nerki może dostarczyć cennych informacji na temat istniejących wcześniej chorób dawcy i zmian naczyniowych, jednak pozostaje procedurą inwazyjną.

Przeglądu ograniczeń i zalet konwencjonalnych metod diagnostycznych oraz szeregu nowych potencjalnych narzędzi w odniesieniu do oceny jakości przeszczepu dawcy, identyfikacji uszkodzenia niedokrwienno-reperfuzyjnego (IRI, ang. ischemia-reperfusion injury), kontroli perfuzji i przewidywania DGF dokonano w pracy poglądowej pt. „A review of current and emerging trends in donor graft-quality assessment techniques” (J. Clin. Med., 2022, 11, 487), będącej częścią cyklu publikacji prezentowanych w tej rozprawie doktorskiej (publikacja P.1.).

## Review

# A Review of Current and Emerging Trends in Donor Graft-Quality Assessment Techniques

Natalia Warmuzińska, Kamil Łuczykowski and Barbara Bojko \* 

Department of Pharmacodynamics and Molecular Pharmacology, Faculty of Pharmacy, Collegium Medicum in Bydgoszcz, Nicolaus Copernicus University in Torun, 85-089 Bydgoszcz, Poland; n.warmuzinska@cm.umk.pl (N.W.); k.luczykowski@cm.umk.pl (K.L.)

\* Correspondence: bbojko@cm.umk.pl

**Abstract:** The number of patients placed on kidney transplant waiting lists is rapidly increasing, resulting in a growing gap between organ demand and the availability of kidneys for transplantation. This organ shortage has forced medical professionals to utilize marginal kidneys from expanded criteria donors (ECD) to broaden the donor pool and shorten wait times for patients with end-stage renal disease. However, recipients of ECD kidney grafts tend to have worse outcomes compared to those receiving organs from standard criteria donors (SCD), specifically increased risks of delayed graft function (DGF) and primary nonfunction incidence. Thus, representative methods for graft-quality assessment are strongly needed, especially for ECDs. Currently, graft-quality evaluation is limited to interpreting the donor's recent laboratory tests, clinical risk scores, the visual evaluation of the organ, and, in some cases, a biopsy and perfusion parameters. The last few years have seen the emergence of many new technologies designed to examine organ function, including new imaging techniques, transcriptomics, genomics, proteomics, metabolomics, lipidomics, and new solutions in organ perfusion, which has enabled a deeper understanding of the complex mechanisms associated with ischemia-reperfusion injury (IRI), inflammatory process, and graft rejection. This review summarizes and assesses the strengths and weaknesses of current conventional diagnostic methods and a wide range of new potential strategies (from the last five years) with respect to donor graft-quality assessment, the identification of IRI, perfusion control, and the prediction of DGF.

**Keywords:** kidney transplantation; graft quality assessment; biomarkers; machine perfusion; IRI; DGF



**Citation:** Warmuzińska, N.; Łuczykowski, K.; Bojko, B. A Review of Current and Emerging Trends in Donor Graft-Quality Assessment Techniques. *J. Clin. Med.* **2022**, *11*, 487. <https://doi.org/10.3390/jcm11030487>

Academic Editor: Eytan Mor

Received: 13 December 2021

Accepted: 14 January 2022

Published: 18 January 2022

**Publisher's Note:** MDPI stays neutral with regard to jurisdictional claims in published maps and institutional affiliations.



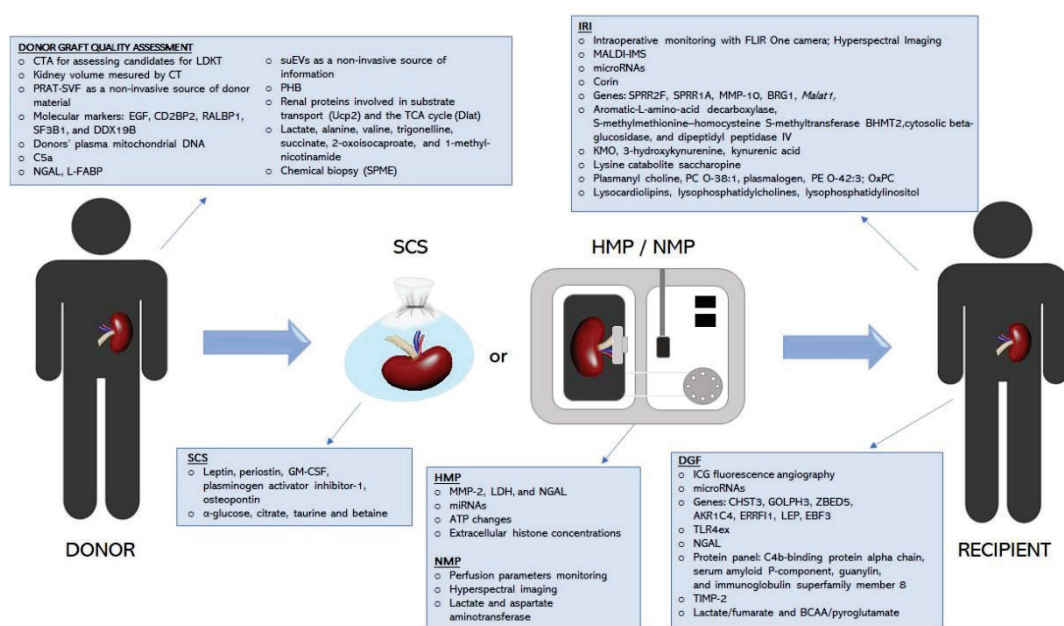
**Copyright:** © 2022 by the authors. Licensee MDPI, Basel, Switzerland. This article is an open access article distributed under the terms and conditions of the Creative Commons Attribution (CC BY) license (<https://creativecommons.org/licenses/by/4.0/>).

## 1. Introduction

Kidney transplantation (KTx) is a life-saving treatment for patients with end-stage renal dysfunction that is characterized by higher survival rates and greater quality of patient life compared to dialysis treatment [1]. Unfortunately, the number of patients placed on kidney transplant waiting lists is rapidly increasing, resulting in a growing gap between organ demand and the availability of kidneys for transplantation. Standard criteria donors (SCD) are preferred for kidney transplants because organs from these individuals typically result in more favourable outcomes compared to other donor types [2]. However, the shortage of available kidneys has forced medical professionals to utilize marginal kidneys from expanded criteria donors (ECD) to broaden the donor pool and shorten wait times for patients with end-stage renal disease. Nonetheless, it is well known that donor organ quality affects long-term outcomes for renal transplant recipients, and ECD kidney grafts have been shown to have worse outcomes compared to SCD grafts, including an increased risk of delayed graft function (DGF) and primary nonfunction incidence (PNF) [2,3]. Thus, representative methods of assessing graft-quality are urgently needed, especially for ECDs. Currently, the surgeon decides whether to accept or decline a kidney based on their interpretation of the donor's recent laboratory tests and a visual evaluation of the organ, with a biopsy being employed in some cases for direct tissue analysis [4,5].

Notably, the rapid emergence of techniques such as imaging, omics, and organ perfusion has provided surgeons with a wide range of new potential tools and biomarkers that could be used to evaluate graft quality.

In this paper, we review and evaluate the limits and advantages of current conventional diagnostic methods and a range of new potential tools (from the last five years) with respect to donor graft-quality assessment, the identification of ischemia-reperfusion injury (IRI), perfusion control, and the prediction of DGF (Figure 1).



**Figure 1.** Emerging techniques and biomarkers in graft quality assessment, the identification of ischemia-reperfusion injury, perfusion control, and the prediction of DGF.

## 2. Current Conventional Diagnostic Methods

### 2.1. Visual Assessment

A visual evaluation of the kidney by the transplant team is a critical step in determining whether it will be accepted for transplantation or rejected. Macroscopic examination is useful for identifying kidney tumors, anatomical changes, damage, fibrosis, and scars that indicate the quality of the graft. However, this method is subjective and depends on the transplant team's level of experience [4]. Recent findings showed that surgeons were able to reliably predict the occurrence of postperfusion syndrome through visual assessments of liver graft quality, thus emphasizing the importance of visual appraisals by the surgical team [6]. However, no prior studies have evaluated intra-observer variability and the predictive value of visual kidney assessment. Thus, there is a need for new standardized diagnostic solutions for graft-quality assessment.

### 2.2. Clinical Risk Scores

Clinical information and laboratory results for a potential donor are crucial for an initial assessment of organ quality. Consequently, several scoring systems have been created to comprehensively analyse the risk of long-term graft failure or DGF [7–10]. At present, the Kidney Donor Risk Index (KDRI) and the Kidney Donor Profile Index (KDPI) are recognized as the most effective systems for scoring kidney graft quality. The KDRI was created by Rao et al., to quantify the risk of graft failure from deceased donors (DDs) based

on donor and transplant variables, such as age, serum creatinine (CR), diabetes, HCV status, and cause of death [10]. The KDPI is a percentile measure based on the KDRI that was designed to assess how long a kidney from a DD is expected to function relative to all kidneys recovered in the U.S. during the previous year. The KDPI score is calculated based on ten variably weighted donor parameters that relevantly affect organ quality, with an emphasis on nephron mass. Lower KDPI scores are linked with longer estimated organ function, while higher KDPI scores are associated with a shorter estimated organ lifespan [11,12]. The KDRI and KDPI are regarded as reliable predictors of graft outcomes, and they are expected to increase the prevalence of marginal kidney grafting and reduce the unnecessary discard rate [11,13]. However, these indexes are not intended to be used as the only metric for determining donor suitability; rather, they should be utilized as a part of a comprehensive assessment along with other factors, including pre-implant biopsy histopathology and hypothermic machine perfusion (HMP) parameters [11,14]. Because age is the most influential factor in calculating the KDRI and KDPI scores, it is unclear whether the scores for these indexes can be applied to elderly and pediatric DDs. Recent studies suggest that the KDPI does not precisely predict pediatric kidney graft survival, while the KDRI has been found to be more reliable for elderly DDs. Overall, more research is needed to assess how reliably KDPI and KDRI scores predict postoperative renal function for grafts using kidneys from pediatric and elderly donors [13,15].

### 2.3. Biopsy

Pretransplant biopsy is currently one of the most widely used diagnostic methods and is recognized as the gold standard for confirming allograft injury. However, the frequency with which biopsies are performed varies between medical facilities and countries. In the United States, up to 85% of higher-risk kidneys are biopsied, whereas pretransplant biopsies are rarely conducted in European medical facilities. Histological evaluation is usually applied selectively, predominantly in ECD and donor after cardiac death (DCD) kidneys, and can help surgeons decide whether a kidney should be selected for transplantation or rejected [4,5,16].

In contrast to most laboratory data, histopathological assessments of biopsies do not yield a single value; rather, they produce comprehensive diagnoses that consider all available information. Although glomerulosclerosis, vascular disease, and interstitial fibrosis are the most frequently reported kidney parameters associated with worse graft outcomes [4,16], there is no consensus on the relative importance of each factor and which threshold values should be used to define the acceptable limit values. A further difficulty is the low reproducibility of kidney biopsy evaluations between on-call pathologists and renal pathologists described in many prior studies. The clear need to improve reproducibility and to objectivize the procedure and reporting of results prompted the development of several new composite histopathological scoring systems, including the Remuzzi score, the Maryland Aggregate Pathology Index, Banff criteria, and the Chronic Allograft Damage Index. Nevertheless, even with all these scoring systems, there are still doubts relating to the sampling, processing, and evaluation of biopsies [4,5,16].

In daily practice, it may be necessary to obtain quick results. In such circumstances, frozen section (FS) evaluation is often used for decision making. Producing paraffin sections (PS) is time consuming, which can cause histological evaluations to require up to 3 h to complete, even with the use of high-speed processing methods [5,17,18]. However, reports of reproducibility and prognostic value are based on paraffin-embedded tissue [18]. Recent studies have shown discrepancies in the results obtained with the use of FS and PS, but these variances had no significant impact on the outcomes for the transplanted organs [18]. Observed changes could be subtler in frozen sections than in paraffin sections, which may be a limitation, particularly in the hands of inexperienced pathologists [17,19]. On the other hand, it is also critical to consider logistics when choosing an optimal biopsy technique. For instance, FS is able to provide a diagnosis in less than 30 min, whereas PS requires at

least 3 h. In selecting the proper technique, it is important to strike a balance between the benefits and risks associated with increased cold ischemia [4,18].

A lack of uniformity with respect to procedural standards has resulted in the use of a variety of biopsy techniques. The majority of medical facilities seem to prefer wedge biopsy (WB) over needle biopsy (NB) because NB carries a greater risk of injuring larger blood vessels, potentially resulting in uncontrolled bleeding after reperfusion. However, most recent reports comparing WB and NB have found that NB provides a much better evaluation of vascular lesions and has a higher overall correlation with the state of the whole kidney [5,16,17].

Ultimately, the most crucial factor is how the histopathological results correlate with long-term graft survival. Many studies have attempted to address the predictive value of renal biopsy with respect to graft outcomes, but the results of these studies have been predominantly inconclusive [20–23]. For instance, Traynor et al., conducted a retrospective study that examined kidney transplants over a 10-year period to determine whether pretransplant histology is able to predict graft outcomes at 5 years, and whether donor histology adds incremental data to the current clinical parameters. While the results of these reports suggest that that histological assessment adds little additional prognostic information aside from clinical parameters [20], Yap et al., found that the histological evaluation of ECD kidneys was associated with improved long-term graft survival. Their results suggest that pretransplant biopsy assessment can enable ECD kidneys to be used as a safe and viable option during persistent shortages of kidney donors [21]. The divergence between recent studies highlights the need for a prospective controlled trial to evaluate the predictive value of pretransplant biopsies. Until a standardized and comprehensive evaluation protocol has been developed, biopsy findings remain only one component of a donor organ assessment and should not be taken as the sole determinant in deciding whether to discard or transplant donor kidneys [19,24,25].

#### 2.4. Perfusion Control

Static cold storage (SCS) and HMP are the main techniques of kidney graft preservation [26]. HMP has become a frequently and widely used procedure in kidney transplantation over the past few years [26–28]. Indeed, several reports have shown that the HMP reconditioning effect results in better postoperative outcomes with respect to reducing DGF and better long-term graft survival after transplantation [29–31]. An important benefit of HMP is that it enables the monitoring of perfusion parameters that could predict post-transplant organ viability. In particular, flow rate and renal resistance (RR) have been among the most frequently used perfusion parameters in predicting post-transplant function [27,32–34]. Previous studies have produced findings suggesting that real-time RR detection provides good predictive value. As Bissolati et al., showed, the RR trend during HMP can be used to predict post-transplantation outcomes, especially in relation to kidneys procured from ECD [28]. Patel et al., conducted a retrospective study that included 190 kidneys in order to evaluate the prognostic utility of HMP in DD transplantation. Their findings showed that resistances at two hours and beyond predicted DGF, while initial resistance to machine perfusion predicted one-year graft survival post-transplantation [35]. On the other hand, some studies found no association between hemodynamic parameters during HMP and the development of DGF [27]. Thus, due to these inconclusive results, the perfusion parameters cannot be regarded as stand-alone criteria. However, the undoubted advantage of perfusion parameters is that they are easy to obtain in a non-invasive manner. As such, Jochmans et al., and Zheng et al., have suggested that HMP parameters should be included as part of a comprehensive graft assessment [14,32]. DGF has a complex pathogenesis and cannot be predicted with precision using the HMP parameters as a stand-alone assessment tool. However, RR represents an additional source of information that can help clinicians in their decision-making process. Attaining more accurate predictions of graft outcomes will require integrating the perfusion parameters into multifactorial graft quality scoring systems. A combination of the donor's clinical data, kidney pre-implant

histopathology, and HMP parameters may provide a more effective prediction of DGF than any of the measures alone [14,32].

### 2.5. Microbiological Analysis of Preservation Fluid

Organ transplant recipients are prone to infectious complications, and despite many advances, post-operative infections remain associated with significant morbidity and mortality [36–38]. Early post-transplant infections among kidney transplant recipients may be transmitted via the donor, or the donated organ may be contaminated during the transplantation procedure [36,38]. Moreover, pathogens can be transmitted via preservation solution, which is required to maintain kidney viability, but due to its biochemical characteristics, it can also keep microorganisms alive and serve as an infection vector [36,38,39]. For that reason, some transplant centres collect preservation fluid for microbiological analysis in addition to standard screening for donor infections. However, there are no widely accepted recommendations for managing positive preservation fluid cultures [36,38]. Moreover, it remains unanswered whether intra-operative preservation fluid routine screening should be performed because the clinical impact of this practice is still not well established. Some studies have evaluated the risk factors associated with culture-positive preservation fluid and determined the benefit of routine screening of preservation solutions for the management of kidney transplant recipients [36–38,40]. Corbel et al., demonstrated that 24% of DD preservation fluid cultures were positive, and these contaminations were mainly a consequence of procurement procedures [37]. Reticker et al. [36] and Oriol et al. [38] showed that the prevalence of culture-positive preservation fluid was up to 60%; however, the vast majority of microbial growth was consistent with skin flora or low-virulence pathogens. In addition, Oriol et al., indicated that pre-emptive antibiotic therapy for recipients with high-risk culture-positive preservation fluid might improve the outcomes and help to avoid preservation-fluid-related infections [38]. Moreover, Stern et al., reported that fungal contamination of preservation fluid was infrequent, although yeast contamination of preservation solutions was associated with high mortality [40]. In parallel, Reticker et al., suggested that antibiotic therapy for recipients with preservation solutions contaminated by low virulence pathogens may not be necessary, reducing antibiotic overuse [36]. In conclusion, routine screening of preservation solutions could improve graft outcomes and pre-emptive antibiotic therapy and be helpful to avoid preservation-fluid-related infections. However, future studies are needed to establish guidelines for preservation fluid microbiological analysis and handling culture-positive preservation fluid.

## 3. Emerging Techniques

### 3.1. Imaging

Diagnostic imaging methods are mainly used to evaluate kidneys from living donors (LD) prior to acceptance for transplantation, as well as for assessing post-renal transplant complications. In the case of living donor surgeries, non-invasive preoperative evaluation of the quality of the graft organ is especially critical, which allows surgeons to assess certain vital features, such as size, the presence/absence of focal cystic or solid lesions, and the condition of vascular structures, to establish whether it is appropriate for transplantation. While most of these features can be visualized via Doppler ultrasound, computed tomography angiography (CTA) is usually necessary for a more accurate assessment of the vascular anatomy [41–43]. However, given the critical role of careful evaluation and suitable preparation when dealing with living donor transplantation, it will be imperative to continue to conduct new research aimed at improving transplantation outcomes.

Sarier et al., conducted a retrospective study wherein they compared pretransplant CTA images to intraoperative findings to evaluate renal artery variations in a large sample of LD. They found that laparoscopic donor nephrectomy enabled the detection of the same number of renal arteries as CTA in 97.9% of the analysed kidneys, but less than CTA in the remaining 2.1%. Notably, a greater number of renal arteries were not detected in any of the studied kidneys via nephrectomy compared to CTA. These results indicate that CTA

is more accurate than intraoperative findings, and is an effective method for evaluating candidate donors for living donor kidney transplantation (LDKT), as well as for identifying renovascular variations [42].

Al-Adra et al., employed computed tomography (CT) scans to assess the influence of donor kidney volume on recipient estimated glomerular filtration rate (eGFR) in a large cohort of patients undergoing LDKT. The resultant statistical models showed a significant correlation between donor kidney volume and recipient eGFR at 1, 3, and 6 months ( $p < 0.001$ ). These findings indicate that donor kidney volume is a strong independent predictor of recipient eGFR in LDKT and may therefore be a valuable addition to predictive models of eGFR after transplantation. Further research could examine whether addition of donor kidney volume in matching algorithms can improve recipient outcomes [43].

Although the ability to monitor graft status intraoperatively is limited at present, several novel solutions have been proposed over the past few years to evaluate graft quality during transplantation and predict DGF.

In 2019, Fernandez et al., proposed a novel approach that utilized infrared imaging to monitor the reperfusion phase during kidney transplantation in real-time. To this end, they used a long-wave infrared camera (FLIR One) with a visual resolution of  $1440 \times 1080$  pixels and a thermal resolution of  $160 \times 120$  to study the grafts in 10 pediatric patients undergoing kidney transplantation. During the study, images were acquired at several key time points. The authors observed a correlation between changes in intraoperative graft temperature and decreases in postoperative creatinine levels in all of the analysed subjects. Given these results, Fernandez et al., concluded that infrared thermal imaging could be a promising option for non-invasive graft perfusion monitoring. However, additional work is required to confirm Fernandez et al.'s results because they were somewhat limited due to the relatively small number of patients included and the short follow-up period [44].

In another study, Sucher et al., employed Hyperspectral Imaging (HSI) as a noncontact, non-invasive, and non-ionizing method of acquiring quantitative information relating to kidney viability and performance during transplantation. Specifically, they used HSI to study seventeen consecutive deceased donor kidney transplants prior to transplantation, while stored on ice, and again at 15 and 45 min after reperfusion. After computation time of less than 8 s, the analysis software was able to provide an RGB image and 4 false color images representing the physiological parameters of the recorded tissue area, namely, tissue oxygenation, perfusion, organ hemoglobin, and tissue water index. The obtained results revealed that allograft oxygenation and microperfusion were significantly lower in patients with DGF. Future applications might also utilize HSI during donor surgery to assess kidney quality prior to cold perfusion and procurement. However, HSI can only be used intraoperatively and requires a direct view of the kidney because the maximum penetration depth for microcirculation measurements is currently 4–6 millimetres, making transcutaneous applications impossible. Thus, this technique's main limitations are its inability to provide continuous or intermittent transcutaneous follow-up measurements, as well as its small sample size. Thus, further studies are required to confirmed these results [45].

In the recent article, Gerken et al., documented a prospective diagnostic study that they had conducted in two German transplantation centres wherein allograft microperfusion was assessed intraoperatively via near-infrared fluorescence angiography with indocyanine green (ICG). While previous studies have shown that ICG fluorescence angiography can be applied safely during kidney transplantation, none have provided a quantitative assessment of the use of fluorescence video. To fill this gap, Gerken et al., evaluated the benefits of coupling quantitative intraoperative fluorescence angiography with ICG to predict post-operative graft function and the occurrence of DGF. Their findings indicated that the impairment of intraoperative microperfusion in the allograft cortex is a risk factor for the occurrence of DGF, and that ICG Ingress is an independent predictor of DGF. Further studies are warranted to analyse the effect of applying early therapeutic approaches to prevent DGF in kidney transplant recipients, thus improving long-term graft success [46].

The use of imaging techniques to diagnose post-renal transplant complications has been discussed extensively in recent reviews [47–49]; therefore, the present work will only examine a few of the most recent studies in this field. Promising results have been reported with respect to combining positron emission tomography (PET) with CT or magnetic resonance imaging (MRI) using the glucose analogue radiotracer, 2-deoxy-2-fluoro-D-glucose (FDG), to detect acute kidney allograft rejection, for diagnostic applications, for the functional assessment of grafts, and for therapeutic monitoring [50,51]. In another study, the utility of arterial spin labeling (ASL) magnetic resonance imaging was evaluated for its ability to identify kidney allografts with underlying pathologies. ASL uses endogenous water as a tracer, and it has previously been used in applications relating to the brain. Moreover, there have been reports demonstrating that ASL can be used to categorize stages of chronic kidney disease [52]. Wang et al., demonstrated that ASL might be a non-invasive tool for differentiating kidneys with subclinical pathology from those with stable graft function. However, more research should be performed to verify these findings [53].

### 3.2. Omics

The last few years has seen the emergence of many new technologies that examine organ function on a molecular level, which has enabled the discovery of numerous potential biomarkers of renal injury. High-throughput omics technologies allow researchers to obtain a large amount of data about specific types of molecules, providing a holistic picture that captures the complex and dynamic interactions within a biological system. These innovative methods, including transcriptomics, genomics, proteomics, metabolomics, and lipidomics, provide a deeper understanding of the complex mechanisms associated with IRI, inflammatory processes, and graft rejection [5,54]. This section surveys some promising methods and techniques that could be successfully translated to clinical settings in the foreseeable future (Table 1).

#### 3.2.1. Transcriptomics/Genomics

Several studies have examined how graft quality and donor category impact graft and patient survival. Giraud et al., proposed an open-ended approach based on microarray technology to understand IRI occurring in DCD kidneys in a preclinical porcine model that had been subjected to warm ischemia (WI) followed by cold ischemia. Giraud et al.'s findings indicated that hundreds of cortex and corticomedullary junction genes were significantly regulated after WI or after WI followed by cold storage compared to healthy kidneys. In addition, they also analysed the kinetics of the most differentially expressed genes. They hypothesized that these genes played a key role in IRI and could be divided into eight categories: mitochondria and redox state regulation; inflammation and apoptosis; and protein folding and proteasome; cell cycle, cellular differentiation and proliferation; nucleus genes and transcriptional regulation; transporters; metabolism regulation; mitogen-activated protein kinase and GTPase (guanosine triphosphate, GTP) activity [55].

Boissier et al., performed a comparative study of cellular components, transcriptomics, and the vasculogenic profiles obtained from 22 optimal donors and 31 deceased ECDs. They hypothesized that as an easily accessible source of donor-derived material, perirenal adipose tissue (PRAT) can be used to assess the quantitative and functional features that characterize donor cells. In addition, adipose tissue can be enzymatically processed to obtain stromal vascular fraction (SVF), which is a heterogeneous cellular mixture free of adipocytes. In their study, Boissier et al., performed a transcriptomic analysis in order to differentiate the PRAT-SVF molecular transcript in ECD and other donors. The upregulated genes demonstrated a strong association with the inflammatory response, cytokine secretion, and circulatory system development, while the downregulated genes were associated with regulating metabolic processes and circulatory system development. Importantly, Boissier et al.'s findings provide new evidence that PRAT-SVF serves as a non-invasive source of donor material that can be highly valuable in the assessment of inflammatory features affecting the quality and function of the graft [56].

The midterm outcomes of kidney transplant recipients with early borderline changes between ECD, SCD, and LD were compared in a retrospective observational study. In the ECD group, microarray analysis showed a higher expression of 244 transcripts than the SCD group, and 437 more than the LD group. Compared to both the SCD and LD groups, gene annotation analysis of transcripts with elevated expression in ECD group revealed enhancement in the inflammatory response, the response to wounding, the defence response, and the ECM-receptor interaction pathway. ECD-related transcripts were likely increased by already occurred vascular changes compared to SCD group, and, similarly in SCD group, by longer ischemia compared with LD group. Therefore, chronic vascular changes and cold ischemia time enhance inflammation and thus contribute to poor outcomes for these grafts [57].

Another novel organ-evaluation tool was proposed in a retrospective open-cohort study that examined donors' plasma mitochondrial DNA (mtDNA), which can be easily and non-invasively assayed in the pre-transplant period, and may be a promising predictive biomarker for allograft function [58]. The mtDNA levels in the plasma of DCD were determined via real-time polymerase chain reaction (RT-PCR) and then statistically analysed in relation to the recipient's mtDNA levels and DGF. The linear prediction model, which included plasma mtDNA, donor serum creatinine, and warm ischemia time (WIT), showed high predictive value for reduced graft function. Moreover, the findings indicated that plasma mtDNA might be a novel non-invasive predictor of DGF and allograft function at six months after transplantation, in addition to correlating to allograft survival. Furthermore, mtDNA may serve as a surrogate predictive marker for PNF [58].

The vast majority of studies aiming to identify novel biomarkers involved in IRI have used murine or rat models. A growing body of evidence indicates that the aberrant expression of microRNAs (miRNA/miR) is closely associated with IRI pathogenesis [59–64]. MiRNAs are small, noncoding RNAs that mediate mRNA cleavage, translational repression, or mRNA destabilization [59]. For instance, Chen et al.'s findings suggest that miR-16 may serve as a potential biomarker of IRI-induced acute kidney injury (AKI) [59], while Zhu et al., found that miR-142-5p and miR-181a might be responsible for modulating renal IRI development [63]. On the other hand, some studies have pointed that miR-17-92, miR-139-5p, and miR-27a may play a protective role in IRI [61,62,64]. For example, Song et al., suggest that the overexpression of miR-17-92 could partly reverse the side-effects of IRI on the proximal tubules in vivo [61]. Furthermore, Wang et al., have reported that the overexpression of miR-27a results in the downregulation of toll-like receptor 4 (TLR4), which in turn inhibits inflammation, cell adhesion, and cell death in IRI [62].

Other murine-model-based studies have explored new candidate genes associated with renal IRI. In one such study, Su et al., found that IRI caused the upregulation of SPRR2F, SPRR1A, MMP-10, and long noncoding RNA (lncRNA) *Malat1* in kidney tissues. These genes are involved in keratinocyte differentiation, regeneration, and the repair of kidney tissues; extracellular matrix degradation and remodeling; inflammation; and cell proliferation in renal IRI [64]. In a separate study, Liu et al., investigated the role of BRG1 in IRI-induced AKI with a focus on its role in regulating IL-33 expression in endothelial cells. Their findings revealed that endothelial BRG1 deficiency reduces renal inflammation following ischemia-reperfusion in mice with a simultaneous reduction in IL-33 levels [65].

Comparisons of IRI in murine-based models and clinical studies have yielded valuable results [66,67]. For instance, Cippà et al., employed RNA-sequencing-mediated transcriptional profiling and machine learning computational approaches to analyse the molecular responses associated with IRI, which emphasized early markers of kidney disease progression and outlined transcriptional programs involved in the transition to chronic injury [66]. Other studies have demonstrated that Corin is downregulated in renal IRI and may be associated with DGF after kidney transplantation. Researchers have also screened differentially expressed genes in a murine model of IRI, with findings identifying Corin as one of the most relevant downregulated genes among 2218 differentially expressed genes. Moreover, 11 recipients with complications due to DGF and 16 without DGF were recruited

for an ELISA to determine their plasma Corin concentrations. The findings of this study showed downregulation of plasma Corin concentrations in transplant recipients with DGF complications, indicating that Corin could be a potential biomarker of DGF [67]. DGF may result from early ischemic injury and potentially contribute to poor long-term survival following kidney transplantation [68,69]. For this reason, much research has been devoted to devising reliable methods for predicting the extent of IRI, and hence, DGF.

Hence, as with the IRI, miRNA was evaluated as a biomarker of DGF. In one study, Khalid et al., quantified microRNAs in urine samples from kidney transplant patients to determine whether this approach can be used to predict who will develop DGF following kidney transplantation. To this end, they used unbiased profiling to identify microRNAs that are predictive of DGF following kidney transplantation (i.e., miR-9, -10a, -21, -29a, -221, and -429), and afterward confirmed their findings by measuring specific microRNAs via RT-PCR. The biomarker panel was then assessed using an independent cohort at a separate transplant centre, with urine samples being collected at varying times during the first week after transplantation. When considered individually, all miRs in the panel showed a trend towards an increase or relevant increase in patients with DGF [68].

Wang et al., used high-throughput sequencing to investigate the miRNA expression profiling of exosomes in the peripheral blood of kidney recipients with and without DGF, and explain the regulation of miRNAs in the DGF pathogenesis [69]. Exosomes are cell-derived membrane vesicles present in numerous bodily fluids that play a crucial role in processes such as the regulation of cellular activity, intercellular communication, and waste management [69,70]. Wang et al., identified 52 known and 5 conserved exosomal miRNAs specifically expressed in transplant recipients with DGF. Additionally, their findings showed that transplant recipients with DGF also exhibited the upregulation of three co-expressed miRNAs: hsa-miR-33a-5p R-1, hsa-miR-98-5p, and hsa-miR-151a-5p. Moreover, hsa-miR-151a-5p was positively correlated with the kidney recipients' serum CR, blood urea nitrogen (BUN), and uric acid (UA) levels in the first week post-transplantation [69].

MicroRNA expression in kidney transplant recipients with DGF has also been assessed in another recently published study [71]. In this work, the researchers employed RT-PCR to analyse the expression of miRNA-146-5p in peripheral blood and renal tissue obtained from kidney transplant recipients who had undergone a surveillance graft biopsy during the DGF period. In the renal tissue, the expression of miR-146a-5p was significantly increased among the DGF patients compared to the stable and acute rejection (AR) patients. Similarly, microRNA 146a-5p had heightened expression in the peripheral blood samples from the DGF group compared to those of the acute rejection and stable groups; however, these differences were not statistically significant ( $p = 0.083$ ) [71].

Overall, all these reports indicate that miRNAs are emerging as essential biomarkers in the molecular diagnosis of DGF. The above-discussed findings identify biomarkers that could contribute to the development of tools for predicting DGF and, as such, represent an important area of focus for future research.

Zmonarski et al., applied PCR to nonstimulated peripheral blood mononuclear cells (PBMCs) to examine the averaged mRNA toll-like receptor 4 expression (TLR4ex). The sample for this study consisted of 143 kidney transplant patients, 46 of whom had a history of DGF, and a control group of 38 healthy volunteers. The patients with a history of DGF were divided into two subgroups based on the median TLR4ex: low-TLR4 expression and high-TLR4 expression. Zmonarski et al.'s findings showed that patients with DGF had a much lower TLR4ex and worse parameters of kidney function. In addition, while a comparison of the DGF patients with low and high TLR4ex revealed no initial differences in kidney transplant function, differences were observed in the post-follow-up period. Furthermore, regression analysis showed that TLR4ex was related to recipient age, tacrolimus concentration, and uremic milieu. Consequently, the authors concluded that the low TLR4 expression in patients with DGF may be associated with poor graft-capacity prognosis, and that analysis of changes in TLR4ex may be valuable for assessing immunosuppression efficacy [72].

Another study aiming to identify potential biomarkers of DGF and AKI was recently conducted by Bi et al. [73]. In this study, the authors obtained two mRNA expression profiles from the National Center of Biotechnology Information Gene Expression Omnibus repository, including 20 DGF and 68 immediate graft function (IGF) samples. Differentially expressed genes (DEGs) in the DGF and IGF groups were identified, and pathway analysis of these DEGs was conducted using the Gene Ontology and Kyoto Encyclopedia of Genes and Genomes. Next, a protein–protein interaction analysis extracted hub genes. The essential genes were then searched in the literature and cross-validated based on the training dataset. In total, 330 DEGs were identified in the DGF and IGF samples, including 179 upregulated and 151 downregulated genes. Of these, OLIG3, EBF3, and ETV1 were transcription factor genes, while LEP, EIF4A3, WDR3, MC4R, PPP2CB, DDX21, and GPT served as hub genes in the PPI network. In addition, the findings suggested that EBF3 may be associated with the development of AKI following renal transplantation because it was significantly upregulated in the validation dataset (GSE139061), which is consistent with the initial gene differential expression analysis. Moreover, the authors found that LEP had a good diagnostic value for AKI (AUC = 0.740). Overall, these findings provided more profound insights into the diagnosis of AKI following kidney transplantation [73].

Elsewhere, McGuinness et al., combined epigenetic and transcriptomic data sets to determine a molecular signature for loss of resilience and impaired graft function. Notably, at a translational level, this study also provided a platform for developing a universal IRI signature and the ability to link it to post-transplant outcomes. Furthermore, McGuinness et al.'s findings relate DNA methylation status to reperfusion injury and DGF outcome. In this study, 24 paired pre- and post-perfusion renal biopsies defined as either meeting the extreme DGF phenotype or exhibiting IGF were selected for analysis. The findings of this analysis showed that the molecular signature contained 42 specific transcripts, related through IFN $\gamma$  signaling, which, in allografts displaying clinically impaired function (DGF), exhibited a major change in transcriptional amplitude and increased expression of noncoding RNAs and pseudogenes, which is consistent with increased allostatic load. This phenomenon was attended by an increase in DNA methylation within the promoter and intragenic regions of the DGF panel in pre-perfusion allografts with IGF. Overall, McGuinness et al.'s findings suggest that kidneys exhibiting DGF suffer from an impaired ability to restore physiological homeostasis in response to stress that is commensurate to their biological age and associated allostatic load. This outcome is reflected in changes in the epigenome and transcriptome, as well as in the dysregulation of RNA metabolism [3].

### 3.2.2. Proteomics

Proteomics approaches have also been used to identify donor biomarkers that may predict graft dysfunction in order to alleviate organ shortages and address the lack of representative methods for assessing graft quality. To date, several studies have focused on identifying novel proteomic biomarkers of graft quality in donor urine [74–77]. Koo et al.'s study aimed to investigate the viability of using the levels of neutrophil gelatinase-associated lipocalin (NGAL), kidney injury molecule-1 (KIM-1), and L-type fatty acid binding protein (L-FABP) in donor urine samples to predict reduced graft function (RGF). In addition, Koo et al., also created a prediction model of early graft dysfunction based on these donor biomarkers. This model, which includes donor urinary NGAL, L-FABP, and serum CR, has been shown to provide better predictive value for RGF than donor serum CR alone. Based on this model, a nomogram for a scoring method to predict RGF was created to help guide the allocation of DD and maximize organ utilization [74]. On the other hand, another large prospective study has shown that donor injury biomarkers such as microalbumin, NGAL, KIM-1, IL-18, and L-FABP have limited utility in predicting outcomes among kidney transplant recipients [75]. This study evaluated the associations between injury biomarkers in the urine of DD and donor AKI, recipient DGF, and recipient six-month eGFR. Each of the tested biomarkers was strongly associated with donor AKI in the adjusted analyses. However, although the levels of all five donor biomarkers were higher in

recipients with DGF than in those without DGF, the fully adjusted analyses revealed an association between higher donor urinary NGAL concentrations and a modest increase in the relative risk of recipient DGF. Moreover, the results of this study indicated that donor urinary biomarkers add minimal value in predicting recipient allograft function at six months post-transplantation [75]. In both studies, the tested biomarkers were strongly associated with donor AKI, while NGAL concentration was associated with DGF. A potential explanation for the different conclusions of these studies may be that Koo et al., used RGF as an outcome in their study, while Reese et al., used DGF due to different donor characteristics. Furthermore, it is worth emphasizing that, while these proteins are upregulated and secreted in urine in response to tubular injury, they were reported to have low specificity for tubular epithelial cell injury and were observed to increase in patients with urinary tract infections and sepsis [78,79].

In another study, the potential utility of C3a and C5a in DD urine samples as biomarkers for early post-transplant outcomes was investigated [76]. The results of this large, prospective, observational cohort study indicated a three-fold increase in C5a concentrations in urine samples from donors with stage 2 and 3 AKI compared to donors without AKI. In addition, donor C5a was positively correlated with the occurrence of DGF in recipients. In adjusted analyses, C5a remained independently correlated with recipient DGF only for donors without AKI. Moreover, the authors observed a tendency to indicate better 12-month organ functioning from donors with the lowest urinary C5a [76].

Monocyte chemoattractant protein-1 (MCP-1) has also been proposed as a potential biomarker of donor kidney quality. For example, Mansour et al., evaluated the association between graft outcomes and levels of MCP-1 in urine from DD at the time of organ procurement. In particular, they measured MCP-1 concentration to determine its correlation to donor AKI, recipient DGF, six-month estimated eGFR, and graft failure. Unfortunately, Mansour et al.'s results suggested that urinary MCP-1 has minimal clinical utility. Although median urinary MCP-1 concentrations were elevated in donors with AKI compared to those without AKI, higher MCP-1 levels were independently associated with a higher six-month eGFR in those without DGF. However, MCP-1 was not independently associated with DGF, and no independent associations between MCP-1 and graft failure were observed over a median follow-up of ~two years [77].

Recently, Braun et al., demonstrated the potential of using small urinary extracellular vesicles (suEVs) as a non-invasive source of data regarding early molecular processes in transplant biology. Their unbiased proteomic analysis revealed temporal patterns in the signature of suEV proteins, as well as cellular processes involved in both early response and longer-term graft adaptation. In addition, a subsequent correlative analysis identified potential prognostic markers of future graft function, such as phosphoenol pyruvate carboxykinase (PCK2). However, while Braun et al.'s study showed the potential of suEVs as biomarkers, the small number of patients in their sample did not allow for a conclusive statement on the predictive value of suEV PCK2. Therefore, the potential use of this biomarker will depend on larger trials in the future [80].

Studies focusing on the use of kidney tissue as a sample matrix to evaluate donor organ quality have also been performed. Using a rabbit model of brain death (BD), Li et al., employed two-dimensional gel electrophoresis and Matrix Assisted Laser Desorption/Ionization Time-of-Flight Mass Spectrometry (MALDI-TOF-MS)-based comparative proteomic analysis to profile the differentially-expressed proteins between BD and renal tissue collected from a control group. The authors were able to acquire five downregulated proteins and five upregulated proteins, which were then classified according to their function, including their association with proliferation and differentiation, signal transduction, protein modification, electron transport chain, and oxidation-reduction. Moreover, immunohistochemical analysis indicated that the expression of prohibitin (PHB) gradually elevated in a time-dependent manner. These data showed alterations in the levels of certain proteins in the organs from the BD group, even in the case of non-obvious functional and morphological changes. Given their results, Li et al., suggested that PHB may

be an innovative biomarker for the primary assessment of the quality of kidneys from BD donors [81].

Conversely, van Erp et al., used a multi-omics approach and a rat model to investigate organ-specific responses in the kidneys and liver during BD. The application of proteomics analysis enabled them to quantify 50 proteins involved in oxidative phosphorylation, tricarboxylic acid (TCA) cycle, fatty acid oxidation (FAO), substrate transport, and several antioxidant enzymes in isolated hepatic and renal mitochondria. The most relevant changes were observed in the reduced peptide levels in the kidneys, which were related to complex I (Ndufs1), the TCA cycle (Aco2, Fh, and Suc1g2), FAO (Hadhb), and the connection between FAO and the electron transport chain (Etfdh). The expression of two renal proteins, which were associated with substrate transport (Ucp2) and the TCA cycle (Dlat), was significantly increased in samples from the BD group compared to the sham-operated group. Interestingly, van Erp et al.'s findings showed that BD pathophysiology affects systemic metabolic processes, alongside organ-explicit metabolic changes, manifest in the kidneys by metabolic shutdown and suffering from oxidative stress, and a shift to anaerobic energy production, while kidney perfusion decreases. Ultimately, van Erp et al., concluded that an organ-specific strategy focusing on metabolic changes and graft perfusion should be part of novel procedures for assessing graft quality in organs from brain-dead donor, and may be the key to improving transplantation outcomes [82].

The vast majority of studies focusing on IRI have used animal models. In one proteo-metabolomics study using rat models, coagulation, complement pathways, and fatty acid (FA) signaling were observed following the elevation of proteins belonging to acute phase response due to IRI. Moreover, after 4 h of reperfusion, analysis of metabolic changes showed an increase in glycolysis, lipids, and FAs, while mitochondrial function and adenosine triphosphate (ATP) production were impaired after 24 h [83]. The authors of another study that used a porcine model of IRI found that integrative proteome analysis can provide a panel of potential—and predominantly renal—biomarkers at many levels, as changes occurring in the tissue are reflected in serum and urine protein profiles. This conclusion was based on the use of urine, serum, and renal cortex samples. In the renal cortex proteome, the authors observed an elevation in the synthesis of proteins in the ischemic kidney (vs. the contralateral kidney), which was highlighted by transcription factors and epithelial adherens junction proteins. Intersecting the set of proteins up- or downregulated in the ischemic tissue with both serum and urine proteomes, authors identified six proteins in the serum that may provide a set of targets of kidney injury. In addition, four urinary proteins with predominantly renal gene expression were also identified: aromatic-L-amino-acid decarboxylase (AADC), S-methylmethionine–homocysteine S-methyltransferase BHMT2 (BHMT2), cytosolic beta-glucosidase (GBA3), and dipeptidyl peptidase IV (DPP4) [84]. Recent research by Moser et al., has examined kidney preservation injury and the nephro-protective activity of doxycycline (Doxy). In this work, rat kidneys were cold perfused with and without Doxy for 22 h, followed by the extraction of proteins from the renal tissue. Subsequent analysis showed a significant difference in eight enzymes involved in cellular and mitochondrial metabolism. Interestingly, the levels of N(G),N(G)-dimethylarginine dimethylaminohydrolase and phosphoglycerate kinase 1 decreased during cold perfusion on its own but increased during cold perfusion with Doxy [85]. The influence of perfusion type on graft quality has also been evaluated by Weissenbacher et al., who applied proteomics analysis to determine the differences between normothermally perfused (normothermic machine perfusion, NMP) human kidneys with urine recirculation (URC) and urine replacement (UR). Their findings revealed that damage-associated patterns in the kidney tissue decreased after 6 h of NMP with URC, suggesting decreased inflammation. Furthermore, they also observed that vasoconstriction in the kidneys was also attenuated with URC, as indicated by a reduction in angiotensinogen levels. The kidneys became metabolically active during NMP, which could be improved and prolonged by applying URC. The application of URC also enhanced mitochondrial succinate dehydrogenase enzyme levels and carbonic anhydrase, which contributed to pH stabilization. Key enzymes

involved in glucose metabolism increased after 12 and 24 h of NMP with URC, including mitochondrial malate dehydrogenase and glutamic-oxaloacetic transaminase, predominantly in DCD tissue. The authors concluded that NMP with URC can prolong organ preservation and revitalize metabolism to possibly better mitigate IRI in discarded kidneys [86].

Ischemic injury may result in DGF, which is associated with a more complicated post-operative course, including a higher risk of AR [87]. Therefore, the early evaluation of kidney function following transplantation is essential for predicting graft outcomes [88]. Several studies have applied proteomic analysis to recipient urine samples in an attempt to identify protein biomarkers of DGF [87–89]. For instance, Lacquaniti et al., evaluated the usefulness of NGAL levels both for the early detection of DGF and as a long-term predictor of graft outcome. Their findings revealed that serum and urine samples from DGF patients contained high levels of NGAL beginning the first day after transplantation. Moreover, in patients who had received a kidney from a living related donor with excellent allograft function, NGAL concentrations lowered quickly during the first 24 h post-transplant period, reflecting a more pronounced reversible short-term injury. Importantly, NGAL levels in urine provided a better diagnostic profile than serum NGAL. Hence, urinary biomarkers on day 1 post-transplant may not only be useful in predicting who will need dialysis within one week, but they may also allow clinicians to discriminate between more subtle allograft recovery patterns [88]. However, as mentioned above, NGAL is characterized by low specificity; hence, its clinical application is limited due to inconclusive results [78,79]. Williams et al., used a Targeted Urine Proteome Assay (TUPA) to identify biomarkers of DGF following kidney transplantation. After employing data quality consideration and rigorous statistical analysis, they identified a panel of the top 4 protein biomarkers, including the C4b-binding protein alpha chain, serum amyloid P-component, guanylin, and immunoglobulin superfamily member 8, which had an AUC of 0.891, a specificity of 82.6%, and a sensitivity of 77.4% [87]. Similarly, urinary tissue inhibitor of metalloproteinases-2 (TIMP-2) and insulin-like growth factor binding protein-7 (IGFBP7) have been evaluated as biomarkers for DGF [89]. The findings of these studies indicated that TIMP-2 was able to adequately identify patients with DGF and prolonged DGF (AUC 0.89 and 0.77, respectively), whereas IGFBP7 was not. Moreover, correcting TIMP-2 for urine osmolality improved predictability (AUC 0.91 for DGF, AUC 0.80 for prolonged DGF), and 24-h urinary CR excretion and TIMP-2/mOsm were found to be significant predictors of DGF, with an AUC of 0.90. Hence, the obtained results indicated that TIMP-2 might be a promising, non-invasive indicator for predicting the occurrence and duration of DGF in individual patients [89].

### 3.2.3. Metabolomics and Lipidomics

In the absence of good quantitative biomarkers correlating to pre-transplantation organ quality, van Erp et al., examined metabolic alterations during BD using hyperpolarized magnetic resonance (MR) spectroscopy and ex vivo graft glucose metabolism during normothermic isolated perfused kidney (IPK) machine perfusion [90]. To this end, they employed hyperpolarized  $^{13}\text{C}$ -labeled pyruvate MR spectroscopy to quantify pyruvate metabolism in the kidneys and liver at three time points during BD in a rat model. Following BD, glucose oxidation was measured using tritium-labeled glucose ( $\text{D-6-3H-glucose}$ ) during IPK reperfusion. In addition, enriched  $^{13}\text{C}$ -pyruvate was injected repetitively to evaluate the metabolic profile at  $T = 0$ ,  $T = 2$ , and  $T = 4$  h via the relative conversion of pyruvate into lactate, alanine, and bicarbonate. The rats showed significantly higher lactate levels immediately following the induction of BD, with alanine production decreasing in the kidneys 4 h post-BD. However, it should be emphasized that this study's results did not assess whether these metabolic alterations can be associated with graft quality, or if they are suitable predictors of transplant outcome [90].

Another study using a rodent model of IRI examined the potential of using Hyperpolarized  $^{13}\text{C}$ -labeled pyruvate to evaluate the metabolic profile directly in the kidneys [91]. The in vivo responses observed at 24 h and 7 d following ischemic injury demonstrated a

similar trend towards a general decrease in the overall metabolism in the ischemic kidney and a compensatory increase in anaerobic metabolism, which is evidenced by elevated lactate production, compared to aerobic metabolism. In addition, a correlation was found between the intra-renal metabolic profile 24 h after reperfusion and 7 d after injury induction, as well as a correlation with the plasma CR. As a result, the authors suggest that using hyperpolarized  $^{13}\text{C}$ -labeled pyruvate to identify the balance between anaerobic and aerobic metabolism has great future potential as a prognostic biomarker [91].

Increased lactate levels due to IRI were also observed in another study [92]. However, analysis of urine samples via nuclear magnetic resonance (NMR) spectroscopy showed higher levels of valine and alanine and decreased levels of metabolites such as trigonelline, succinate, 2-oxoisocaproate, and 1-methyl-nicotinamide following IRI, which was likely due to altered kidney function or metabolism [92].

A novel and minimally invasive metabolomic and lipidomic diagnostic protocol based on solid-phase microextraction (SPME) has been proposed to address the lack of representative methods of assessing graft quality [93,94]. The small size of the SPME probe allows the performance of chemical biopsy, which enables metabolites to be extracted directly from the kidney without any tissue collection. Furthermore, SPME's minimally invasive nature permits multiple analyses over time. For instance, ischemia-induced alterations in the metabolic profile of the kidneys and oxidative stress as a function of cold storage were observed in one study that used an animal model, with the most pronounced alterations being observed in the levels of essential amino acids and purine nucleosides [93]. However, more work is required to discriminate a set of characteristic compounds that could serve as biomarkers of graft quality and indicators of possible development of organ dysfunction.

In response to reports that the pharmacological inhibition of kynurenine 3-monooxygenase (KMO), and, separately, the transcriptional blockage of the *Kmo* gene, reduces 3-hydroxykynurenine formation and protects against secondary AKI, Zheng et al., investigated whether mice lacking functional KMO (*Kmo*<sup>null</sup> mice) are protected from AKI experimentally induced by the direct induction of renal IRI [95]. KMO plays a crucial role in kynurenine metabolism. Kynurenine metabolites are generated by tryptophan catabolism and are involved in the regulation of various biological processes, including host-microbiome signaling, immune cell response, and neuronal excitability. The kynurenine pathway diverges into two distinct branches, which are regulated by kynurenine aminotransferases (KATs) and KMO, respectively. KMO is the only route of 3-hydroxykynurenine production that is known to be injurious to cells and tissue. Kynurenine may also be metabolized into kynurenic acid by KATs and to anthranilic acid by kynureninase [95]. Following the experimental induction of AKI via renal IRI, Zheng et al., observed that the *Kmo*<sup>null</sup> mice had kept renal function, decreased renal tubular cell injury, and fewer infiltrating neutrophils than the wild-type control mice. Given these results, they suggested that KMO is a critical regulator of renal IRI. Moreover, higher levels of kynurenine and kynurenic acid were observed in the *Kmo*<sup>null</sup> IRI mice compared to the *Kmo*<sup>null</sup> sham-operated mice. This result may indicate that these metabolites help to protect against AKI after renal IRI, particularly because kynurenic acid has been demonstrated to have protective properties in other inflammatory situations due to its activity at glutamate receptors [95].

A 12.5-fold increase in the lysine catabolite saccharopine in IRI kidneys was observed in a recent study examining the differences between renal allograft acute cellular rejection (ACR) and IRI. The findings of this work indicated that the accumulation of saccharopine causes mitochondrial toxicity and may contribute to IRI pathophysiology. Moreover, similar to other reports, increased levels of itaconate and kynurenine were also observed in ACR kidneys. However, the detected changes in metabolites seemed to be unique for IRI and ACR, respectively, indicating that these two conditions have distinct tissue metabolomic signatures [96].

Several reports have also demonstrated that IRI can alter the lipidome. For example, Rao et al., evaluated lipid changes in an IRI mouse model using sequential window acqui-

sition of all theoretical spectra-mass spectrometry (SWATH-MS) lipidomics. Their findings indicated that four lipids increased significantly at 6 h after IRI: plasmalogen, phosphatidylcholine (PC) O-38:1 (O-18:0, 20:1), plasmalogen, and phosphatidylethanolamine (PE) O-42:3 (O-20:1, 22:2). As anticipated, statistically significant changes were observed in many more lipids at 24 h after IRI. Interestingly, elevated levels of PC O-38:1 persisted at 24 h post-IRI, while renal levels of PE O-42:3 decreased alongside all ether PEs detected by SWATH-MS at this later time point. Overall, the authors found that coupling SWATH-MS lipidomics with MALDI-IMS (Imaging Mass Spectrometry, IMS) for lipid localization provided a better understanding of the role played by lipids in the pathobiology of acute kidney injury [97].

Researchers have also tested whether oxidized phosphatidylcholine (OxPC) molecules are generated following renal IRI. Solati et al., identified fifty-five distinct OxPC molecules in rat kidneys following IRI, including various fragmented (aldehyde and carboxylic-acid-containing species) and nonfragmented products. Among these, 1-stearoyl-2-linoleoyl-phosphatidylcholine (SLPC-OH) and 1-palmitoyl-2-azelaoyl-sn-glycero-3-phosphocholine (PAzPC) were the most abundant after 6 h and 24 h IRI, respectively. The total number of fragmented aldehyde OxPC molecules was significantly elevated in the 6 h and 24 h IRI groups compared to the sham-operated group, while an increase in the level of fragmented carboxylic acid was observed in the 24 h group compared to the sham and 6 h groups. In addition, fragmented OxPC levels were found to be significantly correlated with CR levels [98].

In their recent paper, van Smaalen et al., introduced and employed an interesting new approach based on IMS to rapidly and accurately evaluate acute ischemia in kidney tissue from a porcine model. First, ischemic tissue damage was systematically evaluated by two pathologists; this was followed by the application of MALDI-IMS to study the spatial distributions and compositions of lipids in the same tissues. Whereas the histopathological analysis revealed no significant difference between the tested groups, the MALDI-IMS analysis provided detailed discrimination of severe and mild ischemia based on the differential expression of characteristic lipid-degradation products throughout the tissue. In particular, elevated levels of lysolipids, including lysocardiolipins, lysophosphatidylcholines, and lysophosphatidylinositol, were present after severe ischemia. This data shows IMS's potential for use in differentiating and identifying early ischemic injury molecular patterns, and as a future tool that can be deployed in kidney assessment [99].

Because ischemia and reperfusion are inevitable consequences of kidney transplantation, and because DGF is a manifestation of IRI, Wijermars et al., used kidney transplantation as a clinical model of IRI to evaluate the role of the hypoxanthine-xanthine oxidase (XO) axis in human IRI. The sample group for this study consisted of patients undergoing renal allograft transplantation ( $n = 40$ ), who were classified into three groups based on the duration of ischemia: short, intermediate, and prolonged. The results of the analysis confirmed the progressive accumulation of hypoxanthine during ischemia. However, differences in arteriovenous concentrations of UA and an *in situ* enzymography of XO did not indicate relevant XO activity in IRI kidney grafts. Moreover, renal malondialdehyde and isoprostane levels and allantoin formation were assessed during the reperfusion period to determine whether a putative association exists between hypoxanthine accumulation and renal oxidative stress. The absence of the release of these markers indicated the lack of an association between ischemic hypoxanthine accumulation and post-reperfusion oxidative stress. Based on these results, the authors suggest that the hypoxanthine-xanthine oxidase axis is not involved in the initial phase of clinical IRI [100]. In their clinical study, Kostidis et al., employed NMR spectroscopy to analyse the urinary metabolome of DCD transplant recipients at multiple time points in an attempt to identify markers that predict the prolonged duration of functional DGF [79]. To this end, urine samples were collected at 10, 42, 180, and 360 days post-transplantation. Their analysis revealed that samples collected on day 10 had a different profile than samples obtained at the other time points. At day 10, D-glucose, 2-aminobutyrate, valine, p-hydroxyhippurate,

fumarate, 2-ethylacrylate, leucine, and lactate were significantly elevated in patients with DGF compared to those without DGF, while asparagine, DMG, 3-hydroxyisobutyrate, 3-hydroxyisovalerate, 2-hydroxy-isobutyrate, and histidine were significantly reduced in the DGF group. Urine samples from patients with prolonged DGF ( $\geq 21$  days) showed increased levels of lactate and lower levels of pyroglutamate compared to participants with limited DGF ( $< 21$  days). Moreover, the ratios of all metabolites were analysed via logistic regression analysis in an attempt to further distinguish prolonged DGF from limited DGF. The results of this analysis showed that the combination of lactate/fumarate and branched chain amino acids (BCAA)/pyroglutamate provided the best outcome, predicting prolonged DGF with an AUC of 0.85. Given these results, the authors concluded that it is possible to identify kidney transplant recipients with DGF based on their altered urinary metabolome, and that it may also be possible to use these two ratios to predict prolonged DGF [79].

In another study, Lindeman et al., examined possible metabolic origins of clinical IRI by integrating data from 18 pre- and post-reperfusion tissue biopsies with 36 sequential arteriovenous blood samplings from grafts in three groups of subjects, including LD and DD grafts with and without DGF. The integration of metabolomics data enabled Lindeman et al., to determine a discriminatory profile that can be used to identify future DGF. This profile was characterized by impaired recovery of the high-energy phosphate-buffer, phosphocreatine, in DGF grafts post-reperfusion, as well as by persistent post-reperfusion ATP/GTP catabolism and significant ongoing tissue damage. The impaired recovery of high-energy phosphate occurred despite the activation of glycolysis, fatty acid oxidation, glutaminolysis, autophagia and was found to be related to a defect at the level of the oxoglutarate dehydrogenase complex in the Krebs cycle. Hence, Lindeman et al.'s findings suggest that DGF is preceded by a post-reperfusion metabolic collapse, leading to an inability to sustain the organ's energy requirements. Thus, efforts aimed at preventing DGF should aim to preserve or restore metabolic competence [101].

### 3.3. New Solutions in Perfusion Control

Organ-preservation technologies have been garnering significant interest for graft quality assessment, advanced organ monitoring, and treating transplanted kidneys during machine perfusion. As mentioned above, SCS and HMP are two of the more common methods of hypothermic preservation applied in clinical settings at present. In SCS, the kidney is submerged in a cold preservation fluid and placed on ice in an icebox; in HMP, a device pumps cold preservation fluid through the renal vasculature, which has been revealed to improve post-transplant outcomes [102]. NMP is another dynamic preservation strategy that involves the circulation of a perfusion solution through the kidney. The NMP conditions are designed to nearly replicate physiological conditions, which makes a real-life assessment of the graft possible prior to transplantation [103,104]. NMP has been recently translated into clinical practice, but this application is still at an experimental stage. However, early clinical results are promising [103,105]. Because preservation/perfusion solutions serve as a non-invasive source for the analysis of biomarkers, numerous studies have employed it for the purposes of graft quality assessment. In this section of this paper, we summarize the latest findings and studies that have used preservation/perfusion fluid and perfusion control in kidney transplantation (Table 1).

Coskun et al., used proteomic techniques to analyse the protein profiles of preservation fluid used in SCS kidneys. Their findings revealed significant correlations between protein levels and donor age (23 proteins), cold ischemia time (5 proteins), recipients' serum BUN (12 proteins), and CR levels (7 proteins). The identified proteins belonged to groups related to the structural constituent of the cytoskeleton, serine-type endopeptidase inhibitor activity, peptidase inhibitor activity, cellular component organization or biogenesis, and cellular component morphogenesis, among others [106]. In another proteomic study of preservation fluid, five potential biomarkers (leptin, periostin, granulocyte-macrophage colony-stimulating factor (GM-CSF), plasminogen activator inhibitor-1, and osteopontin)

were identified in a discovery panel for differentiating kidneys with immediate function from those with DGF. Further analysis yielded a prediction model based on leptin and GM-CSF. Receiver-operating characteristic analysis revealed an AUC of 0.87, and the addition of recipient BMI significantly increased the model's predictive power, resulting in an AUC of 0.89 [107]. The metabolomic study compared the level of metabolites in perfusate samples collected prior to transplantation, during static cold storage, and between the allografts exhibiting DGF and IGF, while an integrated NMR-based analysis revealed a significant elevation in  $\alpha$ -glucose and citrate levels, and significant decreases in taurine and betaine levels in the perfusate of DGF allografts [108].

In the last few years, several studies have documented the benefits of HMP over SCS, including improved short-term outcomes and reduced risk of DGF [109–111]. However, reports suggesting that HMP improves long-term graft function are inconclusive [102,111]. Some research groups have compared HMP with SCS to evaluate HMP's potential to improve kidney-graft outcomes [109,112] and to better understand the long-term benefits associated with its use [111,113]. At the same time, other groups have investigated how the use of oxygenated HMP impacts post-transplant outcomes, and how it can be used to further optimize kidney preservation, thereby expanding the number of organs available for transplant [102,114]. Furthermore, perfusion solution has been used in the search for useful biomarkers of graft quality and potential therapeutic targets. The analysis of perfusates from donor after brain death (DBD), DCD, and LD kidneys showed that DCD kidneys contained the highest levels of matrix metalloproteinase-2 (MMP-2), lactate dehydrogenase (LDH), and NGAL, followed by DBD and LD kidneys, respectively, suggesting a greater amount of injury in the DCD kidneys. Moreover, the DCD kidney perfusate contained significantly higher levels of protein compared to the DBD and LD perfusates, with quantitative analysis of the protein spots revealing significant differences between the groups in relation to seven spots: peroxiredoxin-2, FABP, A1AT, heavy chain of immunoglobulin, serum albumin, fragment of collagen 1, and protein deglycase (DJ-1) [115]. In another proteomic study, perfusate analysis of DBD kidneys preserved via HMP was performed to identify differences between the proteomic profiles of kidneys with good (GO) and suboptimal outcomes (SO) one-year post-transplantation. Analysis of samples collected 15 min after the start of HMP (T1) and before the termination of HMP (T2) indicated that the 100 most abundant proteins demonstrated discrimination between grafts, with a GO and SO at T1. Increased proteins were involved in classical complement cascades at both T1 and T2, while a decreased abundance of lipid metabolism at T1 and cytoskeletal proteins at T2 in GO (vs. SO) was also observed. Perfusate analysis at T1 revealed a predictive value of 91% for ATP-citrate synthase and fatty acid-binding protein 5, and analysis at T2 showed a predictive value of 86% for immunoglobulin heavy variable 2–26 and desmoplakin. In summary, HMP perfusate profiles for DBD kidneys can distinguish between outcomes one-year post-transplantation, providing a potential non-invasive method of assessing donor organ quality [2].

MicroRNAs in kidney machine perfusion solutions have also been considered as new biomarkers for graft function. For instance, Gómez dos Santos et al., conducted a prospective cohort study to investigate graft dysfunction in kidney transplantation from ECD. To this end, they employed a mean expression value approach, which confirmed the significance of a subset of the miRNAs previously identified with the development of delayed graft function, namely, miR-486-5p, miR-144-3p, miR-142-5p, and miR-144-5p. These results confirmed that perfusion fluid can be a valuable pre-transplantation source of organ-viability biomarkers [116].

In another study, Teichman et al., assessed oxidative stress markers from the hypothermic preservation of transplanted kidneys. In particular, they sought to analyse the activity of enzymes and levels of non-enzymatic compounds involved in antioxidant defense mechanisms. These compounds, which included glutathione (GSH), glutathione peroxidase (GPX), catalase (CAT), superoxide dismutase (SOD), glutathione reductase (GR), glutathione transferase (GST), thiobarbituric acid reactive substances (TBARS), malondi-

aldehyde (MDA), were measured in preservation solutions before the transplantation of human kidneys grafted from DBD. The study group was divided into two groups based on the method of kidney storage, with Group 1 consisting of HMP kidneys ( $n = 26$ ) and Group 2 consisting of SCS kidneys ( $n = 40$ ). There were aggregations of significant correlations between kidney function parameters after KTx and oxidative stress markers, namely: diuresis and CAT;  $\text{Na}^+$  and CAT;  $\text{K}^+$  and GPX; and urea and GR. Moreover, there were aggregations of correlations between recipient blood count and oxidative stress markers, including CAT and monocyte count; SOD and white blood cell count; and SOD and monocyte count. However, there was an issue of unequivocal interpretation because none of the observed aggregations constituted conditions that supported the authors' hypothesis that kidney function after KTx can be predicted based on oxidative stress markers measured during preservation. Moreover, it would be hard to conclude that the blood count alterations observed in the repeated measurements after KTx were unrelated to factors other than oxidative stress or acidosis. As the authors suggest, many other factors may modify blood count, including operative stress, bleeding, immunosuppression, and microaggregation [117].

Longchamp et al., presented an interesting and non-invasive method of assessing graft quality during perfusion based on the use of  $^{31}\text{P}$  pMRI spectroscopy to detect high-energy phosphate metabolites, such as ATP. Thus, pMRI can be used to predict the energy state of a kidney and its viability before transplantation. In addition, Longchamp et al., also performed gadolinium perfusion sequences, which allowed them to observe the internal distribution of the flow between the cortex and the medulla. pMRI showed that warm ischemia caused a reduction in ATP levels, but not its precursor, adenosine monophosphate (AMP). Moreover, they found that ATP levels and cortical and medullary gadolinium elimination were inversely correlated with the severity of kidney histological injury. Thus, the measured parameters may be considered as biomarkers of kidney injury after warm ischemia, and Longchamp et al.'s method provides an innovative non-invasive approach to assessing kidney viability prior to transplantation [118].

Other researchers have examined whether a correlation exists between the level of extracellular histones in machine perfusates and the viability of DD kidneys. Extracellular histone levels were significantly elevated in the perfusates of kidneys with post-transplant graft dysfunction, and they were considered an independent risk factor for DGF and one-year graft failure, but not for PNF. One-year graft survival was 12% higher in the low-histone-concentration group ( $p = 0.008$ ) compared to the higher-histone-concentration group. Hence, the quantitation of extracellular histones might contribute to the evaluation of post-transplant graft function and survival [119].

NMP is an emerging approach for donor organ preservation and functional improvements in kidney transplantation. However, methods for evaluating organs via NMP have yet to be developed, and the development of novel graft quality assessment solutions has only recently come into focus.

Kaths et al., used a porcine model to investigate whether NMP is suitable for graft quality assessment prior to transplantation. They found that intra-renal resistance was lowest in the HBD group and highest in the severely injured DCD group (60 min of warm ischemia), and that the initiation of NMP was correlated with post-operative renal function. Markers of acid-base homeostasis ( $\text{pH}$ ,  $\text{HCO}_3^-$ , base excess) correlated with post-transplantation renal function. Furthermore, concentrations of lactate and aspartate aminotransferase were lowest in perfusate from non-injured grafts (vs. DCD kidneys) and were correlated with post-transplantation kidney function. Kaths et al., found that perfusion characteristics and clinically available perfusate biomarkers during NMP were correlated with post-transplantation kidney graft injury and function. However, further research is needed to identify perfusion parameter thresholds for DGF and PNF [120].

HSI combined with NMP was introduced as a novel approach for monitoring physiological kidney parameters. The experimental results of an HSI-based oxygen-saturation calculation indicated that HSI is useful for monitoring oxygen saturation distribution

and identifying areas with a reduced oxygen supply prior to transplantation. Moreover, camera-based measurements are easy to integrate with a perfusion setup and allow the fast and non-invasive measurement of tissue characteristics [121]. Subsequent research has explored how to improve algorithms for determining kidney oxygen saturation [122]. Unfortunately, the application of HSI is limited by the propagating light's low penetration depth, which makes it impossible to detect deeper tissue injuries. However, based on the fact that most metabolic activity occurs in the kidney cortex, the combined use of HSI and NMP offers a promising and easy-to-use method for assessing the status of the organ and for chemical imaging [121,122].

Hyperpolarized MRI and spectroscopy (MRS) using pyruvate and other  $^{13}\text{C}$ -labeled molecules offers a novel approach to monitoring the state of ex vivo perfused kidneys. In one study, the state of a porcine kidney was quantified using acquired anatomical, functional, and metabolic data. The findings showed an apparent reduction in pyruvate turnover during renal metabolism compared with the typical in vivo levels observed in pigs, while perfusion and blood gas parameters were found to be in the normal ex vivo range. Mariager et al.'s findings demonstrate the applicability of these techniques for monitoring ex vivo graft metabolism and function in a large animal model that resembles human renal physiology [123].

In another study, researchers sought to investigate the link between the urinary biomarkers, endothelin-1 (ET-1), NGAL, and KIM-1, and NMP parameters in order to improve kidney assessment prior to transplantation. Fifty-six kidneys from DD were used in this work, with each kidney being subjected to 1 h of NMP, followed by assessment based on macroscopic examination, renal blood flow, and urine output. The levels of ET-1 and NGAL measured in the urine samples after 1 h of NMP were significantly associated with perfusion parameters during NMP. These biomarkers and NMP perfusion parameters were also significantly associated with terminal graft function in the donor. However, KIM-1 was not correlated with the perfusion parameters or the donor's renal function. Larger studies are required to determine the usefulness of using these biomarkers with NMP to predict transplant outcomes. Despite this limitation, this study undoubtedly demonstrates that measuring urinary biomarkers during NMP provides additional information about graft quality [124].

**Table 1.** Emerging trends in donor graft quality assessment techniques.

Application	Category	Model	Type of Sample	Main Conclusions	Author
Evaluation of gene expression profile of kidney submitted to ischemic injury	Donor graft quality	Pig	Tissue	<ul style="list-style-type: none"> <li>ischemia leads to the full reprogramming of the transcriptome of major pathways such those related to oxidative stress responses, cell reprogramming, cell-cycle, inflammation and cell metabolism</li> </ul>	Giraud et al. [55]
Investigation of the features of perirenal adipose tissue as an indicator of the detrimental impact of the ECD microenvironment on a renal transplant	Donor graft quality	Human	Perirenal adipose tissue	<ul style="list-style-type: none"> <li>↑ genes associated with the inflammatory response, cytokine secretion, and circulatory system development</li> <li>↓ genes associated with regulating metabolic processes and regulating the circulatory system development</li> </ul>	Boissier et al. [56]
Evaluation of donor category influence on borderline changes in kidney allografts by molecular fingerprints	Donor graft quality	Human	Tissue	<ul style="list-style-type: none"> <li>early borderline changes in ECD kidneys were characterized by the most increased regulation of inflammation, extracellular matrix remodeling, and AKI transcripts compared to SCD and LD groups</li> </ul>	Hruba et al. [57]

Table 1. Cont.

Application	Category	Model	Type of Sample	Main Conclusions	Author
Exploration of the association between plasma mtDNA levels and post-transplant renal allograft function	Donor graft quality	Human	Plasma	<ul style="list-style-type: none"> <li>plasma mtDNA may be a non-invasive predictor of DGF and allograft function at 6 months after transplantation, and it also correlates with allograft survival</li> <li>mtDNA may serve as a surrogate predictive marker for PNF</li> </ul>	Han et al. [58]
Searching for urinary miRs that can be a biomarker for AKI	IRI	<ul style="list-style-type: none"> <li>Mouse</li> <li>Human</li> </ul>	<ul style="list-style-type: none"> <li>Urine; Tissue</li> <li>Urine; Serum</li> </ul>	<ul style="list-style-type: none"> <li>urinary miR-16 may serve as a valuable indicator for AKI patients</li> </ul>	Chen et al. [59]
Determination of the role of miR-17-92 in IRI-induced AKI	IRI	Mouse	Tissue	<ul style="list-style-type: none"> <li>overexpression of miR-17-92 may antagonize the side-effects of IRI on the proximal tubules in vivo</li> </ul>	Song et al. [61]
Investigation of the expression of renal miRNAs following renal IRI	IRI	Rat	Tissue	<ul style="list-style-type: none"> <li>↑ miR-27a downregulated the expression of TLR 4, which resulted in inhibition of inflammation, cell adhesion and cell death in IRI</li> </ul>	Wang et al. [62]
Identification of candidate genes involved in renal IRI	IRI	Mouse	Tissue	<ul style="list-style-type: none"> <li>IRI induces changes in the expression of SPRR2F, SPRR1A, MMP-10, <i>Malat1</i>, and <i>miR-139-5p</i> in the kidney, suggesting the utility of this panel as a biomarker of the renal IRI</li> </ul>	Su et al. [64]
Examination of a link between activation of IL-33 transcription by BRG1 in endothelial cells and renal IRI	IRI	Mouse	Tissue	<ul style="list-style-type: none"> <li>endothelial BRG1 deficiency alleviates renal inflammation following IRI in mice with a concomitant reduction in IL-33 levels</li> </ul>	Liu et al. [65]
Screening for differentially expressed genes in renal IR-injured mice using a high-throughput assay	IRI; DGF	<ul style="list-style-type: none"> <li>Mouse</li> <li>Human</li> </ul>	<ul style="list-style-type: none"> <li>Tissue, Serum</li> <li>Plasma</li> </ul>	<ul style="list-style-type: none"> <li>plasma Corin was downregulated in kidney transplantation recipients complicated with DGF</li> <li>Corin might be a potential biomarker that is associated with DGF of kidney transplantation</li> </ul>	Hu et al. [67]
Unbiased urinary microRNA profiling to identify DGF predictors after kidney transplantation.	DGF	Human	Urine	<ul style="list-style-type: none"> <li>combined measurement of six microRNAs (miR-9, miR-10a, miR-21, miR-29a, miR-221, miR-429) had predictive value for DGF following KT</li> </ul>	Khalid et al. [68]
High-throughput sequencing to expression profiling of exosomal miRNAs obtained from the peripheral blood of patients with DGF	DGF	Human	Plasma	<ul style="list-style-type: none"> <li>↑ hsa-miR-33a-5p R-1, hsa-miR-98-5p, hsa-miR-151a-5p in kidney recipients with DGF</li> </ul>	Wang et al. [69]
Examination of miR-146a-5p expression in kidney transplant recipients with DGF	DGF	Human	Tissue; Whole blood	<ul style="list-style-type: none"> <li>miR-146a-5p expression has a unique pattern in the renal tissue and perhaps in a blood sample in the presence of DGF</li> </ul>	Milhoransa et al. [71]
Evaluation of PBMC TLR4 expression of renal graft recipients with DGF	DGF	Human	Tissue; Whole blood	<ul style="list-style-type: none"> <li>low TLR4 expression in patients with DGF may be related to a poor prognosis for graft capability</li> <li>analysis of TLR4 expression change may be a valuable parameter for the evaluation of immunosuppression effectiveness</li> </ul>	Zmonarski et al. [72]

Table 1. Cont.

Application	Category	Model	Type of Sample	Main Conclusions	Author
Profiling of molecular changes associated with decreased resilience and impaired function of human renal allografts	DGF	Human	Tissue	<ul style="list-style-type: none"> <li>identified 42 transcripts associated with IFN<math>\gamma</math> signaling, which in allografts with DGF exhibited a greater magnitude of change in transcriptional amplitude and higher expression of noncoding RNAs and pseudogenes identified</li> </ul>	McGuinness et al. [3]
Searching for urinary biomarkers that predict reduced graft function after DD kidney transplantation	RGF	Human	Urine	<ul style="list-style-type: none"> <li>utility of donor urinary NGAL, KIM-1, L-FABP levels in predicting RGF</li> <li>the model including donor urinary NGAL, L-FABP, and serum CR showed a better predictive value for RGF than donor serum CR alone</li> </ul>	Koo et al. [74]
Evaluation of associations between DD urine injury biomarkers and kidney transplant outcomes	DGF	Human	Urine	<ul style="list-style-type: none"> <li>higher urinary NGAL and L-FABP levels correlated with slightly decreased 6-month eGFR only among patients without DGF</li> <li>donor urine injury biomarkers correlate with donor AKI but have poor predictive value for outcomes in kidney transplant recipients</li> </ul>	Reese et al. [75]
Assessment of C3a and C5a in urine samples as biomarkers for post-transplant outcomes	DGF	Human	Urine	<ul style="list-style-type: none"> <li>urinary C5a was associated with the degree of donor AKI</li> <li>in the absence of clinical donor AKI, donor urinary C5a concentrations associate with recipient DGF</li> </ul>	Schröppel et al. [76]
Assessment of urinary and perfusate concentrations of MCP-1 from kidneys on HMP as an organ function indicator	AKI; DGF	Human	Urine; Perfusate	<ul style="list-style-type: none"> <li>higher concentrations of uMCP-1 are independently associated with donor AKI</li> <li>donor uMCP-1 concentrations were modestly associated with higher recipient six-month eGFR in those without DGF</li> <li>donor uMCP-1 has low clinical utility due to the lack of correlation with graft failure</li> </ul>	Mansour et al. [77]
Evaluation of the proteome of suEVs and its changes throughout LD transplantation	Donor graft quality	Human	Urine; Tissue	<ul style="list-style-type: none"> <li>the abundance of PCK2 in the suEV proteome 24 h after transplantation may have a predictive value for overall kidney function one year after transplantation</li> </ul>	Braun et al. [80]
Proteomic study of differentially expressed proteins in BD rabbits kidneys	Donor graft quality	Rabbit	Tissue; Serum	<ul style="list-style-type: none"> <li>the results indicated alterations in levels of several proteins in the kidneys of those with BD, even if the primary function and the structural changes were not obvious</li> <li>PHB may be a novel biomarker for primary quality evaluation of kidneys from DBD</li> </ul>	Li et al. [81]
Investigation of the influence of BD on systemic and specifically hepatic and renal metabolism in a rodent BD model	Donor graft quality	Rat	Plasma; Urine; Tissue	<ul style="list-style-type: none"> <li>the kidneys undergo metabolic arrest and oxidative stress, turning to anaerobic energy generation as renal perfusion diminishes</li> </ul>	Van Erp et al. [82]

Table 1. Cont.

Application	Category	Model	Type of Sample	Main Conclusions	Author
Unbiased integrative proteo-metabolomic study in combination with mitochondrial function analysis of kidneys exposed to IRI to investigate its effects at the molecular level	IRI	Rat	Tissue	<ul style="list-style-type: none"> <li>proteins belonging to the acute phase response, coagulation and complement pathways, and FA signaling were elevated after IRI</li> <li>metabolic changes showed increased glycolysis, lipids, and FAs after 4 h reperfusion</li> <li>mitochondrial function and ATP production were impaired after 24 h</li> </ul>	Huang et al. [83]
Integrative proteome analysis of potential and predominantly renal injury biomarkers considering changes occurring in the tissue and echo in serum and urine protein profiles	IRI	Pig	Serum; Urine; Tissue	<ul style="list-style-type: none"> <li>four urinary proteins with primarily renal gene expression were changed in response to managed kidney IRI and may be biomarkers of kidney dysfunction: aromatic-L-amino-acid decarboxylase (AADAC), S-methylmethionine-homocysteine S-methyltransferase BHMT2 (BHMT2), cytosolic beta-glucosidase (GBA3), and dipeptidyl peptidase IV (DPPIV)</li> </ul>	Malagrino et al. [84]
Evaluation of the changes in the proteome of kidney subjected to ischemia during machine cold perfusion with doxycycline	IRI	Rat	Tissue; Perfusate	<ul style="list-style-type: none"> <li>analysis showed a significant difference in 8 enzymes, all involved in cellular and mitochondrial metabolism</li> <li>N(G),N(G)-dimethylarginine dimethylaminohydrolase and phosphoglycerate kinase 1 were decreased by cold perfusion, and perfusion with Doxy led to an increase in their levels</li> </ul>	Moser et al. [85]
Proteomics analysis determinating the molecular differences between NMP human kidneys with URC and UR	IRI	Human	Tissue	<ul style="list-style-type: none"> <li>NMP with URC permits prolonged preservation and revitalizes metabolism to possibly better cope with IRI in discarded kidneys</li> </ul>	Weissenbacher et al. [86]
TUPA to identify protein biomarkers of delayed recovery following KTx	DGF	Human	Urine	<ul style="list-style-type: none"> <li>C4b-binding protein alpha chain, serum amyloid P-component, Guanylin, and Immunoglobulin Super-Family Member 8 were identified that together distinguished DGF with a sensitivity of 77.4%, specificity of 82.6%</li> </ul>	Williams et al. [87]
Assessment of the diagnostic and prognostic role of NGAL in DGF and chronic allograft nephropathy	DGF	Human	Serum; Urine	<ul style="list-style-type: none"> <li>high levels of NGAL characterized DGF patients since the first day after transplantation in urine and serum</li> <li>urine NGAL presented a better diagnostic profile than serum NGAL</li> </ul>	Lacquaniti et al. [88]
Investigation of changes of urinary TIMP-2 and IGFBP7 in the first days after KTx and their diagnostic utility for predicting DGF outcomes	DGF	Human	Urine	<ul style="list-style-type: none"> <li>urinary TIMP-2, but not IGFBP7, is a potential biomarker to predict the occurrence and duration of DGF in DCD kidney transplant recipients</li> </ul>	Bank et al. [89]

Table 1. Cont.

Application	Category	Model	Type of Sample	Main Conclusions	Author
Investigation of organ-specific metabolic profiles of the liver and kidney during BD and afterwards during NMP of the kidney	Donor graft quality	Rat	Tissue; Plasma; Urine	<ul style="list-style-type: none"> <li>immediately following BD induction, BD animals demonstrated significantly increased lactate levels, and after 4 h of BD, alanine production decreased in the kidney</li> <li>during IPK perfusion, renal glucose oxidation was decreased following BD vs sham animals</li> </ul>	van Erp et al. [90]
Investigation of the acute and prolonged metabolic consequences associated with IRI, and elucidation whether the early injury mediated metabolic reprogramming can predict the outcome of the injury	IRI	Rat	Tissue; Plasma	<ul style="list-style-type: none"> <li>significant correlation between the intra-renal metabolic profile 24 h after reperfusion and 7 d after injury induction</li> <li>identifying the balance between the anaerobic and aerobic metabolism with the use of hyperpolarized <sup>13</sup>C-labeled pyruvate has a great potential to be used in the future as a prognostic biomarker</li> </ul>	Nielsen et al. [91]
NMR identification of metabolic alterations to the kidney following IRI	IRI	Mouse	Urine; Serum; Tissue	<ul style="list-style-type: none"> <li>higher levels of valine and alanine and decreased metabolites such as trigonelline, succinate, 2-oxoisocaproate, and 1-methyl-nicotinamide were found in urine following IRI due to altered kidney function or metabolism</li> </ul>	Chihanga et al. [92]
Monitoring of the effect of oxidative stress and ischemia on the condition of kidneys using SPME-LC-HRMS platform	Organ ischemia	Rabbit	Tissue	<ul style="list-style-type: none"> <li>pronounced alterations in metabolic profile in kidneys induced by ischemia and oxidative stress as a cold storage function were reflected in levels of essential amino acids and purine nucleosides</li> </ul>	Stryjak et al. [93]
Assessment of the role of kynurenine 3-monooxygenase as an essential regulator of renal IRI	IRI	Mouse	Plasma; Urine; Tissue	<ul style="list-style-type: none"> <li>KMO is highly expressed in the kidney and exerts major metabolic control over the biologically active kynurenine metabolites 3-hydroxykynurenine, kynurenine acid, and downstream metabolites</li> <li>mice lacking functional KMO kept renal function, decreased renal tubular cell injury, and fewer infiltrating neutrophils compared with control mice</li> </ul>	Zheng et al. [95]
Unbiased tissue metabolomic profiling of IRI and ACR in murine models to identify novel biomarkers and to provide a better understanding of the pathophysiology	IRI; ACR	Mouse	Tissue	<ul style="list-style-type: none"> <li>the lysine catabolite saccharopine 12.5-fold was increased in IRI kidneys and caused mitochondrial toxicity</li> <li>itaconate and kynurenine increased levels were found in ACR kidneys</li> </ul>	Beier et al. [96]

Table 1. Cont.

Application	Category	Model	Type of Sample	Main Conclusions	Author
Detection of early lipid changes in AKI using SWATH lipidomics coupled with MALDI tissue imaging	IRI	Mouse	Tissue	<ul style="list-style-type: none"> <li>increase in plasmalogen choline, phosphatidylcholine (PC) O-38:1 (O-18:0, 20:1), plasmalogen, and phosphatidylethanolamine (PE) O-42:3 (O-20:1, 22:2) concentrations at 6 h after IRI</li> <li>PC O-38:1 elevations were maintained at 24 h post-IR, while renal PE O-42:3 levels reduced, as were all other PEs detected by SWATH-MS at this later time point</li> </ul>	Rao et al. [97]
Determination of the individual OxPC molecules generated during renal IRI	IRI	Rat	Tissue	<ul style="list-style-type: none"> <li>SLPC-OH and PAzPC were the most abundant OxPC species after 6 h and 24 h IRI, respectively</li> <li>total fragmented aldehyde OxPC were significantly elevated in IRI groups than sham groups</li> <li>fragmented carboxylic acid elevated in 24 h group compared with other groups</li> </ul>	Solati et al. [98]
Rapid identification of IRI in renal tissue by Mass-Spectrometry Imaging	IRI	Pig	Tissue	<ul style="list-style-type: none"> <li>MALDI-IMS provided of detailed discrimination of severe and mild ischemia by differential expression of characteristic lipid-degradation products throughout the tissue</li> <li>lysolipids, including lysocardiolipins, lysophosphatidylcholines, and lysophosphatidylinositol were elevated after severe ischemia</li> </ul>	Van Smaalen et al. [99]
Evaluation of the involvement of the hypoxanthine-XO axis in the IRI that occurs during kidney transplantation	IRI	Human	Plasma; Tissue	<ul style="list-style-type: none"> <li>arteriovenous concentration differences of UA and in situ enzymography of XO did not indicate significant XO activity in IRI kidney grafts</li> <li>absent release of malondialdehyde, isoprostane and allantoin is not consistent with an association between ischemic hypoxanthine accumulation and postreperfusion oxidative stress</li> </ul>	Wijermars et al. [100]
Prediction of prolonged duration of DGF in DCD kidney transplant recipients by urinary metabolites profiling	DGF	Human	Urine	<ul style="list-style-type: none"> <li>the metabolites associated with prolonged DGF are handled by proximal tubular epithelial cells and reflect tubular (dys)function</li> <li>lactate/fumarate and BCAAs/pyroglutamate ratios were useful to predict prolonged duration of DGF</li> </ul>	Kostidis et al. [79]
Explorative metabolic assessment based on an integrated, time-resolved strategy involving sequential evaluation of AV differences over reperfused grafts and parallel profiling of graft biopsies	DGF	Human	Tissue; Plasma	<ul style="list-style-type: none"> <li>DGF is preceded by a post-reperfusion metabolic collapse, leading to an inability to sustain the organ's energy requirements</li> </ul>	Lindeman et al. [101]

Table 1. Cont.

Application	Category	Model	Type of Sample	Main Conclusions	Author
Analysis of the proteins and peptides that are passed from the kidneys to the preservation fluid during organ preservation	Perfusion control	Human	Preservation fluid	<ul style="list-style-type: none"> <li>the relevant correlations between the levels of proteins and donors' age (23 proteins), cold ischemia time (5), recipients' serum BUN (12), and CR (7) levels were observed</li> <li>identified proteins belonged to groups related to the structural constituent of the cytoskeleton, serine-type endopeptidase inhibitor activity, peptidase inhibitor activity, cellular component organization or biogenesis, and cellular component morphogenesis</li> </ul>	Coskun et al. [106]
Searching for proteins accumulating in preservation solutions during SCS as biomarkers to predict posttransplantation graft function	Perfusion control	Human	Preservation fluid	<ul style="list-style-type: none"> <li>five potential biomarkers (leptin, periostin, GM-CSF, plasminogen activator inhibitor-1, and osteopontin) were identified in a discovery panel, differentiating kidneys with IGF versus DGF</li> <li>prediction model based on leptin and GM-CSF and recipient BMI showed an AUC of 0.89</li> </ul>	van Balkom et al. [107]
Analysis of perfusates during SCS to obtain the metabolite profiles of DGF and IGF allografts	Perfusion control	Human	Preservation fluid	<ul style="list-style-type: none"> <li>significant elevation in <math>\alpha</math>-glucose and citrate levels and significant decreases in taurine and betaine levels in the perfusate of DGF allografts</li> </ul>	Wang et al. [108]
Proteomic study of perfusate from HMP of transplant kidneys	Perfusion control	Human	Perfusate	<ul style="list-style-type: none"> <li>the highest levels of MMP-2, LDH, and NGAL were seen for the DCD kidneys, followed by the DBD kidneys and then LD</li> <li>total protein in the perfusate from DCD was significantly increased than that in the perfusate from other donors</li> </ul>	Moser et al. [115]
Proteomic perfusate analysis of DBD kidneys preserved using HMP to identify the differences between proteomic profiles of kidneys with a good and suboptimal outcome	Perfusion control	Human	Perfusate	<ul style="list-style-type: none"> <li>DBD kidney HMP perfusate profiles can distinguish between outcome one year after transplantation</li> <li>increased proteins involved in classical complement cascades and a decreased levels of lipid metabolism at T1 and cytoskeletal proteins at T2 in GO versus SO were observed</li> </ul>	van Leeuwen et al. [2]
Evaluation of miRNAs in kidney machine perfusion fluid as novel biomarkers for graft function	Perfusion control	Human	Perfusate	<ul style="list-style-type: none"> <li>confirmation of the significance of a subset of the miRNAs previously identified for DGF development and composed of miRNAs miR-486-5p, miR-144-3p, miR-142-5p, and miR-144-5p</li> </ul>	Gómez-Dos-Santos et al. [116]
Influence of method of kidney storage on oxidative stress and post-transplant kidney function parameters	Perfusion control	Human	Perfusate; Whole blood	<ul style="list-style-type: none"> <li>correlations between kidney function parameters after KTx and oxidative stress markers: diuresis or <math>\text{Na}^+</math> and CAT, <math>\text{K}^+</math> and GPX, urea and GR were found</li> </ul>	Tejchman et al. [117]

Table 1. Cont.

Application	Category	Model	Type of Sample	Main Conclusions	Author
Ex vivo evaluation of kidney graft viability during perfusion using $^{31}\text{P}$ MRI spectroscopy	Perfusion control	Pig	n.a.	<ul style="list-style-type: none"> <li>warm ischemia induced significant histological damages, delayed cortical and medullary Gadolinium elimination (perfusion), and decreased ATP levels, but not AMP</li> <li>ATP levels and kidney perfusion are both inversely linked to the degree of kidney histological damage</li> </ul>	Longchamp et al. [118]
Assessment of an association between the presence of extracellular histones in machine perfusates and deceased donor kidney viability	Perfusion control	Human	Perfusate	<ul style="list-style-type: none"> <li>extracellular histone concentrations were significantly higher in perfusates of kidneys with posttransplant graft dysfunction and were an independent risk factor for DGF and one-year graft failure, but not for primary nonfunction</li> </ul>	van Smaalen et al. [119]
Organ quality assessment during NMP	Perfusion control	Pig	Perfusate; Whole blood; Urine	<ul style="list-style-type: none"> <li>intra-renal resistance was lowest in the HBD group and highest in the severely injured DCD group and at the initiation of NMP correlated with postoperative renal function</li> <li>markers of acid-base homeostasis, lactate and aspartate aminotransferase perfusate concentrations were correlated with post-transplantation renal function</li> </ul>	Kaths et al. [120]
Hyperpolarized MRI and spectroscopy using pyruvate and other $^{13}\text{C}$ -labeled molecules as a novel tool for monitoring the state of ex vivo perfused kidneys	Perfusion control	Pig	n.a.	<ul style="list-style-type: none"> <li>renal metabolism displayed an apparent reduction in pyruvate turnover compared with pigs' usual in vivo levels</li> <li>perfusion and blood gas parameters were in the normal ex vivo range</li> </ul>	Mariager et al. [123]
Examination of the relationship between urinary biomarkers and NMP parameters in a series of human kidneys	Perfusion control	Human	Urine; Serum	<ul style="list-style-type: none"> <li>urinary ET-1 and NGAL assessed after 1 h of NMP were significantly associated with perfusion parameters during NMP and terminal renal function in the donor</li> <li>KIM-1 was not linked with perfusion parameters or donor's renal function</li> </ul>	Hosgood et al. [124]

↑—increase of expression; ↓—decrease of expression; n.a.—not applicable.

#### 4. Conclusions

New diagnostic solutions for accurately assessing renal graft quality are needed to improve the process for selecting suitable donors, more efficiently managing complications, and prolonging graft survival. Rapid advances in imaging, omics technology, and perfusion methods have led to the development of a wide range of new tools and biomarkers that could be applied to evaluate graft quality. Unfortunately, most of the methods mentioned in the review are based on animal models or require sophisticated technology with a long turn-around time to obtain the results, which significantly limits their potential for clinical use in the form of rapid commercial tests at present. However, non-invasive solutions, including imaging and the measurement of biomarkers in urine, blood, and perfusion fluid, appear to be promising with respect to their ability to be translated to a clinical setting. These studies include mtDNA and miRNAs determination based on commercially available kits

for the isolation of genetic material in combination with the RT-PCR technique widely used in laboratory practice. A similar clinical potential is demonstrated by the determination of biomarkers such as NGAL, KIM-1, L-FABP and C5a in urine by ELISA, also routinely used in diagnostics. Nevertheless, the translation of biomarkers from the discovery stage to clinical practice is still challenging due to the complex and multifactorial type of injuries, the absence of standard guidelines for method validation, and adequate prospective and retrospective cohort studies. Larger, multi-centre validation studies are needed before new solutions can be widely implemented in clinics. Moreover, it will be imperative for future research to explore new technologies and integrate molecular measurements from large data sets reported in different experiments.

**Author Contributions:** Writing—original draft preparation, N.W.; designing writing—review and editing, N.W., K.L., B.B.; funding acquisition, B.B. All authors have read and agreed to the published version of the manuscript.

**Funding:** This study was funded by National Science Centre, grant Opus number 2017/27/B/NZ5/01013.

**Data Availability Statement:** No new data were created or analyzed in this study. Data sharing is not applicable to this article.

**Conflicts of Interest:** The authors declare no conflict of interest.

## Abbreviations

ACR	acute cellular rejection
AKI	acute kidney injury
AMP	adenosine monophosphate
AR	acute rejection
ASL	arterial spin labelling
ATP	adenosine triphosphate
AUC	area under the curve
BCAA	branched chain amino acids
BD	brain death
BMI	body mass index
BUN	blood urea nitrogen
CAT	catalase
CR	creatinine
CTA	computed tomography
CTA	computed tomography angiography
DBD	donor after brain death
DCD	donor after cardiac death
DD	deceased donors
DEG	Differentially expressed genes
DGF	delayed graft function
DJ-1	protein deglycase
Doxy	doxycycline
ECD	expanded criteria donors
eGFR	estimated glomerular filtration rate
ET-1	endothelin-1
FA	fatty acid
FABP	fatty acid-binding protein
FAO	fatty acid oxidation
FC	fold change
FS	frozen section
GM-CSF	Granulocyte-macrophage colony-stimulating factor
GO	good outcome
GPX	glutathione peroxidase
GR	glutathione reductase

GSH	glutathione
GST	glutathione transferase
GTP	guanosine triphosphate
HMP	Hypothermic machine perfusion
HSI	Hyperspectral Imaging
ICG	indocyanine green
IGF	immediate graft function
IGFBP7	insulin-like growth factor binding protein-7
IL-18	Interleukin-18
IPK	normothermic isolated perfused kidney
IRI	ischemia-reperfusion injury
KATs	kynurenine aminotransferases
KDPI	Kidney Donor Profile Index
KDRI	Kidney Donor Risk Index
KIM-1	kidney injury molecule-1
KMO	kynurenine 3-monooxygenase
KTx	Kidney transplantation
LD	living donor
LDH	lactate dehydrogenase
LDKT	living donor kidney transplantation
L-FABP	L-type fatty acid binding protein
lncRNA	long noncoding RNA
MALDI-IMS	Matrix Assisted Laser Desorption/Ionization-Imaging Mass Spectrometry
MALDI-TOF-MS	Matrix Assisted Laser Desorption/Ionization Time-of-Flight Mass Spectrometry
MCP-1	Monocyte chemoattractant protein-1
MDA	malondialdehyde
miRNA/miR	microRNA
MMP-2	matrix metalloproteinase-2
MR	magnetic resonance
MRI	magnetic resonance imaging
MRS	magnetic resonance spectroscopy
MS	mass spectrometry
MSI	mass spectrometry imaging
mtDNA	mitochondrial DNA
NB	needle biopsy
NGAL	neutrophil gelatinase-associated lipocalin
NMP	normothermic machine perfusion
NMR	nuclear magnetic resonance
OxPC	oxidized phosphatidylcholine
PBMC	peripheral blood mononuclear cells
PC	phosphatidylcholine
PCK2	phosphoenol pyruvate carboxykinase
PE	phosphatidylethanolamine
PET	positron emission tomography
PHB	prohibitin
pMRI	<sup>31</sup> P magnetic resonance imaging
PNF	primary nonfunction
PRAT	perirenal adipose tissue
PS	paraffin sections
RGB	Red Green Blue (colour model)
RGF	reduced graft function
RR	renal resistance
RT-PCR	real-time polymerase chain reaction
SCD	standard criteria donors
SCS	Static cold storage
SO	suboptimal outcome
SOD	superoxide dismutase
SPME	solid-phase microextraction
suEVs	small urinary extracellular vesicles

SVF	stromal vascular fraction
SWATH-MS	sequential window acquisition of all theoretical spectra-mass spectrometry
TBARS	thiobarbituric acid reactive substances
TCA	tricarboxylic acid
TIMP-2	tissue inhibitor of metalloproteinases-2
TLR4	Toll-like receptor 4
TUPA	Targeted Urine Proteome Assay
UA	uric acid
UR	urine replacement
URC	urine recirculation
WB	wedge biopsy
WI	warm ischemia
WIT	warm ischemia time
XO	hypoxanthine-xanthine oxidase

## References

- Swanson, K.J.; Aziz, F.; Garg, N.; Mohamed, M.; Mandelbrot, D.; Djamali, A.; Parajuli, S. Role of novel biomarkers in kidney transplantation. *World J. Transplant.* **2020**, *10*, 230–255. [\[CrossRef\]](#)
- Van Leeuwen, L.L.; Sprakman, N.A.; Brat, A.; Huang, H.; Thorne, A.M.; Bonham, S.; van Balkom, B.W.M.; Ploeg, R.J.; Kessler, B.M.; Leuvenink, H.G.D. Proteomic analysis of machine perfusion solution from brain dead donor kidneys reveals that elevated complement, cytoskeleton and lipid metabolism proteins are associated with 1-year outcome. *Transpl. Int.* **2021**, *34*, 1618–1629. [\[CrossRef\]](#)
- McGuinness, D.; Mohammed, S.; Monaghan, L.; Wilson, P.A.; Kingsmore, D.B.; Shapter, O.; Stevenson, K.S.; Coley, S.M.; Devey, L.; Kirkpatrick, R.B.; et al. A molecular signature for delayed graft function. *Aging Cell* **2018**, *17*, e12825. [\[CrossRef\]](#)
- Dare, A.J.; Pettigrew, G.J.; Saeb-parsy, K. Preoperative Assessment of the Deceased-Donor Kidney: From Macroscopic Appearance to Molecular Biomarkers. *Transplantation* **2014**, *97*, 797–807. [\[CrossRef\]](#)
- Moeckli, B.; Sun, P.; Lazeyras, F.; Morel, P.; Moll, S.; Pascual, M.; Bühler, L.H. Evaluation of donor kidneys prior to transplantation: An update of current and emerging methods. *Transpl. Int.* **2019**, *32*, 459–469. [\[CrossRef\]](#) [\[PubMed\]](#)
- Kork, F.; Rimek, A.; Andert, A.; Becker, N.J.; Heidenhain, C.; Neumann, U.P.; Kroy, D.; Roehl, A.B.; Rossaint, R.; Hein, M. Visual quality assessment of the liver graft by the transplanting surgeon predicts postreperfusion syndrome after liver transplantation: A retrospective cohort study. *BMC Anesthesiol.* **2018**, *18*, 29. [\[CrossRef\]](#) [\[PubMed\]](#)
- Nyberg, S.L.; Matas, A.J.; Kremers, W.K.; Thostenson, J.D.; Larson, T.S.; Prieto, M.; Ishitani, M.B.; Sterioff, S.; Stegall, M.D. Improved scoring system to assess adult donors for cadaver renal transplantation. *Am. J. Transplant.* **2003**, *3*, 715–721. [\[CrossRef\]](#) [\[PubMed\]](#)
- Schold, J.D.; Kaplan, B.; Baliga, R.S.; Meier-Kriesche, H.-U. The broad spectrum of quality in deceased donor kidneys. *Am. J. Transplant.* **2005**, *5*, 757–765. [\[CrossRef\]](#) [\[PubMed\]](#)
- Watson, C.J.E.; Johnson, R.J.; Birch, R.; Collett, D.; Bradley, J.A. A simplified donor risk index for predicting outcome after deceased donor kidney transplantation. *Transplantation* **2012**, *93*, 314–318. [\[CrossRef\]](#) [\[PubMed\]](#)
- Rao, P.S.; Schaubel, D.E.; Guidinger, M.K.; Andreoni, K.A.; Wolfe, R.A.; Merion, R.M.; Port, F.K.; Sung, R.S. A comprehensive risk quantification score for deceased donor kidneys: The kidney donor risk index. *Transplantation* **2009**, *88*, 231–236. [\[CrossRef\]](#)
- U.S. Department of Health and Human Services. Organ Procurement and Transplantation Network: KDPI Calculator. Available online: <https://optn.transplant.hrsa.gov/resources/guidance/kidney-donor-profile-index-kdpi-guide-for-clinicians> (accessed on 9 November 2021).
- Dahmen, M.; Becker, F.; Pavenstädt, H.; Suwelack, B.; Schütte-Nütgen, K.; Reuter, S. Validation of the Kidney Donor Profile Index (KDPI) to assess a deceased donor's kidneys' outcome in a European cohort. *Sci. Rep.* **2019**, *9*, 11234. [\[CrossRef\]](#)
- Jun, H.; Yoon, H.E.; Lee, K.W.; Lee, D.R.; Yang, J.; Ahn, C.; Han, S.Y. Kidney Donor Risk Index Score Is More Reliable Than Kidney Donor Profile Index in Kidney Transplantation From Elderly Deceased Donors. *Transplant. Proc.* **2020**, *52*, 1744–1748. [\[CrossRef\]](#)
- Zheng, J.; Hu, X.; Ding, X.; Li, Y.; Ding, C.; Tian, P.; Xiang, H.; Feng, X.; Pan, X.; Yan, H.; et al. Comprehensive assessment of deceased donor kidneys with clinic al characteristics, pre-implant biopsy histopathology and hypothermic mechanical perfusion parameters is highly predictive of delayed graft function. *Ren. Fail.* **2020**, *42*, 369–376. [\[CrossRef\]](#) [\[PubMed\]](#)
- Parker, W.F.; Thistlethwaite, J.R., Jr.; Ross, L.F. Kidney Donor Profile Index (KDPI) Does Not Accurately Predict the Graft Survival of Pediatric Deceased Donor Kidneys. *Transplantation* **2016**, *100*, 2471–2478. [\[CrossRef\]](#)
- Hopfer, H.; Kemény, E. Assessment of donor biopsies. *Curr. Opin. Organ. Transplant.* **2013**, *18*, 306–312. [\[CrossRef\]](#) [\[PubMed\]](#)
- Naesens, M. Zero-time renal transplant biopsies: A comprehensive review. *Transplantation* **2016**, *100*, 1425–1439. [\[CrossRef\]](#) [\[PubMed\]](#)
- Sagasta, A.; Sánchez-Escuredo, A.; Oppenheimer, F.; Paredes, D.; Musquera, M.; Campistol, J.M.; Solé, M. Pre-implantation analysis of kidney biopsies from expanded criteria donors: Testing the accuracy of frozen section technique and the adequacy of their assessment by on-call pathologists. *Transpl. Int.* **2016**, *29*, 234–240. [\[CrossRef\]](#) [\[PubMed\]](#)

19. Cooper, M.; Formica, R.; Friedewald, J.; Hirose, R.; O'Connor, K.; Mohan, S.; Schold, J.; Axelrod, D.; Pastan, S. Report of National Kidney Foundation Consensus Conference to Decrease Kidney Discards. *Clin. Transplant.* **2019**, *33*, e13419. [\[CrossRef\]](#)
20. Traynor, C.; Saeed, A.; O'Ceallaigh, E.; Elbadri, A.; O'Kelly, P.; de Freitas, D.G.; Dorman, A.M.; Conlon, P.J.; O'Seaghdha, C.M. Pre-transplant histology does not improve prediction of 5-year kidney allograft outcomes above and beyond clinical parameters. *Ren. Fail.* **2017**, *39*, 671–677. [\[CrossRef\]](#)
21. Yap, Y.T.; Ho, Q.Y.; Kee, T.; Ng, C.Y.; Chionh, C.Y. Impact of pre-transplant biopsy on 5-year outcomes of expanded criteria donor kidney transplantation. *Nephrology* **2021**, *26*, 70–77. [\[CrossRef\]](#)
22. De Vusser, K.; Lerut, E.; Kuypers, D.; Vanrenterghem, Y.; Jochmans, I.; Monbaliu, D.; Pirenne, J.; Naesens, M. The predictive value of kidney allograft baseline biopsies for long-term graft survival. *J. Am. Soc. Nephrol.* **2013**, *24*, 1913–1923. [\[CrossRef\]](#)
23. Phillips, B.L.; Kassimatis, T.; Atalar, K.; Wilkinson, H.; Kessaris, N.; Simmonds, N.; Hilton, R.; Horsfield, C.; Callaghan, C.J. Chronic histological changes in deceased donor kidneys at implantation do not predict graft survival: A single-centre retrospective analysis. *Transpl. Int.* **2019**, *32*, 523–534. [\[CrossRef\]](#)
24. Liapis, H.; Gaut, J.P.; Klein, C.; Bagnasco, S.; Kraus, E.; Farris III, A.B.; Honsova, E.; Perkowska-Ptasinska, A.; David, D.; Goldberg, J.; et al. Banff Histopathological Consensus Criteria for Preimplantation Kidney Biopsies. *Am. J. Transplant.* **2017**, *17*, 140–150. [\[CrossRef\]](#)
25. Hall, I.E.; Parikh, C.R.; Schröppel, B.; Weng, F.L.; Jia, Y.; Thiessen-Philbrook, H.; Reese, P.P.; Doshi, M.D. Procurement biopsy findings versus kidney donor risk index for predicting renal allograft survival. *Transplant. Direct* **2018**, *4*, e373. [\[CrossRef\]](#) [\[PubMed\]](#)
26. Peng, P.; Ding, Z.; He, Y.; Zhang, J.; Wang, X.; Yang, Z. Hypothermic Machine Perfusion Versus Static Cold Storage in Deceased Donor Kidney Transplantation: A Systematic Review and Meta-Analysis of Randomized Controlled Trials. *Artif. Organs* **2019**, *43*, 478–489. [\[CrossRef\]](#) [\[PubMed\]](#)
27. Peris, A.; Fulceri, G.E.; Lazzeri, C.; Bonizzoli, M.; Li Marzi, V.; Serni, S.; Ciraami, L.; Migliaccio, M.L. Delayed graft function and perfusion parameters of kidneys from uncontrolled donors after circulatory death. *Perfusion* **2021**, *36*, 299–304. [\[CrossRef\]](#)
28. Bissolati, M.; Gazzetta, P.G.; Caldara, R.; Guarneri, G.; Adamenko, O.; Giannone, F.; Mazza, M.; Maggi, G.; Tomanin, D.; Rosati, R.; et al. Renal Resistance Trend During Hypothermic Machine Perfusion Is More Predictive of Postoperative Outcome Than Biopsy Score: Preliminary Experience in 35 Consecutive Kidney Transplantations. *Artif. Organs* **2018**, *42*, 714–722. [\[CrossRef\]](#) [\[PubMed\]](#)
29. Moers, C.; Smits, J.M.; Maathuis, M.-H.J.; Treckmann, J.; van Gelder, F.; Napieralski, B.P.; van Kasterop-Kutz, M.; van der Heide, J.J.H.; Squifflet, J.-P.; van Heurn, E.; et al. Machine Perfusion or Cold Storage in Deceased-Donor Kidney Transplantation. *N. Engl. J. Med.* **2009**, *360*, 7–19. [\[CrossRef\]](#) [\[PubMed\]](#)
30. Lindell, S.L.; Muir, H.; Brassil, J.; Mangino, M.J. Hypothermic Machine Perfusion Preservation of the DCD Kidney: Machine Effects. *J. Transplant.* **2013**, *2013*, 802618. [\[CrossRef\]](#)
31. De Deken, J.; Kocabayoglu, P.; Moers, C. Hypothermic machine perfusion in kidney transplantation. *Curr. Opin. Organ. Transplant.* **2016**, *21*, 294–300. [\[CrossRef\]](#)
32. Jochmans, I.; Moers, C.; Smits, J.M.; Leuvenink, H.G.D.; Treckmann, J.; Paul, A.; Rahmel, A.; Squifflet, J.P.; van Heurn, E.; Monbaliu, D.; et al. The prognostic value of renal resistance during hypothermic machine perfusion of deceased donor kidneys. *Am. J. Transplant.* **2011**, *11*, 2214–2220. [\[CrossRef\]](#)
33. Mozes, M.F.; Skolek, R.B.; Korf, B.C. Use of perfusion parameters in predicting outcomes of machine-preserved kidneys. *Transplant. Proc.* **2005**, *37*, 350–351. [\[CrossRef\]](#)
34. Bunegin, L.; Tolstykh, G.P.; Gelineau, J.F.; Cosimi, A.B.; Anderson, L.M. Oxygen consumption during oxygenated hypothermic perfusion as a measure of donor organ viability. *ASAIO J.* **2013**, *59*, 427–432. [\[CrossRef\]](#) [\[PubMed\]](#)
35. Patel, S.K.; Pankewycz, O.G.; Nader, N.D.; Zachariah, M.; Kohli, R.; Laftavi, M.R. Prognostic utility of hypothermic machine perfusion in deceased donor renal transplantation. *Transplant. Proc.* **2012**, *44*, 2207–2212. [\[CrossRef\]](#) [\[PubMed\]](#)
36. Reticker, A.; Lichvar, A.; Walsh, M.; Gross, A.E.; Patel, S. The Significance and Impact of Screening Preservation Fluid Cultures in Renal Transplant Recipients. *Prog. Transplant.* **2021**, *31*, 40–46. [\[CrossRef\]](#) [\[PubMed\]](#)
37. Corbel, A.; Ladrière, M.; Le Berre, N.; Durin, L.; Rousseau, H.; Frimat, L.; Thilly, N.; Pulcini, C. Microbiological epidemiology of preservation fluids in transplanted kidney: A nationwide retrospective observational study. *Clin. Microbiol. Infect.* **2020**, *26*, 475–484. [\[CrossRef\]](#) [\[PubMed\]](#)
38. Oriol, I.; Sabe, N.; Càmarà, J.; Berbel, D.; Ballesteros, M.A.; Escudero, R.; Lopez-Medrano, F.; Linares, L.; Len, O.; Silva, J.T.; et al. The impact of culturing the organ preservation fluid on solid organ transplantation: A prospective multicenter cohort study. *Open Forum Infect. Dis.* **2019**, *6*, 1–7. [\[CrossRef\]](#)
39. Yu, X.; Wang, R.; Peng, W.; Huang, H.; Liu, G.; Yang, Q.; Zhou, J.; Zhang, X.; Lv, J.H.; Lei, W.; et al. Incidence, distribution and clinical relevance of microbial contamination of preservation solution in deceased kidney transplant recipients: A retrospective cohort study from China. *Clin. Microbiol. Infect.* **2019**, *25*, 595–600. [\[CrossRef\]](#)
40. Stern, S.; Bezinover, D.; Rath, P.M.; Paul, A.; Saner, F.H. Candida contamination in kidney and liver organ preservation solution: Does it matter? *J. Clin. Med.* **2021**, *10*, 2022. [\[CrossRef\]](#)
41. Sjekavica, I.; Novosel, L.; Rupčić, M.; Smiljanić, R.; Muršić, M.; Duspara, V.; Lušić, M.; Perković, D.; Hrabak-Paar, M.; Zidanić, M.; et al. Radiological imaging in renal transplantation. *Acta Clin. Croat.* **2018**, *57*, 694–712. [\[CrossRef\]](#)

42. Sarier, M.; Callioglu, M.; Yuksel, Y.; Duman, E.; Emek, M.; Usta, S.S. Evaluation of the Renal Arteries of 2144 Living Kidney Donors Using Computed Tomography Angiography and Comparison with Intraoperative Findings. *Urol. Int.* **2020**, *104*, 637–640. [\[CrossRef\]](#)
43. Al-Adra, D.P.; Lambadaris, M.; Barbas, A.; Li, Y.; Selzner, M.; Singh, S.K.; Famure, O.; Kim, S.J.; Ghanekar, A. Donor kidney volume measured by computed tomography is a strong predictor of recipient eGFR in living donor kidney transplantation. *World J. Urol.* **2019**, *37*, 1965–1972. [\[CrossRef\]](#)
44. Fernandez, N.; Lorenzo, A.; Chua, M.; Koyle, M.A.; Farhat, W.; Matava, C. Real-time kidney graft perfusion monitoring using infrared imaging during pediatric kidney transplantation. *J. Pediatr. Urol.* **2019**, *15*, 222.e1–222.e7. [\[CrossRef\]](#)
45. Sucher, R.; Wagner, T.; Köhler, H.; Sucher, E.; Guice, H.; Recknagel, S.; Lederer, A.; Hau, H.M.; Rademacher, S.; Schneeberger, S.; et al. Hyperspectral Imaging (HSI) of Human Kidney Allografts. *Ann. Surg.* **2020**. [\[CrossRef\]](#)
46. Gerken, A.L.H.; Nowak, K.; Meyer, A.; Weiss, C.; Krüger, B.; Nawroth, N.; Karampinis, I.; Heller, K.; Apel, H.; Reissfelder, C.; et al. Quantitative Assessment of Intraoperative Laser Fluorescence Angiography with Indocyanine Green Predicts Early Graft Function after Kidney Transplantation. *Ann. Surg.* **2020**. [\[CrossRef\]](#) [\[PubMed\]](#)
47. Yu, Y.M.; Ni, Q.Q.; Wang, Z.J.; Chen, M.L.; Zhang, L.J. Multiparametric functional magnetic resonance imaging for evaluating renal allograft injury. *Korean J. Radiol.* **2019**, *20*, 894–908. [\[CrossRef\]](#) [\[PubMed\]](#)
48. Schutter, R.; Lantinga, V.A.; Borra, R.J.H.; Moers, C. MRI for diagnosis of post-renal transplant complications: Current state-of-the-art and future perspectives. *Magn. Reson. Mater. Physics Biol. Med.* **2020**, *33*, 49–61. [\[CrossRef\]](#) [\[PubMed\]](#)
49. Jehn, U.; Schuette-Nuetgen, K.; Kentrup, D.; Hoerr, V.; Reuter, S. Renal allograft rejection: Noninvasive ultrasound- and mri-based diagnostics. *Contrast Media Mol. Imaging* **2019**, *2019*, 3568067. [\[CrossRef\]](#) [\[PubMed\]](#)
50. Pajenda, S.; Rasul, S.; Hacker, M.; Wagner, L.; Geist, B.K. Dynamic 2-deoxy-2[18F] fluoro-D-glucose PET/MRI in human renal allotransplant patients undergoing acute kidney injury. *Sci. Rep.* **2020**, *10*, 8270. [\[CrossRef\]](#)
51. Jadoul, A.; Lovinfosse, P.; Bouquegneau, A.; Weekers, L.; Pottel, H.; Hustinx, R.; Jouret, F. Observer variability in the assessment of renal 18F-FDG uptake in kidney transplant recipients. *Sci. Rep.* **2020**, *10*, 4617. [\[CrossRef\]](#)
52. Cai, Y.; Li, Z.; Zuo, P.; Pfeuffer, J.; Li, Y.; Liu, F.; Liu, R. Diagnostic value of renal perfusion in patients with chronic kidney disease using 3D arterial spin labeling. *J. Magn. Reson. Imaging* **2017**, *46*, 589–594. [\[CrossRef\]](#)
53. Wang, W.; Yu, Y.; Li, X.; Chen, J.; Zhang, Y.; Zhang, L.; Wen, J. Early detection of subclinical pathology in patients with stable kidney graft function by arterial spin labeling. *Eur. Radiol.* **2021**, *31*, 2687–2695. [\[CrossRef\]](#)
54. Bontha, S.V.; Maluf, D.G.; Mueller, T.F.; Mas, V.R. Systems Biology in Kidney Transplantation: The Application of Multi-Omics to a Complex Model. *Am. J. Transplant.* **2017**, *17*, 11–21. [\[CrossRef\]](#) [\[PubMed\]](#)
55. Giraud, S.; Steichen, C.; Allain, G.; Couturier, P.; Labourdette, D.; Lamarre, S.; Ameteau, V.; Tillet, S.; Hannaert, P.; Thuillier, R.; et al. Dynamic transcriptomic analysis of Ischemic Injury in a Porcine Pre-Clinical Model mimicking Donors Deceased after Circulatory Death. *Sci. Rep.* **2018**, *8*, 5986. [\[CrossRef\]](#) [\[PubMed\]](#)
56. Boissier, R.; François, P.; Tellier, B.G.; Meunier, M.; Lyonnet, L.; Simoncini, S.; Magalon, J.; Legris, T.; Arnaud, L.; Giraudo, L.; et al. Perirenal Adipose Tissue Displays an Age-Dependent Inflammatory Signature Associated With Early Graft Dysfunction of Marginal Kidney Transplants. *Front. Immunol.* **2020**, *11*, 445. [\[CrossRef\]](#)
57. Hrubá, P.; Krejčík, Z.; Dostalova Merkerova, M.; Klema, J.; Stranecky, V.; Slatinska, J.; Maluskova, J.; Honsova, E.; Viklicky, O. Molecular Fingerprints of Borderline Changes in Kidney Allografts Are Influenced by Donor Category. *Front. Immunol.* **2020**, *11*, 423. [\[CrossRef\]](#) [\[PubMed\]](#)
58. Han, F.; Wan, S.; Sun, Q.; Chen, N.; Li, H.; Zheng, L.; Zhang, N.; Huang, Z.; Hong, L.; Sun, Q. Donor Plasma Mitochondrial DNA Is Correlated with Posttransplant Renal Allograft Function. *Transplantation* **2019**, *103*, 2347–2358. [\[CrossRef\]](#)
59. Chen, H.-H.; Lan, Y.-F.; Li, H.-F.; Cheng, C.-F.; Lai, P.-F.; Li, W.-H.; Lin, H. Urinary miR-16 transactivated by C/EBP $\beta$  reduces kidney function after ischemia/reperfusion-induced injury. *Sci. Rep.* **2016**, *6*, 27945. [\[CrossRef\]](#)
60. Zhang, W.; Shu, L. Upregulation of miR-21 by Ghrelin Ameliorates Ischemia/Reperfusion-Induced Acute Kidney Injury by Inhibiting Inflammation and Cell Apoptosis. *DNA Cell Biol.* **2016**, *35*, 417–425. [\[CrossRef\]](#)
61. Song, T.; Chen, M.; Rao, Z.; Qiu, Y.; Liu, J.; Jiang, Y.; Huang, Z.; Wang, X.; Lin, T. miR-17-92 ameliorates renal ischemia reperfusion injury. *Kaohsiung J. Med. Sci.* **2018**, *34*, 263–273. [\[CrossRef\]](#)
62. Wang, Y.; Wang, D.; Jin, Z. miR-27a suppresses TLR4-induced renal ischemia-reperfusion injury. *Mol. Med. Rep.* **2019**, *20*, 967–976. [\[CrossRef\]](#)
63. Zhu, K.; Zheng, T.; Chen, X.; Wang, H. Bioinformatic analyses of renal ischaemia-reperfusion injury models: Identification of key genes involved in the development of kidney disease. *Kidney Blood Press. Res.* **2018**, *43*, 1898–1907. [\[CrossRef\]](#) [\[PubMed\]](#)
64. Su, M.; Hu, X.; Lin, J.; Zhang, L.; Sun, W.; Zhang, J.; Tian, Y.; Qiu, W. Identification of Candidate Genes Involved in Renal Ischemia/Reperfusion Injury. *DNA Cell Biol.* **2019**, *38*, 256–262. [\[CrossRef\]](#) [\[PubMed\]](#)
65. Liu, L.; Mao, L.; Wu, X.; Wu, T.; Liu, W.; Yang, Y.; Zhang, T.; Xu, Y. BRG1 regulates endothelial-derived IL-33 to promote ischemia-reperfusion induced renal injury and fibrosis in mice. *Biochim. Biophys. Acta Mol. Basis Dis.* **2019**, *1865*, 2551–2561. [\[CrossRef\]](#)
66. Cippà, P.E.; Sun, B.; Liu, J.; Chen, L.; Naesens, M.; McMahon, A.P. Transcriptional trajectories of human kidney injury progression. *JCI insight* **2018**, *3*, e123151. [\[CrossRef\]](#)
67. Hu, X.; Su, M.; Lin, J.; Zhang, L.; Sun, W.; Zhang, J.; Tian, Y.; Qiu, W. Corin is downregulated in renal ischemia/reperfusion injury and is associated with delayed graft function after kidney transplantation. *Dis. Markers* **2019**, *2019*, 9429323. [\[CrossRef\]](#)

68. Khalid, U.; Newbury, L.J.; Simpson, K.; Jenkins, R.H.; Bowen, T.; Bates, L.; Sheerin, N.S.; Chavez, R.; Fraser, D.J. A urinary microRNA panel that is an early predictive biomarker of delayed graft function following kidney transplantation. *Sci. Rep.* **2019**, *9*, 3584. [\[CrossRef\]](#)
69. Wang, J.; Li, X.; Wu, X.; Wang, Z.; Zhang, C.; Cao, G.; Yan, T. Expression Profiling of Exosomal miRNAs Derived from the Peripheral Blood of Kidney Recipients with DGF Using High-Throughput Sequencing. *Biomed. Res. Int.* **2019**, *2019*, 1759697. [\[CrossRef\]](#)
70. Mirzakhani, M.; Mohammadnia-Afrouzi, M.; Shahbazi, M.; Mirhosseini, S.A.; Hosseini, H.M.; Amani, J. The exosome as a novel predictive/diagnostic biomarker of rejection in the field of transplantation. *Clin. Immunol.* **2019**, *203*, 134–141. [\[CrossRef\]](#) [\[PubMed\]](#)
71. Milhoransa, P.; Montanari, C.C.; Montenegro, R.; Manfro, R.C. Micro RNA 146a-5p expression in Kidney transplant recipients with delayed graft function. *J. Bras. Nefrol.* **2019**, *41*, 242–251. [\[CrossRef\]](#) [\[PubMed\]](#)
72. Zmonarski, S.; Madziarska, K.; Banasik, M.; Mazanowska, O.; Magott-Procelewska, M.; Hap, K.; Krajewska, M. Expression of PBMC TLR4 in Renal Graft Recipients Who Experienced Delayed Graft Function Reflects Dynamic Balance Between Blood and Tissue Compartments and Helps Select a Problematic Patient. *Transplant. Proc.* **2018**, *50*, 1744–1749. [\[CrossRef\]](#)
73. Bi, H.; Zhang, M.; Wang, J.; Long, G. The mRNA landscape profiling reveals potential biomarkers associated with acute kidney injury AKI after kidney transplantation. *PeerJ* **2020**, *8*, e10441. [\[CrossRef\]](#)
74. Koo, T.Y.; Jeong, J.C.; Lee, Y.; Ko, K.-P.; Lee, K.-B.; Lee, S.; Park, S.J.; Park, J.B.; Han, M.; Lim, H.J.; et al. Pre-transplant evaluation of donor urinary biomarkers can predict reduced graft function after deceased donor kidney transplantation. *Medicine* **2016**, *95*, e3076. [\[CrossRef\]](#)
75. Reese, P.P.; Hall, I.E.; Weng, F.L.; Schröppel, B.; Doshi, M.D.; Hasz, R.D.; Thiessen-Philbrook, H.; Ficek, J.; Rao, V.; Murray, P.; et al. Associations between deceased-donor urine injury biomarkers and kidney transplant outcomes. *J. Am. Soc. Nephrol.* **2016**, *27*, 1534–1543. [\[CrossRef\]](#)
76. Schröppel, B.; Heeger, P.; Thiessen-Philbrook, H.; Hall, I.E.; Doshi, M.D.; Weng, F.L.; Reese, P.P.; Parikh, C.R. Donor Urinary C5a Levels Independently Correlate with Posttransplant Delayed Graft Function. *Transplantation* **2019**, *103*, e29–e35. [\[CrossRef\]](#) [\[PubMed\]](#)
77. Mansour, S.G.; Puthumana, J.; Reese, P.P.; Hall, I.E.; Doshi, M.D.; Weng, F.L.; Schröppel, B.; Thiessen-Philbrook, H.; Bimali, M.; Parikh, C.R. Associations Between Deceased-Donor Urine MCP-1 and Kidney Transplant Outcomes. *Kidney Int. Rep.* **2017**, *2*, 749–758. [\[CrossRef\]](#) [\[PubMed\]](#)
78. Mezzolla, V.; Pontrelli, P.; Fiorentino, M.; Stasi, A.; Franzin, R.; Rascio, F.; Grandaliano, G.; Stallone, G.; Infante, B.; Gesualdo, L.; et al. Emerging biomarkers of delayed graft function in kidney transplantation. *Transplant. Rev.* **2021**, *35*, 100629. [\[CrossRef\]](#) [\[PubMed\]](#)
79. Kostidis, S.; Bank, J.R.; Soonawala, D.; Nevedomskaya, E.; van Kooten, C.; Mayboroda, O.A.; de Fijter, J.W. Urinary metabolites predict prolonged duration of delayed graft function in DCD kidney transplant recipients. *Am. J. Transplant.* **2019**, *19*, 110–122. [\[CrossRef\]](#)
80. Braun, F.; Rinschen, M.; Buchner, D.; Bohl, K.; Plagmann, I.; Bachurski, D.; Späth, M.R.; Antczak, P.; Göbel, H.; Klein, C.; et al. The proteomic landscape of small urinary extracellular vesicles during kidney transplantation. *J. Extracell. Vesicles* **2020**, *10*, e12026. [\[CrossRef\]](#)
81. Li, L.; Li, N.; He, C.; Huang, W.; Fan, X.; Zhong, Z.; Wang, Y.; Ye, Q. Proteomic analysis of differentially expressed proteins in kidneys of brain dead rabbits. *Mol. Med. Rep.* **2017**, *16*, 215–223. [\[CrossRef\]](#)
82. Van Erp, A.C.; Rebollo, R.A.; Hoeksma, D.; Jespersen, N.R.; Ottens, P.J.; Nørregaard, R.; Pedersen, M.; Laustsen, C.; Burgerhof, J.G.M.; Wolters, J.C.; et al. Organ-specific responses during brain death: Increased aerobic metabolism in the liver and anaerobic metabolism with decreased perfusion in the kidneys. *Sci. Rep.* **2018**, *8*, 4405. [\[CrossRef\]](#)
83. Huang, H.; Van Dullemen, L.F.A.; Akhtar, M.Z.; Faro, M.-L.L.; Yu, Z.; Valli, A.; Dona, A.; Thézéas, M.-L.; Charles, P.D.; Fischer, R.; et al. Proteo-metabolomics reveals compensation between ischemic and non-injured contralateral kidneys after reperfusion. *Sci. Rep.* **2018**, *8*, 8539. [\[CrossRef\]](#) [\[PubMed\]](#)
84. Malagrino, P.A.; Venturini, G.; Yogi, P.S.; Dariolli, R.; Padilha, K.; Kiers, B.; Gois, T.C.; Cardozo, K.H.M.; Carvalho, V.M.; Salgueiro, J.S.; et al. Proteome analysis of acute kidney injury—Discovery of new predominantly renal candidates for biomarker of kidney disease. *J. Proteomics* **2017**, *151*, 66–73. [\[CrossRef\]](#) [\[PubMed\]](#)
85. Moser, M.A.J.; Sawicka, K.; Sawicka, J.; Franczak, A.; Cohen, A.; Bil-Lula, I.; Sawicki, G. Protection of the transplant kidney during cold perfusion with doxycycline: Proteomic analysis in a rat model. *Proteome Sci.* **2020**, *18*, 3. [\[CrossRef\]](#) [\[PubMed\]](#)
86. Weissenbacher, A.; Huang, H.; Surik, T.; Faro, M.L.L.; Ploeg, R.J.; Coussios, C.C.; Friend, P.J.; Kessler, B.M. Urine recirculation prolongs normothermic kidney perfusion via more optimal metabolic homeostasis—a proteomics study. *Am. J. Transplant.* **2020**, *21*, 1740–1753. [\[CrossRef\]](#) [\[PubMed\]](#)
87. Williams, K.R.; Colangelo, C.M.; Hou, L.; Chung, L.; Belcher, J.M.; Abbott, T.; Hall, I.E.; Zhao, H.; Cantley, L.G.; Parikh, C.R. Use of a Targeted Urine Proteome Assay (TUPA) to identify protein biomarkers of delayed recovery after kidney transplant. *Proteomics Clin. Appl.* **2017**, *11*, 1600132. [\[CrossRef\]](#)
88. Lacquaniti, A.; Caccamo, C.; Salis, P.; Chirico, V.; Buemi, A.; Cernaro, V.; Noto, A.; Pettinato, G.; Santoro, D.; Bertani, T.; et al. Delayed graft function and chronic allograft nephropathy: Diagnostic and prognostic role of neutrophil gelatinase-associated lipocalin. *Biomarkers* **2016**, *21*, 371–378. [\[CrossRef\]](#)

89. Bank, J.R.; Ruhaak, R.; Soonawala, D.; Mayboroda, O.; Romijn, F.P.; Van Kooten, C.; Cobbaert, C.M.; De Fijter, J.W. Urinary TIMP-2 Predicts the Presence and Duration of Delayed Graft Function in Donation after Circulatory Death Kidney Transplant Recipients. *Transplantation* **2019**, *103*, 1014–1023. [\[CrossRef\]](#)
90. Van Erp, A.C.; Qi, H.; Jespersen, N.R.; Hjortbak, M.V.; Ottens, P.J.; Wiersema-Buist, J.; Nørregaard, R.; Pedersen, M.; Laustsen, C.; Leuvenink, H.G.D.; et al. Organ-specific metabolic profiles of the liver and kidney during brain death and afterwards during normothermic machine perfusion of the kidney. *Am. J. Transplant.* **2020**, *20*, 2425–2436. [\[CrossRef\]](#)
91. Nielsen, P.M.; Qi, H.; Bertelsen, L.B.; Laustsen, C. Metabolic reprogramming associated with progression of renal ischemia reperfusion injury assessed with hyperpolarized [1-<sup>13</sup>C]pyruvate. *Sci. Rep.* **2020**, *10*, 8915. [\[CrossRef\]](#)
92. Chihanga, T.; Ma, Q.; Nicholson, J.D.; Ruby, H.N.; Edelmann, R.E.; Devarajan, P.; Kennedy, M.A. NMR spectroscopy and electron microscopy identification of metabolic and ultrastructural changes to the kidney following ischemia-reperfusion injury. *Am. J. Physiol. Ren. Physiol.* **2018**, *314*, F154–F166. [\[CrossRef\]](#) [\[PubMed\]](#)
93. Stryjak, I.; Warmużińska, N.; Bogusiewicz, J.; Łuczykowski, K.; Bojko, B. Monitoring of the influence of long-term oxidative stress and ischemia on the condition of kidneys using solid-phase microextraction chemical biopsy coupled with liquid chromatography–high-resolution mass spectrometry. *J. Sep. Sci.* **2020**, *43*, 1867–1878. [\[CrossRef\]](#)
94. Stryjak, I.; Warmużińska, N.; Łuczykowski, K.; Hamar, M.; Urbanellis, P.; Wojtal, E.; Masztalerz, M.; Selzner, M.; Włodarczyk, Z.; Bojko, B. Using a chemical biopsy for graft quality assessment. *J. Vis. Exp.* **2020**, e60946. [\[CrossRef\]](#)
95. Zheng, X.; Zhang, A.; Binnie, M.; McGuire, K.; Webster, S.P.; Hughes, J.; Howie, S.E.M.; Mole, D.J. Kynurenine 3-monooxygenase is a critical regulator of renal ischemia–reperfusion injury. *Exp. Mol. Med.* **2019**, *51*, 1–14. [\[CrossRef\]](#)
96. Beier, U.H.; Hartung, E.A.; Concors, S.; Hernandez, P.T.; Wang, Z.; Perry, C.; Baur, J.A.; Denburg, M.R.; Hancock, W.W.; Gade, T.P.; et al. Tissue metabolic profiling shows that saccharopine accumulates during renal ischemic-reperfusion injury, while kynurenine and itaconate accumulate in renal allograft rejection. *Metabolomics* **2021**, *16*, 65. [\[CrossRef\]](#)
97. Rao, S.; Walters, K.B.; Wilson, L.; Chen, B.; Bolisetty, S.; Graves, D.; Barnes, S.; Agarwal, A.; Kabarowski, J.H. Early lipid changes in acute kidney injury using SWATH lipidomics coupled with MALDI tissue imaging. *Am. J. Physiol. Ren. Physiol.* **2016**, *310*, F1136–F1147. [\[CrossRef\]](#)
98. Solati, Z.; Edel, A.L.; Shang, Y.; Karmin, O.; Ravandi, A. Oxidized phosphatidylcholines are produced in renal ischemia reperfusion injury. *PLoS ONE* **2018**, *13*, e0195172. [\[CrossRef\]](#)
99. van Smaalen, T.C.; Ellis, S.R.; Mascini, N.E.; Siegel, T.P.; Cillero-Pastor, B.; Hillen, L.M.; van Heurn, L.W.E.; Peutz-Kootstra, C.J.; Heeren, R.M.A. Rapid Identification of Ischemic Injury in Renal Tissue by Mass-Spectrometry Imaging. *Anal. Chem.* **2019**, *91*, 3575–3581. [\[CrossRef\]](#) [\[PubMed\]](#)
100. Wijermars, L.G.M.; Bakker, J.A.; de Vries, D.K.; van Noorden, C.J.F.; Bierau, J.; Kostidis, S.; Mayboroda, O.A.; Tsikas, D.; Schaapherder, A.F.; Lindeman, J.H.N. The hypoxanthine-xanthine oxidase axis is not involved in the initial phase of clinical transplantation-related ischemia-reperfusion injury. *Am. J. Physiol. Ren. Physiol.* **2017**, *312*, F457–F464. [\[CrossRef\]](#)
101. Lindeman, J.H.; Wijermars, L.G.; Kostidis, S.; Mayboroda, O.A.; Harms, A.C.; Hankemeier, T.; Bierau, J.; Gupta, K.B.S.S.; Giera, M.; Reinders, M.E.; et al. Results of an explorative clinical evaluation suggest immediate and persistent post-reperfusion metabolic paralysis drives kidney ischemia reperfusion injury. *Kidney Int.* **2020**, *98*, 1476–1488. [\[CrossRef\]](#)
102. Jochmans, I.; Brat, A.; Davies, L.; Hofker, H.S.; van de Leemkolk, F.E.M.; Leuvenink, H.G.D.; Knight, S.R.; Pirenne, J.; Ploeg, R.J. Oxygenated versus standard cold perfusion preservation in kidney transplantation (COMPARE): A randomised, double-blind, paired, phase 3 trial. *Lancet* **2020**, *396*, 1653–1662. [\[CrossRef\]](#)
103. Hosgood, S.A.; Hoff, M.; Nicholson, M.L. Treatment of transplant kidneys during machine perfusion. *Transpl. Int.* **2021**, *34*, 224–232. [\[CrossRef\]](#)
104. Resch, T.; Cardini, B.; Oberhuber, R.; Weissenbacher, A.; Dumfarth, J.; Krapf, C.; Boesmueller, C.; Oefner, D.; Grimm, M.; Schneeberger, S. Transplanting Marginal Organs in the Era of Modern Machine Perfusion and Advanced Organ Monitoring. *Front. Immunol.* **2020**, *11*, 631. [\[CrossRef\]](#)
105. Hamar, M.; Selzner, M. Ex-vivo machine perfusion for kidney preservation. *Curr. Opin. Organ. Transplant.* **2018**, *23*, 369–374. [\[CrossRef\]](#)
106. Coskun, A.; Baykal, A.T.; Kazan, D.; Akgoz, M.; Senal, M.O.; Berber, I.; Titiz, I.; Bilsel, G.; Kilercik, H.; Karaosmanoglu, K.; et al. Proteomic analysis of kidney preservation solutions prior to renal transplantation. *PLoS ONE* **2016**, *11*, e0168755. [\[CrossRef\]](#) [\[PubMed\]](#)
107. van Balkom, B.W.M.; Gremmels, H.; Ooms, L.S.S.; Toorop, R.J.; Dor, F.J.M.F.; de Jong, O.G.; Michielsen, L.A.; de Borst, G.J.; De Jager, W.; Abrahams, A.C.; et al. Proteins in preservation fluid as predictors of delayed graft function in kidneys from donors after circulatory death. *Clin. J. Am. Soc. Nephrol.* **2017**, *12*, 817–824. [\[CrossRef\]](#)
108. Wang, Z.; Yang, H.; Zhao, C.; Wei, J.; Wang, J.; Han, Z.; Tao, J.; Xu, Z.; Ju, X.; Tan, R.; et al. Proton nuclear magnetic resonance (1H-NMR)-based metabolomic evaluation of human renal allografts from donations after circulatory death. *Med. Sci. Monit.* **2017**, *23*, 5472–5479. [\[CrossRef\]](#)
109. Nath, J.; Smith, T.B.; Patel, K.; Ebbs, S.R.; Hollis, A.; Tennant, D.A.; Ludwig, C.; Ready, A.R. Metabolic differences between cold stored and machine perfused porcine kidneys: A 1H NMR based study. *Cryobiology* **2017**, *74*, 115–120. [\[CrossRef\]](#)
110. Adani, G.L.; Pravisani, R.; Crestale, S.; Baccarani, U.; Scott, C.A.; D'Ali, L.; Demaglio, G.; Tulissi, P.; Vallone, C.; Isola, M.; et al. Effects of delayed hypothermic machine perfusion on kidney grafts with a preliminary period of static cold storage and a total cold ischemia time of over 24 hours. *Ann. Transplant.* **2020**, *25*, e918997. [\[CrossRef\]](#)

111. Foucher, Y.; Fournier, M.-C.; Legendre, C.; Morelon, E.; Buron, F.; Girerd, S.; Ladrière, M.; Mourad, G.; Garrigue, V.; Glotz, D.; et al. Comparison of machine perfusion versus cold storage in kidney transplant recipients from expanded criteria donors: A cohort-based study. *Nephrol. Dial. Transplant.* **2020**, *35*, 1051–1059. [\[CrossRef\]](#) [\[PubMed\]](#)
112. Tejchman, K.; Sierocka, A.; Kotowski, M.; Zair, L.; Pilichowska, E.; Ostrowski, M.; Sienko, J. Acid-Base Balance Disorders During Kidney Preservation in Cold Ischemia. *Transplant. Proc.* **2020**, *52*, 2036–2042. [\[CrossRef\]](#)
113. He, N.; Li, J.-H.; Jia, J.-J.; Xu, K.-D.; Zhou, Y.-F.; Jiang, L.; Lu, H.-H.; Yin, S.-Y.; Xie, H.-Y.; Zhou, L.; et al. Hypothermic Machine Perfusion's Protection on Porcine Kidney Graft Uncovers Greater Akt-Erk Phosphorylation. *Transplant. Proc.* **2017**, *49*, 1923–1929. [\[CrossRef\]](#) [\[PubMed\]](#)
114. Patel, K.; Smith, T.B.; Neil, D.A.H.; Thakker, A.; Tsuchiya, Y.; Higgs, E.B.; Hodges, N.J.; Ready, A.R.; Nath, J.; Ludwig, C. The Effects of Oxygenation on Ex Vivo Kidneys Undergoing Hypothermic Machine Perfusion. *Transplantation* **2019**, *103*, 314–322. [\[CrossRef\]](#)
115. Moser, M.A.J.; Sawicka, K.; Arcand, S.; O'Brien, P.; Luke, P.; Beck, G.; Sawicka, J.; Cohen, A.; Sawicki, G. Proteomic analysis of perfusate from machine cold perfusion of transplant kidneys: Insights into protection from injury. *Ann. Transplant.* **2017**, *22*, 730–739. [\[CrossRef\]](#) [\[PubMed\]](#)
116. Gómez-Dos-Santos, V.; Ramos-Muñoz, E.; García-Bermejo, M.L.; Ruiz-Hernández, M.; Rodríguez-Serrano, E.M.; Saiz-González, A.; Martínez-Perez, A.; Burgos-Revilla, F.J. MicroRNAs in Kidney Machine Perfusion Fluid as Novel Biomarkers for Graft Function. Normalization Methods for miRNAs Profile Analysis. *Transplant. Proc.* **2019**, *51*, 307–310. [\[CrossRef\]](#)
117. Tejchman, K.; Sierocka, A.; Kotfis, K.; Kotowski, M.; Dolegowska, B.; Ostrowski, M.; Sienko, J. Assessment of oxidative stress markers in hypothermic preservation of transplanted kidneys. *Antioxidants* **2021**, *10*, 1263. [\[CrossRef\]](#)
118. Longchamp, A.; Klauser, A.; Songeon, J.; Agius, T.; Nastasi, A.; Ruttiman, R.; Moll, S.; Meier, R.P.H.; Buhler, L.; Corpataux, J.-M.; et al. Ex Vivo Analysis of Kidney Graft Viability Using <sup>31</sup>P Magnetic Resonance Imaging Spectroscopy. *Transplantation* **2020**, *104*, 1825–1831. [\[CrossRef\]](#)
119. Van Smaalen, T.C.; Beurskens, D.M.H.; Hoogland, E.R.P.; Winkens, B.; Christiaans, M.H.L.; Reutelingsperger, C.P.; van Heurn, L.W.E.; Nicolaes, G.A.F. Presence of Cytotoxic Extracellular Histones in Machine Perfusate of Donation after Circulatory Death Kidneys. *Transplantation* **2017**, *101*, e93–e101. [\[CrossRef\]](#)
120. Kathis, J.M.; Echeverri, J.; Chun, Y.M.; Cen, J.Y.; Goldaracena, N.; Linares, I.; Dingwell, L.S.; Yip, P.M.; John, R.; Bagli, D.; et al. Continuous Normothermic Ex Vivo Kidney Perfusion Improves Graft Function in Donation after Circulatory Death Pig Kidney Transplantation. *Transplantation* **2017**, *101*, 754–763. [\[CrossRef\]](#)
121. Tetschke, F.; Markgraf, W.; Gransow, M.; Koch, S.; Thiele, C.; Kulcke, A.; Malberg, H. Hyperspectral imaging for monitoring oxygen saturation levels during normothermic kidney perfusion. *J. Sensors Sens. Syst.* **2016**, *5*, 313–318. [\[CrossRef\]](#)
122. Markgraf, W.; Feistel, P.; Thiele, C.; Malberg, H. Algorithms for mapping kidney tissue oxygenation during normothermic machine perfusion using hyperspectral imaging. *Biomed. Tech.* **2018**, *63*, 557–566. [\[CrossRef\]](#) [\[PubMed\]](#)
123. Mariager, C.Ø.; Hansen, E.S.S.; Bech, S.K.; Munk, A.; Kjærgaard, U.; Lyhne, M.D.; Søberg, K.; Nielsen, P.F.; Ringgaard, S.; Laustsen, C. Graft assessment of the ex vivo perfused porcine kidney using hyperpolarized [<sup>13</sup>C]pyruvate. *Magn. Reson. Med.* **2020**, *84*, 2645–2655. [\[CrossRef\]](#) [\[PubMed\]](#)
124. Hosgood, S.A.; Nicholson, M.L. An assessment of urinary biomarkers in a series of declined human kidneys measured during ex vivo normothermic kidney perfusion. *Transplantation* **2017**, *101*, 2120–2125. [\[CrossRef\]](#) [\[PubMed\]](#)

## 5.2. Mikroekstrakcja do fazy stałej

Mikroekstrakcja do fazy stałej (SPME, ang. solid-phase microextraction) to nowoczesna technika przygotowania próbek szeroko wykorzystywana w chemii analitycznej i bioanalizie. Jej podstawowym celem jest selektywne wyodrębnienie i skoncentrowanie związków chemicznych z różnorodnych matryc przed ich dalszą analizą, zwykle z wykorzystaniem technik takich jak chromatografia gazowa lub cieczowa sprzężona ze spektrometrią mas. SPME jest dobrze znana ze swojej skuteczności w analizie związków lotnych w różnych obszarach chemii analitycznej [8]. Rozwój biokompatybilnych faz ekstrakcyjnych umożliwił jednak rozszerzenie zastosowania tej techniki na ekstrakcję związków nielotnych poprzez bezpośrednie zanurzenie sondy w badanej próbce, co pozwala na poszerzenie zakresu analizowanych metabolitów. Stosowane powłoki ekstrakcyjne umożliwiają wysoką selektywność wobec małych cząsteczek, zapobiegają współekstrakcji białek i innych makrocząsteczek oraz nie wywołują niepożądanych reakcji po zanurzeniu w próbkach biologicznych, co czyni je odpowiednimi do pobierania próbek *in vivo* ze złożonych matryc [8,9]. Bezpośrednia analiza tkanek za pomocą SPME, określana również mianem "biopsji chemicznej", umożliwia połączenie w jednym kroku procesów pobierania próbki, ekstrakcji metabolitów oraz natychmiastowego wygaszania metabolizmu. Takie podejście pozwala na skuteczną izolację także niestabilnych związków, które często pozostają niewykrywalne w tradycyjnych procedurach przygotowania próbek. Ponadto, brak konieczności fizycznego pobrania fragmentu tkanki oraz małe rozmiary sondy SPME (średnica ~200 µm) zapewniają minimalną inwazyjność i umożliwiają wielokrotne pobieranie próbek z tego samego narządu bez jego uszkodzenia [8]. Dzięki tym właściwościom, technika SPME umożliwia monitorowanie dynamicznych zmian metabolicznych w czasie - aspekt zazwyczaj niedostępny przy zastosowaniu tradycyjnych metod, które wymagają pobrania i homogenizacji tkanki oraz ekstrakcji analitów z użyciem rozpuszczalników wodnych i organicznych [10]. Klasyczne podejścia, choć szeroko stosowane, nie są odpowiednie do ekstrakcji bezpośrednio w miejscu badania ze względu na skomplikowane protokoły przygotowania próbki. Dodatkowo, konieczność fizycznego pobierania tkanki ogranicza możliwość wielokrotnego próbkowania, ponieważ kolejne biopsje zwiększają ryzyko uszkodzenia narządu oraz wystąpienia powikłań.

Połączenie techniki SPME z analizą metabolomiczną i lipidomiczną umożliwia monitorowanie natychmiastowej reakcji organizmu na nagłe zmiany środowiskowe. W kontekście transplantacji pozwala to na wykrywanie zmian zachodzących w narządzie na wszystkich etapach procesu - od momentu pobrania od dawcy, przez przechowywanie i perfuzję, aż do rewaskularyzacji u biorcy. Tego typu analizy dostarczają cennych informacji, umożliwiających lepsze zrozumienie zmian w szlakach biochemicznych związanych z niedokrwieniem, stresem oksydacyjnym, odpowiedzią zapalną oraz innymi procesami zachodzącymi podczas pobierania, przechowywania i reperfuzji narządu.

Analiza lipidomiczna, będąca głównym przedmiotem niniejszej rozprawy doktorskiej, umożliwia kompleksowe badanie lipidów w komórkach, tkankach, narządach oraz całych organizmach. Obejmuje identyfikację, charakterystykę i ilościowe oznaczanie różnych klas lipidów, a także analizę ich funkcji biologicznych oraz roli w szlakach metabolicznych [11].

Lipidy stanowią istotną klasę biomolekuł, które odgrywają kluczową rolę w licznych procesach komórkowych. Są głównymi składnikami błon biologicznych, umożliwiającymi oddzielenie komórki od środowiska zewnętrznego, a ponadto pełnią funkcję magazynowania nadmiaru energii na potrzeby późniejszego wykorzystania. Dodatkowo lipidy uczestniczą w procesach sygnalizacji wewnątrz- i zewnątrzkomórkowej, gdzie odpowiadają za przekazywanie sygnałów oraz wzmacnianie szlaków regulacyjnych [11,12]. W wielu chorobach nerek obserwuje się zaburzenia w metabolizmie lipidów oraz zmiany w ich stężeniach, co odgrywa istotną rolę w progresji choroby [13]. Połączenie profilowania lipidomicznego z ekstrakcją *in vivo* przy użyciu biopsji chemicznej stwarza nowe możliwości w badaniach nad mechanizmami uszkodzenia nerek, identyfikacji biomarkerów jakości narządów oraz prognozowania wystąpienia powikłań.

Zagadnienia związane z zastosowaniem SPME w badaniach koncentrujących się na monitorowaniu przeszczepów w okresie okołoperacyjnym transplantacji oraz omówienie jej potencjału jako narzędzia diagnostycznego zostały szczegółowo opisane w pracy poglądowej pt. „Solid phase microextraction – a promising tool for graft quality monitoring in solid organ transplantation” (Separations, 2023, 10, 153), będącej częścią cyklu publikacji prezentowanych w tej rozprawie doktorskiej (publikacja P.2.).

## Review

# Solid Phase Microextraction—A Promising Tool for Graft Quality Monitoring in Solid Organ Transplantation

Kamil Łuczykowski <sup>†</sup> , Natalia Warmuzińska <sup>†</sup>  and Barbara Bojko <sup>\*</sup> 

Department of Pharmacodynamics and Molecular Pharmacology, Faculty of Pharmacy,  
Collegium Medicum in Bydgoszcz, Nicolaus Copernicus University in Torun, 85-089 Bydgoszcz, Poland  
\* Correspondence: bbojko@cm.umk.pl

<sup>†</sup> These authors contributed equally to this work.

**Abstract:** Solid organ transplantation is a life-saving intervention for patients suffering from end-stage organ failure. Although improvements in surgical techniques, standards of care, and immunosuppression have been observed over the last few decades, transplant centers have to face the problem of an insufficient number of organs for transplantation concerning the growing demand. An opportunity to increase the pool of organs intended for transplantation is the more frequent use of organs from extended criteria and the development of analytical methods allowing for a better assessment of the quality of organs to minimize the risk of post-transplant organ injury and rejection. Therefore, solid-phase microextraction (SPME) has been proposed in various studies as an effective tool for determining compounds of significance during graft function assessment or for the chemical profiling of grafts undergoing various preservation protocols. This review summarizes how SPME addresses the analytical challenges associated with different matrices utilized in the peri-transplant period and discusses its potential as a diagnostic tool in future work.

**Keywords:** solid-phase microextraction; SPME; transplantation; graft quality assessment; biomarkers



**Citation:** Łuczykowski, K.; Warmuzińska, N.; Bojko, B. Solid Phase Microextraction—A Promising Tool for Graft Quality Monitoring in Solid Organ Transplantation. *Separations* **2023**, *10*, 153. <https://doi.org/10.3390/separations10030153>

Academic Editors: Victoria Samanidou, Natasa Kalogiouri and Maria Touraki

Received: 29 December 2022

Revised: 20 February 2023

Accepted: 21 February 2023

Published: 23 February 2023



**Copyright:** © 2023 by the authors. Licensee MDPI, Basel, Switzerland. This article is an open access article distributed under the terms and conditions of the Creative Commons Attribution (CC BY) license (<https://creativecommons.org/licenses/by/4.0/>).

## 1. Introduction

Solid organ transplantation is a life-saving intervention for patients suffering from end-stage organ failure. The transplantation of livers, kidneys, hearts, and lungs has become a routine part of clinical care worldwide, and has contributed to higher survival rates and greater quality of life among patients [1]. Over the last few decades, advancements in surgical techniques, standards of care, and immunosuppression have significantly improved transplantation outcomes. However, the number of patients on waiting lists for all solid organs has rapidly increased, resulting in an ever-growing disparity between organ availability and demand [2]. Furthermore, this shortage of donor organs is exacerbated by the fact that many organs are ultimately deemed unsuitable for transplantation due to strict criteria and are discarded as a result [3]. Indeed, it is estimated that only 20% of lungs and less than 40% of hearts are considered suitable for transplantation [4,5].

Given this scarcity of viable organs, strategies aimed at increasing the donor pool, reducing patient wait times, and decreasing the number of unnecessarily discarded organs are crucial. Among such strategies, one of the most notable is the use of organs from expanded criteria donors (ECD) and donors after circulatory death (DCD) [6,7]. However, it is well known that compared with standard criteria donors (SCD), marginal grafts tend to have worse outcomes, including an increased risk of delayed graft function (DGF) and primary nonfunction incidence (PNF) [8,9]. Hence, there is a great need for accurate methods of assessing graft quality and estimating donor risk, especially in relation to marginal grafts. Currently, an organ's suitability for transplantation is determined based on detailed parameters, including the donor's medical history and examination results. Depending on the organ, different parameters will be considered. The factors taken into account when assessing organ quality include, among others: smoking history, chest X-rays, oxygenation, active

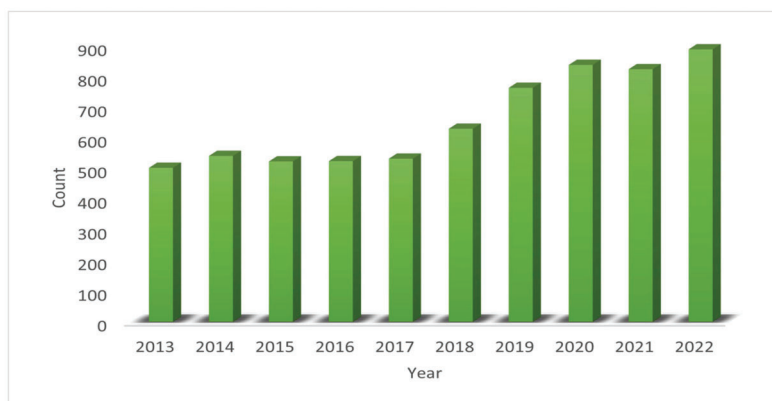
infections, hemodynamic stability, electrocardiograms, echocardiograms, serum bilirubin, AST, ALT, creatinine concentration, visual assessment of the organ, and biopsy [7,10–13]. Unfortunately, the decision-making process for accepting an organ for transplantation is always subjective to some extent and often lacks sufficient overall predictive power. Furthermore, many of the evaluated parameters cannot be used as independent predictors due to their low specificity.

The transplant team's visual assessment of donor organs is often fundamental in decision-making. Although a general inspection can help to identify tumors and anatomical changes, this method is subjective and depends on the transplant team's experience level [12]. In the case of heart transplants, several studies have indicated that elevated troponin levels in donor serum may be related to primary graft dysfunction (PGD). However, higher troponin levels in serum from donors who have experienced brain death may be a result of the brain's degradation rather than an indication of myocardial damage [7,14]. Similarly, left ventricular dysfunction is another common reason for discarding potential transplant organs, but this condition may be caused by a potentially reversible sequela of brain death, rather than a defective heart [14]. For lung transplants, non-smokers are ideal donors, as a donor history of smoking has been related to PGD. Nonetheless, findings have shown that recipients who received a graft from an actively smoking donor have significantly lower mortality compared to patients who remained on the waiting list [15]. In the case of kidney and liver transplantation, pre-transplant biopsies remain the gold standard for diagnosing organ injury. However, histological assessments are usually applied selectively, predominantly in ECD and DCD grafts, and the frequency of performed biopsies varies between medical facilities and countries. Although biopsies can provide comprehensive information relating to organ status, the role of a pre-transplant biopsy in graft evaluation is intensely debated. The use of biopsies to evaluate graft quality is hampered by two major limitations: the low reproducibility of results between on-call pathologists, and their time-consuming nature. Previous studies have analyzed the consistency of scores assigned to kidney donor biopsies by different on-call pathologists and the retrospective evaluation of the same sections performed by the renal pathologist. Interestingly, a correlation between donor histology and graft outcome was observed in the evaluations performed by the renal pathologists, but not in the evaluations performed by the on-call pathologists [16]. Thus, histological evaluation remains only one component of graft assessment and should not be the sole determinant in deciding whether to accept an organ for transplantation or to discard it. All of the above examples illustrate the comprehensiveness and complexity of organ-quality assessment and the decision-making processes. In an attempt to improve and standardize the evaluation process, researchers have developed several scoring systems aimed at providing an objective estimate of post-transplant survival based on donors' and/or recipients' characteristics. Two of these systems, the Kidney Donor Risk Index (KDRI) and the Liver Donor Risk Index (LDRI), are among the most established metrics for estimating graft survival; however, new solutions are still being proposed [17]. Although risk indices can facilitate and improve the decision-making process, they are not intended to serve as the only metric for determining donor suitability; rather, they should be utilized as part of a comprehensive evaluation along with other factors. Furthermore, while donor age is one of the most influential factors in calculating most risk indexes, it is not well-established whether these indexes can be applied to elderly and pediatric donors [18,19].

Another way to increase the donor pool is the implementation of new organ preservation methods. At present, static cold storage (SCS) is the standard technique for organ preservation in clinical practice due to its readily available logistics and low cost. The hypothermic conditions of SCS reduce the organ's metabolic activity and oxygen demand, thereby reducing ischemic injury. However, ECD grafts appear to be more prone to prolonged ischemia, resulting in increased morbidity and mortality in recipients. Thus, the technique of preserving these types of organs is crucial [20,21]. In recent years, numerous preclinical and clinical studies have sought to develop and optimize alternative organ-

preservation methods in an attempt to improve the outcomes of ECD graft transplantation. Currently, the proposed machine perfusion methods can be divided into three categories based on the pumping temperature of the preservation solution and the oxygen supply (i.e., with or without oxygen): normothermic (35–37 °C), sub-normothermic (20–25 °C), and hypothermic (4–10 °C) [22]. These methods are advantageous because they minimize the risk of organ damage and early allograft dysfunction (EAD), in addition to allowing the administration of additional pharmacological agents for protective ischemic postconditioning and for assessing organ function immediately before transplantation [4,5]. Unfortunately, although machine perfusion enables the monitoring of perfusion parameters that can predict organ viability after transplantation, there is still a lack of representative methods for assessing graft quality.

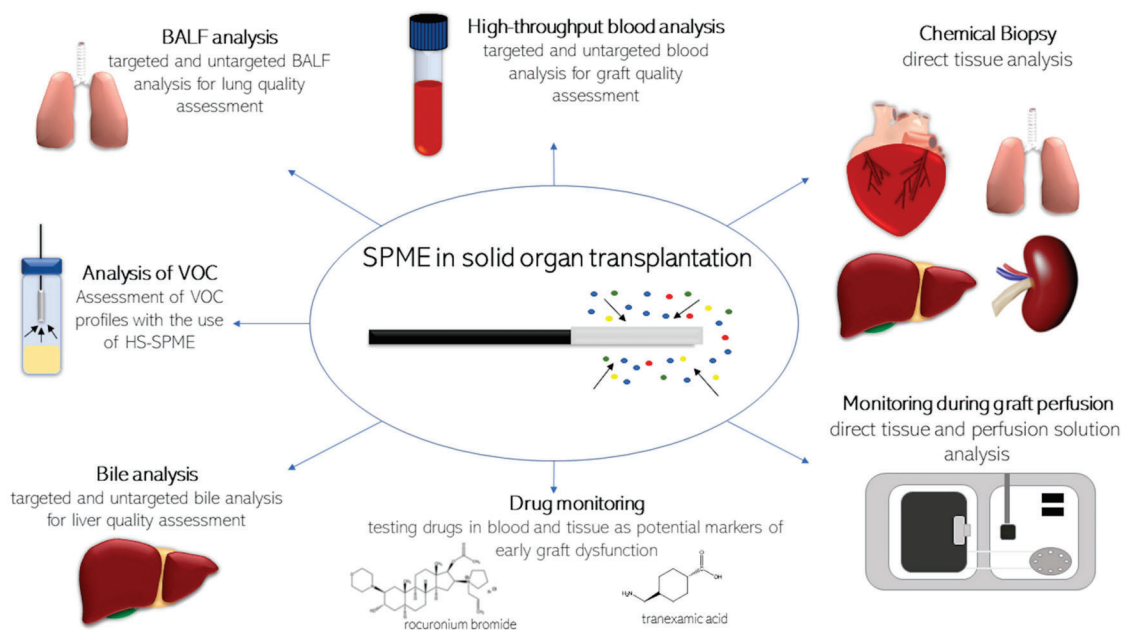
Solid-phase microextraction (SPME) is a widely accepted analytical method in bioanalysis. Undoubtedly, the analysis of volatile compounds in the headspace of a given sample is both the original and most studied application of SPME. However, in recent years, the direct extraction of non-volatile compounds from complex matrices has emerged as a very attractive alternative to conventional sample preparation methods in bioanalysis. While SPME fibers—which are probes with a small diameter (ca. 250 nm)—are the most well-known geometry, thin-film devices are also frequently used, as their larger coating area and use of higher sorbent volumes enables greater sensitivity. The literature contains numerous reviews detailing developments in and applications of SPME [23–30]. In addition, there is an ever-growing trend showing that the SPME technique is increasingly used for sample preparation prior to analysis in recent years (Figure 1).



**Figure 1.** The number of articles that include SPME as a sample preparation method. Numbers are based on PubMed searching for “SPME” or “solid-phase microextraction” in titles and/or abstracts.

In brief, SPME is an equilibrium-based technique that extracts via free concentration. In complex matrices containing macromolecules (e.g., proteins), small species equilibrate with the macromolecules so that they are partially bound and partially free. In general, the more hydrophobic the compound, the higher the binding and the lower the free concentration; therefore, one would expect SPME to perform poorly in recovering these species. However, the coatings most commonly used in bioanalysis, such as C18 or mixed-mode coatings, have a high affinity toward hydrophobic compounds, thus compensating for the aforementioned phenomenon. The opposite situation is observed for hydrophilic metabolites, thereby allowing SPME to provide balanced coverage of the compounds. Another feature of SPME that should be emphasized is its capacity for capturing unstable species, which is made possible by its ability to extract small compounds while excluding large molecules. The chemistry and porosity of commonly used SPME coatings restrict the penetration of macromolecules into the sorbent, which protects the absorbed metabolites

from enzymatic degradation. Moreover, due to the small size of probes (e.g., fibers), SPME affords minimal invasiveness and allows the same organ to be sampled several times without damaging the tissue. Conventional sample preparation methods demand the collection and homogenization of tissue, followed by the extraction of analytes with aqueous and organic solvents. Such techniques are widely used; however, their complex protocols make them unsuitable for on-site extraction. Additionally, tissue collection usually restricts analysis to a single sampling because repeated biopsy carries the risk of tissue damage and other side effects [31]. Because of SPME's unique features—which include, but are not limited to, balanced analyte coverage, minimal invasiveness [32], lack of physical sample consumption [33], the ability to extract labile metabolites and determine free (i.e., active) concentrations of metabolites [34], and the biocompatibility of SPME probes—new applications are continually being tested and proposed. As mentioned above, one of the major challenges in transplant surgery is assessing graft quality and function in order to minimize the risk of post-transplant organ injury and rejection. Given the above-discussed possibilities, SPME has been proposed in various studies as an effective tool for determining compounds of significance during graft function assessment, or for the chemical profiling of grafts undergoing various preservation protocols. The recent literature contains numerous papers detailing the use of SPME and omics approaches to assess the quality of organs intended for transplantation. As such, this review summarizes how solid-phase microextraction addresses the analytical challenges associated with different matrices utilized in the peri-transplant period (Figure 2) and discusses its potential as diagnostic tool in future work. The main assumptions of the cited studies are summarized in Table 1.



**Figure 2.** Exemplary application of solid-phase microextraction in solid organ transplantation. Details are discussed in the text.

**Table 1.** Applications of solid-phase microextraction in solid organ transplantation.

Monitored Organ	Biological Specimen	Sampling Mode (Ex Vivo/In Vivo; Head-Space/Direct Immersion HS/DI)	Device Geometry and Coating Chemistry	Target Analyte	Comments	Reference
lung	bronchoalveolar lavage fluid (BALF) (human)	ex vivo; DI	TFME, PAN-C18	cholic acid (CA), deoxycholic acid (DCA)	<ul style="list-style-type: none"> <li>comparison of the results with total bile acids concentration performed by enzymatic assay</li> </ul>	[35]
lung	bronchoalveolar lavage fluid (BALF) (human)	ex vivo; DI	fiber, mix-mode	untargeted profiling	<ul style="list-style-type: none"> <li>separation of patients with TBA &lt; and &gt; TBA &gt; 0.05 mmol/L driven by bile acids, steroid, fatty aldehydes, fatty alcohol, prenol lipids, fatty amide, fatty acids suggested re-consideration TBA cut-off value for “healthy/sick” BALF samples</li> </ul>	[35]
lung	bronchoalveolar lavage fluid BALF and blind bronchial aspirate (BBA) (human)	ex vivo; HS	fiber, DVB/CAR/PDMS	untargeted profiling	<ul style="list-style-type: none"> <li>20 compounds selected with support vector machine (SVM) model resulted in a sensitivity of 0.63, specificity of 0.94, positives and negatives predictive value of 0.87 and 0.80, respectively;</li> <li>no relationship between the type of donation, cause of death or time of ischemia and VOC profile was statistically significant;</li> <li>donor BMI correlated with the VOC pattern</li> </ul>	[36]
liver	plasma (human)	ex vivo; DI	TFME, PAN-WCX	rocuronium bromide (ROC), tranexamic acid (TXA)	<ul style="list-style-type: none"> <li>testing drugs as potential markers of early graft dysfunction using living donors (LD) and heart beating brain dead donors (HBD);</li> <li>ROC showed lower liver clearance in HBD group;</li> <li>TXA showed no difference in renal clearance in HBD and LD, but in both cases it was lower than normal; supported by analysis of known biomarkers of liver injury</li> </ul>	[37]
liver	plasma (human)	ex vivo; DI	TFME, HLB	untargeted profiling	<ul style="list-style-type: none"> <li>searching biomarkers of early graft dysfunction;</li> <li>HBD and LD groups discriminated by oxidized lipids and bile acids</li> </ul>	[37]
liver	bile (pig)	ex vivo; DI	TFME, HLB	untargeted profiling	<ul style="list-style-type: none"> <li>evaluation of the metabolomic profile of bile from livers preserved via SCS and NEVLP: Bile produced in the SCS-preserved livers was characterized by increased levels of metabolites such as CDCA, AA, and 5S-HETE, as well as saturated and monounsaturated LPCs. assessment of the effect of the organ's ischemic time on the composition of bile: changes mainly in amino acids and lipids, including bile acids and steroid compounds, along with their derivatives</li> </ul>	[38]

Table 1. Cont.

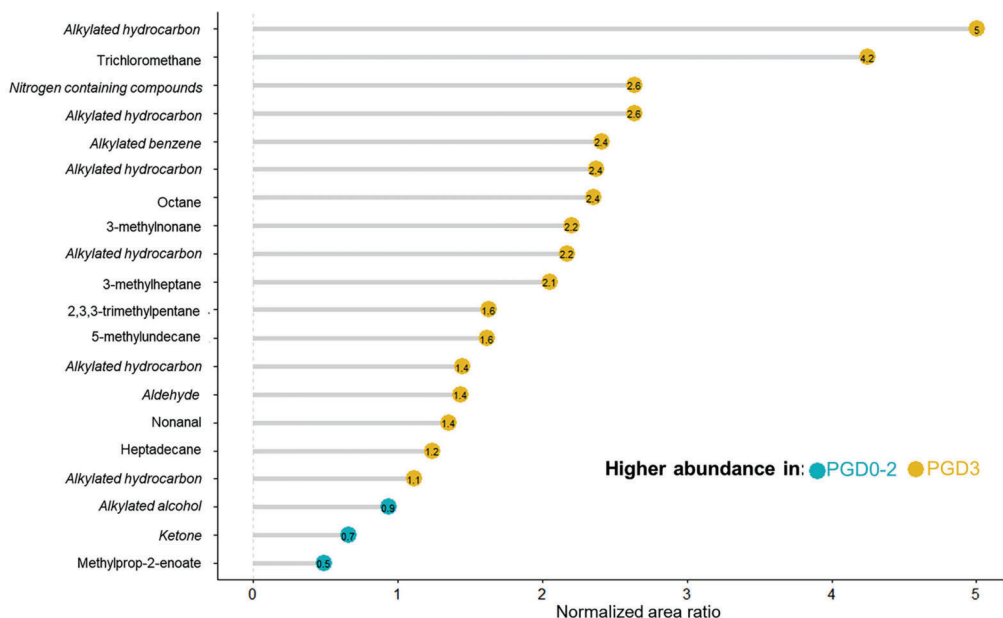
Monitored Organ	Biological Specimen	Sampling Mode (Ex Vivo/In Vivo; Head-Space/Direct Immersion HS/DI)	Device Geometry and Coating Chemistry	Target Analyte	Comments	Reference
liver	bile (pig)	ex vivo; DI	TFME, C18	glycocholic acid (GCA), taurocholic acid (TCA), glycochenodeoxycholic acid (GCDCa), taurothiocholic acid (TLCA), glycooursodeoxycholic acid (GUDCA), taurooursodeoxycholic acid (TUDCA), glycodeoxycholic acid (GDCA), cholic acid (CA), chenodeoxycholic acid (CDCA), deoxycholic acid (DCA), hyocholic acid (HCA), taurochenodeoxycholic acid (TUDCA), ursodeoxycholic acid (UDCA)	<ul style="list-style-type: none"> <li>evaluation of individual bile acid profile of bile samples in the peri-transplant period: the conjugated forms of bile acids were significantly predominant in the bile samples compared to unconjugated forms;</li> <li>high concentration of TCA was characterized the perfusion period and they remained high during reperfusion in the 90'/DCD group; prolonged ischemia caused an increase in TDCA and GDCA levels in the first days after transplantation compared to HBD group</li> </ul>	[39]
lung, liver	tissue (pig)	ex vivo, in vivo; DI	fiber, mix-mode	untargeted profiling	<ul style="list-style-type: none"> <li>evaluation of the method's efficiency, the utilized storage and transportation conditions;</li> <li>in the extracts from ex vivo sampling, the absence of some labile metabolites (e.g., itaconic acid, hypoxanthine, lactaldehyde or hydroxyacetone), but the presence of metabolites recognized as the products of the primary metabolite degradation (e.g., diacylglycerol) were observed;</li> <li>in vivo sampling followed by on-fiber storage was the most convenient strategy;</li> <li>the best sensitivity was observed for the longer coating, while reproducibility was better for the two shorter coatings, which was likely due to the heterogeneity of the liver</li> </ul>	[40]
lung, liver	tissue (pig)	ex vivo, in vivo; DI	fiber, mix-mode	methylprednisolone (MP)	<ul style="list-style-type: none"> <li>monitoring drugs routinely used during the transplantation procedure as markers of changes in liver function;</li> <li>methylprednisolone was only present in non-ischemic organs</li> </ul>	[41]
lung, liver	tissue (pig), perfusate	ex vivo, in vivo; DI	fiber, mix-mode	untargeted profiling	<ul style="list-style-type: none"> <li>evaluation of changes of the metabolic profiling of lungs at different stages of their transplantation procedure;</li> <li>monitoring metabolites in perfusate circulating throughout the graft in a closed circuit as a non-invasive approach for monitoring graft function during perfusion</li> </ul>	[41]

Table 1. Cont.

Monitored Organ	Biological Specimen	Sampling Mode (Ex Vivo/In Vivo; Head-Space/Direct Immersion HS/DI)	Device Geometry and Coating Chemistry	Target Analyte	Comments	Reference
kidney	tissue (rabbit)	ex vivo; DI	fiber, mix-mode	untargeted profiling	<ul style="list-style-type: none"> <li>assessment of the effect of prolonged ischemia and the accompanying oxidative stress affected the condition of kidneys subjected to static cold storage;</li> <li>a significant change in the metabolic profile of the kidney over the first 4 h of storage;</li> <li>the most pronounced alterations were observed in the levels of essential amino acids, which changed depending on exposure to the ischemic milieu, and purine nucleosides, which are associated with various metabolic pathways involved in the production of reactive oxygen species (ROS)</li> </ul>	[42]
					<ul style="list-style-type: none"> <li>presentation of a metabolomic and lipidomic protocol for untargeted analyses for graft quality assessment</li> </ul>	
					<ul style="list-style-type: none"> <li>evaluation of kidney quality during the transplantation procedure with particular emphasis on HBD and DCD donors; revealed changes in purine and LPC levels between the HBD and DCD groups;</li> <li>level of certain amino acids and LPC were correlated with the organ's warm ischemia duration;</li> <li>the decreased PC/PE ratio in the DCD organs during reperfusion</li> </ul>	
kidney	tissue (pig)	ex vivo, in vivo; DI	fiber, mix-mode	untargeted profiling	<ul style="list-style-type: none"> <li>comparison of the effects of SCS, NEVKP, and HMP on the lipidomic profile of a kidney graft;</li> <li>the preservation temperature had a more significant impact on the lipidomic profile than its mechanical characteristics;</li> <li>higher levels of CARs, PCs and PEs (including ether-linked), PIs, TCs, most LPCs, and LPIs were observed in the hypothermic preservation group;</li> <li>lower accumulation of pro-inflammatory lipids during NEKVP method</li> </ul>	[45]
heart	tissue (pig), perfusate	ex vivo, in vivo; DI	fiber, mix-mode, C18, HLB	untargeted profiling	<ul style="list-style-type: none"> <li>assessment of protocol feasibility for metabolomic and lipidomic profiling of changes associated with declines in myocardial function during ESHF;</li> <li>comparison of the results obtained with SPME and those obtained via solid-liquid extraction (SLE) performed on biopsies</li> </ul>	[5]
heart	tissue (human), perfusate	ex vivo; DI	fiber, mix-mode, C18	untargeted profiling	<ul style="list-style-type: none"> <li>validation of the experimental protocol and the metabolomic findings during ESHF</li> </ul>	[5]

## 2. Monitoring Graft Function in Donor Specimens

One of the first protocols involving both thin-film and solid-phase microextraction explored the diagnostic value of bronchoalveolar lavage fluid (BALF) in lung transplant patients [35]. The presence of bile acids (BAs) and pepsin in BALF is a marker of the aspiration of gastric components, which carries a risk of obliterative bronchiolitis and allograft dysfunction. In routine clinical practice, the total concentration of bile acids is measured using an enzymatic assay; however, this method is not specific and might be associated to cross-reactions. Mass spectrometry coupled to liquid chromatography is capable of successfully measuring individual bile acids. As such, Bessonneau et al. combined this approach with PAN-C18-coated thin-film microextraction (TFME) blades for the determination of cholic acid (CA) and deoxycholic acid (DCA), which served as representatives of di- and trihydroxy bile acids, respectively. Their method-validation results showed good figures of merit, with an RSD < 4% and an LOQ of 0.02  $\mu\text{mol/L}$ . In addition, the results obtained for the clinical samples revealed that the proposed method was able to detect the investigated bile acids at concentrations below the LOQ. The summary concentration of the two acids ranged from 0.02 to 0.06  $\mu\text{mol/L}$  and was correlated with the results of the enzymatic assay (TBA 0.01 to 0.24  $\mu\text{mol/L}$ ). While no correlation was found ( $R^2 = 0.11$ ) when all of the studied samples were included in the comparison, the removal of one patient's data resulted in a correlation coefficient of 0.92. BALF samples were also extracted using fibers with a mix-mode coating, followed by untargeted profiling on a high-resolution orbitrap mass spectrometer. Here, the results revealed that of the few thousand detected features, three belonged to bile acids, with 7-ketolithocholic acid as the predominant type (ca. 94% of all BAs). The summary peak area of the identified bile acids correlated with the TBA enzymatic assay data ( $R^2 = 0.86$ ). Interestingly, the principal component analysis plot showed clear separation between two groups of patients, which was characterized by the TBA value < and > 0.05  $\mu\text{mol/L}$ . This separation was driven by the 13 metabolites in the "TBA > 0.05  $\mu\text{mol/L}$ " group but was absent in the other. Among these compounds were three bile acids, one steroid, three fatty aldehydes, one fatty alcohol, two prenol lipids, one fatty amide, and two fatty acids ( $p$ -value < 0.01 and fold change  $\geq 5$ ). These results highlighted the importance of re-considering the TBA cut-off value for "healthy/sick" BALF samples, which is currently set for 0.2  $\mu\text{mol/L}$ . Furthermore, Bessonneau et al.'s work also demonstrated the potential diagnostic value of metabolites apart from BAs in assessing the risk of obliterative bronchiolitis and lung allograft dysfunction. Elsewhere, Stefanuto et al. proposed a different SPME-based approach for identifying PGD after lung transplantation in BALF and blind bronchial aspirate (BBA) samples [36]. To this end, the authors employed 2 cm divinylbenzene/carboxen/polydimethylsiloxane (DVB/CAR/PDMS) fibers to extract volatile compounds from the headspace of 20 mL headspace vial that contained 500  $\mu\text{L}$  of lung fluid samples and was sealed with a PTFE/silicone cap. The extracted analytes were then analyzed via two-dimensional gas chromatography coupled to a time-of-flight mass spectrometer (HS-SPME-GC  $\times$  GC-TOFMS). In the first step, samples obtained at the end of transplant surgery were profiled and the VOC patterns of patients who later developed severe PGD and those who either did not develop PGD, or who only developed low-grade PGD (0-2), were compared. In the next step, a support vector machine (SVM) with a linear kernel on the training set model was built to select features discriminating the studied groups at the first 6 h after transplantation. For 20 selected compounds, the SVM model provided sensitivity of 0.63, specificity of 0.94, and positive and negative predictive value of 0.87 and 0.80, respectively. The majority of the detected compounds were up-regulated in grade 3 PGD (Figure 3).



**Figure 3.** Ratio of the normalized areas of the 20 selected features. Reprinted from [36] with permission under a Creative Commons Attribution 4.0 International License.

Given the complexity of the factors influencing the VOC profiles, the authors employed a multivariate analysis of variance (MANOVA) to assess how clinical risk factors influenced the VOC patterns. The results showed no statistically significant relationships between the VOC profile and the type of donation, cause of death, or time of ischemia. Instead, the donor's body mass index (BMI) was found to be most strongly correlate with the VOC pattern ( $p < 0.05$ ). From a biochemical point of view, the results indicated the potential importance of lipid peroxidation in the development of PGD; from a diagnostic point of view, the findings demonstrated that the analysis of volatile compounds in lung fluids may be applicable in clinical practice.

Yang et al. tested a completely different hypothesis in liver transplant patients [37]. In this work, they sought to determine the concentrations of two drugs (i.e., rocuronium bromide (ROC) and tranexamic acid (TXA)) routinely used during transplant surgery in order to evaluate liver and kidney performance in patients receiving grafts from living donors (LD) or heart beating brain dead donors (HBD). Although the transplanted grafts in living donors were smaller (<50%) compared to those from the HBDs (full size), the latter group of grafts may result in worse outcomes due to the longer ischemia times required for graft preservation. Rocuronium bromide is primarily eliminated through hepatobiliary excretion (up to 90%), with the kidneys excreting only about 10%. In contrast, the kidneys are the main route through which TXA is eliminated (>95%). Therefore, the simultaneous monitoring of these two drugs can potentially provide insight into the development of multiorgan dysfunction in the neohepatic phase. The extractions were performed using high-throughput TFME with stainless steel blades coated with polyacrylonitrile (PAN) and weak cation exchange (WCX) particles according to a previously published method [46]. The WCX particles were selected to compensate for the characteristics of ROC; specifically, as a quaternary ammonium compound, sample preparation for ROC can be challenging due to its propensity to interact with glass surfaces. Moreover, prior studies have reported that due to its instability in collected blood samples, ROC analysis requires sample acidification, which may affect the analysis of other metabolites and drugs from the same sample. The

method proposed by Gorynski et al. [46] enabled the effective extraction of both analytes of interest without the need for matrix modification. The obtained data was further used to build pharmacokinetic profiles of the targeted drugs using a two-compartment model. In the case of ROC, liver clearance was lower in the HBD group, while the LD group showed similar clearance to that observed in people with normal liver function. While the comparison of TXA renal clearance did not reveal any significant differences between the HBD and LD cohorts, it was found to be slightly lower than normal in both cases. In addition to targeted drug analysis, TFME coated with hydrophilic-lipophilic balance (HLB) particles was applied for the metabolomic profiling of plasma. The HBD and LD groups formed separate clusters, with oxidized lipids and bile acids being identified as the main discriminating metabolites. The SPME-LC-MS measurements were supplemented by determining the relative expression of miR-122, miR-148a, and  $\gamma$ -glutamyltranspeptidase (GGT), a known biomarker of liver injury. Indeed, GGT levels were significantly higher in HBD patients, suggesting that this increase may have been the result of cold ischemia time (CIT) and may result in injury to the sinusoidal epithelial cells. The study's findings demonstrated that ROC analysis may be a good indicator of early liver function, while TXA clearance may be a promising marker of the granular filtration rate and, consequently, chronic or acute renal injury, which may lead to early graft dysfunction. On the other hand, metabolomic profiling may help to develop a more detailed understanding of the mechanisms underlying the development of graft injury, in addition to identifying potential diagnostic biomarkers.

Łuczykowski et al. developed a high-throughput sample-analysis protocol based on TFME to evaluate the metabolomic profiles of bile samples from porcine model donors with mild (HBD) and moderate warm ischemia (DCD) grafts that had been subjected to SCS or normothermic ex vivo liver perfusion (NEVLP) prior to transplantation [38]. Extraction was performed using steel blades coated with an HLB sorbent, and each sample consisted of 10  $\mu$ L of bile diluted in phosphate-buffered saline (1:99). The extraction and desorption times were 120 min, and an ACN:H<sub>2</sub>O (80:20, *v:v*) mixture was selected as the desorption solution. The findings showed that the bile produced in the SCS-preserved livers was characterized by increased levels of chenodeoxycholic acid, arachidonic acid, and 5S-hydroxyeicosatetraenoic acid, as well as saturated and monounsaturated LPCs, which may be due to changes in the bile acid synthesis pathways and organ inflammation. In addition, the metabolomic profile of bile produced by the SCS-preserved livers changed after a short-term (30 min) ischemia (22 and 7 statistically significant differentiating compounds for reperfusion and POD, respectively), while significant changes only appeared in the NEVLP group after 90 min. These metabolites primarily consisted of amino acids and lipids, including bile acids and steroid compounds, along with their derivatives. Moreover, a linear relationship was observed between levels of lipids from the LPC group and the organ ischemia time. Ultimately, Łuczykowski et al. identified a number of metabolites worth considering in future targeted and fully validated analyses as potential markers of changes occurring in preserved grafts. Based on the above experiment, Łuczykowski et al. conducted a subsequent pilot study to assess whether BA concentrations in bile are correlated with changes in the transplanted organ [39]. Here, sample preparation was performed via TFME using C18 sorbent as the extraction phase and methanol as the desorption solvent. Due to the high concentration of BA in this biological matrix, dilution factors of 100x and 20,000x were used to cover a wide range of primary and secondary BA concentrations. Conjugated forms of bile acids (with taurine or glycine) were significantly predominant in the bile samples compared to unconjugated forms. High concentrations of taurocholic acid characterized the perfusion period and they remained high during reperfusion in the 90'DCD group. Furthermore, prolonged ischemia caused an increase in taurodeoxycholic ( $15,87 \pm 8,22$  vs.  $2,83 \pm 0,57$   $\mu$ g/mL) and glycodeoxycholic acid ( $135,82 \pm 78,5$  vs.  $18,56 \pm 4,57$   $\mu$ g/mL) levels in the first days after transplantation compared to the HBD group.

### 3. Monitoring Graft Function by Direct Analysis of Graft

As noted above, the wide range of SPME applications is largely attributable to the tremendous variability of the devices. One unique feature making SPME ideal for *in vivo* and *in situ* analyses of intact tissues and organs is its low invasiveness when using the fiber geometry. There are other restrictions and requirements related to *in vivo* sampling, particularly when human subjects are involved in the studies, such as biocompatibility, single use of the devices, and sterilizability in the conditions established in the given hospital (in most cases, via autoclaving or ethylene oxide sterilization). As previously detailed, SPME is a safe and minimally invasive tissue sampling technique capable of providing coverage for a broad spectrum of metabolites. Moreover, the miniaturized nature of the device enables simultaneous analysis in different areas of the organ and more importantly, multiple analyses of the same organ over time.

The very first trials to use SPME for the direct extraction of metabolites from organ grafts focused on evaluating not only the method's efficiency, but also the utilized storage and transportation conditions [40]. For the latter objective, the authors used pig liver grafts undergoing NEVLP. Six 7 mm mix-mode fibers were used to perform extractions on-site during graft perfusion, while three identical fibers were used to perform extractions from liver fragments, which had been collected at the beginning of the medical procedure and stored at  $-80^{\circ}\text{C}$  after being transported to the laboratory in dry ice. Immediately after sampling, the six fibers were divided into two groups. The first group was subjected to desorption on-site, with the resultant extracts being transported to the laboratory and stored using the same conditions described for the tissue, while the second group of fibers was secured in the empty vials for transportation and storage. As expected, the results revealed marked differences between the three approaches. The authors suggested that the discrepancies between on-fiber storage and *in vivo* sampling followed by extract storage may have been due to the partial evaporation of the desorption solvent, and thus, the preconcentration of the metabolites. To address this issue, complete evaporation and reconstitution in lab would be advisable. On the other hand, the *in vivo* vs. *ex vivo* sampling was characterized by differences in the presence of metabolites. For instance, in the extracts from *ex vivo* sampling, the authors observed the absence of some labile metabolites (e.g., itaconic acid, hypoxanthine, lactaldehyde or hydroxyacetone), but the presence of metabolites recognized as the products of the primary metabolite degradation (e.g., diacylglycerol). Although the untargeted nature of these studies precluded the strict monitoring of the extracted metabolites' stability, the results indicated that *in vivo* sampling followed by on-fiber storage was the most convenient strategy. With regards to method performance, the authors tested three fiber coating lengths (i.e., 4, 7, and 15 mm) for 30 min extractions from liver tissue. The best sensitivity was observed for the 15 mm coating, while reproducibility was better for the two shorter coatings, which was likely due to the heterogeneity of the liver. When selecting the optimum sorbent length, it is very important to carefully consider all aspects of the experiment, including: the main goal of the experiment (spatial resolution studies e.g., characterization of the specific region such as malignant lesion vs. obtaining average information about the studied area); characteristics of the sampled tissue (homo- vs. heterogenous); size of the studied area; and the properties and concentrations of the compounds of interest. Furthermore, in clinical environments, particularly during surgical procedures, restrictions related to sampling time are very challenging from an analytical perspective. Specifically, while the method's overall sensitivity largely depends on the coating length and extraction time, both parameters must be as small as possible to ensure that the method is minimally invasive and disturbs the subject as little as possible. For that reason, the authors of the above study selected probes with a 7 mm coating for use in subsequent experiments. Another practical aspect discussed in [40] was the option of using needle-assembled fibers, which enable penetration through harder tissues such as muscles or barriers (e.g., pleura). Although this approach is slightly more invasive, it is still less so than a regular biopsy, while continuing to allow for sampling with no physical tissue consumption. The extraction coverage results

showed that the proposed method provided coverage ranging from 239 molecular features in negative ionization mode for lung sampling to 1580 in positive ionization mode for liver samples, thus confirming the excellent efficiency reported previously for SPME. As emphasized in previous metabolomics studies using SPME, the number and range of the metabolites extracted via SPME is lower compared to conventional sample preparation methods based on tissue collection, homogenization, and multi-solvent extraction, because SPME is an equilibrium technique that extracts via free fraction of metabolites. Thus, only metabolites present in their free form are available for extraction. This feature can be either an advantage or a disadvantage depending on the biological information the researcher wants to obtain from their study. If the main goal is to identify the active molecules involved in a given mechanism, then SPME is a good choice; however, if the objective is to characterize all molecules in the studied system independently based on their biological activity, then more conventional strategies should be considered. The optimized protocol described in [40] was subsequently used in pilot studies conducted on liver and lungs, wherein sampling times of 20 and 30 min were used, respectively [41]. Similar to the previously described studies on ROC and TXA [37], these studies showed that monitoring drugs routinely used during the transplantation procedure may shed light on changes in liver function. The authors found that methylprednisolone was only present in non-ischemic organs, while no drug metabolites were detected in livers subjected to 38 and 78 min of warm ischemia time (WIT), thus suggesting impaired organ function. This hypothesis was supported by observed alterations in endogenous compounds from the Krebs, pentose cycles, and TCA pathway. The metabolic profiling of lungs at different stages of their transplantation procedure (i.e., CIT, ex vivo perfusion (EVLP) and after revascularization) revealed clear differences between the subsequent groups of samples and enabled the tentative identification of metabolites that have been up- and down-regulated under different conditions and factors. In addition to organ sampling, the authors proposed monitoring metabolites in perfusate circulating throughout the graft in a closed circuit as a non-invasive approach for monitoring graft function during perfusion. In addition, this experiment bypassed the need for sample withdrawal, as extraction was performed by exposing the SPME needle-assembled fibers to the perfusate by inserting them into the three-way stopcock—which was equipped with a Luer-lock connected to the perfusate line—for 2 min. In this study, all sampling was conducted in triplicate. Unsupervised analysis of the data showed clustering of the samples at different perfusion time points, indicating the occurrence of alterations in the studied organs, mainly involving amino acids, fatty acids, and their derivatives.

Stryjak et al. conducted a proof-of-concept study to demonstrate this technology's suitability for characterizing changes during the cold preservation of kidneys [42]. Specifically, Stryjak et al. assessed how prolonged ischemia and the accompanying oxidative stress affected the condition of kidneys subjected to static cold storage using a rabbit model. Extraction was performed by inserting duplicate SPME probes (4 mm length mixed-mode extraction phase) into each kidney cortex for 30 min at 5 different time points: immediately following the removal of kidneys, and after 2, 4, 6, and 21 h of cold preservation. The results revealed a significant change in the metabolic profile of the kidney over the first 4 h of storage. The most pronounced alterations were observed in the levels of essential amino acids, which changed depending on exposure to the ischemic milieu, and purine nucleosides, which are associated with various metabolic pathways involved in the production of reactive oxygen species (ROS). Among the identified metabolites, the presence of adenosine and adenosine monophosphate was notable, as this indicated the adenosine-dependent nature of the mechanisms underlying preconditioning and protection against renal ischemia. Other notable identified metabolites also included inosine, hypoxanthine, and xanthine. Furthermore, the short half-life of some of the identified metabolites highlights this analytical approach's usefulness for capturing unstable and short-lived compounds. Moreover, Stryjak et al. extended the existing protocol for use in lipidomic studies and optimized it for in vivo studies on a porcine model and in human subjects [43].

Since biological applications necessitate a compromise between the method's sensitivity and repeatability and the restrictions inherent to medical procedures, it is necessary to determine the optimal extraction phase length and extraction time. Although equilibrium extraction provides the highest sensitivity, the authors decided to use pre-equilibrium conditions for safety reasons, as this would avoid affecting the operation's total duration. The findings confirmed that a 10-min extraction using probes coated with 7 mm of mix-mode (MM) sorbent provided sufficient sensitivity for a broad spectrum of metabolites, enabling the effective profiling of the renal cortex during ex vivo kidney perfusion, in vivo prior to organ harvest, and in vivo after revascularization. The developed protocol used 100 µL of desorption solutions consisting of ACN:H<sub>2</sub>O (80:20, *v:v*) and IPA:MeOH (50:50) for the metabolomic and lipidomic analyses, respectively. The SPME method's potential for evaluating kidney quality during the transplantation procedure was demonstrated in a pig autotransplantation model, with particular emphasis on HBD and DCD donors [44]. For both donor types, extractions were performed in vivo prior to retrieval; after 1 h, 3 h, 5 h, and 7 h of perfusion; and again in vivo immediately after revascularization. Additionally, the DCD kidneys were also sampled after 45 min and 2 h of warm ischemia. Direct tissue sampling was carried out for 30 min using probes coated with 7 mm of MM extraction phase. The utilized metabolomic and lipidomic platforms enabled the identification of a set of metabolites that may have diagnostic value in monitoring organ function before transplantation. The metabolomic data revealed changes in purine levels between the HBD and DCD groups. The accumulation of adenosine observed during perfusion in the HBD group may be associated with its protective effects against ischemia-reperfusion injury IRI, while the reduced levels of inosine observed during reperfusion in the DCD group may be associated with a worse prognosis after transplantation. In addition, changes in the levels of certain amino acids were found to be correlated with the organ's warm ischemia duration. For instance, increased levels of alanine and valine are associated with impaired organ function, can be a sensitive discriminator of ischemia, and may lead to less favourable outcomes. On the other hand, the decrease in histidine concentrations during WIT may have resulted from ongoing inflammatory processes and the development of oxidative stress. The lipidomic portion of the work revealed differences in LPC levels between the HBD and DCD organs and an upward trend in the level of these metabolites during WIT. Although the exact mechanisms governing the effects of LPC on the graft remain unclear, this group of lipids may be associated with increased oxidative stress, increased inflammatory responses, and the remodelling of cell membranes. Furthermore, the decreased PC/PE ratio in the DCD organs during reperfusion may be associated with impaired liver regeneration, alterations in energy metabolism, increased cell leakage, and endoplasmic reticulum stress. This research was continued by Warmużińska et al., who used an SPME chemical biopsy to compare the effects of SCS, normothermic ex vivo kidney perfusion (NEVKP), and hypothermic machine perfusion (HMP) on the lipidomic profile of a graft in a renal DCD autotransplantation porcine model [45]. Similar to Stryjak et al.'s study, 7 mm length MM fibre probes were employed to perform 30 min direct extractions from the kidney cortex. The samples were harvested in vivo before retrieval; after 1 h and 2 h of warm ischemia; after 1 h, 3 h, 5 h, and 7 h of perfusion; in vivo immediately after reperfusion; and in vivo under deep anesthesia at the time of sacrifice on postoperative day 3. The findings indicated that the preservation temperature had a more significant impact on the lipidomic profile than the mechanical character of perfusion. Higher levels of CARs, PCs and PEs (including ether-linked), PIs, TGs, most LPCs, and LPEs were observed in the hypothermic preservation group, which may be related to IRI, mitochondrial dysfunction, and oxidative stress. The obtained results also revealed that the NEKVP method may have a beneficial effect on graft function. Specifically, NEKVP-perfused kidneys showed lower accumulation of pro-inflammatory lipids, which contributes to improved graft function after perfusion compared to hypothermic preservation methods.

In one of the most recent studies on this topic, SPME was applied to sample myocardium during prolonged ex situ heart perfusion (ESHP) [5]. In this work, a porcine

model was used for protocol development and exploratory analysis, while two explanted human hearts that had been declined for transplantation and used for scientific purposes were treated as validity grafts. In the porcine model, sampling was conducted at various in vivo and ex vivo stages (i.e., heart beating before harvesting the organ and during perfusion, respectively). The human hearts were only monitored during the ESHP procedure. The untargeted screening covered both the polar metabolome and the lipidome, thereby offering a comprehensive insight into the molecular changes taking place within the examined organs. From a biological perspective, increased metabolite dysregulation in response to prolonged organ preservation indicated the presence of inflammatory processes, the progression of mitochondrial oxidative stress, the disturbance of mitochondrial bioenergetics, and the dysregulation of many lipids, with increases in the level of species negatively impacting the tissue. An especially interesting component of the study was the authors' comparison of the results obtained with SPME and those obtained via solid-liquid extraction (SLE) performed on biopsies collected from the same hearts that had been sampled with SPME probes. The results confirmed that SLE enables more comprehensive analyte coverage, particularly with respect to lipid species that are integrated components of cell membranes, and that are not present in free form or are present at concentrations that are too low to be detected by SPME. In contrast to SLE, SPME proved to be more effective in detecting unstable and intermediate compounds and in offering better sample clean-up, which enabled the detection of low abundance species and a greater variety of lipid subclasses. In SLE, sample homogenization followed by solvent extraction releases and dissolves compounds bound to macromolecules located in different organelles and fractions of the cells and tissues, thus providing higher sensitivity; however, this improved sensitivity comes at the cost of compromised extract clean-up and the production of matrix effects.

#### 4. Conclusions

This review's up-to-date survey of SPME-based studies focusing on graft monitoring in the peri-transplant period demonstrates this technology's profound potential for use in the diagnostic process. The ability to process different biofluid samples regardless of their complexity can be effectively exploited to monitor the state of the graft after surgery when access to the organ is very limited or impossible. On the other hand, the minimally invasive nature of SPME fibres creates the unique opportunity to directly monitor biochemical changes occurring in the graft over the entire period of transplantation (i.e., "from donor to recipient"). Furthermore, untargeted studies, particularly on well-controlled animal models, can lead to a better understanding of the mechanisms underlying organ injury and rejection, in addition to identifying metabolites with potential diagnostic value. Considering the fact that SPME devices have been directly coupled with stand-alone instruments (e.g., mass spectrometers) in numerous studies, it can be envisioned that such strategies can be used for determination of discovered biomarkers. Given SPME's short sample preparation time and ability to perform on-site extractions without the need for sample consumption, combined with its ability to provide the rapid, quantitative, and sensitive determination of target analytes, the use of this technology to obtain results in close to real time appears to be an attainable goal.

**Author Contributions:** Writing—original draft preparation, K.L., N.W. and B.B.; writing—review and editing, K.L., N.W. and B.B.; funding acquisition, B.B. All authors have read and agreed to the published version of the manuscript.

**Funding:** This study was funded by National Science Center 2017/27/B/NZ5/01013.

**Data Availability Statement:** Not applicable.

**Conflicts of Interest:** The authors declare no conflict of interest.

## References

1. Kvietkauskas, M.; Zitkute, V.; Leber, B.; Strupas, K.; Stiegler, P.; Schemmer, P. The Role of Metabolomics in Current Concepts of Organ Preservation. *Int. J. Mol. Sci.* **2020**, *21*, 6607. [\[CrossRef\]](#) [\[PubMed\]](#)
2. Warmuzińska, N.; Łuczykowski, K.; Bojko, B. A Review of Current and Emerging Trends in Donor Graft-Quality Assessment Techniques. *J. Clin. Med.* **2022**, *11*, 487. [\[CrossRef\]](#) [\[PubMed\]](#)
3. Bruinsma, B.G.; Sridharan, G.V.; Weeder, P.D.; Avruch, J.H.; Saeidi, N.; Özer, S.; Geerts, S.; Porte, R.J.; Heger, M.; Van Gulik, T.M.; et al. Metabolic Profiling during Ex Vivo Machine Perfusion of the Human Liver. *Sci. Rep.* **2016**, *6*, 22415. [\[CrossRef\]](#) [\[PubMed\]](#)
4. Looby, N.; Roszkowska, A.; Ali, A.; Bojko, B.; Cypel, M.; Pawliszyn, J. Metabolomic Fingerprinting of Porcine Lung Tissue during Pre-Clinical Prolonged Ex Vivo Lung Perfusion Using in Vivo SPME Coupled with LC-HRMS. *J. Pharm. Anal.* **2022**, *12*, 590–600. [\[CrossRef\]](#) [\[PubMed\]](#)
5. Olkowicz, M.; Ribeiro, R.V.P.; Yu, F.; Alvarez, J.S.; Xin, L.; Yu, M.; Rosales, R.; Adamson, M.B.; Bissoondath, V.; Smolenski, R.T.; et al. Dynamic Metabolic Changes During Prolonged Ex Situ Heart Perfusion Are Associated With Myocardial Functional Decline. *Front. Immunol.* **2022**, *13*, 859506. [\[CrossRef\]](#)
6. Mihaylov, P.; Mangus, R.; Ekser, B.; Cabrales, A.; Timsina, L.; Fridell, J.; Lacerda, M.; Ghabril, M.; Nephew, L.; Chalasani, N.; et al. Expanding the Donor Pool With the Use of Extended Criteria Donation After Circulatory Death Livers. *Liver Transplant.* **2019**, *25*, 1198–1208. [\[CrossRef\]](#)
7. Beuth, J.; Falter, F.; Pinto Ribeiro, R.V.; Badiwala, M.; Meineri, M. New Strategies to Expand and Optimize Heart Donor Pool: Ex Vivo Heart Perfusion and Donation after Circulatory Death: A Review of Current Research and Future Trends. *Anesth. Analg.* **2019**, *128*, 406–413. [\[CrossRef\]](#)
8. Ravaioli, M.; Maroni, L.; Angeletti, A.; Fallani, G.; De Pace, V.; Germinario, G.; Odaldi, F.; Corradetti, V.; Caraceni, P.; Baldassarre, M.; et al. Hypothermic Oxygenated Perfusion versus Static Cold Storage for Expanded Criteria Donors in Liver and Kidney Transplantation: Protocol for a Single-Center Randomized Controlled Trial. *JMIR Res. Protoc.* **2020**, *9*, e13922. [\[CrossRef\]](#)
9. McGuinness, D.; Mohammed, S.; Monaghan, L.; Wilson, P.A.; Kingsmore, D.B.; Shapter, O.; Stevenson, K.S.; Coley, S.M.; Devey, L.; Kirkpatrick, R.B.; et al. A Molecular Signature for Delayed Graft Function. *Aging Cell* **2018**, *17*, e12825. [\[CrossRef\]](#)
10. Kurosaki, T.; Miyoshi, K.; Otani, S.; Imanishi, K.; Sugimoto, S.; Yamane, M.; Kobayashi, M.; Toyooka, S.; Oto, T. Low-Risk Donor Lungs Optimize the Post-Lung Transplant Outcome for High Lung Allocation Score Patients. *Surg. Today* **2018**, *48*, 928–935. [\[CrossRef\]](#)
11. D'Errico, A.; Riefole, M.; Serenari, M.; De Pace, V.; Santandrea, G.; Monica, M.; de Cillia, C.; Ravaioli, M.; Cescon, M.; Vasuri, F. The Histological Assessment of Liver Fibrosis in Grafts from Extended Criteria Donors Predicts the Outcome after Liver Transplantation: A Retrospective Study. *Dig. Liver Dis.* **2020**, *52*, 185–189. [\[CrossRef\]](#)
12. Dare, A.J.; Pettigrew, G.J.; Saeb-Parsy, K. Preoperative Assessment of the Deceased-Donor Kidney: From Macroscopic Appearance to Molecular Biomarkers. *Transplantation* **2014**, *97*, 797–807. [\[CrossRef\]](#)
13. Moekli, B.; Sun, P.; Lazeyras, F.; Morel, P.; Moll, S.; Pascual, M.; Bühler, L.H. Evaluation of Donor Kidneys Prior to Transplantation: An Update of Current and Emerging Methods. *Transpl. Int.* **2019**, *32*, 459–469. [\[CrossRef\]](#)
14. Kransdorf, E.P.; Stehlik, J. Donor Evaluation in Heart Transplantation: The End of the Beginning. *J. Heart Lung Transplant.* **2014**, *33*, 1105–1113. [\[CrossRef\]](#)
15. Courtwright, A.; Cantu, E. Evaluation and Management of the Potential Lung Donor. *Clin. Chest Med.* **2017**, *38*, 751–759. [\[CrossRef\]](#)
16. Azancot, M.A.; Moreso, F.; Salcedo, M.; Cantarell, C.; Perello, M.; Torres, I.B.; Montero, A.; Trilla, E.; Sellarés, J.; Morote, J.; et al. The Reproducibility and Predictive Value on Outcome of Renal Biopsies from Expanded Criteria Donors. *Kidney Int.* **2014**, *85*, 1161–1168. [\[CrossRef\]](#)
17. Scheuermann, U.; Truong, T.; Seyferth, E.R.; Freischlag, K.; Gao, Q.; Yerxa, J.; Ezekian, B.; Davis, R.P.; Schroder, P.M.; Peskoe, S.B.; et al. Kidney Donor Profile Index Is a Reliable Alternative to Liver Donor Risk Index in Quantifying Graft Quality in Liver Transplantation. *Transplant. Direct* **2019**, *5*, e511. [\[CrossRef\]](#)
18. Jun, H.; Yoon, H.E.; Lee, K.W.; Lee, D.R.; Yang, J.; Ahn, C.; Han, S.Y. Kidney Donor Risk Index Score Is More Reliable Than Kidney Donor Profile Index in Kidney Transplantation From Elderly Deceased Donors. *Transplant. Proc.* **2020**, *52*, 1744–1748. [\[CrossRef\]](#)
19. Parker, W.F.; Thistlethwaite Jr, J.R.; Ross, L.F. Kidney Donor Profile Index (KDPI) Does Not Accurately Predict the Graft Survival of Pediatric Deceased Donor Kidneys. *Transplantation* **2016**, *100*, 2471–2478. [\[CrossRef\]](#)
20. Verhoeven, C.J.; Farid, W.R.R.; De Jonge, J.; Metselaar, H.J.; Kazemier, G.; Van Der Laan, L.J.W. Biomarkers to Assess Graft Quality during Conventional and Machine Preservation in Liver Transplantation. *J. Hepatol.* **2014**, *61*, 672–684. [\[CrossRef\]](#)
21. Cypel, M.; Keshavjee, S. Extending the Donor Pool: Rehabilitation of Poor Organs. *Thorac. Surg. Clin.* **2015**, *25*, 27–33. [\[CrossRef\]](#) [\[PubMed\]](#)
22. Ravaioli, M.; De Pace, V.; Angeletti, A.; Comai, G.; Vasuri, F.; Baldassarre, M.; Maroni, L.; Odaldi, F.; Fallani, G.; Caraceni, P.; et al. Hypothermic Oxygenated New Machine Perfusion System in Liver and Kidney Transplantation of Extended Criteria Donors: First Italian Clinical Trial. *Sci. Rep.* **2020**, *10*, 6063. [\[CrossRef\]](#) [\[PubMed\]](#)
23. Queiroz, M.E.C.; Souza, I.D.d.; Oliveira, I.G.d.; Grecco, C.F. In Vivo Solid Phase Microextraction for Bioanalysis. *TrAC-Trends Anal. Chem.* **2022**, *153*, 116656. [\[CrossRef\]](#)
24. Ji, X. Applications of Headspace Solid-Phase Microextraction in Human Biological Matrix Analysis. *Rev. Anal. Chem.* **2022**, *41*, 180–188. [\[CrossRef\]](#)

25. Hemmati, M.; Nix, C.; Crommen, J.; Servais, A.C.; Fillet, M. Benefits of Microsampling and Microextraction for Metabolomics Studies. *TrAC-Trends Anal. Chem.* **2020**, *127*, 115899. [\[CrossRef\]](#)
26. Riboni, N.; Fornari, F.; Bianchi, F.; Careri, M. Recent Advances in in Vivo Spme Sampling. *Separations* **2020**, *7*, 6. [\[CrossRef\]](#)
27. Filipiak, W.; Bojko, B. SPME in Clinical, Pharmaceutical, and Biotechnological Research—How Far Are We from Daily Practice? *Trends Anal. Chem.* **2019**, *115*, 203–213. [\[CrossRef\]](#)
28. Reyes-Garcés, N.; Gionfriddo, E. Recent Developments and Applications of Solid Phase Microextraction as a Sample Preparation Approach for Mass-Spectrometry-Based Metabolomics and Lipidomics. *TrAC-Trends Anal. Chem.* **2019**, *113*, 172–181. [\[CrossRef\]](#)
29. Godage, N.H.; Gionfriddo, E. A Critical Outlook on Recent Developments and Applications of Matrix Compatible Coatings for Solid Phase Microextraction. *TrAC-Trends Anal. Chem.* **2019**, *111*, 220–228. [\[CrossRef\]](#)
30. Roszkowska, A.; Miękus, N.; Bączek, T. Application of Solid-Phase Microextraction in Current Biomedical Research. *J. Sep. Sci.* **2019**, *42*, 285–302. [\[CrossRef\]](#)
31. Bojko, B. Solid-Phase Microextraction: A Fit-for-Purpose Technique in Biomedical Analysis. *Anal. Bioanal. Chem.* **2022**, *414*, 7005–7013. [\[CrossRef\]](#)
32. Bojko, B.; Looby, N.; Olkowicz, M.; Roszkowska, A.; Kupcewicz, B.; Reck dos Santos, P.; Ramadan, K.; Keshavjee, S.; Waddell, T.K.; Gómez-Ríos, G.; et al. Solid Phase Microextraction Chemical Biopsy Tool for Monitoring of Doxorubicin Residue during in Vivo Lung Chemo-Perfusion. *J. Pharm. Anal.* **2021**, *11*, 37–47. [\[CrossRef\]](#)
33. Thirukumaran, M.; Singh, V.; Arao, Y.; Fujito, Y.; Nishimura, M.; Ogura, T.; Pawliszyn, J. Solid-Phase Microextraction- Probe Electrospray Ionization Devices for Screening and Quantitating Drugs of Abuse in Small Amounts of Biofluids. *Talanta* **2021**, *231*, 122317. [\[CrossRef\]](#)
34. Lendor, S.; Olkowicz, M.; Boyaci, E.; Yu, M.; Diwan, M.; Hamani, C.; Palmer, M.; Reyes-Garcés, N.; Gómez-Ríos, G.A.; Pawliszyn, J. Investigation of Early Death-Induced Changes in Rat Brain by Solid Phase Microextraction via Untargeted High Resolution Mass Spectrometry: In Vivo versus Postmortem Comparative Study. *ACS Chem. Neurosci.* **2020**, *11*, 1827–1840. [\[CrossRef\]](#)
35. Bessonneau, V.; Bojko, B.; Azad, A.; Keshavjee, S.; Azad, S.; Pawliszyn, J. Determination of Bronchoalveolar Lavage Bile Acids by Solid Phase Microextraction Liquid Chromatography-Tandem Mass Spectrometry in Combination with Metabolite Profiling: Comparison with Enzymatic Assay. *J. Chromatogr. A* **2014**, *1367*, 33–38. [\[CrossRef\]](#)
36. Stefanuto, P.H.; Romano, R.; Rees, C.A.; Nasir, M.; Thakuria, L.; Simon, A.; Reed, A.K.; Marczin, N.; Hill, J.E. Volatile Organic Compound Profiling to Explore Primary Graft Dysfunction after Lung Transplantation. *Sci. Rep.* **2022**, *12*, 2053. [\[CrossRef\]](#)
37. Yang, Q.J.; Kluger, M.; Goryński, K.; Pawliszyn, J.; Bojko, B.; Yu, A.-M.; Noh, K.; Selzner, M.; Jerath, A.; McCluskey, S.; et al. Comparing Early Liver Graft Function from Heart Beating and Living-Donors: A Pilot Study Aiming to Identify New Biomarkers of Liver Injury. *Biopharm. Drug Dis.* **2017**, *38*, 326–339. [\[CrossRef\]](#)
38. Łuczykowski, K.; Warmuzińska, N.; Kollmann, D.; Selzner, M.; Bojko, B. Biliary Metabolome Profiling for Evaluation of Liver Metabolism and Biliary Tract Function Related to Organ Preservation Method and Degree of Ischemia in a Porcine Model. *Int. J. Mol. Sci.* **2023**, *24*, 2127. [\[CrossRef\]](#)
39. Łuczykowski, K.; Warmuzińska, N.; Stryjak, I.; Kollmann, D.; Selzner, M.; Bojko, B. Analysis of Changes in Bile Acids Concentration in Bile in Response to the Degree of Liver Ischemia and the Method of Organ Preservation. *Mass Spectrom. Advances Clin. Lab.* **2019**. Available online: [https://www.msacsl.org/program/view\\_abstract\\_selection.php?id=1146&event=2019%20EU](https://www.msacsl.org/program/view_abstract_selection.php?id=1146&event=2019%20EU) (accessed on 28 December 2022).
40. Bojko, B.; Goryński, K.; Gomez-Rios, G.A.; Knaak, J.M.; Machuca, T.; Spetzler, V.N.; Cudjoe, E.; Hsin, M.; Cypel, M.; Selzner, M.; et al. Solid Phase Microextraction Fills the Gap in Tissue Sampling Protocols. *Anal. Chim. Acta* **2013**, *803*, 75–81. [\[CrossRef\]](#)
41. Bojko, B.; Goryński, K.; Gomez-Rios, G.A.; Knaak, J.M.; Machuca, T.; Cudjoe, E.; Spetzler, V.N.; Hsin, M.; Cypel, M.; Selzner, M.; et al. Low Invasive in Vivo Tissue Sampling for Monitoring Biomarkers and Drugs during Surgery. *Lab. Investig.* **2014**, *94*, 586–594. [\[CrossRef\]](#) [\[PubMed\]](#)
42. Stryjak, I.; Warmuzińska, N.; Bogusiewicz, J.; Łuczykowski, K.; Bojko, B. Monitoring of the Influence of Long-Term Oxidative Stress and Ischemia on the Condition of Kidneys Using Solid-Phase Microextraction Chemical Biopsy Coupled with Liquid Chromatography–High-Resolution Mass Spectrometry. *J. Sep. Sci.* **2020**, *43*, 1867–1878. [\[CrossRef\]](#) [\[PubMed\]](#)
43. Stryjak, I.; Warmuzińska, N.; Łuczykowski, K.; Hamar, M.; Urbanellis, P.; Wojtal, E.; Masztalerz, M.; Selzner, M.; Włodarczyk, Z.; Bojko, B. Using a Chemical Biopsy for Graft Quality Assessment. *J. Vis. Exp.* **2020**, *2020*, 1–12. [\[CrossRef\]](#)
44. Stryjak, I.; Warmuzińska, N.; Łuczykowski, K.; Urbanellis, P.; Selzner, M.; Bojko, B. Metabolomic and Lipidomic Landscape of Porcine Kidney Associated with Kidney Perfusion in Heart Beating Donors and Donors after Cardiac Death. *Sci. Rep.* **2022**. [\[CrossRef\]](#)
45. Warmuzińska, N.; Stryjak, I.; Łuczykowski, K.; Hamar, M.; Urbanellis, P.; Selzner, M.; Bojko, B. Low Invasive SPME Tissue Sampling As A New Tool For Graft Quality Assessment. *Eur. Soc. Organ Transplant. Congr.* **2021**, *316*, F1714–F1719. [\[CrossRef\]](#)
46. Goryński, K.; Bojko, B.; Kluger, M.; Jerath, A.; Wasowicz, M.; Pawliszyn, J. Development of SPME Method for Concomitant Sample Preparation of Rocuronium Bromide and Tranexamic Acid in Plasma. *J. Pharm. Biomed. Anal.* **2014**, *92*, 183–192. [\[CrossRef\]](#)

**Disclaimer/Publisher’s Note:** The statements, opinions and data contained in all publications are solely those of the individual author(s) and contributor(s) and not of MDPI and/or the editor(s). MDPI and/or the editor(s) disclaim responsibility for any injury to people or property resulting from any ideas, methods, instructions or products referred to in the content.

## 6. Cel rozprawy doktorskiej

Głównym celem niniejszej rozprawy było zaadresowanie problemu nieefektywnej diagnostyki okołotransplantacyjnej poprzez wykazanie potencjału metody SPME w ocenie jakości nerek. Badania zakładały przetestowanie nowego podejścia analitycznego opartego na bezpośredniej analizie tkanki *in vivo* z wykorzystaniem biopsji chemicznej w połączeniu z profilowaniem lipidomicznym.

W pierwszym etapie badań wykorzystano model zwierzęcy w celu oceny wpływu niedokrwienia na jakość narządu bazując na dwóch typach dawców oraz porównania różnych metod konserwacji narządu i określenia ich oddziaływania na profil lipidomiczny nerki.

Kończącym celem badań było zastosowanie SPME w warunkach klinicznych w celu predykcji ryzyka wystąpienia powikłań oraz wyodrębnienia panelu metabolitów i lipidów o potencjalnym znaczeniu diagnostycznym.

## 7. Wyniki badań

### 7.1. Zastosowanie biopsji chemicznej do oceny jakości przeszczepu. Analiza porównawcza profilu lipidomicznego nerki związanego z perfuzją u dawców po śmierci mózgowej oraz po zatrzymaniu krążenia – P.3. oraz P.4.

#### Opis dotyczy prac:

- Stryjak\*, **N. Warmuzińska\***, K. Łuczykowski, M. Hamar, P. Urbanellis, E. Wojtal, M. Masztalerz, M. Selzner, Z. Włodarczyk, B. Bojko: ***Using a chemical biopsy for graft quality assessment.*** Jove-J. Vis. Exp, 2020, 160, e60946  
\* [Dwóch równorzędnych pierwszych autorów; IS – analiza metabolomiczna, NW – analiza lipidomiczna]
- Stryjak\*, **N. Warmuzińska\***, K. Łuczykowski, K. Jaroch, P. Urbanellis, M. Selzner, B. Bojko: ***Metabolomic and lipidomic landscape of porcine kidney associated with kidney perfusion in heart beating donors and donors after cardiac death.*** Transl Res., 2024, 267:79-90  
\* [Dwóch równorzędnych pierwszych autorów; IS – analiza metabolomiczna, NW – analiza lipidomiczna]

Ośrodki transplantacyjne mierzą się z brakiem skutecznych narzędzi do oceny jakości narządów oraz poważnym niedoborem dawców nerek. Rosnąca liczba pacjentów oczekujących na przeszczep pogłębia dysproporcję między zapotrzebowaniem a dostępnością organów. W związku z tym konieczne staje się efektywne wykorzystanie dostępnych zasobów i poszerzanie bazy dawców.

Przeszczepy od żywych dawców cechują się lepszym funkcjonowaniem, szybszą rekonwalescencją biorcy i wyższą przeżywalnością. Jednocześnie, uzyskanie nerki od dawcy o rozszerzonych kryteriach bywa korzystniejsze niż pozostawanie w programie przewlekłej dializy, zwłaszcza w przypadku starszych pacjentów. Jedną z obiecujących metod poszerzania puli dawców jest wykorzystanie nerek od dawców po zatrzymaniu krążenia (DCD, ang. donor after cardiac death), jednak są one narażone na ciepłe niedokrwienie - okres między zatrzymaniem krążenia a rozpoczęciem konserwacji - co może zwiększać ryzyko wystąpienia DGF lub nawet PNF.

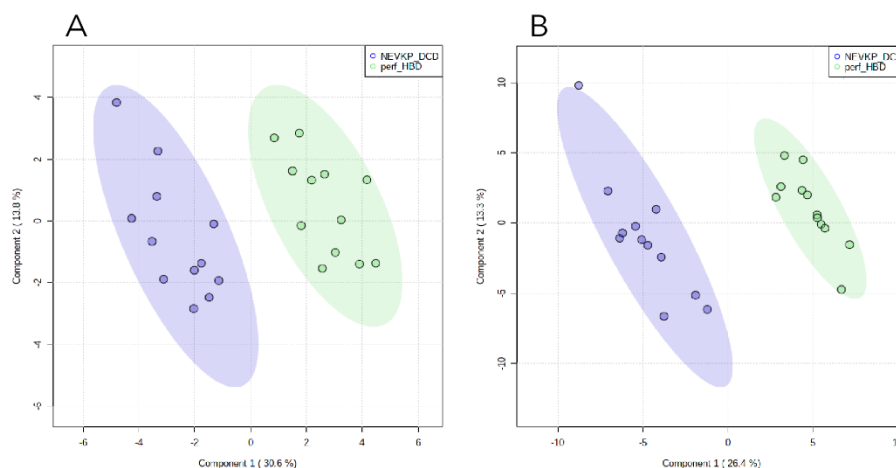
Ocena jakości narządu przed przeszczepieniem wciąż stanowi istotne wyzwanie. Obecnie decyzje opierają się głównie na wynikach badań laboratoryjnych i wizualnej ocenie nerki, a biopsja, mimo swojej niepodważalnej wartości diagnostycznej, jest ograniczona ze

względem na inwazyjność. Potrzebne są nowe, mniej inwazyjne i bardziej wiarygodne metody oceny jakości narządów przeznaczonych do przeszczepienia. W odpowiedzi na tę potrzebę, celem niniejszego badania było wykazanie potencjału metody SPME w ocenie jakości nerek w trakcie procedury przeszczepienia, ze szczególnym uwzględnieniem dwóch typów dawców: dawców z bijącym sercem (HBD, ang. heart beating donor) oraz DCD.

W pierwszym etapie podjęto próbę opracowania i optymalizacji niskoinwazyjnego protokołu bazującego na biopsji chemicznej pozwalającego na wielokrotne pobieranie próbek z tej samej tkanki, co umożliwi śledzenie zmian zachodzących w narządzie na wszystkich etapach procedury przeszczepienia - od pobrania narządu, przez jego przechowywanie, aż po reperfuzję. Każde kliniczne zastosowanie wymaga optymalizacji, aby zachować kompromis pomiędzy czułością i powtarzalnością protokołu analitycznego a ograniczeniami związanymi z procedurą medyczną i warunkami sali operacyjnej. Szczegółowy protokół został opisany w publikacji P.3., której część dotycząca analizy lipidomicznej składa się na cykl publikacji prezentowanych w tej rozprawie doktorskiej.

W kolejnym etapie, opracowany protokół został wykorzystany do profilowania lipidomicznego nerek w trakcie procedury przeszczepienia. Bezpośrednie pobieranie próbek z nerki przeprowadzono za pomocą sond SPME pokrytych sorbentem typu mixed-mode o długości 7 mm. Ze względu na niejednorodną budowę nerki, tj. obecność kory i rdzenia, do uzyskania powtarzalnych wyników wybrano odpowiednio krótką długość fazy ekstrakcyjnej, umożliwiającą pobór próbek wyłącznie z kory nerkowej. Autoprzeszczepienie nerki wykonano na modelu wieprzowym w celu zasymulowania dwóch typów dawców: HBD oraz DCD. Wszystkie przeszczepy nerkowe były perfundowane w normotermicznych warunkach *ex vivo* (NEVKP, ang. normothermic *ex vivo* kidney perfusion). W obu scenariuszach dawców pobieranie próbek przeprowadzono *in vivo* przed pobraniem narządu; następnie po 1, 3, 5 i 7 godzinach perfuzji; oraz ponownie *in vivo* bezpośrednio po rewaskularyzacji. Dodatkowo, w przypadku nerek DCD, próbki pobrano także po 45 minutach i 2 godzinach ciepłego niedokrwienia. Analizę lipidomiczną przeprowadzono z użyciem ultrasprawnej chromatografii cieczowej (UHPLC, ang. Ultra-High-Performance Liquid Chromatography) sprzężonej ze spektrometrem mas Q-Exactive Focus Orbitrap (MS, ang. mass spectrometry).

Monitorowanie profili lipidomicznych nerek pozwoliło zaobserwować zmiany biochemiczne zachodzące w narządzie podczas jego konserwacji, a także różnice między typami dawców HBD i DCD (Rycina 1.).



**Rycina 1.** Wykresy punktowe PLS-DA przedstawiające rozdział między perfuzjami HBD i DCD. Analizy lipidomiczne z użyciem rozdziału (A) HILIC i (B) RP.

Zaobserwowane zmiany dotyczyły głównie poziomów trójglicerydów (TG, ang. triacylglycerol), lizofosfatydylocholin (LPC, ang. lysophosphocholine), oraz fosfatydyloetanoloamin (PE, ang. phosphoethanolamine). Porównanie przeszczepów HBD i DCD podczas perfuzji wykazało niższe poziomy LPC 16:1, LPC 18:1, LPC 20:4, LPC P-16:0, LPC 18:0 oraz wyższe poziomy TG 30:0, TG 32:0, TG 34:0, TG 36:0, TG 38:0, TG 40:0 w nerkach DCD. Spadek poziomów LPC może wskazywać, że przebudowa błon komórkowych jest tymczasowo zahamowana po niedokrwieniu. Natomiast zwiększenie TG może wiązać się z aktywacją mitochondrialnej  $\beta$ -oksydacji kwasów tłuszczowych, na co wskazują wcześniejsze badania. Choć akumulacja neutralnych lipidów może prowadzić do lipotoksyczności, toksyczność nerkowa TG zależy od długości łańcucha acylowego i liczby wiązań podwójnych. Wzrost utleniania kwasów tłuszczowych oraz większa ilość nasyconych TG o stosunkowo krótszych łańcuchach może odzwierciedlać mechanizm adaptacyjny, służący detoksykacji nasyconych kwasów tłuszczowych.

Podsumowując, zastosowanie metody SPME umożliwiło pobranie próbek na wszystkich etapach procedury - od pobrania narządu, przez jego przechowywanie, aż po reperfuzję, co w połączeniu z analizą UHPLC-MS pozwoliło na identyfikację licznych związków o zróżnicowanej polarności. Wśród związków różnicujących dawców HBD i DCD najbardziej obiecującymi lipidami do stworzenia zawężonego panelu analitycznego służącego ocenie funkcji i jakości przeszczepu są TG o różnej długości łańcuchów acylowych i liczbie wiązań podwójnych, LPC oraz PE. Konieczne są jednak dalsze badania, które zweryfikują te wyniki i pozwolą ocenić wartość predykcyjną wybranych metabolitów.

# Using a Chemical Biopsy for Graft Quality Assessment

Iga Stryjak<sup>\*,1</sup>, Natalia Warmużńska<sup>\*,1</sup>, Kamil Łuczykowski<sup>1</sup>, Matyas Hamar<sup>2</sup>, Peter Urbanellis<sup>2</sup>, Emilia Wojtal<sup>3</sup>, Marek Masztalerz<sup>3</sup>, Markus Selzner<sup>2,4</sup>, Zbigniew Włodarczyk<sup>3</sup>, Barbara Bojko<sup>1</sup>

<sup>1</sup> Department of Pharmacodynamics and Molecular Pharmacology, Faculty of Pharmacy, Nicolaus Copernicus University in Torun, Collegium Medicum in Bydgoszcz <sup>2</sup> Multi Organ Transplant Program, Department of Surgery, Toronto General Hospital, University Health Network <sup>3</sup> Department of Transplantation and General Surgery, Collegium Medicum in Bydgoszcz, Antoni Jurasz University Hospital No. 1 in Bydgoszcz, Nicolaus Copernicus University in Torun, Bydgoszcz, Poland <sup>4</sup> Department of Medicine, Toronto General Hospital

\* These authors contributed equally

## Corresponding Author

Barbara Bojko  
bbojko@cm.umk.pl

## Citation

Stryjak, I., Warmużńska, N., Łuczykowski, K., Hamar, M., Urbanellis, P., Wojtal, E., Masztalerz, M., Selzner, M., Włodarczyk, Z., Bojko, B. Using a Chemical Biopsy for Graft Quality Assessment. *J. Vis. Exp.* (160), e60946, doi:10.3791/60946 (2020).

## Date Published

June 17, 2020

## DOI

10.3791/60946

## URL

jove.com/video/60946

## Abstract

Kidney transplantation is a life-saving treatment for a large number of people with end-stage renal dysfunction worldwide. The procedure is associated with an increased survival rate and greater quality of patient's life when compared to conventional dialysis. Regrettably, transplantology suffers from a lack of reliable methods for organ quality assessment. Standard diagnostic techniques are limited to macroscopic appearance inspection or invasive tissue biopsy, which do not provide comprehensive information about the graft. The proposed protocol aims to introduce solid phase microextraction (SPME) as an ideal analytical method for comprehensive metabolomics and lipidomic analysis of all low molecular compounds present in kidneys allocated for transplantation. The small size of the SPME probe enables performance of a chemical biopsy, which enables extraction of metabolites directly from the organ without any tissue collection. The minimum invasiveness of the method permits execution of multiple analyses over time: directly after organ harvesting, during its preservation, and immediately after revascularization at the recipient's body. It is hypothesized that the combination of this novel sampling method with a high-resolution mass spectrometer will allow for discrimination of a set of characteristic compounds that could serve as biological markers of graft quality and indicators of possible development of organ dysfunction.

## Introduction

According to the United States' Organ Procurement and Transplantation Network, there were 94,756 patients waiting for kidney transplants in the US in 2019; while in Europe in 2018, that number was 10,791. Every ten minutes,

someone is added to the national transplant waiting list in the U.S., and it is estimated that 20 people die each day waiting for a transplant<sup>1,2</sup>. Kidney transplantation is a life-saving treatment for a large number of people suffering with

end-stage renal dysfunction worldwide. The procedure is associated with increased survival rate and greater quality of life when compared to conventional dialysis.

However, transplantation faces many serious problems, such as organ shortage or lack of effective tools for organ quality assessment. The standard protocols are limited to macroscopic appearance inspection or invasive tissue biopsy, which do not provide comprehensive information regarding the quality of the graft. While a visual appraisal allows for identification of tumors visible to the eye, anatomical abnormalities, or extensive damage to the grafts, this approach is very subjective, varying in its effectiveness according to the experience of the observers. Biopsy, on the other hand, can provide valuable information regarding pre-existing renal disorders, and is thus considered to be a method of objective and evidenced value in determining graft outcomes. However, the biopsy procedure is not free of flaws; there is the risk of potential complications such as bleeding and an additional 4-5 hours of sample preparation is required, which significantly prolongs the cold ischemic time. Therefore, especially in Europe, the use of direct tissue analysis is limited to expanded criteria donors (ECD) and donors after circulatory death (DCD)<sup>3,4</sup>.

Metabolomics and lipidomics have been recently recognized as promising approaches to attaining a better understanding of the changes in biochemical pathways occurring during organ preservation. Metabolomic and lipidomic profiling enables monitoring of immediate responses of the system to sudden environmental changes related to organ removal with subsequent consequences: ischemia, oxidative stress, or inflammatory responses<sup>5,6,7,8</sup>. The kidney is an organ that is largely associated with metabolic processes, thus measurements of metabolites and lipids concentrations may

permit identification of potential organ quality biomarkers and enable better predictions of graft outcome.

Given the above complications and limitations associated with current organ quality assessment methods, a less invasive diagnostic solution is needed for quick and complex organ quality assessment. Solid phase microextraction (SPME) complies with these requirements as a minimally invasive analytical method that enables coverage of a broad spectrum of metabolites and lipids. The technique is based on the insertion of a thin (~200 µm), biocompatible, titanium-nickel alloy probe covered with a selective extraction phase into the examined organ for a short time. It should be emphasized that SPME prevents protein extraction, and hence enables metabolism inhibition already at the stage of sample collection, which is a significant advantage over alternative methods. Moreover, the miniaturization of the device allows for the execution of repetitive and simultaneous analyses of few structures of the organ<sup>9,10,11</sup>.

## Protocol

All animals received humane care in compliance with the "Principles of Laboratory Animal Care" formulated by the National Society for Medical Research and the "Guide for the Care of Laboratory Animals" published by the National Institute of Health, Ontario, Canada. The Animal Care Committee of the Toronto General Research Institute approved all studies. The research involved human subjects was approved by the Bioethical Committee at Collegium Medicum in Bydgoszcz Nicolaus Copernicus University in Torun.

**NOTE:** Obtain approval from appropriate ethical boards. Remember to always wear safety gloves. Do not touch the

extraction phase of SPME probes. The use of deactivated glass vials is recommended for lipidomic analyses.

## 1. Preparation of probes

1. Prepare titanium-nickel alloy probes (40 mm length; 0.2 mm diameter) coated with 7 mm mix-mode sorbent. The number of probes depends on the time points targeted during the entire procedure and the number of replicates (3 is recommended per time point).

**NOTE:** The length and type of extraction phase may be adjusted based on the mode of study, the polarity of metabolites, and the sample matrix.

2. Prepare a cleaning mixture composed of 2:1 chloroform:methanol (v/v). Pipet 1.0 mL of the solution to each 2.0 mL glass vial and place one probe, previously pierced through the cap, in each vial.

**NOTE:** Before use, clean all probes to remove contaminating particles.

3. Put the vials on the agitator and set the agitation speed at 1,200 rpm. After 45 min, stop the device and rinse the coatings with LC-MS grade water.
4. As coatings must undergo a preconditioning step to activate them, prepare a preconditioning mixture composed of 1:1 methanol:water (v/v). Pipet 1.0 mL of the solution to each 2.0 mL glass vial and place one probe, previously pierced through the cap, in each vial.
5. Put the vials on the vortex agitator and set the agitation speed at 1,200 rpm.
6. After 60 min, stop the agitator and rinse the coatings with LC-MS grade water.
7. Sterilize probes according to the standard surgical equipment sterilization protocol.

## 2. Extraction

1. Open the sterile package right before sampling to ensure a sterile environment.
2. Insert two probes directly into the kidney cortex for 10 min at each time point. The entire length of the coating must be covered by the tissue matrix; no specific angle is required, but ca. 90 deg is usually used.

**NOTE:** The entire medical procedure follows standard protocols in given institution. No modification concerning SPME sampling is considered. The procedure involves the six following sampling time points:

- a) before kidney resection, in vivo from donor;
- b)-e) after 1 h, 3 h, 5 h, 7 h of kidney perfusion, ex vivo in organ chamber;
- f) after reperfusion, in vivo from recipient.

3. Retract the probes by pulling it out from the tissue and then rinse coatings with LC-MS grade water to clear any remaining blood from the coating surface. Rinse away from the surgical site, and immediately after removal of the probes.

## 3. Transport and storage

1. Place probes in separate vials and close them.
2. Place vials in a Styrofoam box filled with dry ice or in liquid nitrogen for transport.
3. Store samples in a freezer (-80 °C), or immediately commence the desorption step.

## 4. Desorption

1. Prepare desorption solutions composed of 80:20 acetonitrile:water (v/v) for metabolomic analysis, and 1:1 isopropanol:methanol (v/v) for lipidomic analysis.

2. Pipet 100  $\mu$ L of the solution to inserts placed into 2.0 mL labeled vials and place one probe, previously pierced through the cap, in each vial.
3. Put the vials on the vortex agitator and set the agitation speed at 1,200 rpm for 120 min.
4. Remove probes from the vials. Obtained extracts are now ready for instrumental analysis.

## 5. LC-MS analysis

1. Place vials containing extracts in the autosampler of the LC-MS system.  
**NOTE:** Liquid chromatography (RP, HILIC) coupled with high resolution mass spectrometry and an orbitrap mass analyzer were used for this study. For metabolomic analysis parameters, go to step 5.2. For lipidomic analysis parameters, go to step 5.6.
2. Use a pentafluorophenyl (PFP) column (2.1 mm x 100 mm, 3  $\mu$ m) for reversed phase separation.
  1. Set the flow rate to 300  $\mu$ L/min, and autosampler and column temperatures to 4 °C and 25 °C, respectively.
  2. Prepare mobile phases according to the following proportions: mobile phase A: water:formic acid (99.9:0.1, v/v), and mobile phase B: acetonitrile:formic acid (99.9:0.1, v/v). Set the mobile phase flow according to the following parameters: starting mobile phase flow (0-3 min): 100% A followed by a linear gradient to 10% A (3-25 min), ending with isocratic flow of 10% A until 34 min, followed by 6 min of column re-equilibrium time.
  3. For HILIC separation, use a HILIC column (2.0 mm x 100 mm, 3  $\mu$ m, 200A). Set the flow rate to 400  $\mu$ L/min.
1. Prepare mobile phases according to the following proportions: mobile phase A: acetonitrile:ammonium acetate buffer (9:1, v/v, effective salt concentration 20 mM), mobile phase B: acetonitrile:ammonium acetate buffer (1:1, v/v, effective salt concentration 20 mM).
2. Set the mobile phase flow according to the following parameters: starting mobile phase flow (0-3 min) at 100% A, hold for 3.0 min and then ramp to 100% B within 5 min. Hold with 100% B until 12 min, followed by 8 min of column re-equilibrium time.
4. Set the scan range to 85-1000 m/z. Set HESI ion source parameters in positive ionization mode to: spray voltage 1,500 V, capillary temperature 300 °C, sheath gas 40 a.u., aux gas flow rate 15 a.u., probe heater temperature 300 °C, S-Lens RF level 55%.
5. Run QC samples composed of 10  $\mu$ L of each analyzed sample (regularly, every 10-12 samples) to monitor instrument performance.
6. For reversed phase separation, use a C18 column (2.1 mm x 75 mm, 3.5  $\mu$ m).
  1. Set the flow rate to 200  $\mu$ L/min, and autosampler and column temperatures to 4 °C and 55 °C, respectively. Prepare mobile phases according to the following proportions: mobile phase A: H<sub>2</sub>O:MeOH (60:40, v/v), 10 mM ammonium acetate and 1 mM acetic acid; mobile phase B: IPA:MeOH (90:10, v/v), 10 mM ammonium acetate and 1 mM acetic acid.
  2. Set the mobile phase flow according to the following parameters: 0-1 min (20% B), 1-1.5 min (20-50% B), 1.5-7.5 min (50-70% B), 7.5-13 min (70-95% B), 13-17 min (95% B), 17-17.1 min (95-20% B), 17.1-23 min (20%).

7. For HILIC separation, use a HILIC column (100 x 2.1 mm, 3  $\mu$ m).
  1. Set the flow rate to 400  $\mu$ L/min, and autosampler and column temperatures to 4  $^{\circ}$ C and 40  $^{\circ}$ C, respectively.
  2. Prepare mobile phases according to the following proportions: mobile phase A: ACN; mobile phase B: 5 mM ammonium acetate in water. Set the mobile phase flow according to the following parameters: 0-2 min (96% B), 2-15 min (96-80% B), 15-15.1 min (80-96% B), 15.1-21 min (96% B).
8. Set HESI ion source parameters in positive ionization mode to spray voltage 3,500 V, capillary temperature 275  $^{\circ}$ C, sheath gas 20 a.u., aux gas flow rate 10 a.u., probe heater temperature 300  $^{\circ}$ C, S-Lens RF level 55%.
9. Run QC samples composed of 10  $\mu$ L of each analyzed sample (every 10-12 samples) to monitor instrument performance.
10. Perform data acquisition in software compatible with the instrument.

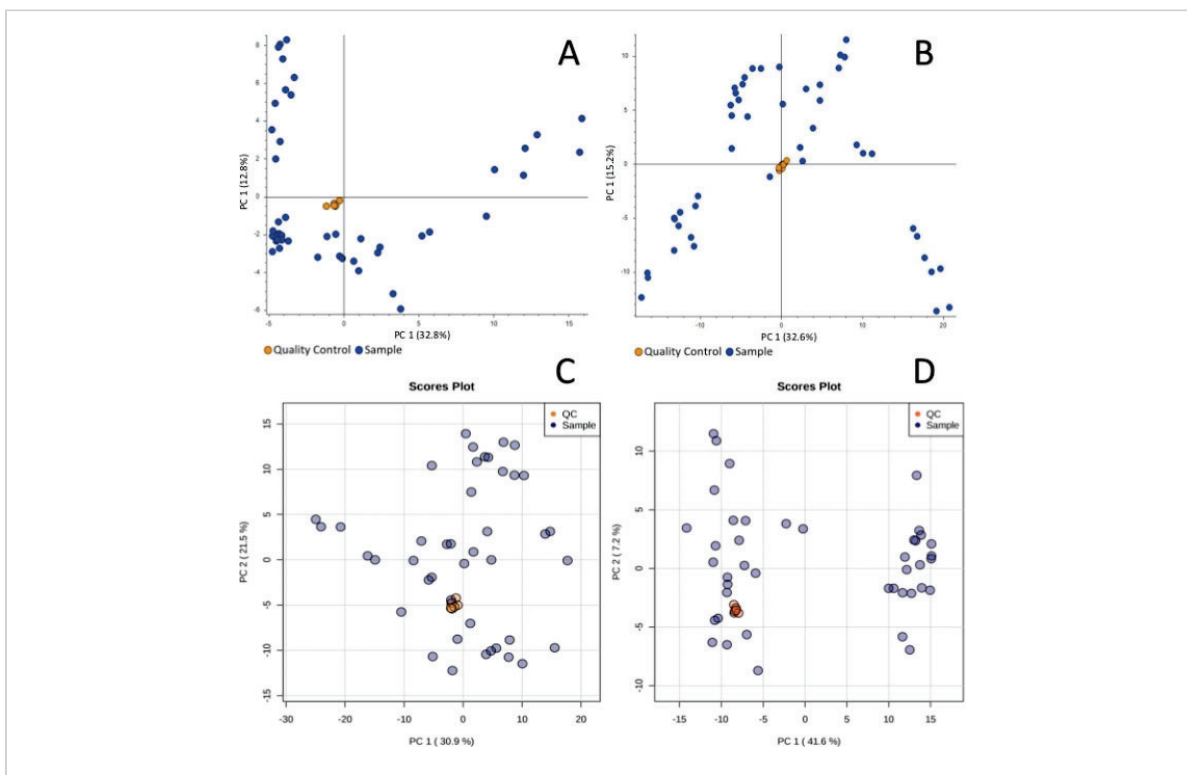
## 6. Data analysis

1. Perform data processing, putative identification, and statistical analysis with the use of software dedicated to untargeted metabolomics and lipidomics analysis.

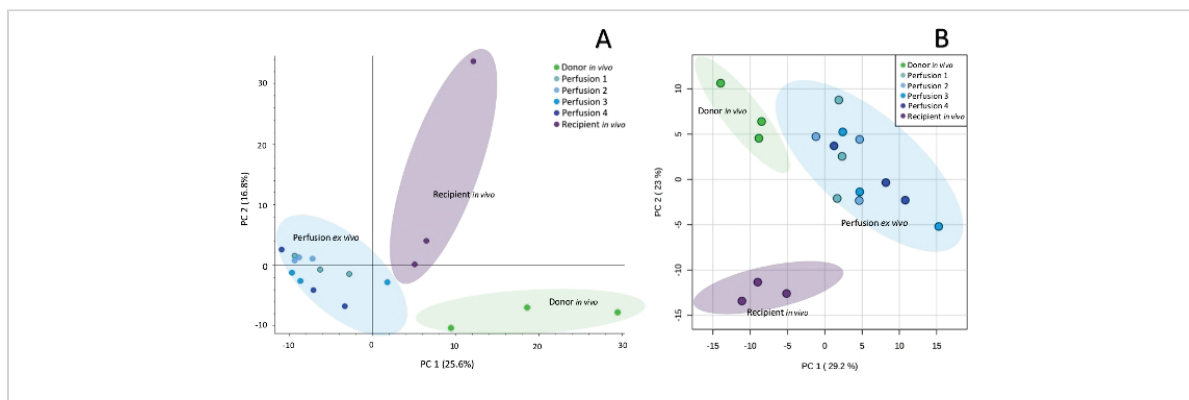
**NOTE:** Principal components analysis (PCA) and box-whisker plots can be obtained to visualize data structure.

## Representative Results

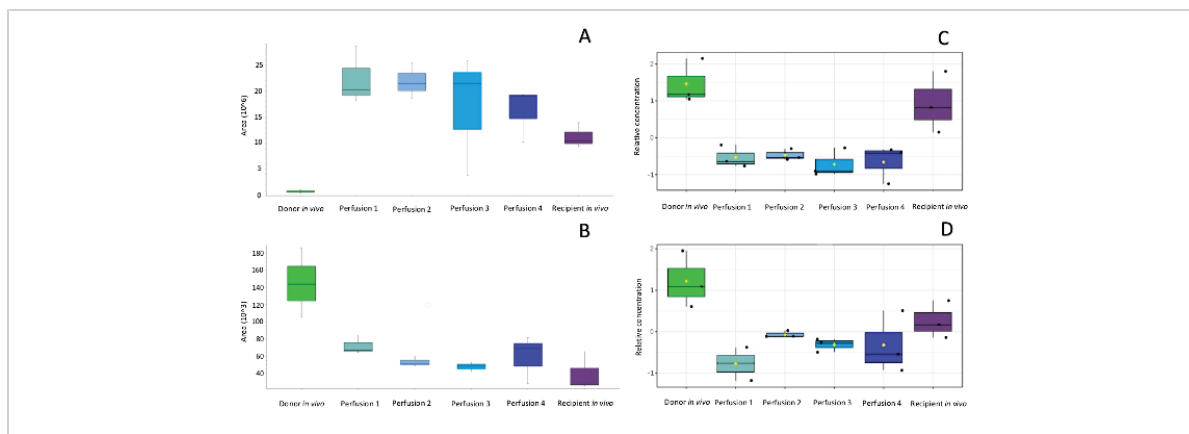
Sample collection was performed according to the SPME method described above, using probes coated with a 7 mm mixed-mode extraction phase. Sampling was conducted directly from the graft tissue (in vivo before transplantation), ex vivo in kidney chamber after 1 h, 3 h, 5 h, and 7 h of perfusion, and in vivo after revascularization in the recipient. Untargeted metabolomic and lipidomic analyses were carried out with the use of liquid chromatography (RP, HILIC) coupled with high resolution mass spectrometry, with the mass analyzer set in positive ionization mode. To assess data quality and attain general insights regarding the results, data was subjected to principal component analysis (PCA). As shown in **Figure 1**, QC samples formed a tight cluster, confirming the quality of the analyses. The studied groups exhibit relatively good separation, allowing for visualization of differences in metabolic and lipidomic profiles before and after transplantation, as well as during organ perfusion (**Figure 2**). SPME sampling permits metabolic profiling of the organ over time. Box-whisker plots of selected metabolites serve to exemplify alterations in metabolite levels throughout the experiment (**Figure 3**). The wide spectrum of extracted features separated on both RP and HILIC columns is shown in **Figure 4**.



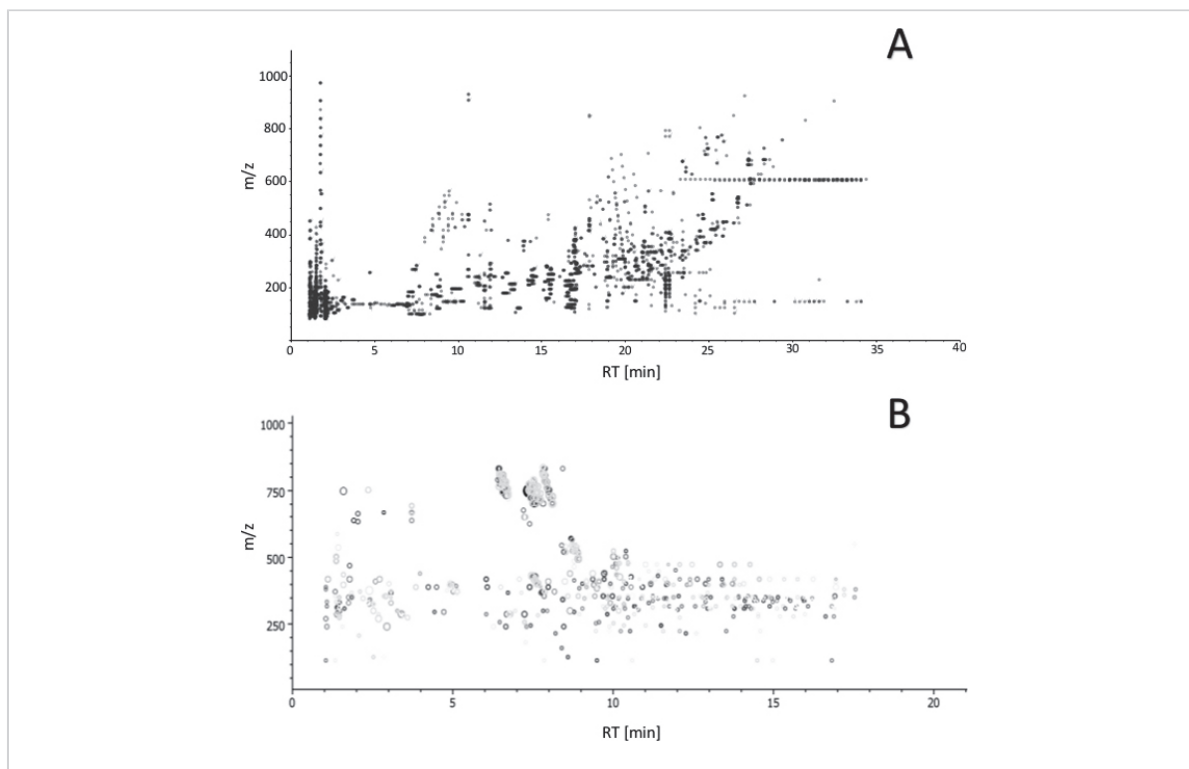
**Figure 1: Principal component analysis showing clustering of quality control samples for metabolomic reversed-phase (A), HILIC (B) and lipidomic reversed-phase (C), HILIC (D) analyses.** The quality control is necessary in untargeted analysis to monitor any possible changes induced by instrumental instability. Tight cluster of QC samples ensures that all changes observed are of biological origin. [Please click here to view a larger version of this figure.](#)



**Figure 2: Principal component analysis showing metabolomic (A) and lipidomic (B) differences between particular sampling points.** Untargeted profiling of kidney with SPME-LC-HRMS enables to observe biochemical differences in organs at subsequent steps of their preservation. [Please click here to view a larger version of this figure.](#)



**Figure 3: Box-whisker plots of selected compounds showing alterations in metabolites (A, B) and lipids (C, D) during the peritransplant period.** After selection and identification of discriminating compounds box-whisker plots enables to monitor changes in levels of these compounds at subsequent steps of the protocol and compare the metabolites levels in organs subjected to different preservation protocols or harvested from different donors e.g. heart beating donors or donors after cardiac death. [Please click here to view a larger version of this figure.](#)



**Figure 4:** Ion map ( $m/z$  versus retention time) of features obtained by LC-MS analysis with (A) reversed-phase and (B) HILIC separation. The plot enables to estimate overall number of features obtained with the proposed protocol (from extraction to detection) and assess analyte coverage based on the polarity. [Please click here to view a larger version of this figure.](#)

## Discussion

Evaluation of organ quality remains a large challenge for physicians, who must make quick informed decisions regarding whether a given organ is viable for transplantation or whether it must be discarded. Multiple factors, such as donor age, duration of ischemia, and infections and inflammatory processes, can affect the long-term graft outcome. While diverse methods have been developed to date to diagnose kidney allograft function, histopathological inspection remains the gold standard in that matter<sup>3, 4, 12</sup>.

Although the biopsy procedure can yield significant information regarding pre-existing donor disease and vascular changes, it is not free of flaws. Sampling errors associated to interobserver variability and sampling of insufficient glomeruli for comprehensive information regarding organ function remain typical concerns in this regard. Moreover, specimen preparation brings some issues such as an incomplete appraisal of the graft in case of frozen sections, and extension of procedure time for paraffin sectioning. However, the increased risk of hemorrhage, which

may appear acutely as microscopic or gross hematuria, is the major life-threatening complication associated with the biopsy procedure. For this reason, the number of allowable biopsies is strictly limited in transplantation procedures, a factor that hampers the capture of dynamic changes and time series analyses via this method<sup>12, 13, 14</sup>. The benefits of a histological analysis must be weighed against the risks associated with the methodology. The value of histological findings is indisputable, but they do not explain the molecular mechanisms of the aberrations.

Metabolomics and lipidomics are the youngest domains of the “-omics” scientific family. The complete set of low molecular (<1,200 Da) human metabolites and lipids connected within a metabolic network is defined as a human metabolome. The genome remains relatively constant throughout its lifetime, with slight modifications caused by mutations occurring infrequently. The metabolome is the product of gene expression, which is highly sensitive to changes in all biological processes as well as environmental factors. The dynamic nature of metabolites and lipids makes them perfect indicators of current organ condition<sup>7, 8, 15, 16</sup>. The SPME method proposed in the abovementioned protocol enables detection of changes occurring in the organ during its preservation, starting from organ removal from the donor's body till revascularization at the recipient's. The small diameter of the probe (~200 µm) provides minimal invasiveness and allows for several samplings from the same organ without causing any damage to the tissue. Conducting studies using kidney, as the most frequently transplanted organ, allows for a better understanding and further characterization of the metabolic pathways responsible for declining the quality and function of grafts. The possibility of monitoring modifications over time certainly is an important advantage of the technique as compared to conventional

invasive methods such as biopsy. The currently presented analysis identified altered concentrations of various groups of lipids and metabolites, especially of essential amino acids, purines, purine nucleosides, and glycerophospholipids. These results are consistent with previous tissue analysis reports<sup>5, 6, 17, 18, 19, 20</sup>. To date, the majority of scientific reports utilizing metabolomics or lipidomics to explain processes inducing complications after transplantation or ischemia/reperfusion injury (IRI) phenomena have been limited to analysis of biofluids<sup>21, 22, 23</sup>.

Each clinical application requires optimization of the sampling protocol to ensure that the performance of the analytical method meets expected criteria. In this regard, the benefit of utilizing SPME is the possibility of adjusting conditions for various experimental designs. The variety of accessible extraction phases provides a broad spectrum of extracted metabolites with diversified polarities. At the same time, this might be considered as a limitation of the method due to the fact that each sorbent provides selectivity towards specific features and does not extract all compounds present in the sample matrix. It should be noted that SPME coatings extract only via free molecules, and simply do not interact with a bound fraction of the analyte. The biocompatibility of the coatings does not introduce toxicity to the tissue while restraining the extraction of large molecules such as proteins; as a consequence, the enzymatic processes are inhibited already at the stage of sample collection and the presence of artefacts is minimized, which is a great advantage over alternative sampling methods. The length of the coating influences the efficiency of extraction (i.e., the length of the coating designates the surface area and the extraction phase volume); thus, longer coatings yield higher recoveries. On the other hand, shorter coatings enable higher spatial resolution. For reliable results, it is crucial

to submerge the probe to the exact same depth of kidney cortex. Insertion too deep causes the risk of entering the kidney medulla. The time of the extraction is also proportional to the extraction efficiency. Therefore, selection of optimum extraction time is one of the most critical steps in SPME method development. The accuracy of time measurement provides the highest repeatability. In biological applications such as the one discussed, there is always a compromise between the sensitivity and repeatability of the analytical protocol and the restrictions of the medical procedure. While equilibrium extraction provides the highest sensitivity, for safety reasons, pre-equilibrium conditions are often used in such applications, as extraction time should not affect the total duration of the surgery. The efficiency of desorption is determined by the time of the process and the composition of the desorption solvent, which should be compatible with the mobile phase used for chromatographic separation<sup>9, 10, 11</sup>.

One of the major requirements for diagnostic instrumentation used for intra-surgical assessments is time of analysis. Current attempts are being made to develop a rapid tool for in vivo SPME extraction coupled directly to a mass spectrometer via microfluidic open interface (MOI)<sup>24</sup> or coated blade spray (CBS)<sup>25</sup>. Such approaches would allow for the disclosure of analytical results in real or close to real time. The use of such methods for pre-intervention analyses of metabolic and lipidomic profiles could enhance the decision-making process during transplantation procedures, enabling the best possible personalized approach and fast response in case of organ failure.

As a summary, it is hypothesized that the proposed protocol will enable attainment of full metabolic and lipidomic profiles of kidney grafts, which in turn would provide a comprehensive assessment of organ quality and

characterization of the processes responsible for ischemia-reperfusion injury. The novelty of the project includes the utilization of solid-phase microextraction (SPME), offering low invasive sampling of living systems, in combination with one of the most innovative technologies available for metabolomics and lipidomics analysis (e.g., the Orbitrap high resolution mass spectrometer). SPME combines sample collection, extraction, and quenching of metabolites in one step, therefore making it a perfect tool for rapid analysis. It is expected that this protocol will help to answer questions related to what pre-transplant conditions of the kidney are responsible for delayed organ function or its dysfunctions after transplantation, as well as to how the graft preservation protocol influences the biochemistry of the organ. Such knowledge would not only have significant impact on the prevention of possible complications related to transplantation, but may help to improve current graft preservation protocols, minimizing loss of viable transplant tissue as well as loss of life. The proposed solution will open the door to further investigations in this field, including the validation of specific potential biomarkers and improvement of therapeutic outcomes in transplantology.

## Disclosures

The authors would like to acknowledge MilliporeSigma (Merck KGaA, Darmstadt, Germany) for providing SPME devices and Thermo Fisher Scientific for access to the Q-Exactive Focus Orbitrap mass spectrometer.

## Acknowledgments

The study was supported by grant Opus UMO-2017/27/B/NZ5/01013 from National Science Centre. The authors would like to acknowledge MilliporeSigma, a business of Merck KGaA, Darmstadt, Germany for providing SPME devices. The

life science business of Merck operates as MilliporeSigma in the U.S. and Canada. Also, the authors want to thank Thermo Fisher Scientific for the access to Q-Exactive Focus orbitrap mass spectrometer. The authors would like to thank Dr. Aleksandra Woderska-Jasńska and the personnel of the Department of Transplantology and General Surgery in Bydgoszcz for their kind assistance in the project. BB want to thank Prof. Janusz Pawliszyn for the opportunity of sample collection at Toronto General Hospital during her stay at University of Waterloo.

## References

1. *Organ Procurement and Transplantation Network*. Official U.S. Government Web site managed by the Health Resources and Services Administration, U.S. Department of Health & Human Services. Available from: <https://optn.transplant.hrsa.gov/> (2019).
2. Branger, P., Undine, S. *Annual Report 2018/ Eurotransplant International Foundation*. Eurotransplant Foundation. Leiden. (2018).
3. Dare, A. J., Pettigrew, G. J., Saeb-Parsy, K. Preoperative assessment of the deceased-donor kidney: From macroscopic appearance to molecular biomarkers. *Transplantation*. **97**, 797–807 (2014).
4. Mueller, T. F., Solez, K., Mas, V. Assessment of kidney organ quality and prediction of outcome at time of transplantation. *Seminars in Immunopathology*. **33**, 185–199 (2011).
5. Xu, J. et al. Lipidomics comparing DCD and DBD liver allografts uncovers lysophospholipids elevated in recipients undergoing early allograft dysfunction. *Scientific Reports*. **5**, 1–10 (2015).
6. Rao, S. et al. Early lipid changes in acute kidney injury using SWATH lipidomics coupled with MALDI tissue imaging. *American Journal of Physiology - Renal Physiology*. **310**, F1136–F1147 (2016).
7. Wishart, D. S. Metabolomics: The principles and potential applications to transplantation. *American Journal of Transplantation*. **5**, 2814–2820 (2005).
8. Kim, S. J., Kim, S. H., Kim, J. H., Hwang, S., Yoo, H. J. Understanding metabolomics in biomedical research. *Endocrinology and Metabolism*. **31**, 7–16 (2016).
9. Bojko, B. et al. Solid phase microextraction fills the gap in tissue sampling protocols. *Analytica Chimica Acta*. **803**, 75–81 (2013).
10. Filipiak, W., Bojko, B. SPME in clinical, pharmaceutical, and biotechnological research – How far are we from daily practice? *TrAC - Trends in Analytical Chemistry*. **115**, 203–213 (2019).
11. Bojko, B. et al. Low invasive in vivo tissue sampling for monitoring biomarkers and drugs during surgery. *Laboratory Investigation*. **94**, 586–594 (2014).
12. Ahmad, I. Biopsy of the transplanted kidney. *Seminars in Interventional Radiology*. **21**, 275–281 (2004).
13. Plattner, B. W. et al. Complications and adequacy of transplant kidney biopsies: A comparison of techniques. *Journal of Vascular Access*. **19**, 291–296 (2018).
14. Tapia-Canelas, C. et al. Complications associated with renal graft biopsy in transplant patients. *Nefrologia*. **34**, 115–119 (2014).
15. Afshinnia, F. et al. Lipidomics and Biomarker Discovery in Kidney Disease. *Seminars in Nephrology*. **38**, 127–141 (2018).

16. Zhao, Y. Y., Vaziri, N. D., Lin, R. C. *Lipidomics: New insight into kidney disease. Advances in Clinical Chemistry.* **68**, 153-175, (2015).
17. Kaminski, J. et al. Oxygen Consumption by Warm Ischemia-Injured Porcine Kidneys in Hypothermic Static and Machine Preservation. *Journal of Surgical Research.* **242**, 78–86 (2019).
18. Wijermars, L. G. M. et al. Defective postreperfusion metabolic recovery directly associates with incident delayed graft function. *Kidney International.* **90**, 181–191 (2016).
19. Huang, H. et al. Proteo-metabolomics reveals compensation between ischemic and non-injured contralateral kidneys after reperfusion. *Scientific Reports.* **8**, 1–12 (2018).
20. Solati, Z., Edel, A. L., Shang, Y., Karmin, O., Ravandi, A. Oxidized phosphatidylcholines are produced in renal ischemia reperfusion injury. *PLoS One.* **13**, 1–24 (2018).
21. Wishart, D. S. Metabolomics in monitoring kidney transplants. *Current Opinion in Nephrology and Hypertension.* **15**, 637–642 (2006).
22. Abbiss, H., Maker, G. L., Trengove, R. D. Metabolomics approaches for the diagnosis and understanding of kidney diseases. *Metabolites.* **9**, (2019).
23. Zhang, Z. H. et al. Metabolomics insights into chronic kidney disease and modulatory effect of rhubarb against tubulointerstitial fibrosis. *Scientific Reports.* **5**, 1–17 (2015).
24. Looby, N. T. et al. Solid phase microextraction coupled to mass spectrometry: Via a microfluidic open interface for rapid therapeutic drug monitoring. *Analyst.* **144**, 3721–3728 (2019).
25. Gómez-Ríos, G. A., Tascon, M., Pawliszyn, J. Coated blade spray: Shifting the paradigm of direct sample introduction to MS. *Bioanalysis.* **10**, 257–271 (2018).



Contents lists available at ScienceDirect

Translational Research

journal homepage: [www.elsevier.com/locate/trsl](http://www.elsevier.com/locate/trsl)

## Metabolomic and lipidomic landscape of porcine kidney associated with kidney perfusion in heart beating donors and donors after cardiac death

Iga Stryjak<sup>a,1</sup>, Natalia Warmużńska<sup>a,1</sup>, Kamil Łuczykowski<sup>a</sup>, Karol Jaroch<sup>a</sup>, Peter Urbanellis<sup>b</sup>, Markus Selzner<sup>b,c</sup>, Barbara Bojko<sup>a,\*</sup>

<sup>a</sup> Department of Pharmacodynamics and Molecular Pharmacology, Faculty of Pharmacy, Collegium Medicum in Bydgoszcz, Nicolaus Copernicus University in Toruń, Bydgoszcz, Poland

<sup>b</sup> Ajmera Transplant Center, Department of Surgery, Toronto General Hospital, University Health Network, Toronto, ON, Canada

<sup>c</sup> Department of Medicine, Toronto General Hospital, Toronto, ON, Canada

### ARTICLE INFO

#### Keywords:

Solid-phase microextraction  
SPME  
LC-MS  
Kidney transplantation  
Metabolomics  
Lipidomics  
Graft quality assessment

### ABSTRACT

Transplant centers are currently facing a lack of tools to ensure adequate evaluation of the quality of the available organs, as well as a significant shortage of kidney donors. Therefore, efforts are being made to facilitate the effective use of available organs and expand the donor pool, particularly with expanded criteria donors. Fulfilling a need, we aim to present an innovative analytical method based on solid-phase microextraction (SPME) - chemical biopsy. In order to track changes affecting the organ throughout the entire transplant procedure, porcine kidneys were subjected to multiple samplings at various time points. The application of small-diameter SPME probes assured the minimal invasiveness of the procedure. Porcine model kidney auto-transplantation was executed for the purpose of simulating two types of donor scenarios: donors with a beating heart (HBD) and donors after cardiac death (DCD). All renal grafts were exposed to continuous normothermic *ex vivo* perfusion. Following metabolomic and lipidomic profiling using high-performance liquid chromatography coupled to a mass spectrometer, we observed differences in the profiles of HBD and DCD kidneys. The alterations were predominantly related to energy and glucose metabolism, and differences in the levels of essential amino acids, purine nucleosides, lysophosphocholines, phosphoethanolamines, and triacylglycerols were noticed. Our results indicate the potential of implementing chemical biopsy in the evaluation of graft quality and monitoring of renal function during perfusion.

### Brief Commentary

**Background:** An ongoing problem of transplantology is organ shortage. To expand the pool of available donors, organs from the expanded criteria donors are considered. Limited analytical tools are accessible to make a decision on organ transplantation or rejection. Reliable no-/low-invasive way of organ's quality

assessment is required to estimate the risk of post-transplant outcomes.

**Translational Significance:** Tissue collection-free chemical biopsy revealed alterations in the levels of essential amino acids, purine nucleosides, lysophosphocholines, phosphoethanolamines, and triacylglycerols in heart beating donors vs. donors after cardiac death in porcine kidney model. Repeated sampling causes no injury enabling temporal and spatial monitoring of graft

**Abbreviations:** ADP, adenosine diphosphate; AMP, adenosine monophosphate; ATP, adenosine triphosphate; CAR, acyl carnitine; CE, cholesterol ester; CKD, chronic kidney disease; Cn, carbon numbers; DCD, donor after cardiac death; DG, diglyceride; DGF, delayed graft function primary nonfunction; ECD, expanded criteria donor; FA, fatty acid; HBD, heart beating donor; HILIC, hydrophilic interaction liquid chromatography; HMP, hypothermic machine perfusion; IGF, immediate graft function; I/R, ischemia/reperfusion; HTK, histidine-tryptophan-ketoglutarate; LPC, lysophosphocholine; MG, monoglyceride; NEVKP, normothermic *ex vivo* kidney perfusion; PC, phosphocholine; PCA, principal component analysis; PE, phosphoethanolamine; PLS-DA, partial least squares discriminant analysis; PNF, primary nonfunction; QC, quality control; ROS, reactive oxygen species; RP, reversed-phase chromatography; SM, sphingomyelin; SPME, solid phase microextraction; TG, triacylglycerol; VIP, The Variable Importance in Projection; WIT, warm ischemia time.

\* Corresponding author.

E-mail address: [bbojko@cm.umk.pl](mailto:bbojko@cm.umk.pl) (B. Bojko).

<sup>1</sup> These authors contributed equally to this work and share first authorship.

<https://doi.org/10.1016/j.trsl.2023.12.001>

Received 20 March 2023; Received in revised form 23 October 2023; Accepted 1 December 2023

Available online 3 December 2023

1931-5244/© 2023 Elsevier Inc. All rights reserved.

biochemistry changes in peritransplant period.

## Introduction

Kidney transplantation is a life-saving treatment for patients with end-stage renal dysfunction that enables higher survival rates and quality of life compared to dialysis treatment.<sup>1</sup> However, the number of patients placed on kidney transplant waiting lists is rapidly increasing, resulting in a growing gap between organ demand and availability. As a result, transplant centers are faced with the challenge of finding ways to maximize their use of all available organ resources and extend the donor pool in an attempt to close this gap.<sup>2,3</sup> Organs obtained from living donors offer several advantages for recipients, such as better graft function, faster recovery, and higher survival rates.<sup>4</sup> At the same time, it is more beneficial to obtain kidneys from expanded criteria donors (ECD) than to remain in a chronic dialysis program, especially in the case of elderly patients.<sup>3</sup> The use of kidneys from deceased donors whose heart has stopped beating—known as “donation after cardiac death” (DCD)—is a promising alternative approach with the potential to expand the donor pool. In contrast to live donations, DCD kidneys are exposed to warm ischemia time during the period between cardiac arrest and graft preservation. This poses a challenge, as prolonged warm ischemia inevitably influences kidney allograft outcomes and can lead to delayed graft function (DGF) or primary nonfunction (PNF).<sup>5,6</sup> An additional problem is the lack of reliable methods of assessing organ quality prior to transplantation. Currently, the surgeon decides whether to accept or decline a potential kidney based on their interpretation of the donor's recent laboratory tests and a visual evaluation of the organ. In some cases, a biopsy is used to evaluate tissue directly.<sup>2,7</sup> Although the biopsy procedure can yield significant information about pre-existing donor disease and vascular changes, it is not free of flaws. For example, the number of allowable biopsies during the transplantation procedure is strictly limited due to the procedure's invasiveness, which restricts its application for capturing dynamic changes and time-series analyses. While the value of histological findings is indisputable, they do not explain the molecular mechanisms of any observed aberrations.<sup>8</sup> Therefore, to increase the number of available organs for transplantation, a better method of assessing organ quality is direly needed.

Solid-phase microextraction (SPME) enables the detection of changes that occur in the organ during its preservation, spanning the period beginning with its removal from the donor's body and ending with its revascularization in the recipient's body.<sup>9</sup> The small diameter of the SPME probe (~200 µm) affords minimal invasiveness and allows the same organ to be sampled several times without damaging the tissue. Notably, SPME combines the sampling, extraction, and quenching of metabolites into a single step, making it a perfect tool for rapid on-site analysis. Furthermore, the biocompatibility of SPME coatings avoids the introduction of toxic compounds to the tissue and prevents the extraction of large molecules, such as proteins; as a result, enzymatic processes are already inhibited and the presence of artefacts are minimized at the time of sample collection, which is a great advantage over alternative sampling methods.<sup>10,11</sup> It is expected that the use of SPME will provide a more detailed understanding of the pre-transplant conditions responsible for delayed kidney function or dysfunction after transplantation, as well as how the graft preservation protocol influences the biochemistry of the organ.

Given that metabolomics and lipidomics enable the monitoring of the organism's immediate response to sudden environmental changes, these techniques may provide a better understanding of the alterations in biochemical pathways related to organ removal, preservation, and reperfusion along with following consequences such as ischemia, oxidative stress or inflammatory response.<sup>12–17</sup> Thus, direct measurements of metabolites and lipids concentrations in kidney tissue may

enable the identification of potential organ quality biomarkers and allow better predictions regarding graft outcomes.

This preliminary study aims to demonstrate the SPME method's potential for evaluating kidney quality during the transplantation procedure, with particular emphasis on two types of donors: heart beating donors (HBD) and DCD. Moreover, the attempts were made to identify the set of metabolites of a potential diagnostic value for further investigation.

## Materials and methods

### Chemicals

Pierce LTQ Velos ESI Positive External Calibrant Solution and Negative Ion Calibration Solution were purchased from Anchem (Anchem, Warsaw, Poland). Water (LC/MS Optima grade), ammonium acetate, formic acid, and acetic acid were purchased from Merck (Merck, Poznań, Poland), and acetonitrile, methanol, and isopropanol (all LC/MS Optima grade) were purchased from Alchem (Alchem, Toruń, Poland). Prototypes of biocompatible SPME mixed-mode probes (C18 and benzenesulfonic acid) were kindly provided by Supelco (Bellefonte, PA, USA).

### Animal

Male Yorkshire six pigs weighing 25–35 kg were used in this study. All animals received humane care in compliance with the “Principles of Laboratory Animal Care” formulated by the National Society for Medical Research and the “Guide for the Care of Laboratory Animals” published by the National Institutes of Health and the ARRIVE guidelines 2.0. All experimental protocols were approved by the Animal Care Committee at the Toronto General Hospital. The detailed autotransplantation procedure, warm ischemia induction, and NEVKP conditions are described elsewhere.<sup>18–20</sup> Briefly, animals were anesthetized using ketamine (20 mg/kg; Bimeda-MTC Animal Health Inc., Cambridge, Canada), atropine (0.04 mg/kg; Rafter 8 Products, Calgary, Canada), and midazolam (0.3 mg/kg; Pharmaceutical Partners of Canada Inc., Richmond Hill, Canada) by intramuscular (IM) injection. Animals were intubated, anesthesia continued using 2.0 % isoflurane (Pharmaceutical Partners of Canada Inc., Richmond Hill, Canada), and a permanent central venous catheter (9.5 French; Cook Medical Company, Bloomington, US) placed into the jugular vein. A midline incision was performed for dissection of right kidneys and clamping of renal vein and artery, in case warm ischemia was applied. Following graft resection, renal artery (1.6”, LivaNova PLC), vein (1/4”x1/8”, LivaNova PLC), and ureter (feeding tube) were cannulated, kidneys cold flushed with 4°C cold histidine-tryptophan-ketoglutarate (HTK) solution (300–500 mL) containing 10,000 IU/L heparin (Sandoz Canada Inc., Toronto Canada) at a pressure of 100 cmH<sub>2</sub>O. Following abdominal closure, animals were recovering from surgery until transplantation procedure was initiated in the evening.

Normothermic *ex vivo* kidney perfusion (NEVKP) was performed using a S3 heart lung machine and neonatal cardiopulmonary bypass equipment from LivaNova (LivaNova PLC, London, United Kingdom). During NEVKP, renal grafts were placed in a heated organ chamber. A physiologic perfusate solution was developed, based on normal values obtained from 20 healthy pigs as previously described elsewhere.<sup>18</sup> Additional pigs served for blood collection. Nonblood group-matched whole blood was washed twice to obtain leukocyte-depleted, plasma-free erythrocytes. The circuit was primed using Ringer's lactate (200 mL), Steen solution<sup>TM</sup> (150 mL), washed erythrocytes (125 mL), double reverse osmosis (DRO) water (27 mL), sodium bicarbonate (8.4 %, 8 mL), calcium gluconate (10 %, 100 mg/mL, 1.8 mL), and heparin (1000 IU). Following flush with HTK, renal grafts were connected to the circuit and perfused at 37°C. Arterial pressure was initially set to 75 mmHg. Throughout perfusion and graft rewarming, pressures dropped

to 65 mmHg and were maintained at this level. Oxygen (2L/min, 95 % O<sub>2</sub>, 5 %CO<sub>2</sub>), nutrition (amino acids and glucose (1 mL/h), insulin (5IU/h), verapamil (0.25 mg/h), and Ringer's lactate (urine and evaporation replacement) were administered continuously. Perfusion circuit characteristics were recorded continuously. Following 8 hours of NEVKP, grafts were flushed with 300–500 mL HTK to surgical implantation.

During the last hour of graft preservation, pigs were re-anesthetized with an intravenous propofol administration. After intubation, anesthesia was maintained using 1.5 % isoflurane per inhalation and 15 mL/h propofol i.v. Repeat laparotomy, contralateral kidney resection, and heterotopic renal autotransplantation were performed. Operative and perioperative procedures, drug administration, and follow up were conducted according to the "Guide for the Care of Laboratory Animals". Animals were followed for 3 days and then sacrificed under anesthesia.

#### Solid-phase microextraction

Direct kidney sampling was conducted using SPME fibers coated with mixed-mode extraction phase to a length of 7 mm. Given that a kidney is an organ which structure is heterogeneous, i.e., consists of cortex and medulla, for replicable results, the short enough length of the extraction phase was selected to sample the kidney cortex only. Renal autotransplantation was performed in porcine models to simulate two types of donor scenarios: HBD and DCD ( $n = 3$  in each group). Based on the results obtained in previous studies (serum creatinine and serum blood urea nitrogen levels), we noticed that kidney function deteriorates with increasing warm ischemia time, therefore we assumed that HBD scenario simulates an ischemia-free control group.<sup>20</sup> All renal grafts were perfused using continuous normothermic *ex vivo* kidney perfusion (NEVKP). For both donor scenarios, sampling was performed *in vivo* before retrieval; after 1 h, 3 h, 5 h, and 7 h of perfusion; and again *in vivo* immediately after revascularization. In addition, kidneys from the DCD cases were also sampled after 45 min and 2 h of warm ischemia time (Fig. 1). Before sampling, all fibers were preconditioned for 60 min in a methanol/water (50:50 v/v) solution followed by rinsing with purified water for a few seconds. The extractions were performed by inserting the SPME fibers into the kidney cortex for 30 min at each time point. After sampling, the fibers were removed from the organ, quickly rinsed with water, and then gently dried with wipes to remove any tissue or blood residue. Next, the fibers were placed into empty glass vials and stored in a freezer at  $-80^{\circ}\text{C}$  until analysis. All fibers were desorbed immediately before instrumental analysis. To this end, the SPME fibers were placed into vials containing 200  $\mu\text{L}$  of desorption solution and agitated (1200 rpm) using a BenchMixer™ MultiTube Vortexer (Benchmark Scientific, Edison, USA) for 120 min. The desorption solutions consisted of acetonitrile: water (80:20, v/v) and isopropanol: methanol (50:50, v/v) for

metabolomic and lipidomic analyses, respectively. To eliminate the analysis of contaminating compounds, extraction blanks were prepared. In this study, the extraction blanks consisted of fibers prepared using the same protocol as the rest of the fibers (preconditioning, desorption, etc.), only they were not used for kidney sampling.

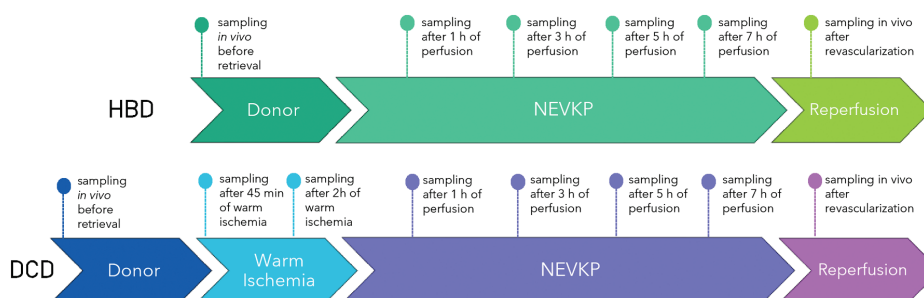
#### Liquid chromatography–high resolution mass spectrometry analysis (LC–HRMS)

Samples were analyzed using an LC–HRMS procedure based on the coupling of an ultra-high performance liquid chromatograph and a Q-Exactive Focus Orbitrap mass spectrometer. Data acquisition was performed using dedicated Thermo Scientific software, namely, Xcalibur 4.2 and Free Style 1.4 (Thermo Fisher Scientific, San Jose, California, USA). The instrument was calibrated via external calibration every 72 h, resulting in a mass accuracy of  $<2$  ppm. Within-sequence samples were randomized, and pooled quality control (QC) samples composed of 10  $\mu\text{L}$  of each sample were run every 8–10 injections to monitor instrument performance.

#### Metabolomic analysis

Chromatographic separation was carried out in reversed-phase (RP) using pentafluorophenyl column (Supelco Discovery HS F5, 2.1 mm  $\times$  100 mm, 3  $\mu\text{m}$ ) in positive and negative ionization mode. Phase A was water + 0.1 % formic acid and phase B was acetonitrile + 0.1 % formic acid. The gradient was as described previously.<sup>9</sup> The flow was set to 0.3 mL/min, and an injection volume of 10  $\mu\text{L}$  was employed. The column temperature was set to  $25^{\circ}\text{C}$ , and the sample vials were held at  $4^{\circ}\text{C}$  in the autosampler. The mass spectrometer parameters in positive ionization mode were as follows: a sheath gas flow rate of 40 a.u.; an aux gas flow rate of 15 a.u.; a spray voltage of 1.5 kV; a capillary temp of  $300^{\circ}\text{C}$ ; an aux gas heater temp of  $300^{\circ}\text{C}$ ; an S-lens radio frequency level of 55 %; an S-lens voltage of 25 V; and a skimmer voltage of 15 V. The scan range was set to  $m/z$  80–1000 with a resolution of 70,000 full width at half maximum (FWHM). Acquisition was performed using an automatic gain control (AGC) target of  $1\text{E}6$ , with the C-trap injection time set to auto. In negative ionization mode, the mass spectrometer parameters were as follows: a sheath gas flow rate of 48 a.u.; an aux gas flow rate of 11 a.u.; a spray voltage of 2.5 kV; a capillary temp of  $256^{\circ}\text{C}$ ; an aux gas heater temp of  $413^{\circ}\text{C}$ ; an S-lens radio frequency level of 55 %; an S-lens voltage of  $-25$  V; and a skimmer voltage of  $-15$  V. In this mode, the scan range was set to  $m/z$  80–1000 with a resolution of 70,000 FWHM. Acquisition was performed using an automatic gain control (AGC) target of  $1\text{E}6$ , with the C-trap injection time set to auto.

The putative identification of compounds was confirmed based on Full MS/dd-MS2 mode. The fragmentation parameters were as follows: mass resolution—35,000 FWHM; AGC target— $2\text{E}4$ ; minimum



**Fig. 1.** Study design. Two types of donor scenarios—heart beating donors (HBD) and donors after cardiac death (DCD)—were examined in porcine models of renal autotransplantation. All renal grafts were perfused at  $37^{\circ}\text{C}$  with the use of continuous normothermic *ex vivo* kidney perfusion (NEVKP). Sampling was performed as follows: *in vivo* before retrieval; after 1 h, 3 h, 5 h, 7 h of perfusion; and *in vivo* immediately after revascularization. In addition, the DCD kidneys were also sampled after 45 min and 2 h of warm ischemia.

AGC—8E3; intensity threshold—auto; maximum IT—auto; isolation window—3.0 *m/z*; stepped collision energy—10 V, 20 V, 40 V; loop count—2; and dynamic exclusion—auto.

#### Lipidomic analysis

Chromatographic separation was carried out on a hydrophilic stationary phase (HILIC) column (SeQuant ZIC-cHILIC, 3  $\mu\text{m}$  100  $\times$  2.1 mm) and in reversed-phase using a C18 column (Waters, XSelect CSH C18, 3.5  $\mu\text{m}$ , 2.1  $\times$  75 mm). The analyses were performed in positive electrospray ionization mode. The mobile phases for the HILIC column were acetonitrile (A) and 5mM ammonium acetate in water (B). The mobile phases for the RP column were: phase A consisted of water: methanol (60:40; v/v) and phase B of isopropanol: methanol (90:10; v/v), both containing 10 mM ammonium acetate and 1 mM acetic acid. The gradients were as described previously.<sup>9</sup> A flow rate of 0.4 mL/min and a temperature of 40°C was used for the HILIC column, while a flow rate of 0.2 mL/min and temperature of 55°C was used for the RP column. The sample vials were held at 4°C in the autosampler, and an injection volume of 10  $\mu\text{L}$  was used. The mass spectrometer parameters for the HILIC separations were as follows: a spray voltage of 1500 V; a capillary temperature of 325°C; sheath gas at 60 a.u.; an aux gas flow rate of 30 a.u.; a spare gas flow rate of 2 a.u.; a probe heater temperature of 325°C; an S-Lens radio frequency level of 55 %; an S-lens voltage of 25 V; and a skimmer voltage of 15 V. For the RP analysis, the following HESI ion source parameters were employed: a spray voltage of 3500V; a capillary temperature of 275°C; sheath gas at 20 a.u.; an aux gas flow rate of 10 a.u.; a spare gas flow rate of 2 a.u.; a probe heater temperature of 300°C; an S-Lens radio frequency level of 55 %; an S-lens voltage of 25 V; and a skimmer voltage of 15 V. For both types of separation, the scan range was set to *m/z* 80–1000 with a resolution 70,000. In addition, in both cases, acquisition was performed using an AGC target of 1E6, and the C-trap injection time was set to auto.

The putative identification of compounds was confirmed based on Full MS/dd-MS2 mode using the following fragmentation parameters: mass resolution—35,000 full width at half maximum (FWHM); AGC target—2E4; minimum AGC—8E3; intensity threshold—auto; maximum IT—auto; isolation window—3.0 *m/z*; stepped collision energy—20 V, 30 V, 50 V; loop count—2; dynamic exclusion—auto.

#### Data processing and statistical analysis

Metabolomic data processing was performed using Compound Discoverer 2.1. (Thermo Fisher Scientific, San Jose, California, USA) software with the following parameters: selected mass tolerance window—max 3 ppm; peak intensity >10 000; signal-to-noise threshold >3; and a max sample-to-blank ratio >5. The QC-based area was used for correction (min 50 % coverage, max 30 % RSD in QC).

Features were putatively identified by searching for their exact molar weights in CEU Mass Mediator. The spectra of fragmented compounds were identified using Thermo Scientific FreeStyle 1.4 software linked to the mzCloud online database and by using MS/MS search in CEU Mass Mediator.

The lipidomic data was processed using LipidSearch 4.1.30 (Thermo Fisher Scientific, San Jose, California, USA) software with the following parameters: peak intensity >10 000; a precursor tolerance of 5 ppm; a product tolerance of 10 ppm; an m-score threshold of 2; a Quan *m/z* tolerance of  $\pm$  5 ppm; a Quan RT (retention time) range of 0.5 min; use of main isomer filter. Protonated, sodiated, potassiated, and ammoniated adducts were considered for positive ion mode. After completing the lipid identification step, peak alignment was performed using the LipidSearch software and the following parameters: an m-Score threshold of 10; a retention time tolerance of 0.25 min; a QC-to-extraction blank ratio >5; and a max 30 % RSD in the QC.

The peak areas for the obtained compounds were analyzed using MetaboAnalyst 4.0 and Statistica 13.3 PL (StatSoft, Inc., Tulsa, Oklahoma, USA) software. All of the missing values were replaced with small

values assumed to be a detection limit. Data were normalized by median, log-transformation, and Pareto scaling. A paired t-test was used to evaluate the statistical significance in normally distributed continuous parameters over time within the same group, while the Mann-Whitney U test was used to compare non-parametric variables. A P-value of < 0.05 was considered significant. In addition, principal component analysis (PCA) and partial least squares discriminant analysis (PLS-DA) were conducted to visually assess separation between sample groups, with variable importance in projection (VIP) scores >1 being considered as significant. The PLS-DA model was cross-validated using leave-one-out cross validation. Two-dimensional score plots were generated to visually assess the separation of sample groups. Pathway analysis was carried out with MetaboAnalyst 5.0, using Homo sapiens Kyoto Encyclopedia of Genes and Genomes (KEGG) metabolic pathway database. The analysis used the hypergeometric test as an enrichment method and relative betweenness centrality for topology analysis, and the results were presented in the form of scatter plots. A pattern matching method based on the Pearson *r* distance measure was implemented to search for compounds with linearly changing relative concentrations over the time of perfusion and warm ischemia (across particular time points).

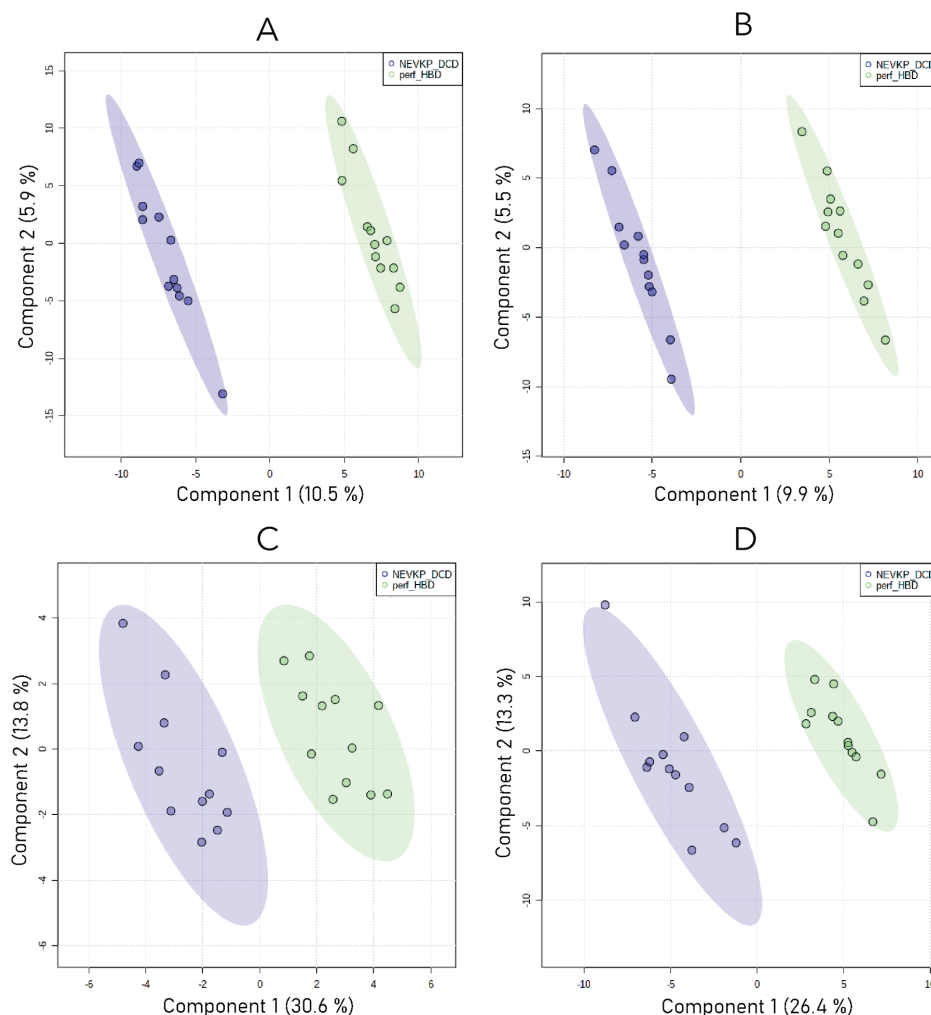
#### Results

Principal component analysis (PCA) was used to confirm the quality of the instrumental analysis. As shown in Fig. S1 (A, B, C, D), the QC samples formed tight clusters, confirming the quality of the obtained results.

Particular time points were compared based on the experiment conditions (i.e., *in vivo* and *ex vivo* during perfusion), with the analysis of the results being divided into three categories: i) changes in the metabolomic and lipidomic profiles of the kidney during perfusion; ii) the influence of the whole transplantation procedure on HBD and DCD kidneys; and iii) comparison of the condition of the HBD and DCD grafts after the use of NEVKP. During the data analysis and discussion of the results, the main emphasis was placed on compounds whose identification was confirmed by comparing the fragmentation spectra with online databases. Lists of the identified metabolites and lipids are provided in Tables S1 and S2, respectively.

#### Evaluation of changes in kidney metabolomic and lipidomic profiles during normothermic *ex vivo* kidney perfusion

The PLS-DA method was employed to obtain a more specific model of the differences in the metabolomic and lipidomic profiles of the HBD and DCD kidneys between perfusions (Fig. 2). Before constructing the PLS-DA models, separations of particular groups were evaluated on PCA scores plots (Fig. S2). Each PLS-DA model was validated using leave-one-out cross validation. This statistical analysis allowed the number of features to be refined, yielding a set of compounds that differentiated the two analyzed groups. The differences observed within the metabolites in both positive and negative ionization modes were mainly related to a large group of amino acids and their derivatives. In terms of nucleosides, higher levels of adenosine and inosine were detected in the DCD grafts. The distinctions observed among lipids were mainly associated with phospholipids and triacylglycerols (TG) for the HILIC and RP separations, respectively. For instance, the DCD samples collected during perfusion contained higher levels of TG with carbon numbers (Cn) 30–40 compared to the corresponding HBD samples. Furthermore, the DCD samples were characterized by lower levels of lysophosphocholines (LPCs) compared to the HBD samples. In addition, volcano plots were generated using the Mann-Whitney U test with FDR correction versus the magnitude of change (fold change > 2.0) and shown in Fig. S3. However, more discriminative compounds of potential biological meaning were identified during chemometric analysis. Differences between levels of selected metabolites identified with chemometric



**Fig. 2.** PLS-DA score plots showing the separation between HBD and DCD perfusions ( $n = 12$ ). RP metabolomic analyses in (A) positive and (B) negative ionization modes; lipidomic analyses with (C) HILIC and (D) RP separations. For the metabolomic analyses, the Q2 and R2 values for the PLS-DA model were 73 % and 96 % for positive ionization mode and 71 % and 96 % for negative ionization mode, respectively. For the lipidomic analyses, the Q2 and R2 values for the PLS-DA model were 85 % and 96 % for HILIC separation and 91 % and 99 % for RP separation, respectively.

analysis are shown in Fig. S4. Furthermore, a pathway analysis was performed to identify relevant networks that undergo changes. Pathway analysis was carried out using the list of significantly differential features from metabolomic and lipidomic analyses. The obtained results are presented in Fig. 3. Table S3 shows the complete list of identified pathways.

The Pearson correlation coefficient was used to evaluate changes across perfusion. The vast majority of the linearly correlated features were found in the metabolomic results rather than the lipidomic results. During perfusion, most of the compounds demonstrated a negative correlation with the HBD kidney, while no predominant trend was observed for the DCD graft. Boxplots of compounds that demonstrated linear correlations are shown in Fig. 4.

#### *Influence of transplantation procedure on HBD and DCD kidneys*

The two-dimensional score plots (PC1 vs. PC2) presented in Figs. S5 and S6 illustrate the differences in the metabolomic and lipidomic patterns of the kidney cortex between consecutive stages of the transplantation procedure. Overlapping distributions can be observed for data points in the score plots for the donor kidney types and reperfusion, which may indicate similarities in their metabolic profiles. In each figure, the cluster linked to the perfusion is noticeably separated, as it refers to the *ex vivo* conditions (Fig. S5 A, B, C, D). In contrast to the lipidome results (Fig. S5 C, D), the metabolome of the kidney during warm ischemia time (Fig. S5 A, B) is distinctly separated from other samples. Similarly, a slight overlapping of data points can be observed for HBD donor and reperfusion, as well as the separation of perfusion clusters (Fig. S6 A, B, C, D). The overall trends in the levels of identified

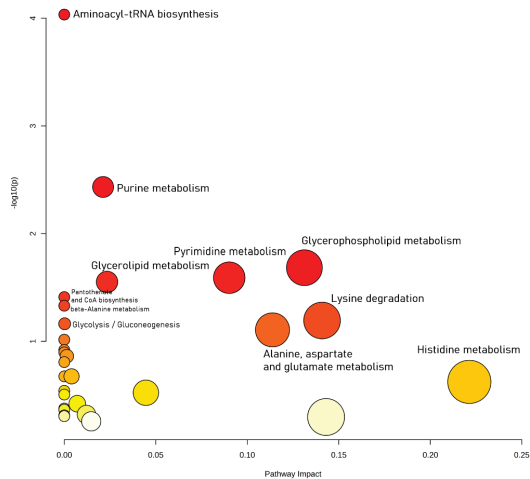


Fig. 3. Pathway analysis of significantly differential features from metabolomic and lipidomic analyses.

compounds are illustrated in the heat-maps shown in Fig. S7.

A paired sample t-test was carried out to determine how the kidney's metabolic profile was affected by the autotransplantation procedure. Discriminative changes were mainly found in the lipidomic analyses. Among the identified lipids, the level of phosphoethanolamines (PEs) increased after the transplant procedure in the DCD grafts. In addition,

decreased levels of LPCs, phosphocholines (PCs), and TG with Cn52 were also observed. Increased levels of TG with Cn30-40 were observed in the HBD kidneys, but no predominant trend for the relative concentrations of phospholipids before and after transplantation was detected. Changes in the levels of the selected metabolites are shown in Fig. 5.

Moreover, the Pearson correlation coefficient was used to evaluate changes across warm ischemia time. The linear correlation of metabolites observed over warm ischemia time indicated dynamic changes within the organ involving positively correlated amino acids such as leucine, alanine, and valine ( $r > 0.7$ ). Boxplots of compounds demonstrating linear correlation are shown in Fig. 6.

#### Comparison of the condition of HBD and DCD grafts after NEVKP

The Mann-Whitney U test was used to compare the condition of the HBD and DCD grafts after NEVKP. In the metabolomic analysis, most of the compounds significantly differentiating the HBD and DCD kidneys after reperfusion were found to be present at higher levels in the DCD kidneys. These compounds included: alanine, glutamine, lysine, histidine, tryptophan, aspartic acid, cystine, adenosine, deoxyguanosine, inosine, pyroglutamic acid, and creatine. Conversely, higher levels of guanine, indolelactic acid, serine, valine, alpha-aminoadipic acid, and acetylcarnitine were observed in the HBD kidneys. In the lipidomic analysis, higher levels of PE P-34:4, PE P-36:5, TG 50:2, TG 52:3, and TG 52:2 were found in the HBD kidneys after perfusion, while higher levels of DG 32:0, TG 36:0, and TG 38:0 were found in the DCD kidneys after perfusion. In addition, plots showing relative concentrations and time relationships were constructed to visualize the results and show trends among the compounds differentiating the perfusion and reperfusion time points (Fig. 7). Interestingly, an investigation of the plots showing relative concentrations and time relationships revealed that 65 % of the

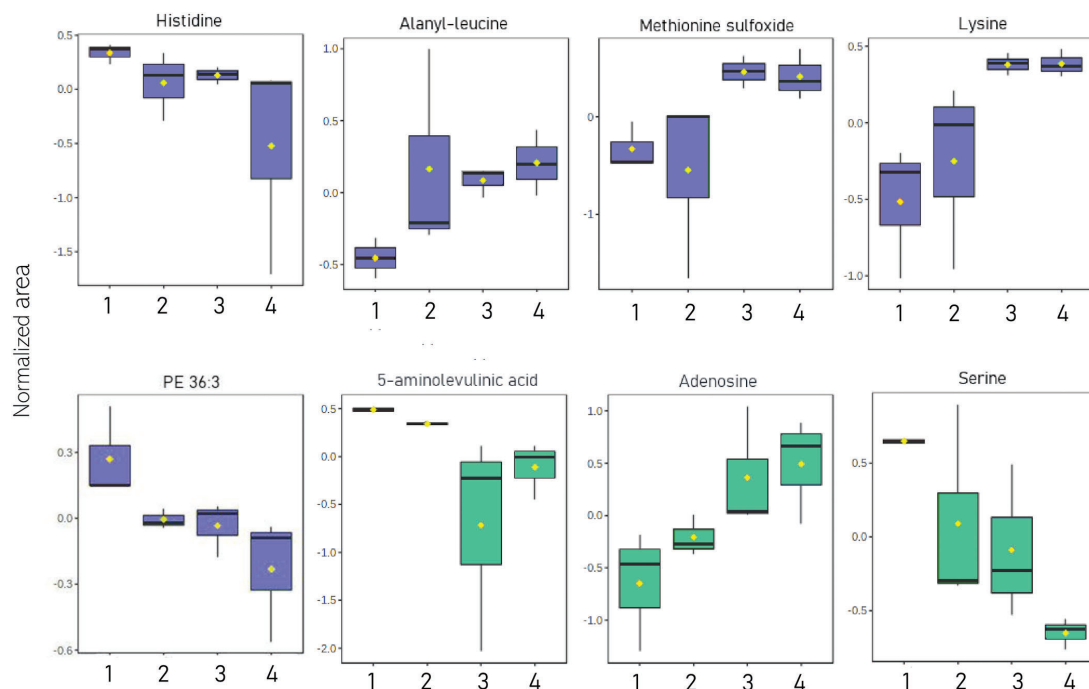
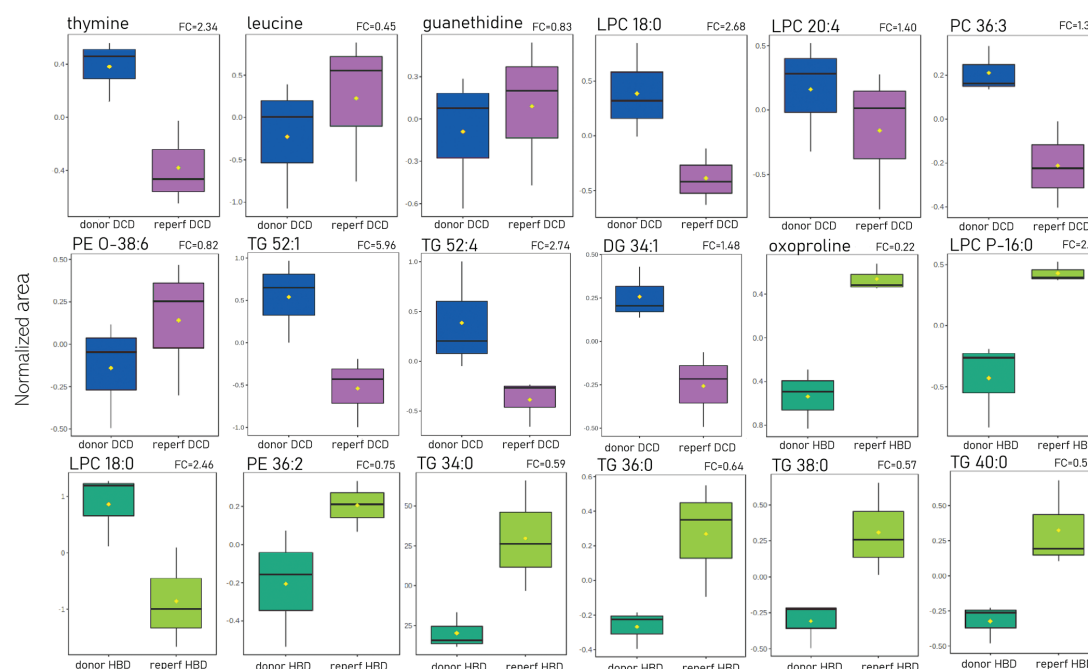


Fig. 4. Linear correlations ( $r > 0.7$ ) between metabolites and four time points across kidney perfusion ( $n = 3$ ). The boxplots display the normalized peak areas, while the notch indicates the 95 % confidence interval around the median of each group. The mean area of each group is indicated with a yellow diamond. Blue box-perfusion of DCD, green box- perfusion of HBD 3,



**Fig. 5.** Change in the levels of selected compounds ( $p < 0.05$ ) before and after the autotransplantation procedure ( $n = 3$ ). The boxplots display the normalized peak areas, while the notch indicates the 95 % confidence interval around the median of each group. The mean area of each group is indicated with a yellow diamond. Blue box- donor DCD, violet box- reperfusion of DCD; dark green box- donor HBD, light green box- reperfusion of HBD; FC- fold change donor/reperfusion.

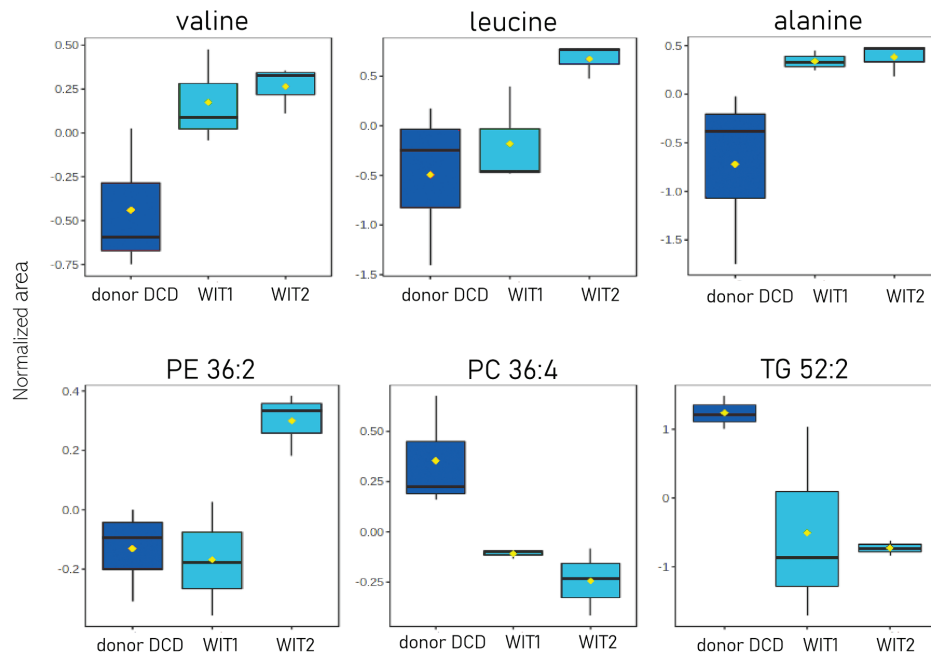
lipids and 44 % of the other metabolites that differentiated perfusion in the PLS-DA models were present in relatively similar concentrations in the HBD and DCD kidneys after reperfusion.

## Discussion

The kidney displays the second highest metabolic rate after the heart.<sup>21</sup> Depending on the segment of the nephron, tubular cells use different substrates such as glucose, amino acids, fatty acids (FA), or ketone bodies to produce energy through fatty acid oxidation (FAO) and glycolysis.<sup>21</sup> Mitochondrial fatty acid  $\beta$ -oxidation serves as the preferred source of adenosine triphosphate (ATP) in the kidney, and its dysfunction results in ATP depletion and lipotoxicity leading to tubular injury and inflammation and subsequent fibrosis progression.<sup>22</sup> Recent lipidomic studies have found that the number of polyunsaturated TGs with higher carbon numbers increases between stage 2 and stage 5 of chronic kidney disease (CKD), while the number of TGs with low carbon numbers and low numbers of double bonds decreases, which indicates impaired  $\beta$ -oxidation.<sup>23</sup> In the present study alterations in neutral glycerolipids, including TG and DG were noticed. In the DCD grafts, significant reductions in DG 34:1, TG 52:1, TG 52:4, TG 52:3, and TG 52:2 were observed following reperfusion. By comparison, significant elevations in TG 38:0, TG 40:0, TG 36:0, TG 34:0, and TG 32:0 were observed in the HBD kidneys. Moreover, a comparison of the HBD and DCD groups during perfusion revealed higher levels of TG with Cn30-40 in the DCD samples. Association of the increase of low double-bond shorter TGs with mitochondrial  $\beta$ -oxidation has been previously reported. Afshinnia et al. demonstrated that a relatively higher abundance of shorter TGs correlates directly with the abundance of longer-chain acylcarnitines which indicates upregulation of FA  $\beta$ -oxidation.<sup>23</sup> The accumulation of neutral lipids in the cell is usually associated with

lipotoxicity; however, the renal toxicity of TGs depends on their acyl length and the number of double bonds.<sup>24,25</sup> Increased FAO and a higher abundance of saturated TGs with relatively shorter acyl chains may reflect an adaptive mechanism for detoxifying toxic saturated FA. In fact, several studies suggest that increased FAO at an early stage of kidney disease may serve as an adaptive phenomenon in response to increased saturated FA.<sup>23,26</sup> However, with the progression of the disease, impairment of  $\beta$ -oxidation prevails and leads to further intracellular accumulation of FA and further mitochondrial damage.<sup>23</sup> An increase of low double-bond shorter TGs after reperfusion and higher levels of these lipids in DCD kidneys observed in this study suggest that I/R injury induces upregulation of FA  $\beta$ -oxidation as an early compensatory mechanism aimed at detoxifying toxic saturated FA.

Additionally, in this study, alterations in glucose and lactic acid levels were noticed. Those changes may be related to modifications in glucose metabolism. Recent studies indicated that in acute and chronic kidney injury, proximal tubular cells metabolism undergo a metabolic shift, moving from oxidative phosphorylation to glycolysis.<sup>21</sup> Glycolysis is the process that converts glucose into pyruvate through ten enzymatic reactions, and depending on oxygen availability, pyruvate is transported into the mitochondria to enter the TCA cycle or, in the absence of oxygen, pyruvate is converted into lactate.<sup>21,27</sup> Increased lactic acid observed during WIT indicated upregulation of glycolysis in response to ischemia and decreased oxygen availability. However, higher glucose level was also observed during WIT, which may indicate increased gluconeogenesis. Gluconeogenesis is a major renal metabolic pathway that can produce glucose from various substrates such as lactate, pyruvate, glycerol, or amino acids, mostly alanine and glutamine.<sup>27</sup> In the kidney, gluconeogenesis relies mainly on lactate, glutamine, and glycerol.<sup>21,27</sup> Although the metabolic shift from  $\beta$ -oxidation of FA toward glycolysis in kidney disease is well-described, there is little data about



**Fig. 6.** Linear correlations ( $r > 0.7$ ) between metabolites and time points across warm ischemia time ( $n = 3$ ). The boxplots display the normalized peak areas, while the notch indicates the 95 % confidence interval around the median of each group. The mean area of each group is indicated with a yellow diamond.

gluconeogenesis regulation during kidney injury.<sup>27</sup> However, based on the results obtained in this study, we hypothesize that injury triggered by warm ischemia caused changes in energy and glucose metabolism but did not lead to a complete switch from oxidative phosphorylation to glycolysis. Moreover, the alterations were temporary as no further lactic acid increase was observed, even after reperfusion. Additionally, a higher glucose level was observed during perfusion in DCD kidneys with no parallel increase of lactic acid, which may indicate further enhanced gluconeogenesis to improve lactate clearance.<sup>27</sup> Importantly, elevated lactate and lower glucose levels have been previously associated with increased mortality in patients with acute kidney injury.<sup>27,28</sup> Hence, the obtained results may indicate a positive effect of normothermic perfusion on organ function, inhibiting further damage to the graft.

Another notable findings of the present study's was alterations in purines and purine derivatives for both the HBD and DCD groups. For the HBD kidneys, an overall decrease in hypoxanthine, adenosine, guanine, and inosine levels was observed after reperfusion, along with a corresponding increase in methyladenosine, deoxyguanosine, adenosine monophosphate (AMP), and allantoin. Similarly, a decrease in the levels of hypoxanthine was observed in the DCD samples following reperfusion. However, in contrast to the HBD samples, the findings showed increased levels of inosine and adenosine, as well as a decline in methyladenosine, deoxyguanosine, and allantoin in the DCD kidneys after transplantation. Furthermore, we observed an increase in hypoxanthine, deoxyguanosine, and methyladenosine, and the downregulation of inosine levels in the DCD samples during WIT. It has been previously hypothesized that, as breakdown products of ATP, purines play an important role in the molecular mechanisms of ischemia and hypoxia. The oxidation of hypoxanthine is disturbed during ischemia and hypoxia, causing the accumulation of hypoxanthine in the cells.<sup>29,30</sup> Once the ischemic tissue is re-supplied with blood, the molecular oxygen catalyzes hypoxanthine conversion by xanthine oxidase, liberating reactive oxygen species (ROS).<sup>31</sup> Moreover, a comparison of the DCD and

HBD grafts during perfusion revealed higher levels of adenosine, inosine, and deoxyguanosine in the DCD samples. The findings of numerous studies suggest the significant role of adenosine in controlling cellular adaptation to hypoxia, ischemia, and inflammatory processes, as well as its protective role in preventing I/R injury. Such conditions wherein oxygen supply is limited are related to intensified extracellular adenosine production due to the associated breakdown of ATP and adenosine diphosphate (ADP).<sup>32–36</sup> Our findings showed that adenosine and urocanic acid were the only metabolites to demonstrate significant linear progressive accumulation during the perfusion of HBD kidneys. Previous reports have well-established the role of adenosine accumulation and the activation of its four receptor subtypes ( $A_1AR$ ,  $A_2AAR$ ,  $A_2BAR$ , and  $A_3AR$ ) in protecting organs from I/R injury.<sup>30,35</sup> Inosine is a breakdown product of adenosine nucleotides, such as ATP, ADP, and AMP. Previous studies focusing on renal DCD allografts have found significantly lower levels of inosine in the perfusate from kidneys with DGF compared to the perfusate from immediate graft function (IGF).<sup>37,38</sup>

A thorough analysis of kidney graft tissue revealed that amino acid pathways were the most modulated. We observed significant linear growth of alanine, leucine, and valine levels during *in vivo* warm ischemia progression in DCD kidneys, as well as the accumulation of these amino acids in both HBD and DCD kidneys during perfusion. Interestingly, during perfusion, significantly higher levels of valine were found in HBD kidneys, while higher levels of alanine were detected in DCD kidneys. Liu et al.'s findings suggest that alanine is a sensitive discriminator of warm ischemia during porcine liver HMP,<sup>39</sup> while Bruinsma et al. observed elevated levels of alanine and valine during sub-normothermic machine perfusion of DCD human livers.<sup>40</sup> Elsewhere, Bon et al. found that increased concentrations of alanine and valine in perfused kidneys tended to result in less favourable outcomes.<sup>41</sup> Additionally, significantly higher levels of alanine and leucine were detected in the perfusate of DGF kidneys, which may be associated with cellular damage that occurs after the release of protein breakdown

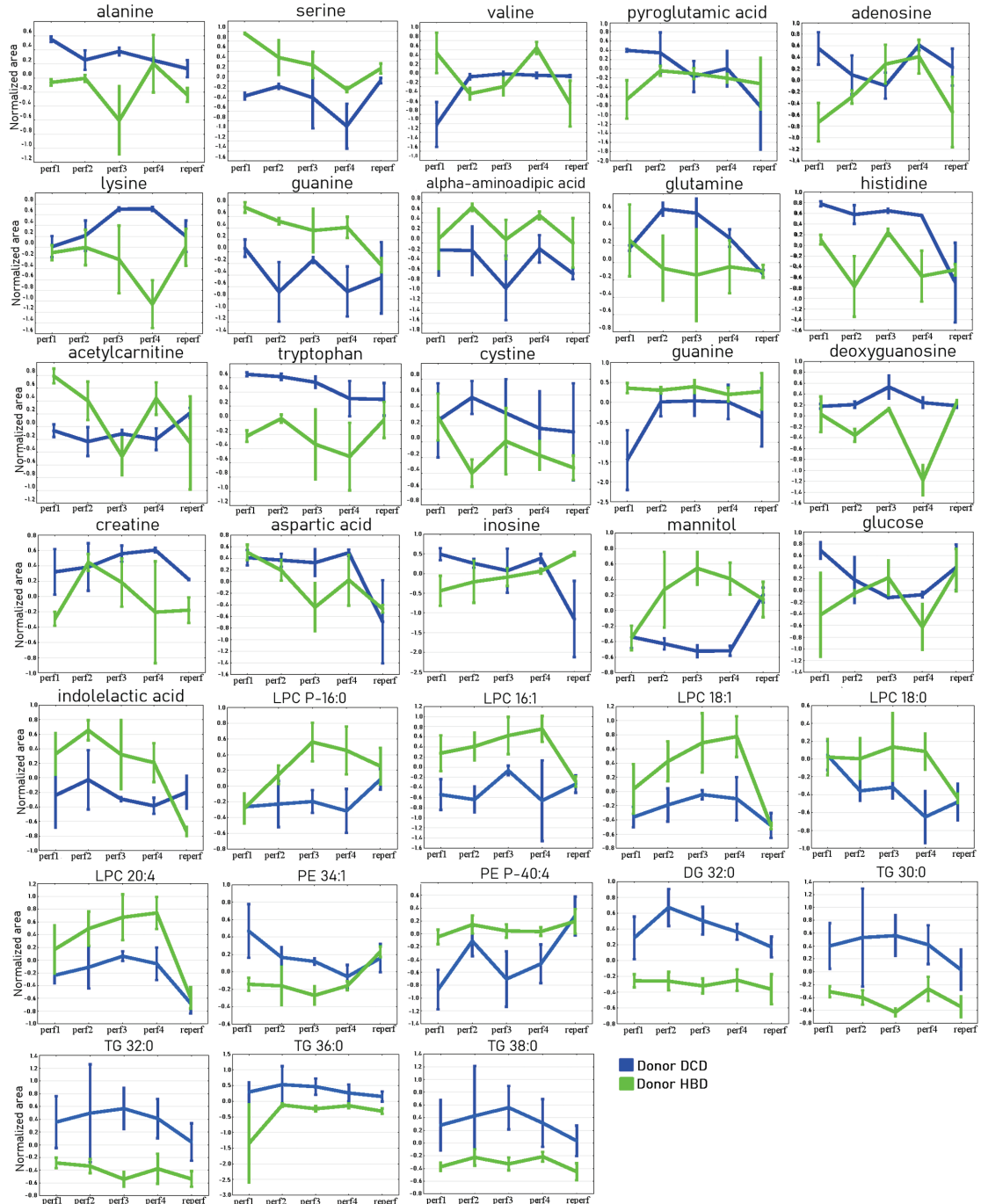


Fig. 7. Change in levels of selected compounds differentiating perfusions across perfusion and reperfusion time points ( $n = 3$ ). The values are presented as mean  $\pm$  SEM. Blue squares—DCD donors; green squares—HBD donors.

products into the perfusate.<sup>37</sup>

In the present study, a significant linear relationship between concentration and perfusion time was observed for several compounds. Linear reductions in serine and phenylalanine levels were noted for the HBD kidneys, while in the DCD kidneys, linear reductions in histidine levels were detected. In contrast, significant linear growth in lysine and methionine sulfoxide levels was observed for the DCD grafts. Moreover, decreases in phenylalanine, histidine, and methionine sulfoxide levels were observed during WIT. Previous reports have indicated that phenylalanine levels decrease as kidney function impairment progresses, which, may complement our findings related to the down-regulation of this amino acid during perfusion.<sup>42</sup> Furthermore, the alleviation of plasma and perfusate phenylalanine levels has been associated with rapid CKD development and DGF, respectively.<sup>38,43</sup> Zhang et al. reported a significant decrease in phenylalanine and histidine levels in the urine of rats with CKD, indicating the possible impairment of these amino acids or intensified catabolism.<sup>44</sup> It has been hypothesized that reduced histidine concentrations are related to protein-energy wasting, systemic inflammatory processes, and oxidative stress development. Histidine is thought to act as an anti-oxidant agent due to its ability to scavenge the ROS generated by cells during inflammation.<sup>44,45</sup> In addition, urinary histidine levels were lower in patients with impaired graft function after renal transplantation compared to those with well-preserved renal function.<sup>46</sup> Our data revealed a significant linear increase in methionine sulfoxide levels throughout the time of preservation for DCD patients. It has been recently established that the cyclic oxidation of methionine to methionine sulfoxide and its subsequent reduction back to methionine is an important protective mechanism against reactive oxygen species. It is believed that the severity of changes in post-ischemic histological kidneys is correlated with methionine sulfoxide reductase A. The accumulation of methionine sulfoxide in renal tissue during the preservation of kidneys may be associated with the ongoing progression of oxidative stress.<sup>47,48</sup>

In the DCD and HBD groups, relevant changes in LPCs levels were observed following reperfusion. For instance, reduced levels of LPC 18:0 were detected in both the HBD and DCD kidneys. Levels of LPC 20:4 were lower than the baseline for both donor types, but this reduction was only significant for the DCD kidneys. Similarly, while increased levels of LPC P-16:0 were observed in both donor types, this increase was only significant in the HBD grafts. Moreover, we observed a non-significant elevation in the overall levels of LPCs during warm ischemia. However, a comparison of the HBD and DCD grafts during perfusion showed lower levels of numerous LPCs in the DCD kidneys. LPCs, via G protein-coupled receptors and Toll-like receptors, activate multiple signalling pathways and may have harmful effects on various cells, including increasing oxidative stress and enhancing inflammatory responses.<sup>16,49</sup> However, recent studies have been inconclusive, and the mechanisms underlying the harmful effects of LPCs have not been fully investigated.<sup>50</sup> Several studies have reported increased levels of LPCs after I/R in animal models<sup>15,51</sup> and patients with stage 4 and 5 CKD.<sup>52</sup> On the other hand, Rhee et al. have reported declining levels of LPCs in patients with CKD and reducing levels of LPC 14:0 in patients with end-stage renal disease,<sup>53,54</sup> while Tsai et al. have recently shown lower levels of LPC 16:0 in recipients with early allograft dysfunction.<sup>55</sup> Interestingly, the current study found that LPCs levels may increase during warm ischemia and decrease after reperfusion and similar results were observed for DCD liver transplant.<sup>49</sup> LPCs with a single acyl chain are breakdown products of membrane phospholipids; hence, previous findings have suggested that a reduction in LPCs indicates that membrane breakdown and remodelling might be transiently inhibited following I/R.<sup>56</sup>

PCs and PEs are the most abundant phospholipids in all mammalian cells and subcellular organelles. While previous research suggests that an alteration in the absolute concentrations of these phospholipids is not a key determinant of cellular processes associated with health and

disease, the PC/PE ratio may be.<sup>57</sup> This work showed a significant reduction in PC 36:3 in the DCD kidneys after reperfusion. Previous studies have also reported reduced levels of different PCs in patients with stage 4 and 5 CKD and patients with end-stage renal disease.<sup>53,54</sup> In the present study, we observed reduction of PEs after warm ischemia and an increase after reperfusion (Fig. S6 E). In the DCD group, we observed significant increases in PE O-38:6, PE O-38:5, and PE 36:2 after reperfusion and non-significant increases in other identified PEs. In addition, the HBD group showed higher PE P-34:4 and PE P-36:5 levels than the DCD group following reperfusion. Previous reports documented reduced PEs levels in animal models of renal I/R<sup>15,51</sup> and elevations in the abundance of PEs in 5-stage CKD patients.<sup>23</sup> PEs are multifunctional lipids that play an essential role in various cellular processes.<sup>24,57,58</sup> However, the mechanism linking PEs and kidney disease progression is not well understood and remains unidentified. In the current study, elevated levels of several PEs and reduced levels of PC 36:4 and PC 36:3 in DCD kidneys were observed, which may impact the overall PC/PE ratio and can, in turn, influence processes in a number of organelles. For instance, a lower PC/PE ratio may impair liver regeneration, affect energy metabolism, increase cell leakage, and cause endoplasmic reticulum stress.<sup>57</sup>

Compared to standard methods such as biopsy or evaluation of donor laboratory results, SPME offers the possibility of multiple direct analyses of kidney tissue, which is hard to perform with other methods while maintaining low invasiveness of the procedure. The frequency of biopsies varies by medical facility and country. In the United States, up to 85 % of high-risk kidneys are biopsied, while pre-transplant biopsies are rarely performed in European medical facilities.<sup>7,59,60</sup> Unlike most laboratory data, histopathological evaluation of a biopsy does not give a single value; instead, they create comprehensive diagnoses that consider all available information. Although glomerulosclerosis, vascular disease, and interstitial fibrosis are the most commonly reported renal parameters associated with worse graft outcomes, there is no consensus on the relative importance of each factor and what threshold values should be used to determine acceptable cutoffs. Results of currently performed studies that address the predictive value of renal biopsy concerning graft outcomes have been predominantly inconclusive.<sup>61–64</sup> Moreover, another difficulty is the low reproducibility of renal biopsy assessments between on-call pathologists and renal pathologists described in many previous studies.<sup>65</sup> Additionally, the number of biopsies is usually limited to single sampling due to the procedure's invasiveness. However, it is worth emphasizing that the indisputable advantage of direct tissue analysis is the detection of organ-specific changes. Traditional clinical diagnoses are usually performed on blood tests and inform of the overall health status of an individual. However, especially with deceased donors, observed changes may not correlate with the status of the organ but can be related to the cause of death or comorbidities. Moreover, in the case of a kidney transplant, blood analysis is possible only before the organ's procurement or after transplantation; thus, there is no possibility of detecting injury triggered by organ ischemia or long preservation. The undoubted advantage of SPME is low-invasiveness which allows for multiple sampling and monitoring changes over time. Moreover, as the obtained results indicate, direct tissue analysis with the use of SPME allows the detection of even subtle differences between the examined organs, which allows us to assume that in future studies, it will be possible to identify a panel of metabolites that will be used to assess the quality of the organs. Targeted analysis for a selected panel of metabolites would shorten the sampling and instrumental analysis time. In this study, the 30-minute extraction time was applied because the animal experiment enabled a relatively long sampling period to evaluate the sampling process fully. However, that long sampling time could be impractical in clinical practice. It could be shortened to 10 or even fewer minutes for clinical application with no noticeable effect on the results' quality.<sup>66</sup> To shorten analysis time, some strategies enable fast determination of selected compounds by direct coupling of SPME probe with a mass spectrometer or other detector, i.e., omitting time-consuming

chromatographic separation.<sup>67–69</sup> Still, it should be emphasized that the extract obtained with the current protocol might be used for both, immediate fast determination of biomarkers as well as untargeted analysis. The latter can be used retrospectively in cases where additional information on the alteration occurring in the graft is needed. Sampling could be performed before organ procurement to evaluate donor organ quality and, for doubtful cases, additionally before organ implementation. Furthermore, using SPME to monitor changes during organ perfusion may contribute to developing new, better perfusion methods thanks to the possibility of tracking dynamic changes that occur in the organ without graft damage. However, further clinical studies on large cohorts must be performed to achieve this long-time goal of implementing SPME chemical biopsy as an additional graft quality assessment method for routine clinical practice.

Despite these promising results, this study has several limitations. Kidneys deemed unsuitable for transplantation were not included in the comparison performed in this study. The complexity of factors contributing to organs' refusal for transplantation forces us to follow successive steps, where the results of one study make a base for the subsequent experimental design. The current study aimed to compare the best possible organs (HBD) and organs with moderate ischemic damage (DCD) to identify compounds and metabolic pathways that will be monitored in further models, for instance different ischemic degrees. It is also important to emphasize that routinely assessed parameters of kidney function were not measured in this research, therefore future studies should compare these results with standard laboratory tests to provide a comprehensive evaluation of the proposed method and its usefulness in graft quality assessment. Another limitation was the small sample sizes. However, this was consistent with the 3R principles (Replacement, Reduction, and Refinement) guiding animal experimentation, which call for the use of as few animals as possible.<sup>70</sup> Moreover, the use of SPME enables multiple analyses over time, which increased the number of samples that can be taken without requiring more animals.

## Conclusion

In summary, SPME followed by LC-MS/MS analysis permits the sampling of biological matrices and the capture and detection of numerous compounds with different polarities. Additionally, the small diameter of SPME probes enables minimally invasive and repeated sampling of the same tissue, thus allowing changes occurring in the organ to be tracked throughout the entire transplantation procedure—from graft collection, through organ storage, to reperfusion. As a result, we hypothesize that metabolites related to metabolic shift moving from oxidative phosphorylation to glycolysis (TGs with different acyl lengths and the number of double bonds, glucose, and lactic acid), and essential amino acids, purine nucleosides, LPCs, PEs are currently the most promising for a smaller panel for targeted analysis evaluating graft function and quality. However, future quantitative targeted studies are required to validate the current findings and to evaluate the predictive value of the selected metabolites.

## Data availability statement

The datasets generated during and/or analysed during the current study are available from the corresponding author on reasonable request

## CRedit authorship contribution statement

**Iga Stryjak:** Methodology, Formal analysis, Investigation, Data curation, Writing – original draft, Writing – review & editing. **Natalia Warmuzińska:** Methodology, Formal analysis, Investigation, Data curation, Writing – original draft, Writing – review & editing, Visualization. **Kamil Łuczykowski:** Investigation, Formal analysis, Writing – review & editing. **Karol Jarocho:** Investigation. **Peter Urbanellis:**

Methodology, Investigation. **Markus Selzner:** Conceptualization, Methodology, Investigation, Resources, Writing – review & editing. **Barbara Bojko:** Conceptualization, Methodology, Investigation, Resources, Writing – review & editing, Supervision, Funding acquisition.

## Declaration of Competing Interest

The authors declare no competing interests.

## Acknowledgment

This study was funded by National Science Centre, grant Opus No. 2017/27/B/NZ5/01013. The authors would like to acknowledge Supelco/MilliporeSigma for kindly supplying the SPME probes and Thermo Fisher Scientific for granting us access to a Q-Exactive Focus mass spectrometer. BB would like to thank Prof. Janusz Pawliszyn for arranging the opportunity to collect the samples used in this work at the Toronto General Hospital during her stay at the University of Waterloo.

## Supplementary materials

Supplementary material associated with this article can be found, in the online version, at [doi:10.1016/j.trsl.2023.12.001](https://doi.org/10.1016/j.trsl.2023.12.001).

## References

- Swanson KJ, Aziz F, Garg N, et al. Role of novel biomarkers in kidney transplantation. *World J Transpl*. 2020;10(9):230–255. <https://doi.org/10.5500/wjt.v10.i9.230>.
- Moekli B, Sun P, Lazeyras F, et al. Evaluation of donor kidneys prior to transplantation: an update of current and emerging methods. *Transpl Int*. 2019;32(5):459–469. <https://doi.org/10.1111/tri.13430>.
- Filiopoulos V, Boletis JN. Renal transplantation with expanded criteria donors: Which is the optimal immunosuppression? *World J Transpl*. 2016;6(1):103. <https://doi.org/10.5500/wjt.v6.i1.103>.
- Bellini MI, Courtney A, McCaughan J. Living donor kidney transplantation improves graft and recipient survival in patients with multiple kidney transplants. *J Clin Med*. 2020;9(7):2118. <https://doi.org/10.3390/jcm9072118>.
- Peters-Sengers H, Houtzager JHE, Idu MM, et al. Impact of cold ischemia time on outcomes of deceased donor kidney transplantation: an analysis of a national registry. *Transpl Direct*. 2019;5(5):1–11. <https://doi.org/10.1097/TXD.0000000000000888>.
- Bellini MI, Nozdrin M, Yiu J, Papalois V. Machine perfusion for abdominal organ preservation: a systematic review of kidney and liver human grafts. *J Clin Med*. 2019;8(8):1221. <https://doi.org/10.3390/jcm8081221>.
- Dare AJ, Pettigrew GJ, Saeb-Parsy K. Preoperative assessment of the deceased-donor kidney: from macroscopic appearance to molecular biomarkers. *Transplantation*. 2014;97(8):797–807. <https://doi.org/10.1097/01.TP.0000441361.34103.53>.
- Plattner BW, Chen P, Cross R, Leavitt MA, Killen PD, Heung M. Complications and adequacy of transplant kidney biopsies: a comparison of techniques. *J Vasc Access*. 2018;19(3):291–296. <https://doi.org/10.1177/1129729817747543>.
- Stryjak I, Warmuzińska N, Łuczykowski K, et al. Using a chemical biopsy for graft quality assessment. *J Vis Exp*. 2020;(160):e60946. <https://doi.org/10.3791/60946>.
- Reyes-Garcés N, Gionfriddo E, Gómez-Ríos GA, et al. Advances in solid phase microextraction and perspective on future directions. *Anal Chem*. 2018;90(1):302–360. <https://doi.org/10.1021/acs.analchem.7b04502>.
- Filiplak W, Bojko B. SPME in clinical, pharmaceutical, and biotechnological research – How far are we from daily practice? *TrAC Trends Anal Chem*. 2019;115:203–213. <https://doi.org/10.1016/j.trac.2019.02.029>.
- Kvietkauskas M, Zitkute V, Leber B, Strupas K, Stiegler P, Schemmer P. The role of metabolomics in current concepts of organ preservation. *Int J Mol Sci*. 2020;21(18):1–17. <https://doi.org/10.3390/ijms21186607>.
- Stryjak I, Warmuzińska N, Bogusiewicz J, Łuczykowski K, Bojko B. Monitoring of the influence of long-term oxidative stress and ischemia on the condition of kidneys using solid-phase microextraction chemical biopsy coupled with liquid chromatography–high-resolution mass spectrometry. *J Sep Sci*. 2020;43(9–10):1867–1878. <https://doi.org/10.1002/jssc.202000032>.
- Raigani S, Karimian N, Huang V, et al. Metabolic and lipidomic profiling of septic human livers during *ex situ* normothermic machine perfusion guides resuscitation strategies. *PLoS One*. 2020;15(1):1–20. <https://doi.org/10.1371/journal.pone.0228011>.
- Rao S, Walters KB, Wilson L, et al. Early lipid changes in acute kidney injury using SWATH lipidomics coupled with MALDI tissue imaging. *Am J Physiol Ren Physiol*. 2016;310(10):F1136–F1147. <https://doi.org/10.1152/ajprenal.00100.2016>.
- Alshinnia F, Rajendiran TM, Wernisch S, et al. Lipidomics and biomarker discovery in kidney disease. *Semin Nephrol*. 2018;38(2):127–141. <https://doi.org/10.1016/j.semnephrol.2018.01.004>.

17. Abbiss H, Maker GL, Trengove RD. Metabolomics approaches for the diagnosis and understanding of kidney diseases. *Metabolites*. 2019;9(2):34. <https://doi.org/10.3390/metabo9020034>.
18. Kathis JM, Spetzler VN, Goldaracena N, et al. Normothermic ex vivo kidney perfusion for the preservation of kidney grafts prior to transplantation. *J Vis Exp*. 2015;2015(101):1–13. <https://doi.org/10.3791/52909>.
19. Kathis JM, Echeverri J, Goldaracena N, et al. Heterotopic renal autotransplantation in a porcine model: a step-by-step protocol. *J Vis Exp*. 2016;2016(108):1–9. <https://doi.org/10.3791/53765>.
20. Kathis JM, Hamar M, Echeverri J, et al. Normothermic ex vivo kidney perfusion for graft quality assessment prior to transplantation. *Am J Transplant*. 2018;18(3):580–589. <https://doi.org/10.1111/ajt.14491>.
21. Faivre A, Verissimo T, Auwerx H, Legouis D, de Seigneux S. Tubular cell glucose metabolism shift during acute and chronic injuries. *Front Med*. 2021;8, 742072. <https://doi.org/10.3389/fmed.2021.742072>.
22. Jang HS, Noh MR, Kim J, Padanilam BJ. Defective mitochondrial fatty acid oxidation and lipotoxicity in kidney diseases. *Front Med*. 2020;7:65. <https://doi.org/10.3389/fmed.2020.00065>.
23. Afshinnia F, Rajendiran TM, Soni T, et al. Impaired b-oxidation and altered complex lipid fatty acid partitioning with advancing CKD. *J Am Soc Nephrol*. 2018;29(1):295–306. <https://doi.org/10.1681/ASN.2017030350>.
24. Afshinnia F, Nair V, Lin J, et al. Increased lipogenesis and impaired B-oxidation predict type 2 diabetic kidney disease progression in American Indians. *JCI Insight*. 2019;4(21):1–19. <https://doi.org/10.1172/jci.insight.130317>.
25. Weinberg JM. Lipotoxicity. *Kidney Int*. 2006;70(9):1560–1566. <https://doi.org/10.1038/sj.ki.5001834>.
26. Afshinnia F, Kretzler M, Afshinnia F, et al. Increased lipogenesis and impaired b-oxidation predict type 2 diabetic kidney disease progression in American Indians. *JCI Insight*. 2019;4(21):1–19. <https://doi.org/10.1172/jci.insight.130317>.
27. Legouis D, Faivre A, Cipà PE, De Seigneux S. Renal gluconeogenesis: an underestimated role of the kidney in systemic glucose metabolism. *Nephrol Dial Transpl*. 2022;37(8):1417–1425. <https://doi.org/10.1093/ndt/gfaa302>.
28. Freire Jorge P, Wieringa N, de Felice E, van der Horst ICC, Oude Lansink A, Nijsten MW. The association of early combined lactate and glucose levels with subsequent renal and liver dysfunction and hospital mortality in critically ill patients. *Crit Care*. 2017;21(1):1–11. <https://doi.org/10.1186/s13054-017-1785-z>.
29. Wijermans LGM, Schaapherder AF, de Vries DK, et al. Defective postreperfusion metabolic recovery directly associates with incident dialysis graft function. *Kidney Int*. 2016;90(1):181–191. <https://doi.org/10.1016/j.kint.2016.02.034>.
30. Fujii K, Kubo A, Miyashita K, et al. Xanthine oxidase inhibitor ameliorates postischemic renal injury in mice by promoting resynthesis of adenine nucleotides. *JCI Insight*. 2019;4(22):1–20. <https://doi.org/10.1172/jci.insight.124816>.
31. Prieto-Moure B, Carabén-Redaño A, Aliena-Valero A, et al. Allopurinol in renal ischemia. *J Invest Surg*. 2014;27(5):304–316. <https://doi.org/10.3109/08941939.2014.911395>.
32. Rabadi MM, Lee TH. Adenosine Receptors and Renal Ischemia Reperfusion Injury. *Acta Physiol*. 2015;213(1):222–231. <https://doi.org/10.1038/jid.2014.371>.
33. Bauerle JD, Grenz A, Kim JH, Lee HT, Eltzschig HK. Adenosine generation and signaling during acute kidney injury. *J Am Soc Nephrol*. 2011;22(1):14–20. <https://doi.org/10.1681/ASN.2009121217>.
34. Zimmerman MA, Kam I, Eltzschig H, Grenz A. Biological implications of extracellular adenosine in hepatic ischemia and reperfusion injury. *Am J Transpl*. 2013;13(10):2524–2529. <https://doi.org/10.1111/ajt.12398>.
35. Han SJ, Thomas Lee H. Mechanisms and therapeutic targets of ischemic acute kidney injury. *Kidney Res Clin Pract*. 2019;38(4):427–440. <https://doi.org/10.23876/j.krcp.19.062>.
36. Fisher O, Benson RA, Imray CH. The clinical application of purine nucleosides as biomarkers of tissue ischemia and hypoxia in humans in vivo. *Biomark Med*. 2018;13(11):953–965. <https://doi.org/10.2217/bmm-2019-0049>.
37. Guy AJ, Nath J, Cobbold M, et al. Metabolomic analysis of perfusate during hypothermic machine perfusion of human cadaveric kidneys. *Transplantation*. 2015;99(4):754–759. <https://doi.org/10.1097/TP.0000000000000398>.
38. Wang Z, Yang H, Zhao C, et al. Proton nuclear magnetic resonance (1H-NMR)-based metabolomic evaluation of human renal allografts from donations after circulatory death. *Med Sci Monit*. 2017;23:5472–5479. <https://doi.org/10.12659/MSM.905168>.
39. Liu Q, Vekemans K, van Pelt J, et al. Discriminate liver warm ischemic injury during hypothermic machine perfusion by proton magnetic resonance spectroscopy: a study in a porcine model. *Transpl Proc*. 2009;41(8):3383–3386. <https://doi.org/10.1016/j.transproceed.2009.09.025>.
40. Bruinsma BG, Sridharan GV, Weeder PD, et al. Metabolic profiling during ex vivo machine perfusion of the human liver. *Sci Rep*. 2016;6:22415. <https://doi.org/10.1038/srep22415>.
41. Bon D, Claire B, Thuillier R, et al. Analysis of perfusates during hypothermic machine perfusion by NMR spectroscopy: a potential tool for predicting kidney graft outcome. *Transplantation*. 2014;97(8):810–816. <https://doi.org/10.1097/TP.0000000000000046>.
42. Li R, Dai J, Kang H. The construction of a panel of serum amino acids for the identification of early chronic kidney disease patients. *J Clin Lab Anal*. 2018;32(3):1–7. <https://doi.org/10.1002/jcla.22282>.
43. Rhee EP, Clish CB, Wenger J, et al. Metabolomics of chronic kidney disease progression: a case-control analysis in the chronic renal insufficiency cohort study. *Am J Nephrol*. 2016;43(5):366–374. <https://doi.org/10.1159/000446484>.
44. Zhang ZH, Wei F, Vaziri ND, et al. Metabolomics insights into chronic kidney disease and modulatory effect of rhubarb against tubulointerstitial fibrosis. *Sci Rep*. 2015;5:14472. <https://doi.org/10.1038/srep14472>.
45. Watanabe M, Suliman ME, Qureshi AR, et al. Consequences of low plasma histidine in chronic kidney disease patients: Associations with inflammation, oxidative stress, and mortality. *Am J Clin Nutr*. 2008;87(6):1860–1866. <https://doi.org/10.1093/ajcn/87.6.1860>.
46. Bassi R, Niewczas MA, Biancone L, et al. Metabolomic profiling in individuals with a failing kidney allograft. *PLoS One*. 2017;12(1):1–14. <https://doi.org/10.1371/journal.pone.0169077>.
47. Hayashi K, Sasamura H, Hishiki T, et al. Use of serum and urine metabolome analysis for the detection of metabolic changes in patients with stage 1–2 chronic kidney disease. *Nephrourol Mon*. 2011;3(3):164–171.
48. Tolun AA, Zhang H, Li D, Sztáray J, Young SP, Millington DS. Allantoin in human urine quantified by UPLC-MS/MS. *Anal Biochem*. 2010;402(2):191–193. <https://doi.org/10.1016/j.ab.2010.03.033>.
49. Xu J, Casas-Ferreira AM, Ma Y, et al. Lipidomics comparing DCD and DBD liver allografts uncovers lysophospholipids elevated in recipients undergoing early allograft dysfunction. *Sci Rep*. 2015;5:17737. <https://doi.org/10.1038/srep17737>.
50. Law S, Chan M, Marathe GK, Parveen F, Chen C, Ke L. An updated review of lysophosphatidylcholine metabolism in human diseases. *Int J Mol Sci*. 2019;20:1149. <https://doi.org/10.3390/ijms20051149>.
51. Solati Z, Edel AL, Shang Y, Karmin O, Ravandi A. Oxidized phosphatidylcholines are produced in renal ischemia reperfusion injury. *PLoS One*. 2018;13(4), e0195172. <https://doi.org/10.1371/journal.pone.0195172>.
52. Chen H, Chen L, Liu D, Chen D, Vaziri ND. A combined clinical phenotype and lipidomic analysis reveals the impact of chronic kidney disease on lipid metabolism. *J Proteome Res*. 2017;16(4):1566–1578. <https://doi.org/10.1021/acs.jproteome.6b00956>.
53. Rhee EP, Souza A, Farrell L, et al. Metabolite profiling identifies markers of uremia. *J Am Soc Nephrol*. 2010;21(6):1041–1051. <https://doi.org/10.1681/ASN.2009111132>.
54. Rhee EP, Clish CB, Ghorbani A, et al. A combined epidemiologic and metabolomic approach improves CKD prediction. *J Am Soc Nephrol*. 2013;24(8):1330–1338. <https://doi.org/10.1681/ASN.2012101006>.
55. Tsai HI, Lo CJ, Zheng CW, et al. A lipidomics study reveals lipid signatures associated with early allograft dysfunction in living donor liver transplantation. *J Clin Med*. 2018;8(1):30. <https://doi.org/10.3390/jcm8010030>.
56. Wei Q, Xiao X, Fogle P, Dong Z. Changes in metabolic profiles during acute kidney injury and recovery following ischemia/reperfusion. *PLoS One*. 2014;9(9):1–13. <https://doi.org/10.1371/journal.pone.0106647>.
57. van der Veen JN, Kennelly JP, Wan S, Vance JE, Vance DE, Jacobs RL. The critical role of phosphatidylcholine and phosphatidylethanolamine metabolism in health and disease. *Biochim Biophys Acta Biomembr*. 2017;1859(9):1558–1572. <https://doi.org/10.1016/j.bbamem.2017.04.006>.
58. Calzada E, Onguka O, Claypool SM. Phosphatidylethanolamine metabolism in health and disease. *Int Rev Cell Mol Biol*. 2016;321:29–88. <https://doi.org/10.1016/b.sicrmb.2015.10.001>.
59. Hopfer H, Kemény E. Assessment of donor biopsies. *Curr Opin Organ Transpl*. 2013;18(3):306–312. <https://doi.org/10.1097/MOT.0b013e3283607a6e>.
60. Warmuzińska N, Łuczykowski K, Bojko B. A review of current and emerging trends in donor graft-quality assessment techniques. *J Clin Med*. 2022;11(3):487. <https://doi.org/10.3390/jcm11030487>.
61. Traynor C, Saeed A, O'Ceallaigh E, et al. Pre-transplant histology does not improve prediction of 5-year kidney allograft outcomes above and beyond clinical parameters. *Ren Fail*. 2017;39(1):671–677. <https://doi.org/10.1080/0886022X.2017.1363778>.
62. Yap YT, Ho QY, Kee T, Ng CY, Chionh CY. Impact of pre-transplant biopsy on 5-year outcomes of expanded criteria donor kidney transplantation. *Nephrology*. 2021;26(1):70–77. <https://doi.org/10.1111/nep.13788>.
63. De Vusser K, Lerut E, Kuypers D, et al. The predictive value of kidney allograft baseline biopsies for long-term graft survival. *J Am Soc Nephrol*. 2013;24(11):1913–1923. <https://doi.org/10.1681/ASN.2012111081>.
64. Phillips BL, Kassimatis T, Atalar K, et al. Chronic histological changes in deceased donor kidneys at implantation do not predict graft survival: a single-centre retrospective analysis. *Transpl Int*. 2019;32(5):523–534. <https://doi.org/10.1111/tri.13398>.
65. Antonieta Azancot M, Moreso F, Salcedo M, et al. The reproducibility and predictive value on outcome of renal biopsies from expanded criteria donors. *Kidney Int*. 2014;85(5):1161–1168. <https://doi.org/10.1038/ki.2013.461>.
66. Bogusiewicz J, Burlikowska K, Łuczykowski K, et al. New chemical biopsy tool for spatially resolved profiling of human brain tissue in vivo. *Sci Rep*. 2021;11(1):19522. <https://doi.org/10.1038/s41598-021-98973-y>.
67. Gómez-Ríos GA, Tascon M, Reyes-Garcés N, Boyaci E, Poole JJ, Pawliszyn J. Rapid determination of immunosuppressive drug concentrations in whole blood by coated blade spray-tandem mass spectrometry (CBS-MS/MS). *Anal Chim Acta*. 2018;999:69–75. <https://doi.org/10.1016/j.aca.2017.10.016>.
68. Looby NT, Tascon M, Acquaro VR, et al. Solid phase microextraction coupled to mass spectrometry: Via a microfluidic open interface for rapid therapeutic drug monitoring. *Analyst*. 2019;144(12):3721–3728. <https://doi.org/10.1039/c9an00041k>.
69. Gómez-Ríos GA, Mirabelli MF. Solid Phase Microextraction-mass spectrometry: Metaanalysis. *TrAC Trends Anal Chem*. 2019;112:201–211. <https://doi.org/10.1016/j.trac.2018.12.030>.
70. National Centre for the Replacement Refinement & Reduction of Animals in Research. The 3Rs. <https://nc3rs.org.uk/who-we-are/3rs> Last accessed: 4 December 2023.

## Supplementary Material

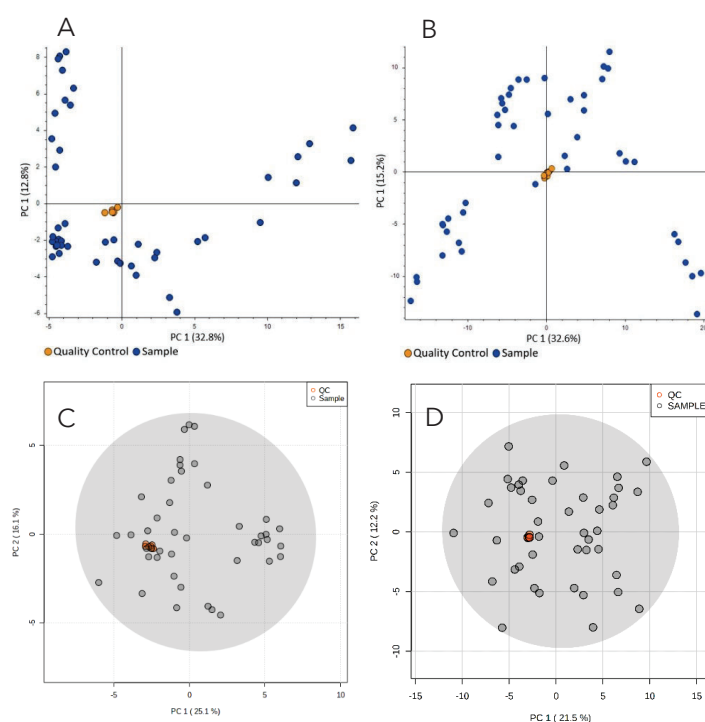
### Metabolomic and lipidomic landscape of porcine kidney associated with kidney perfusion in heart beating donors and donors after cardiac death

Iga Stryjak<sup>1†</sup>, Natalia Warmuzińska<sup>1†</sup>, Kamil Łuczykowski<sup>1</sup>, Karol Jaroń<sup>1</sup>, Peter Urbanellis<sup>2</sup>, Markus Selzner<sup>2,3</sup>, Barbara Bojko<sup>1\*</sup>

<sup>1</sup>Department of Pharmacodynamics and Molecular Pharmacology, Faculty of Pharmacy, Nicolaus Copernicus University in Toruń, Collegium Medicum in Bydgoszcz, Bydgoszcz, Poland

<sup>2</sup>Ajmera Transplant Center, Department of Surgery, Toronto General Hospital, University Health Network, Toronto, ON, Canada.

<sup>3</sup>Department of Medicine, Toronto General Hospital, Toronto, ON, Canada.



**Fig. S1** Principal component analysis (PCA) score plots of all analyzed samples and extraction quality control (QC) samples. A- metabolomics, RP, positive ionization mode; B- metabolomics, RP, negative ionization mode; C- lipidomics, HILIC, positive ionization mode; D – lipidomic, RP, positive ionization mode;

**Table S1.** The list of metabolites identified with the use of MS/MS mode

<b>Molecular Weight [u]</b>	<b>RT [min]</b>	<b>Name</b>
<b>positive ionization mode</b>		
109.06421	1.818	2-amino-4-methylpyrimidine
131.05824	1.262	5-Aminolevulinic acid
145.05268	11.58	8-Hydroxyquinoline
203.11575	8.904	Acetylcarnitine
174.10035	1.51	Acetylmethionine
246.10022	11.572	Acetyltryptophan
267.0965	7.452	Adenosine
347.06276	1.51	Adenosine monophosphate
89.04817	1.834	Alanine
202.13174	7.69	Alanyl-Leucine
161.06869	1.511	alpha-Aminoadipic acid
174.11161	1.931	Arginine
132.05339	1.252	Asparagine
133.0375	1.268	Aspartic acid
175.09561	1.435	Citrulline
131.06947	1.875	Creatine
240.02358	1.216	Cystine
315.27694	16.619	Dehydrophytosphingosine
267.09664	7.24	Deoxyguanosine
296.2349	16.964	Dimorphecolic acid
147.05303	1.413	Glutamic acid
146.06901	1.315	Glutamine
198.18576	22.404	Guanethidine
151.0493	3.737	Guanine
179.05828	9.63	Hippuric acid
155.06941	1.816	Histidine
136.03852	7.064	Hypoxanthin
156.05345	2.484	Imidazolelactic acid
131.09468	7.127	Leucine

146.10547	1.832	Lysine
126.06544	2.484	Melamine
149.05098	3.017	Methionine
165.0459	1.366	Methionine sulfoxide
281.11213	7.505	Methyladenosine
257.10258	1.272	Methylcytidine
169.08505	1.934	Methylhistidine
219.11051	1.514	Pantothenic acid
115.0635	1.505	Proline
143.09453	1.512	Proline
129.04257	1.511	Pyroglutamic acid
105.0429	1.259	Serine
281.27146	21.522	Sphingosine
119.05837	1.339	Threonine
126.04298	2.691	Thymine
204.08995	11.574	Tryptophan
244.06921	1.5	Uridine
138.04274	6.97	Urocanic acid
117.07907	2.41	Valine
<hr/> <b>negative ionization mode</b> <hr/>		
195.05258	8.343	3-Hydroxyhippuric acid
207.08896	12.458	Acetylphenylalanine
246.10028	11.833	Acetyltryptophan
158.04289	1.235	Allantoin
138.04164	6.93	Aminonicotinic acid
133.03617	1.207	Aspartic acid
131.06815	1.833	Creatine
240.02358	1.159	Cystine
196.0576	1.117	Gluconic acid
180.06273	1.096	Glucose
147.05194	1.35	Glutamic acid
146.06794	1.252	Glutamine
465.30937	13.764	Glycocholic Acid

437.29105	18.422	Glycoursodeoxycholic acid
151.0483	3.722	Guanine
155.06828	1.756	Histidine
156.05237	2.426	Imidazolelactic acid
205.0732	11.808	Indolelactic acid
205.07328	12.086	Indolelactic acid
268.08096	7.067	Inosine
90.03009	1.438	Lactic acid
182.07823	1.098	Mannitol
262.04852	11.523	Mannitol-1-phosphate
193.07312	10.128	Methylhippuric acid
129.04104	1.349	Oxoproline
165.07795	8.856	Phenylalanine
368.16614	14.772	Testosterone sulfate
370.23588	12.907	Thromboxane B2
204.08919	11.521	Tryptophan
181.07305	7.237	Tyrosine
138.04168	7.8	Urocanic acid

RT – retention time

**Table S2.** The list of lipid species identified with the use of MS/MS mode

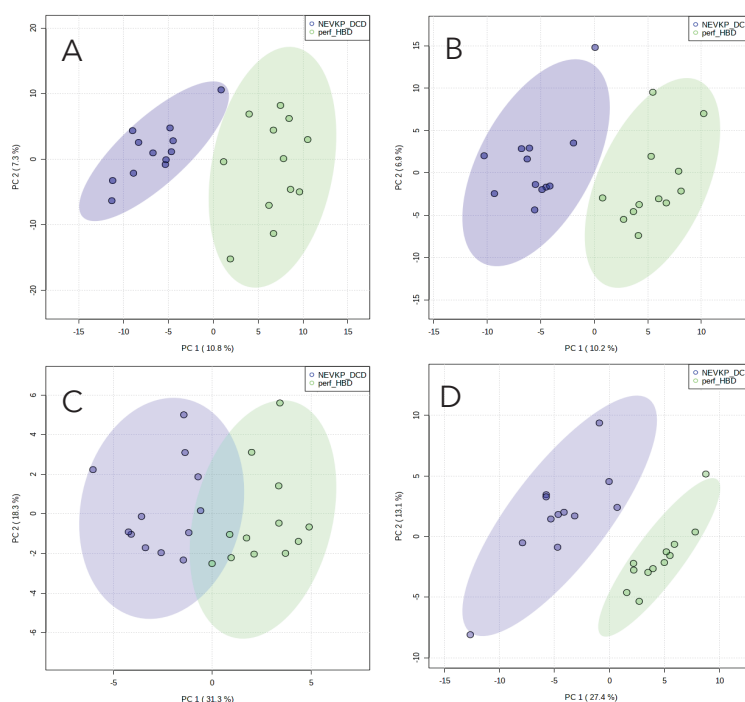
m/z	RT [min]	adduct	Lipid Species Shorthand
<b>HILIC</b>			
480.3448	8.13	+H	LPC P-16:0
494.3241	8.62	+H	LPC 16:1
522.3554	8.06	+H	LPC 18:1
522.3554	8.48	+H	LPC 18:1
524.3710	8.45	+H	LPC 18:0
544.3397	8.46	+H	LPC 20:4
566.3217		+Na	
696.4962	7.14	+H	PE P-34:4
700.5275	7.22	+H	PE P-34:2
702.5432	7.19	+H	PE P-34:1

722.5119	7.08	+H	PE P-36:5
724.5275	7.08	+H	PE P-36:4
746.5095		+Na	
728.5588	7.08	+H	PE P-36:2
740.5200	7.25	+Na	PE 34:1
744.5537	7.23	+H	PE 36:2
766.5357		+Na	
750.5432	7.01	+H	PE P-38:5
752.5564	7.00	+Na	PE O-36:2
752.5588	7.00	+H	PE P-38:4
774.5408		+Na	
764.5200	7.18	+Na	PE 36:3
764.5200	7.49	+Na	PE 36:3
766.5381	7.13	+H	PE 38:5
788.5200		+Na	
768.5513	7.13	+Na	PE 36:1
772.5251	6.97	+Na	PE O-38:6
774.5408	6.97	+Na	PE O-38:5
780.5901	6.87	+H	PE P-40:4
790.5357	7.13	+Na	PE 38:4
804.5513	6.06	+Na	PC 36:4
806.5670	6.48	+Na	PC 36:3
725.5592	7.78	+H	SM 36:4;O2
<b>RP</b>			
331.2842	4.77	+H	MG 16:0
376.3421	5.58	+NH4	MG 18:0
572.4884	10.66	+NH4	TG 30:0
586.5405	10.76	+NH4	DG 32:0
600.5197	10.59	+NH4	TG 32:0
605.4751		+Na	
612.5561	10.94	+NH4	DG 34:1
614.5718	11.35	+NH4	DG 34:0
628.5510	11.19	+NH4	TG 34:0

633.5064		+Na	
638.5718	11.09	+NH4	DG 36:2
656.5823	11.71	+NH4	TG 36:0
661.5377		+Na	
662.5718	11.10	+NH4	DG 38:4
666.6183	13.90	+NH4	CE 18:2
684.6136	12.17	+NH4	TG 38:0
689.5690		+Na	
712.6449	12.57	+NH4	TG 40:0
724.5275	9.45	+H	PE P-36:4
740.6762	12.93	+NH4	TG 42:0
771.6497	5.74	+H	TG 46:4
794.7232	13.33	+NH4	TG 46:1
796.7388	13.56	+NH4	TG 46:0
820.7388	13.41	+NH4	TG 48:2
822.7545	13.64	+NH4	TG 48:1
827.7099		+Na	
846.7545	13.48	+NH4	TG 50:3
848.7701	13.70	+NH4	TG 50:2
850.7858	13.90	+NH4	TG 50:1
862.7858	13.83	+NH4	TG 51:2
864.8014	14.02	+NH4	TG 51:1
872.7701	13.56	+NH4	TG 52:4
877.7255		+Na	
874.7858	13.75	+NH4	TG 52:3
879.7412		+Na	
876.8014	13.96	+NH4	TG 52:2
881.7568		+Na	
878.8171	14.14	+NH4	TG 52:1
896.7701	13.41	+NH4	TG 54:6
898.7858	13.63	+NH4	TG 54:5
903.7412		+Na	
900.8014	13.82	+NH4	TG 54:4

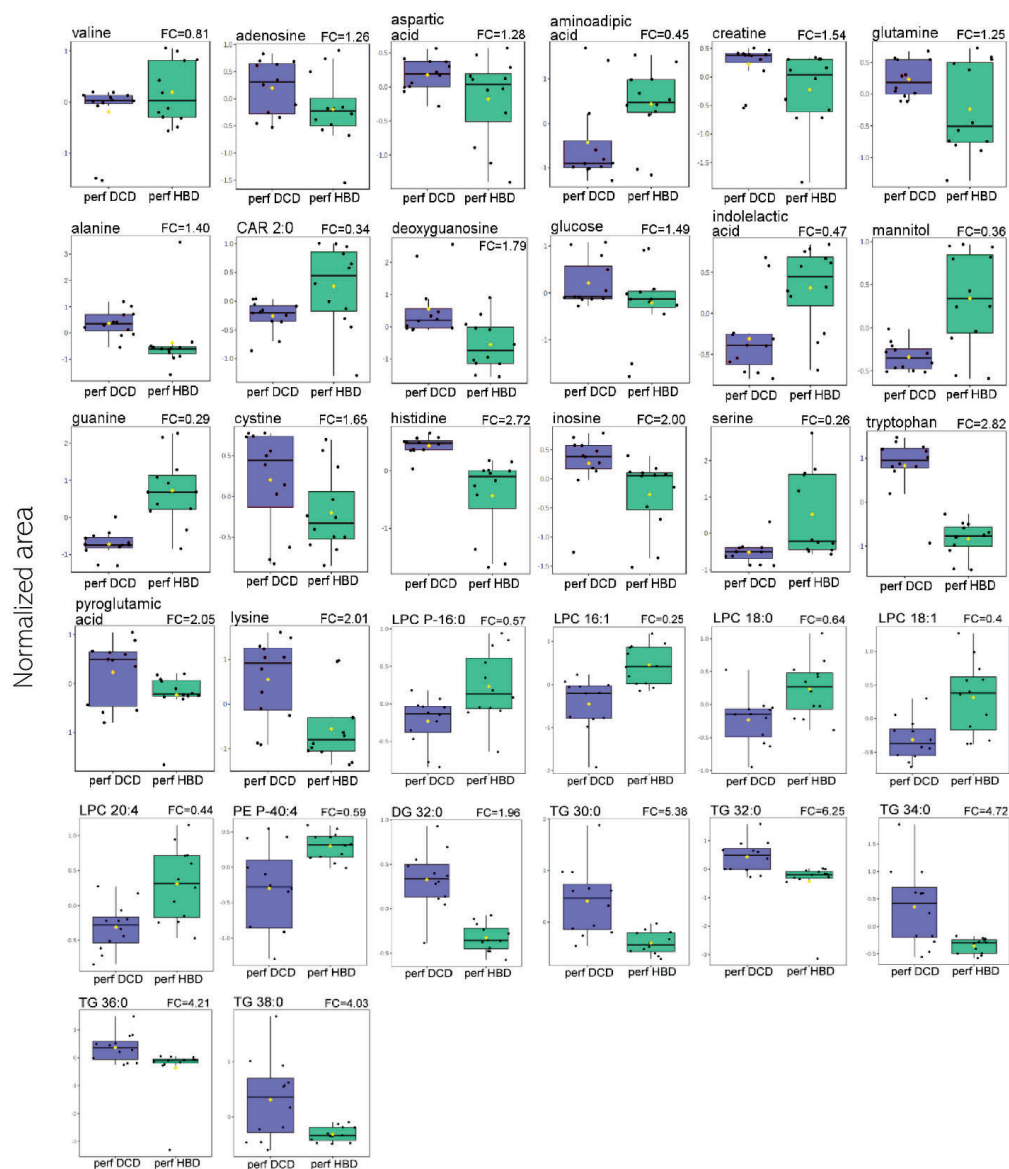
902.8171	14.00	+NH4	TG 54:3
907.7725		+Na	
904.8327	14.19	+NH4	TG 54:2
909.7881		+Na	

m/z – mass to charge ratio; RT – retention time



**Fig. S2** PCA score plots showing separation between HBD and DCD perfusions. RP metabolomic analyses in positive (A) and negative (B) ionization modes, lipidomic analyses with HILIC (C) and RP (D) separations





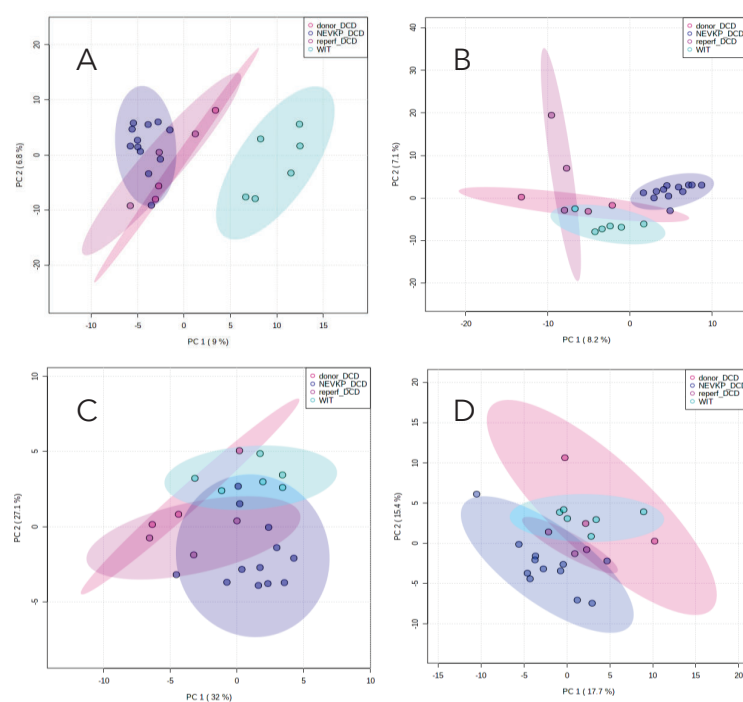
**Fig. S4** Levels of selected compounds (VIP>1.0) detected between perfusions of HBD and DCD kidneys (n=12). The boxplots display normalized peak areas, with the notch indicating the 95% confidence interval around the median of each group. The mean area of each group is indicated with a

yellow diamond. Blue box- perfusion of DCD, green box- perfusion of HBD; FC- fold change perfusion DCD/perfusion HBD

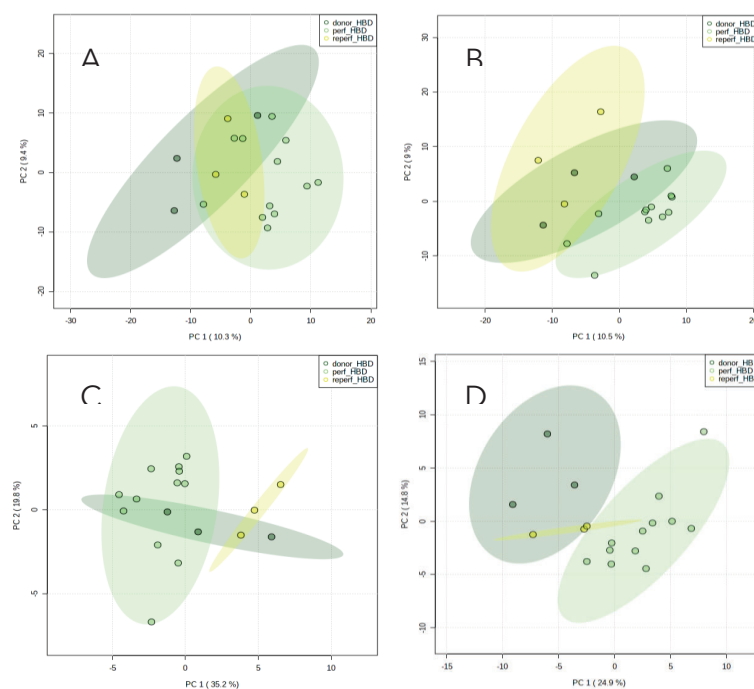
**Table S3.** Result from Pathway Analysis

Pathway Name	Match Status	p	FDR
Aminoacyl-tRNA biosynthesis	6/48	9.2384E-5	0.0077602
Purine metabolism	5/65	0.0036878	0.15489
Glycerophospholipid metabolism	3/36	0.020733	0.47228
Pyrimidine metabolism	3/39	0.025669	0.47228
Glycerolipid metabolism	2/16	0.028112	0.47228
Pantothenate and CoA biosynthesis	2/19	0.038846	0.54384
beta-Alanine metabolism	2/21	0.046739	0.56087
Lysine degradation	2/25	0.0641	0.64156
Glycolysis / Gluconeogenesis	2/26	0.068738	0.64156
Alanine, aspartate and glutamate metabolism	2/28	0.078339	0.65805
D-Glutamine and D-glutamate metabolism	1/6	0.096667	0.67667
Nitrogen metabolism	1/6	0.096667	0.67667
Biosynthesis of unsaturated fatty acids	2/36	0.12042	0.76106
Valine, leucine and isoleucine biosynthesis	1/8	0.12684	0.76106
Fatty acid degradation	2/39	0.13743	0.76959
Biotin metabolism	1/10	0.15605	0.81926
Arginine biosynthesis	1/14	0.21167	0.98779
Glycosylphosphatidylinositol (GPI)-anchor biosynthesis	1/14	0.21167	0.98779
Histidine metabolism	1/16	0.23814	1.0
Selenocompound metabolism	1/20	0.28854	1.0
Sphingolipid metabolism	1/21	0.30063	1.0
Pyruvate metabolism	1/22	0.31252	1.0
Glutathione metabolism	1/28	0.3799	1.0
Glyoxylate and dicarboxylate metabolism	1/32	0.42124	1.0
Glycine, serine and threonine metabolism	1/33	0.43115	1.0
Cysteine and methionine metabolism	1/33	0.43115	1.0
Arginine and proline metabolism	1/38	0.47832	1.0

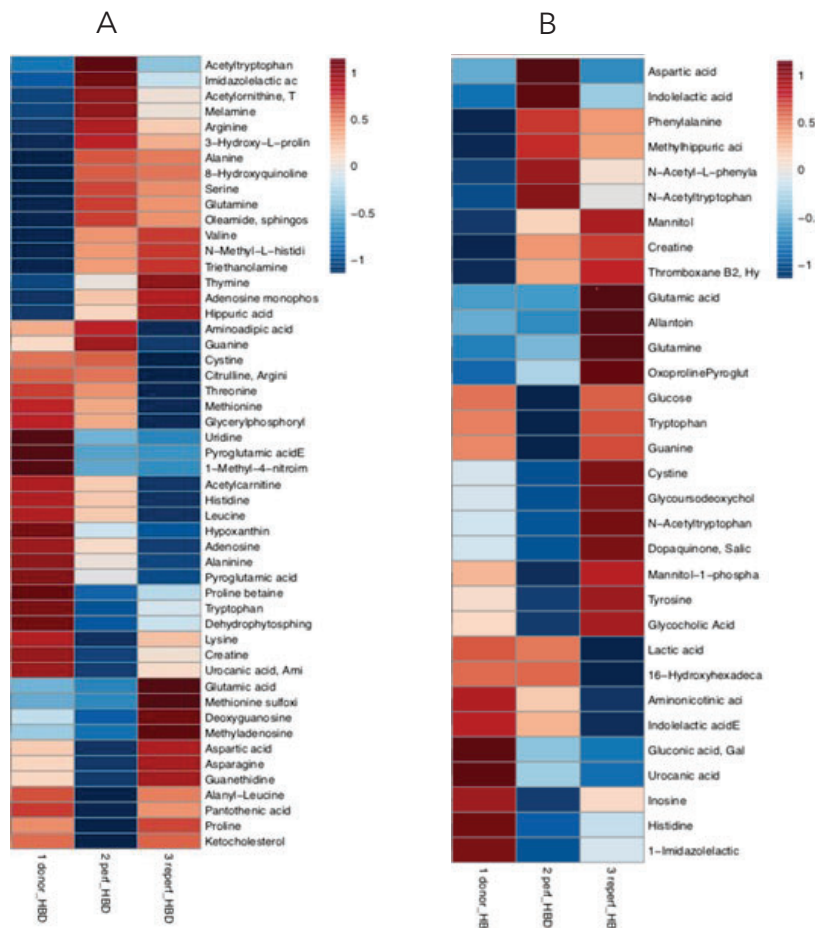
Fatty acid elongation	1/39	0.48729	1.0
Valine, leucine and isoleucine degradation	1/40	0.49611	1.0
Tryptophan metabolism	1/41	0.50478	1.0
Fatty acid biosynthesis	1/47	0.5539	1.0

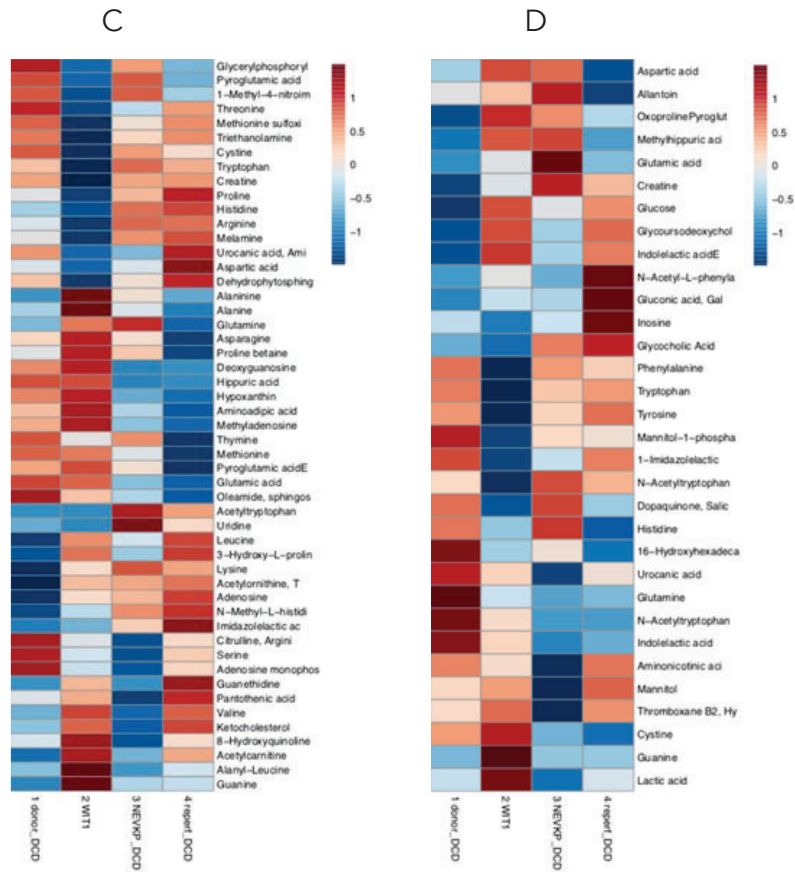


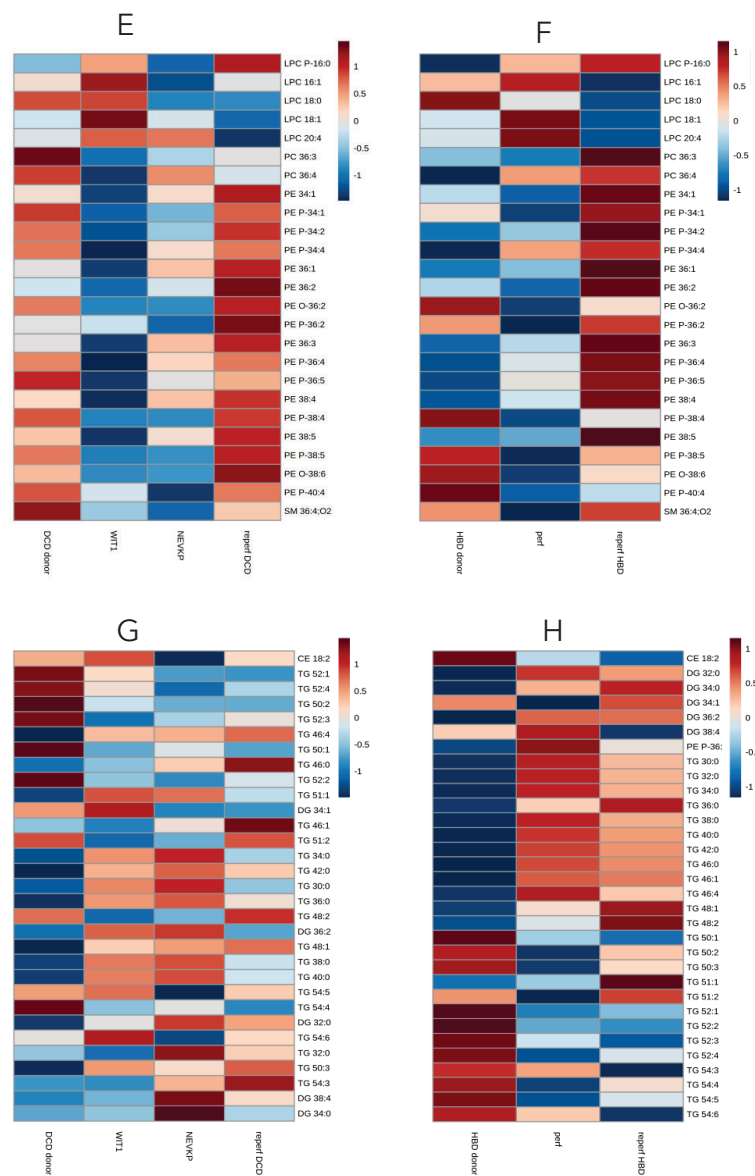
**Fig. S5** PCA score plots of DCD metabolomic and lipidomic data. A – metabolomics, RP, positive ionization mode; B – metabolomics, RP, negative ionization mode; C – lipidomics, HILIC, positive ionization mode; D – lipidomics, RP, positive ionization mode



**Fig. S6** Principal Component Analysis score plots of HBD metabolomic and lipidomic data. A – metabolomics, RP, positive ionization mode; B – metabolomics, RP, negative ionization mode; C – lipidomics, HILIC, positive ionization mode; D – lipidomics, RP, positive ionization mode







**Fig. S7** Heat-maps showing overall trends in identified metabolites levels during autotransplantation procedure. A- HBD donor, metabolomics, RP, positive ionization mode; B- HBD donor, metabolomics, RP, negative ionization mode; C- DCD donor, metabolomics, RP, positive ionization mode; D- DCD donor, metabolomics, RP, negative ionization mode; E- DCD donor, lipidomics, HILIC; F- HBD donor, lipidomics, HILIC; G- DCD donor, lipidomic RP; H- HBD donor, lipidomic, RP

## 7.2. Wpływ normotermicznych i hipotermicznych metod konserwacji na lipidom nerek — badanie porównawcze z wykorzystaniem biopsji chemicznej – P.5.

**Opis dotyczy pracy:** N. Warmuzińska, K. Łuczykowski, I. Stryjak, H. Rosales-Solano, P. Urbanellis, J. Pawliszyn, M. Selzner, B. Bojko: *The impact of normothermic and hypothermic preservation methods on kidney lipidome—comparative study using chemical biopsy with microextraction probes*. Front. Mol. Biosci., 2024, 11, 1341108;

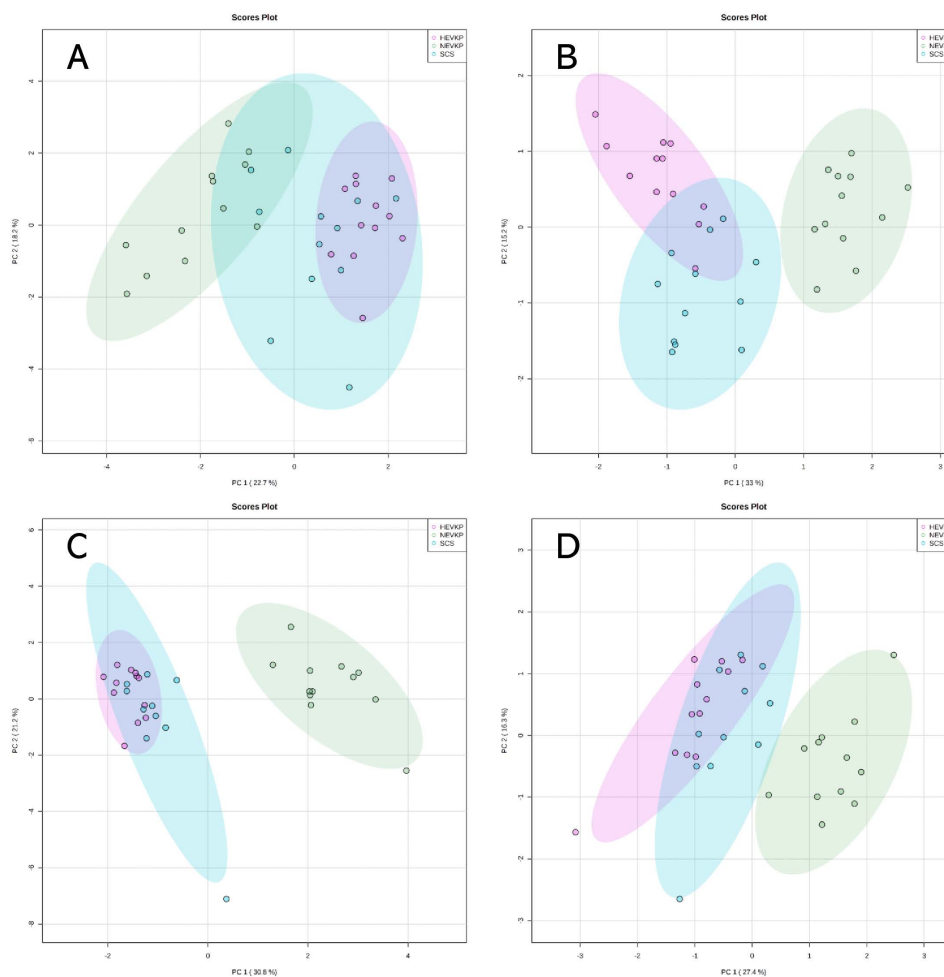
Jedną ze strategii walki z niedoborem dostępnych narządów jest wprowadzanie nowych metod przechowywania mających na celu ograniczanie uszkodzeń oraz poprawę jakości narządu, co może zwiększyć szanse na udany przeszczep. Obecnie najczęściej stosowanymi w praktyce klinicznej metodami konserwacji są hipotermia prosta (SCS, ang. static cold storage) oraz hipotermiczna perfuzja maszynowa (HMP, ang. hypothermic machine perfusion). SCS polega na zanurzeniu nerki w zimnym płynie konserwującym i umieszczeniu jej w pojemniku z lodem, natomiast HMP wykorzystuje urządzenie do pompowania zimnego płynu przez naczynia krwionośne nerki, co - jak wykazano - skuteczniej chroni przeszczepy marginalne i DCD w porównaniu do SCS. Normotermiczna perfuzja maszynowa (NEVKP, ang. normothermic ex vivo kidney perfusion) to nowa, dynamiczna metoda konserwacji, polegająca na cyrkulacji roztworu perfuzyjnego przez nerkę w warunkach jak najbardziej zbliżonych do fizjologicznych, w celu ograniczenia uszkodzeń spowodowanych zimnym niedokrwieniem i poprawy wyników przeszczepiania.

Celem niniejszego badania była ocena wpływu technik konserwacji hipotermicznej i normotermicznej na profil lipidomiczny nerki przy użyciu mikroekstrakcji do fazy stałej jako metody poboru i preparatyki próbek.

Bezpośrednie pobieranie próbek z nerki przeprowadzono przy użyciu sond SPME pokrytych fazą ekstrakcyjną typu mixed-mode w wieprzowym modelu autotransplantacji nerki, odzwierciedlającym dawcę po zatrzymaniu krążenia. Porównano trzy metody konserwacji: SCS, NEVKP oraz HMP. Analizę lipidomiczną przeprowadzono za pomocą wysokosprawnej chromatografii cieczowej sprzężonej ze spektrometrem masowym Q-Exactive Focus Orbitrap.

Analiza chemometryczna wykazała, że temperatura przechowywania ma większy wpływ na profil lipidomiczny nerki niż mechaniczny charakter metody konserwacji. We wszystkich

analizach lipidomety tkanki nerkowej z grupy NEVKP wykazywały wyraźne oddzielenie od tych z grup SCS i HMP. Natomiast grupy SCS i HMP miały częściowo nakładające się rozkłady. Wykresy analizy głównych składowych (PCA, ang. Principal Component Analysis) zostały przedstawione na Rycinie 2.



**Rycina 2.** Wykresy analizy PCA przedstawiające rozdzielenie pomiędzy różnymi typami konserwacji nerek. Analiza HILIC w trybie jonizacji dodatniej (A) i ujemnej (B) oraz analiza RP w trybie jonizacji dodatniej (C) i ujemnej (D).

W grupie przechowywanej w warunkach hipotermii stwierdzono wyższe poziomy acylokarnityn (CAR, ang. acylcarnitine), fosfatydylocholin (PC, ang. phosphatidylcholine), fosfolipidów z wiązaniem eterowym (PC i PE), fosfatydyloinozytoli (PI, ang. phosphatidylinositol), TG, większości LPC i lizofosfatydyloetanolamin (LPE, ang. lysophosphatidylethanolamine) oraz PE o dłuższych łańcuchach.

Zwiększenie poziomów lipidów ze wskazanych grup może być związane z uszkodzeniem niedokrwienno-reperfuzyjnym, dysfunkcją mitochondrialną, działaniem prozapalnym i stresem oksydacyjnym. Uzyskane wyniki sugerują, że zastosowanie normotermicznej perfuzji nerki może korzystnie wpływać na funkcję przeszczepu.



## OPEN ACCESS

EDITED BY  
Danuta Dudzik,  
Medical University of Gdańsk, Poland

REVIEWED BY  
Oleg Mayboroda,  
Leiden University Medical Center (LUMC),  
Netherlands  
Danuta Siluk,  
Medical University of Gdańsk, Poland

\*CORRESPONDENCE  
Barbara Bojko,  
✉ bbojko@cm.umk.pl

RECEIVED 19 November 2023  
ACCEPTED 15 April 2024  
PUBLISHED 09 May 2024

CITATION  
Warmuzińska N, Łuczykowski K, Stryjak I,  
Rosales-Solano H, Urbanellis P, Pawliszyn J,  
Selzner M and Bojko B (2024), The impact of  
normothermic and hypothermic preservation  
methods on kidney lipidome—comparative  
study using chemical biopsy with  
microextraction probes.  
*Front. Mol. Biosci.* 11:1341108.  
doi: 10.3389/fmolb.2024.1341108

COPYRIGHT  
© 2024 Warmuzińska, Łuczykowski, Stryjak,  
Rosales-Solano, Urbanellis, Pawliszyn, Selzner  
and Bojko. This is an open-access article  
distributed under the terms of the [Creative  
Commons Attribution License \(CC BY\)](#). The use,  
distribution or reproduction in other forums is  
permitted, provided the original author(s) and  
the copyright owner(s) are credited and that the  
original publication in this journal is cited, in  
accordance with accepted academic practice.  
No use, distribution or reproduction is  
permitted which does not comply with these  
terms.

# The impact of normothermic and hypothermic preservation methods on kidney lipidome—comparative study using chemical biopsy with microextraction probes

Natalia Warmuzińska<sup>1</sup>, Kamil Łuczykowski<sup>1</sup>, Iga Stryjak<sup>1</sup>,  
Hernando Rosales-Solano<sup>2</sup>, Peter Urbanellis<sup>3</sup>, Janusz Pawliszyn<sup>2</sup>,  
Markus Selzner<sup>3,4</sup> and Barbara Bojko<sup>1\*</sup>

<sup>1</sup>Department of Pharmacodynamics and Molecular Pharmacology, Faculty of Pharmacy, Nicolaus Copernicus University in Toruń, Collegium Medicum in Bydgoszcz, Bydgoszcz, Poland, <sup>2</sup>Department of Chemistry, University of Waterloo, Waterloo, ON, Canada, <sup>3</sup>Ajmera Transplant Center, Department of Surgery, Toronto General Hospital, University Health Network, Toronto, ON, Canada, <sup>4</sup>Department of Medicine, Toronto General Hospital, Toronto, ON, Canada

**Introduction:** Normothermic ex vivo kidney perfusion (NEVKP) is designed to replicate physiological conditions to improve graft outcomes. A comparison of the impact of hypothermic and normothermic preservation techniques on graft quality was performed by lipidomic profiling using solid-phase microextraction (SPME) chemical biopsy as a minimally invasive sampling approach.

**Methods:** Direct kidney sampling was conducted using SPME probes coated with a mixed-mode extraction phase in a porcine autotransplantation model of the renal donor after cardiac death, comparing three preservation methods: static cold storage (SCS), NEVKP, and hypothermic machine perfusion (HMP). The lipidomic analysis was done using ultra-high-performance liquid chromatography coupled with a Q-Exactive Focus Orbitrap mass spectrometer.

**Results:** Chemometric analysis showed that the NEVKP group was separated from SCS and HMP groups. Further in-depth analyses indicated significantly ( $p < 0.05$ , VIP  $> 1$ ) higher levels of acylcarnitines, phosphocholines, ether-linked and longer-chain phosphoethanolamines, triacylglycerols and most lysophosphocholines and lysophosphoethanolamines in the hypothermic preservation group. The results showed that the preservation temperature has a more significant impact on the lipidomic profile of the kidney than the preservation method's mechanical characteristics.

**Conclusion:** Higher levels of lipids detected in the hypothermic preservation group may be related to ischemia-reperfusion injury, mitochondrial dysfunction, pro-inflammatory effect, and oxidative stress. Obtained results suggest the NEVKP method's beneficial effect on graft function and confirm that SPME

chemical biopsy enables low-invasive and repeated sampling of the same tissue, allowing tracking alterations in the graft throughout the entire transplantation procedure.

#### KEYWORDS

solid-phase microextraction, SPME, LC-MS, kidney transplantation, lipidomics, graft quality assessment, kidney perfusion

## 1 Introduction

Kidney transplantation is a life-saving method for patients with end-stage renal dysfunction that enables higher survival rates and patient quality of life compared to dialysis treatment. Unfortunately, an ongoing organ shortage has led to the rapid growth in the number of patients on kidney waiting lists (Swanson et al., 2020; Warmuzińska et al., 2022). This growing gap in supply and demand has led clinicians to explore the possibility of using kidneys recovered from extended criteria donors (ECD) or donation after circulatory death (DCD) donors; however, recipients of ECD kidney grafts tend to have worse outcomes than those receiving organs from standard criteria donors, including being at a higher risk of delayed graft function (DGF) and primary nonfunction incidence (Urbanellis et al., 2020; Warmuzińska et al., 2022). Hence, strategies for reducing preservation injury and monitoring graft function are of intense interest. At present, static cold storage (SCS) and hypothermic machine perfusion (HMP) are the most common preservation methods applied in clinical settings. SCS involves submerging the kidney in a cold preservation fluid and then placing it on ice in an icebox; in contrast, HMP entails using a device to pump cold preservation fluid through the renal vasculature, which has been demonstrated to be more effective at preserving marginal and DCD grafts compared to SCS (Lindell et al., 2013; Urbanellis et al., 2020; Warmuzińska et al., 2022). Normothermic *ex vivo* kidney perfusion (NEVKP) is a novel dynamic preservation strategy applying a perfusion solution's circulation through the kidney. NEVKP conditions are developed to replicate physiological conditions as closely as possible to reduce cold ischemia damage and improve graft outcome (Resch et al., 2020; Hosgood et al., 2021). While several studies have attained promising results indicating NEVKP's superiority over SCS, this application is still in the experimental stage (Kaths et al., 2017; Urbanellis et al., 2020). One notable problem is the need for more accurate methods of evaluating graft quality and assessing donor risk, especially concerning marginal grafts. A kidney's suitability for transplantation is determined based on detailed parameters, including the donor's medical history, visual assessment, and examination results (Warmuzińska et al., 2022). The visual evaluation of donor organs is frequently fundamental in decision-making. However, although macroscopic inspection can help diagnose tumors and anatomical changes, this method is subjective and depends on the transplant team's experience level (Dare et al., 2014). Consequently, pretransplant biopsies remain the gold standard for identifying donor kidney injury. Histological examinations are often applied selectively, mainly in marginal grafts, and the frequency of performed biopsies varies between medical facilities and countries (Dare et al., 2014; Moeckli et al., 2019; Warmuzińska et al., 2022).

Moreover, the use of biopsies is hampered by two significant limitations: the low reproducibility of results between on-call pathologists and their time-consuming nature (Azancot et al., 2014). Additionally, the number of allowable biopsies during the transplantation procedure is usually restricted to a single sampling due to their invasiveness, which limits their application for capturing dynamic changes and time-series analyses (Bojko, 2022). Therefore, new representative organ-quality assessment methods are needed to increase the number of organs available for transplantation. In this study, we assess the viability of solid-phase microextraction (SPME) chemical biopsy as a method for evaluating the impact of hypothermic and normothermic preservation techniques on the lipidomic profile of the kidney. The small diameter of the SPME probe (~200 µm) enables minimal invasiveness and allows for several samplings of the same organ without damaging the tissue. Furthermore, SPME combines sampling, extraction, and metabolite quenching into a single step, which makes it a valuable tool for on-site analysis. Finally, SPME's low invasiveness enables its application for monitoring of changes in the organ throughout the entire transplantation procedure, beginning with its removal from the donor's body, through its preservation, and ending with its revascularization in the recipient's body (Łuczykowski et al., 2023).

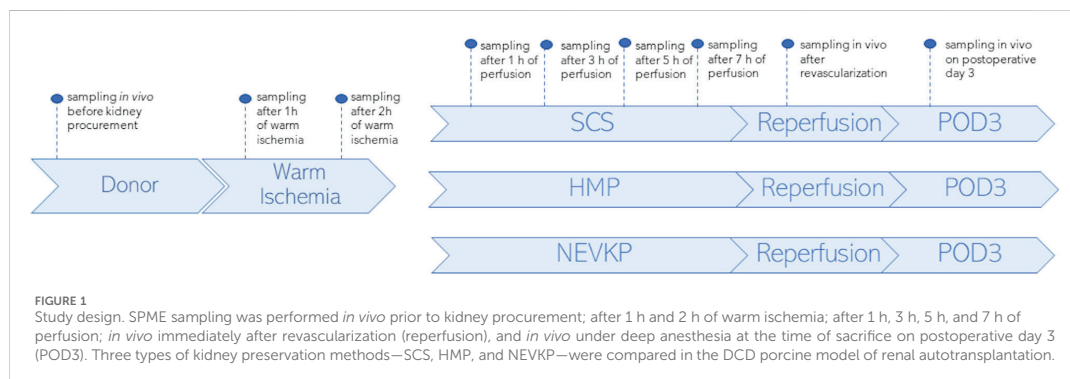
## 2 Materials and methods

### 2.1 Animals

Eight 3-month-old male Yorkshire pigs (≈30 kg) were housed for 1 week prior to the experiments, with water and food being provided *ad libitum*. All animals received humane care in compliance with the "Principles of Laboratory Animal Care" formulated by the National Society for Medical Research and the "Guide for the Care of Laboratory Animals" published by the National Institutes of Health and the ARRIVE guidelines 2.0. The study protocol was approved by the Animal Care Committee at the Toronto General Research Institute, Ontario, Canada.

### 2.2 Study design

SPME fibers coated with a mixed-mode extraction phase (coating length: 7 mm) were applied for direct kidney sampling in three porcine models of renal DCD autotransplantation using different preservation methods: an 8-h SCS group ( $n = 3$ ), an 8-h NEVKP group ( $n = 3$ ), and an 8-h HMP group ( $n = 2$ ). The autotransplantation and anesthetic procedures, warm ischemia induction, and NEVKP, HMP, and SCS conditions are described elsewhere (Kaths et al., 2015; Kaths et al., 2016; Kaths et al., 2018;



Urbanellis et al., 2020). SPME sampling was performed *in vivo* prior to kidney procurement; after 1 h and 2 h of warm ischemia; after 1 h, 3 h, 5 h, and 7 h of perfusion; *in vivo* immediately after revascularization (reperfusion), and *in vivo* under deep anesthesia at the time of sacrifice on postoperative day 3 (POD3). The study protocol is illustrated in Figure 1. Before sampling, all fibers were preconditioned for 60 min in a methanol/water (50:50 v/v) solution, followed by rinsing with purified water for a few seconds. The extractions were performed by inserting the SPME fiber into the kidney cortex for 30 min at each time point. After sampling, the fibers were removed from the organ, quickly rinsed with water, and then gently dried with kimwipes to remove any tissue or blood residue. Next, the fibers were placed into empty glass vials and stored in a freezer at  $-80^{\circ}\text{C}$  until analysis. All fibers were desorbed immediately before instrumental analysis. For desorption, the fibers were inserted into 200  $\mu\text{L}$  of isopropanol:methanol (1:1 v/v) solution with the use of silanized inserts and agitated (1,200 rpm) using a BenchMixer™ MultiTube Vortexer (Benchmark Scientific, Edison, United States) for 120 min. After desorption, extracts were ready for instrumental analysis. The extraction blanks consisted of fibers that were prepared using the same protocol as the rest of the fibers, but with the extraction step being omitted.

## 2.3 Liquid chromatography–high resolution mass spectrometry analysis (LC–HRMS)

Untargeted lipidomics analysis was performed using an LC–HRMS procedure based on the coupling of an ultra-high performance liquid chromatograph and a Q-Exactive Focus Orbitrap mass spectrometer. Data acquisition was performed using dedicated Thermo Scientific software, namely, Xcalibur 4.2 and Free Style 1.4 (Thermo Fisher Scientific, San Jose, California, United States). The instrument was calibrated by injecting calibrants every 72 h, resulting in a mass accuracy of  $<2$  ppm. During analysis, the samples were randomized and pooled quality control (QC) samples containing 10  $\mu\text{L}$  of each sample were run every 8–10 injections to monitor instrument performance and analyte stability. Chromatographic separation was carried out on a hydrophilic interaction liquid chromatography (HILIC) column (SeQuant ZIC–chILIC, 3  $\mu\text{m}$ , 100 mm  $\times$  2.1 mm) and in reversed-phase (RP) using a C18 column (Waters, XSelect CSH C18, 3.5  $\mu\text{m}$ , 2.1 mm  $\times$  75 mm) to

cover a wide range of lipids. The mobile phases for the HILIC column were 5 mM ammonium acetate in water (A) and acetonitrile (B). The mobile phases for the RP column were: phase A consisted of water: methanol (60:40; v/v) and phase B of isopropanol: methanol (90:10; v/v), both containing 10 mM ammonium acetate and 1 mM acetic acid. The gradients were as described previously (Stryjak et al., 2020). The analyses were performed in positive and negative electrospray ionization mode. For positive ionization mode, the mass spectrometer parameters for the HILIC separations were as follows: a spray voltage of 1,500V; a capillary temperature of  $325^{\circ}\text{C}$ ; sheath gas at 60 a.u.; an aux gas flow rate of 30 a.u.; a spare gas flow rate of 2 a.u.; a probe heater temperature of  $325^{\circ}\text{C}$ ; an S-Lens radio frequency level of 55%; an S-lens voltage of 25 V; and a skimmer voltage of 15 V. For the RP analysis, the following parameters were employed: a spray voltage of 3500V; a capillary temperature of  $275^{\circ}\text{C}$ ; sheath gas at 20 a.u.; an aux gas flow rate of 10 a.u.; a spare gas flow rate of 2 a.u.; a probe heater temperature of  $300^{\circ}\text{C}$ ; an S-Lens radio frequency level of 55%; an S-lens voltage of 25 V; and a skimmer voltage of 15 V. For negative ionization mode, the mass spectrometer parameters for the HILIC separations were as follows: a spray voltage of 1300V; a capillary temperature of  $263^{\circ}\text{C}$ ; sheath gas at 60 a.u.; an aux gas flow rate of 30 a.u.; a spare gas flow rate of 2 a.u.; a probe heater temperature of  $425^{\circ}\text{C}$ ; an S-Lens radio frequency level of 55%; an S-lens voltage of 25 V; and a skimmer voltage of 15 V. For the RP analysis, the following HESI ion source parameters were employed: a spray voltage of 3,500V; a capillary temperature of  $275^{\circ}\text{C}$ ; sheath gas at 30 a.u.; an aux gas flow rate of 10 a.u.; a spare gas flow rate of 2 a.u.; a probe heater temperature of  $300^{\circ}\text{C}$ ; an S-Lens radio frequency level of 55%; an S-lens voltage of 25 V; and a skimmer voltage of 15 V. The putative identification of compounds was confirmed in Full MS/dd-MS2 mode using the following fragmentation parameters: mass resolution—35,000 full width at half maximum (FWHM); AGC target—2E4; minimum AGC—8E3; intensity threshold—auto; maximum IT—auto; isolation window—3.0 m/z; stepped collision energy—20 V, 30 V, 50 V; loop count—2; dynamic exclusion—auto.

## 2.4 Data processing and statistical analysis

Raw data from each LC–HRMS analysis were processed independently using LipidSearch 4.1.30 (Thermo Fisher Scientific, San Jose, California, United States) software with the following

parameters: peak intensity >10,000; a precursor tolerance of 5 ppm; a product tolerance of 10 ppm; an m-score threshold of 2; a Quan *m/z* tolerance of  $\pm 5$  ppm; a Quan RT (retention time) range of 0.5 min; and the use of a main isomer filter.  $H^+$ ,  $NH_4^+$ , and  $Na^+$  adducts were considered in positive ion mode, while  $H^-$  and  $CH_3COO^-$  were considered in negative ion mode. After completing the lipid identification step, the alignment process was performed using the LipidSearch software with the following parameters: an m-Score threshold of 10; a retention time tolerance of 0.25 min; a QC-to-extraction-blank ratio of >5; and a max 30% RSD in the QC. The search mode function of the software sought matches of parent peaks (full scan MS) and product peaks (fragments, MS/MS) with the lipid database entries. The software assigns four grades of identification of decreasing quality (A–D) to each feature. Identification grade filtering was applied to filter false positive lipid ID from LipidSearch results. Only lipids species with grades A and B were considered in further analyses. Grade A indicates that both lipid class and all fatty acid chains belonging to a given lipid were completely identified; grade B indicates full identification of lipid class and partial identification of fatty acid chains. The peak areas for the obtained compounds were analyzed using MetaboAnalyst 4.0 and Statistica 13.3 PL software (StatSoft, Inc., Tulsa, Oklahoma, United States). All missing values were replaced with small values that were assumed to be a detection limit. A UpSet plot was made with the lists of compounds annotated in the different LC-HRMS analyses using the UpSet plot generator tool ([https://www.chipplot.online/upset\\_plot.html](https://www.chipplot.online/upset_plot.html)) to evaluate the number of lipids species identified in each analytical block. Data were normalized by median, log-transformation, and Pareto scaling, and statistical significance was calculated based on the Kruskal-Wallis test and the Mann–Whitney U test with FDR correction. A *post hoc* test with multiple comparisons of mean ranks for all groups with a Bonferroni correction followed the Kruskal-Wallis test. A *p*-value of <0.05 was considered significant. In addition, principal component analysis (PCA) and partial least squares discriminant analysis (PLS-DA) were conducted to visually assess the separation between sample groups, with variable importance in projection (VIP) scores >1 being used as a criterion for detecting the relevant variables in the context of the model's predictive capability. Each model was validated via Leave-one-out cross-validation and refined with a permutation test. The model was considered to have passed permutation when the *p*-value was lower than 0.05. The Friedman test was employed to search for compounds with relative concentrations that changed throughout perfusion (across specific time points). After statistical analysis, the results from each LC-HRMS block were combined in tables to increase the clarity of the results. If a compound was considered statistically significant from more than one analytical condition, it was placed in tables only once with the most significant *p*-value to avoid duplication of information.

### 3 Results

The proposed method was employed to investigate changes in the lipidomic profiles of kidneys during transplantation and preservation. Principal component analysis was employed to confirm the quality of the instrumental analysis for all

combinations of chromatographic separation and ionization mode. As shown in [Supplementary Figure S1](#), the pooled QC samples formed a tight cluster, thus confirming the good quality of the analytical performance. Using all four blocks of LC-HRMS analysis, 128 lipid species belonging to 14 lipid classes were annotated with level 2 confidence in metabolomics compound identification. A UpSet plot representing the number of compounds annotated in each analytical block is shown in [Figure 2](#). A list of the identified lipid species is provided in [Supplementary Table S1](#).

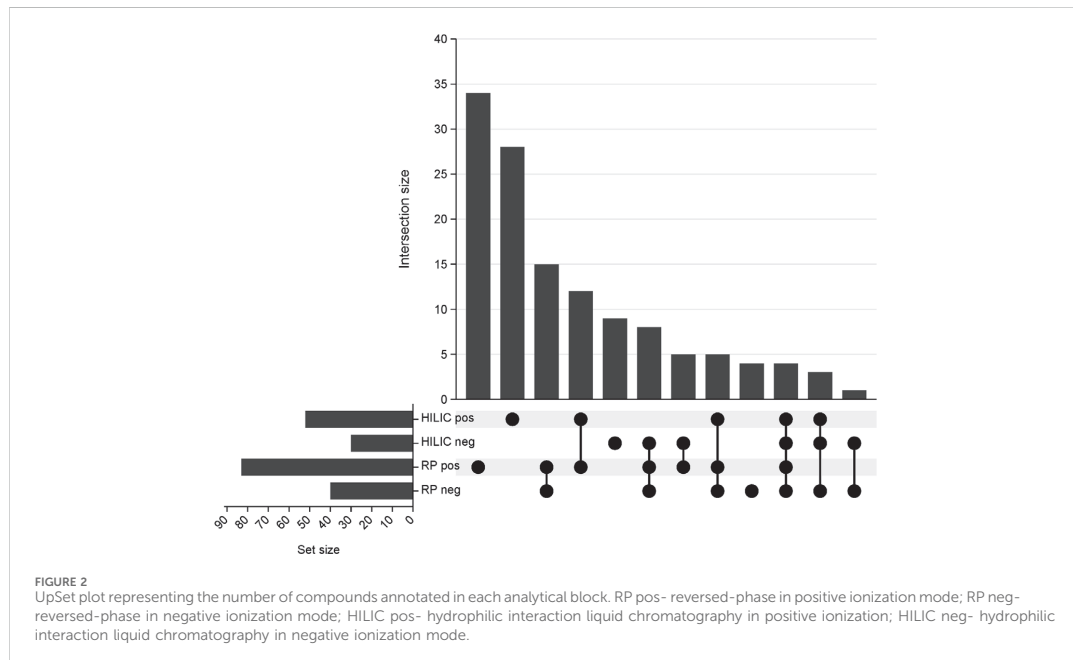
The analysis of the results was divided into four parts: 1) analysis of how warm ischemia influenced the lipidomic profiles of the kidneys; 2) comparison of the three organ-preservation methods; 3) monitoring changes across time; and 4) investigation of the influence of transplantation procedure on kidney grafts.

#### 3.1 Influence of warm ischemia on kidney lipidomic profiles

The Kruskal-Wallis test, followed by *post hoc* test, was used to identify changes that occurred during warm ischemia. The results indicated that discriminative changes were mostly visible at the first sampling point of warm ischemia time (WIT). Among the identified lipids, an increase in acylcarnitines (CARs), lysophosphocholines (LPCs), and lysophosphoethanolamines (LPEs) was observed after 45 min of warm ischemia, while a corresponding decrease in phosphocholines (PCs) and sphingomyelins (SMs) was also noted. Boxplots of statistically significant lipids are shown in [Figure 3](#).

#### 3.2 Comparison of different kidney preservation methods

Chemometric analysis was conducted to visualize the data and investigate the differences in the kidney lipidomic profiles in the SCS, NEVKP, and HMP groups. The two-dimensional scoring plots (PC1 vs. PC2) presented in [Supplementary Figure S2](#) revealed major differences in the lipidomic patterns of samples harvested under different preservation conditions. In all analyses, the lipidomes of the renal tissue from the NEVKP group showed clear separation from those of the SCS and HMP groups. In contrast, the data points in the scoring plots for the SCS and HMP groups had slightly overlapping distributions ([Supplementary Figure S2](#)). PLS-DA was applied to more accurately model differences in the lipidomic profiles of the kidneys in each preservation method group ([Figure 4](#)). Each model was validated via leave-one-out cross-validation and refined using a permutation test (permutation number = 1,000), which yielded significant ( $p < 0.05$ ) quality parameters. This statistical analysis produced a set of compounds that successfully differentiated the different types of kidney preservation. A VIP score value > 1 was selected as a cut-off value. Furthermore, the Kruskal-Wallis test ( $p < 0.05$ ) was used to compare the NEVKP, HMP, and SCS groups, while the discriminative compounds were selected based on chemometric and univariate analysis. [Supplementary Table S2](#) lists the compounds meeting the above-mentioned criteria.



Given that unsupervised analysis indicated that the observed differences were mainly related to the preservation temperature, additional PCA (Supplementary Figure S3) and PLS-DA (Figure 5) analyses were conducted to identify the compounds that statistically differentiated the hypothermic and normothermic preservation methods. These analyses were confirmed via leave-one-out cross-validation and a positive permutation test (permutation number = 1,000;  $p < 0.05$ ). In addition, the Mann-Whitney U test with FDR correction was also applied to select statistically important compounds. Supplementary Table S3 lists the compounds with a  $p$ -value  $< 0.05$  and/or a VIP value  $> 1$ . Moreover, samples collected from all preservation groups after reperfusion were compared to identify differences occurring in kidney tissue *in vivo* after using a given preservation method. Strip plots of statistically significant compounds are shown in Figure 6. After reperfusion, significantly fewer differentiating compounds were identified than during preservation. A similar comparison was performed for samples collected on postoperative day 3. However, this comparison was possible only for the samples from the NEVKP and SCS groups, as the POD3 samples from the HMP group were rendered unrepresentative due to damage, and therefore had to be omitted. Nonetheless, a comparison of samples collected from the NEVKP and SCS groups at POD3 did not reveal any significant differentiating lipids.

### 3.3 Changes across time

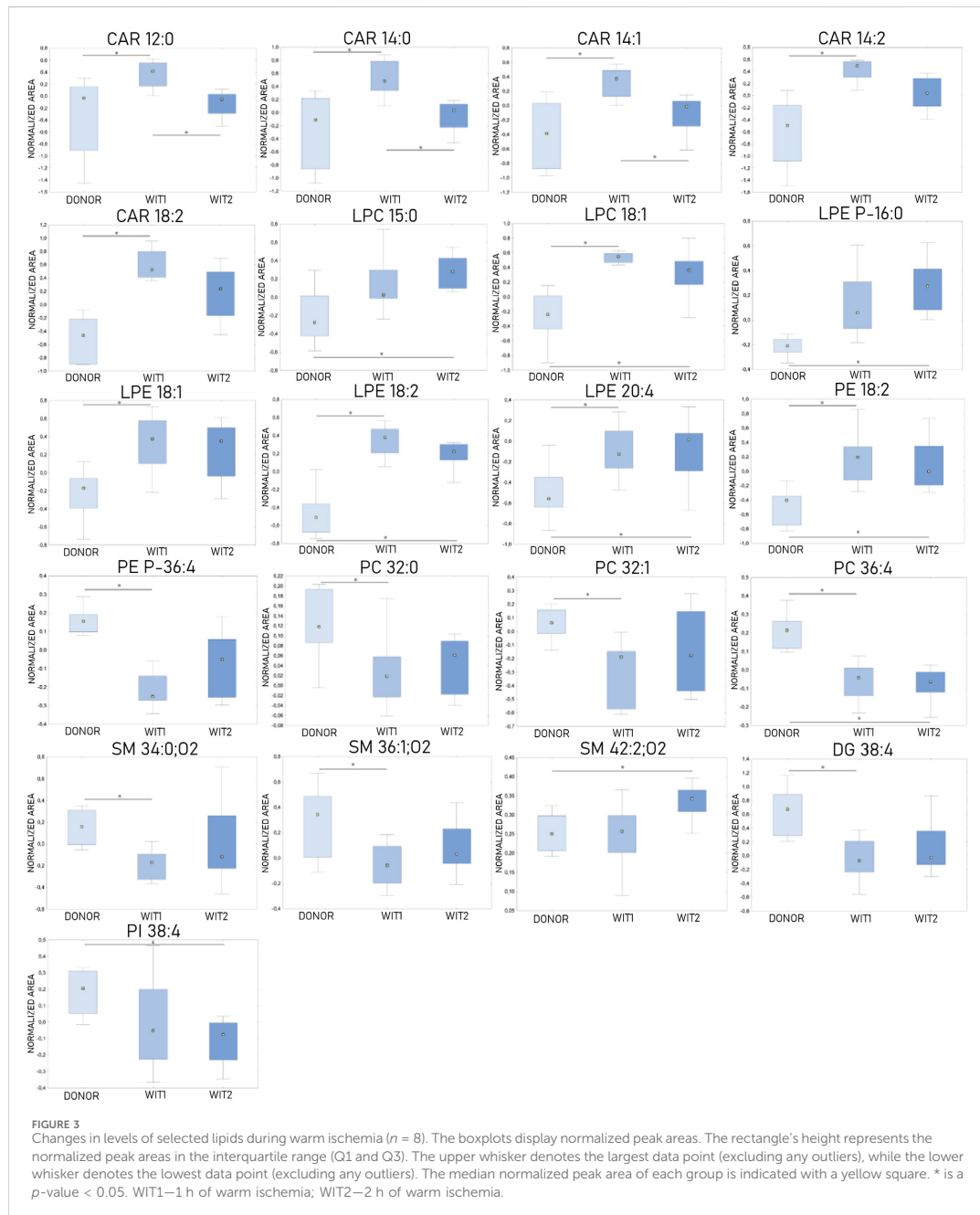
The Friedman test was used to evaluate changes throughout perfusion. The majority of statistically significant changes in lipids

levels were found in the samples collected during mechanical perfusion (especially HMP). For NEVKP, a decrease was observed for CARs (CAR 12:0, CAR 14:1) and triacylglycerol (TG) 56:7. For HMP samples, changes throughout perfusion were mainly observed for PCs, phosphoethanolamines (PEs), and SMs but no dominant trend was observed. Strip plots of the selected compounds are shown in Figure 7, and a list of statistically significant compounds is provided in Supplementary Table S4.

Next, differences between the reperfusion and POD3 samples were evaluated. As mentioned before, the POD3 samples from the HMP group were removed from the analysis; hence, comparisons were performed only for the samples from the NEVKP and SCS groups. The analysis revealed more differentiating lipids in the SCS group (21 compounds) than in the NEVKP group (3 compounds). In the NEVKP group, all statistically significant lipids were present at higher levels on POD3 than after reperfusion. In the SCS group, elevated levels of ether-linked phospholipids and PCs with 32 carbon chains were observed on POD3, along with a corresponding reduction in SMs, PEs, PC 35:6, and PC 38:5. A list of statistically significant compounds is shown in Supplementary Table S5.

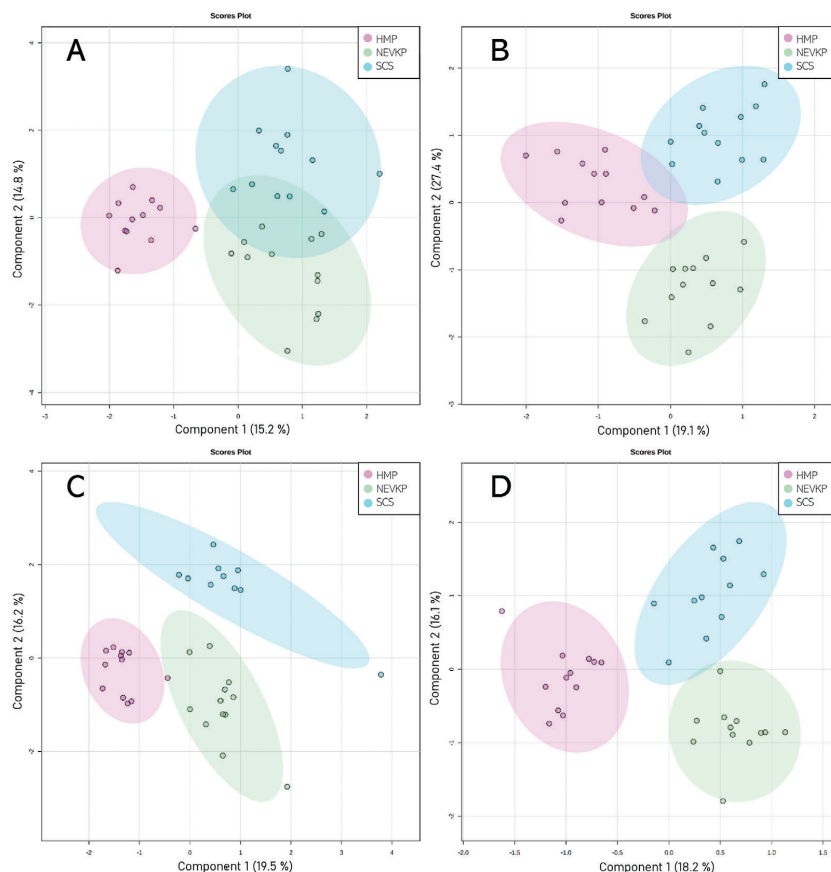
### 3.4 Influence of transplantation procedure on kidney grafts

A Mann-Whitney U test with FDR correction was carried out to determine how the transplantation and preservation procedures affected the lipidomic profiles of the kidneys. For the SCS and NEVKP groups, comparisons of lipidomic profiles at donation and



reperfusion and donation and POD3 were performed. For the HMP group, a comparison at donation and reperfusion was conducted. As shown in [Supplementary Table S6](#), most of the statistically significant compounds in the SCS group were found in the donor and POD3 comparison. Conversely, in the comparison of

donors and reperfusion, most of the significantly differentiating compounds were found in the NEVKP group; however, most of these compounds were present at lower levels after reperfusion. While the comparison of donors and POD 3 revealed similar change trends for the SCS and NEVKP groups, the alterations were usually



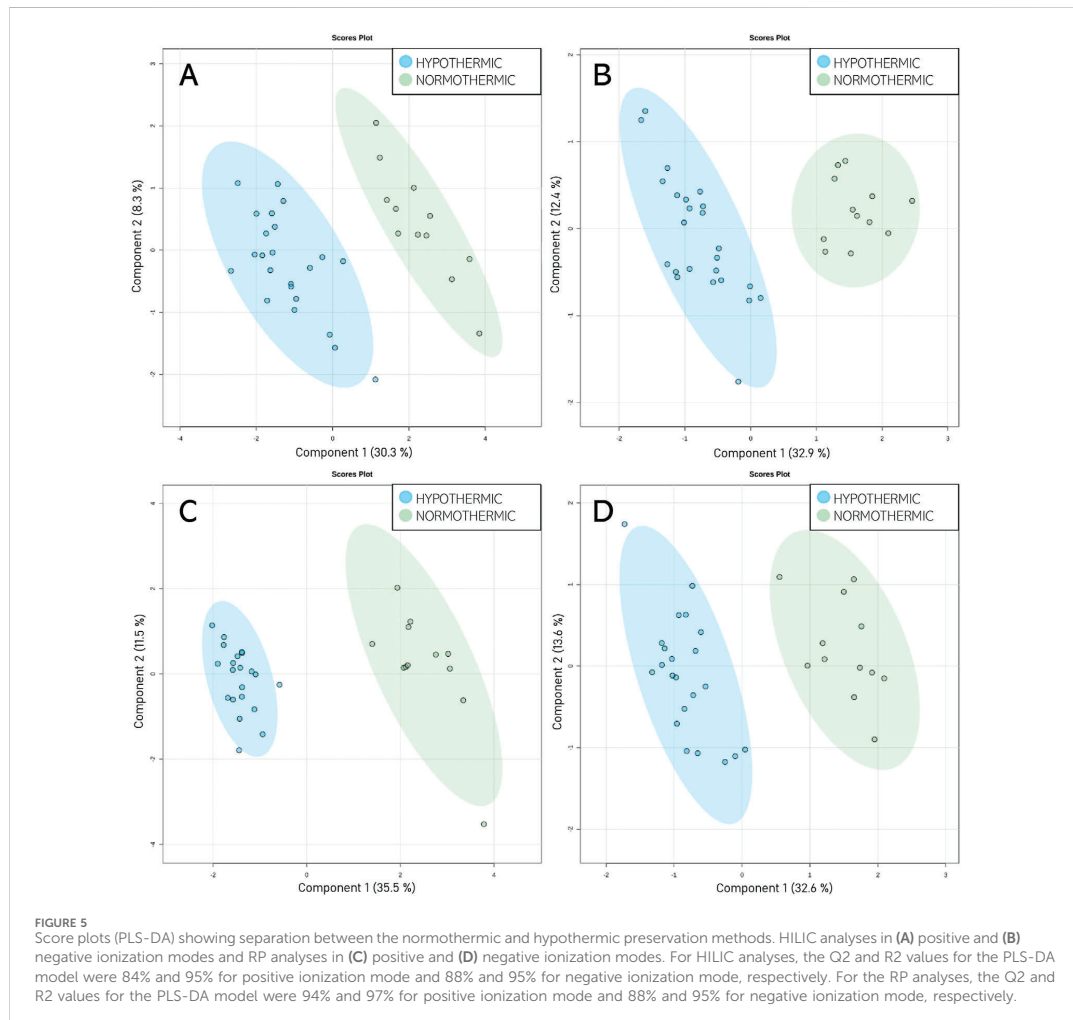
**FIGURE 4**  
Score plots (PLS-DA) showing separation based on different types of kidney preservation. HILIC analyses in (A) positive and (B) negative ionization modes and RP analyses in (C) positive and (D) negative ionization modes. For HILIC analyses, the Q2 and R2 values for the PLS-DA model were 71% and 88% for positive ionization mode and 57% and 74% for negative ionization mode, respectively. For the RP analyses, the Q2 and R2 values for the PLS-DA model were 76% and 92% for positive ionization mode and 59% and 87% for negative ionization mode, respectively.

more noticeable in the SCS group, as evidenced by the fold change. On POD3, both groups exhibited elevated levels CARs, LPEs, and PCs and PEs (including ether-linked) with relatively shorter chains, along with a corresponding in PCs with longer chains. Additionally, a reduction in PSs, SMs, and PEs with longer chains was also observed in the SCS group.

## 4 Discussion

Organ-preservation methods have garnered significant interest in graft quality evaluation, advanced organ monitoring, and the treatment of transplanted kidneys during machine perfusion. This study further explores these trends and, to the best of our knowledge, it is the first to apply SPME to compare SCS, NEVKP, and HMP preservation methods in a porcine DCD autotransplantation model.

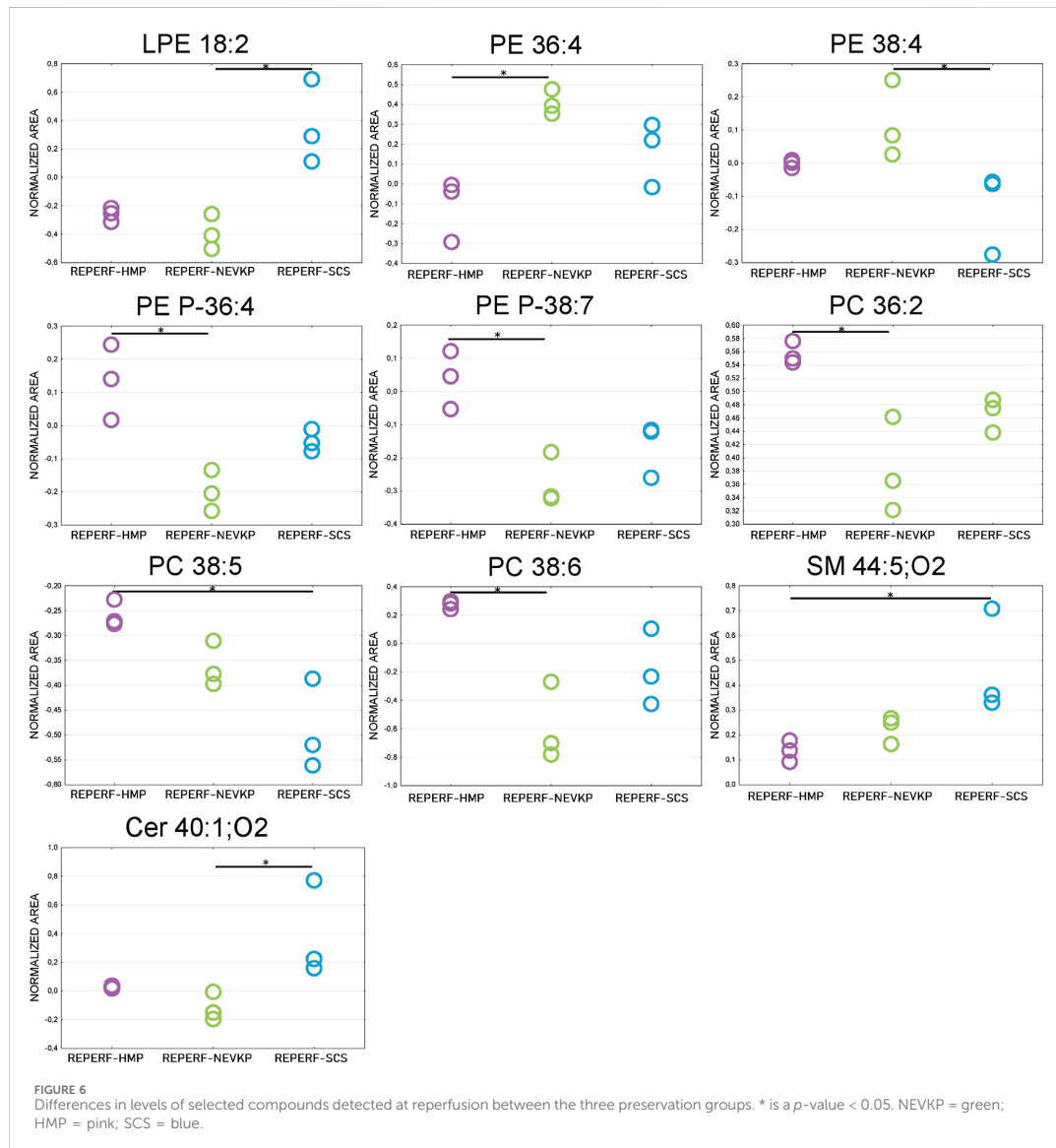
Moreover, this study highlights the alterations in the lipidomic profile during warm ischemia and perfusion, as well as after transplantation. The minimally invasive SPME chemical biopsy allows for the repeated direct sampling of the organ, as it does not require any tissue collection. Thanks to this undisputed advantage, it was possible to validate the PLS-DA models and identify significantly differentiating lipids using a relatively small number of animals. Additionally, this study employed four LC-HRMS analyses to cover a wide range of lipids. The analysis showed that this approach allowed the identification of more lipids than was possible using only one type of chromatographic separation. The largest number of unique compounds were identified with the use of RP and HILIC separation in positive ionization mode. In negative ionization mode, using HILIC and RP separations, 9 and 4 unique compounds were identified, respectively. Therefore, based on the results obtained and taking into account the time-consuming nature



of the analyses, the consumption of organic reagents, the amount of data obtained, and the benefits of using additional LC-HRMS analyses in future studies, it is worth considering limiting the number of analyzes used, thus choosing the best compromise between advantages and disadvantages.

A thorough analysis of kidney graft tissue during warm ischemia indicated increased levels of CARs, LPCs, and LPEs. CARs are established mitochondrial biomarkers in neonatal screening; however, they are not routinely used beyond this screening, despite the growing evidence of their biomarker potential among disorders such as diabetes, sepsis, cancer, and heart failure (Breit and Weinberger, 2016; McCann et al., 2021). Moreover, alterations of CARs related to kidney disease, including acute kidney injury, progression of chronic kidney disease (CKD), and diabetic nephropathy, have been previously reported in several reports (Breit and Weinberger, 2016; Hoher and Adamski, 2017; Afshinnia et al., 2018; Kordalewska et al., 2019; Andrianova

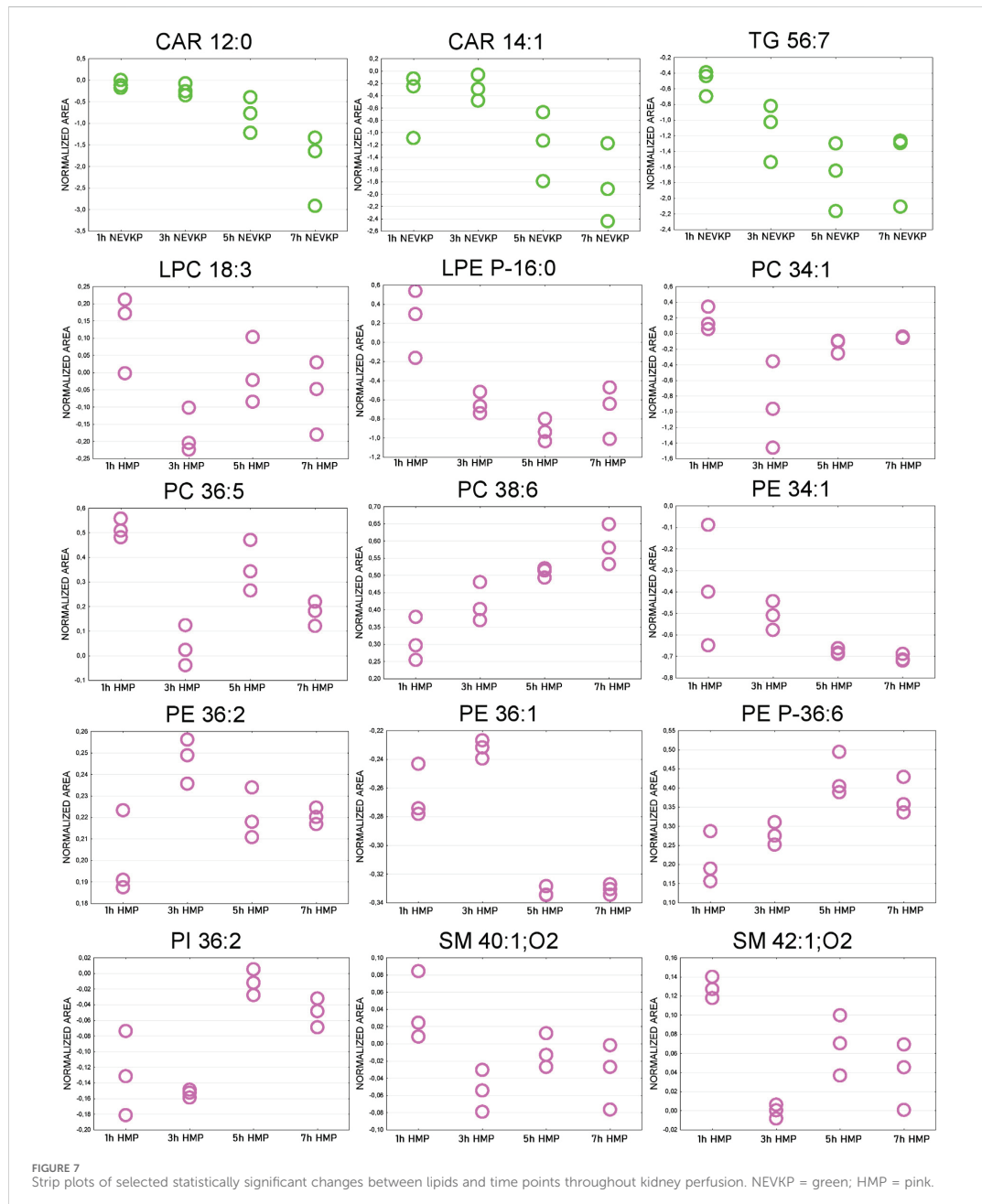
et al., 2020). In this study, significantly elevated levels of four long-chain CARs (CAR 14:0, CAR 14:1, CAR 14:2, CAR 18:2) and one medium-chain CAR (CAR 12:0) were mainly observed after 45 min of warm ischemia. CARs are crucial for transporting long-chain fatty acids into the mitochondria to ensure the  $\beta$ -oxidation process (Breit and Weinberger, 2016; Kordalewska et al., 2019). Thus, the increase of CARs observed during warm ischemia may be related to mitochondria dysfunction. Indeed, a similar accumulation of long-chain CARs in ischemic tissue has been reported elsewhere, and it is thought that this accumulation inhibits oxidative phosphorylation, induces mitochondrial membrane hyperpolarization, and stimulates the production of reactive oxygen species (ROS) (Liepinsh et al., 2016; Andrianova et al., 2020). LPCs and LPEs are the products of the phospholipase-induced hydrolysis of PCs and PEs (Xu et al., 2015; Law et al., 2019). These compounds play a role in cellular signal transduction, tumorigenesis, angiogenesis, immunity, atherosclerosis, cancer,



and neuronal survival (Kordalewska et al., 2019). Previously, higher levels of LPCs have been associated with oxidative stress and pro-inflammatory effects (Kordalewska et al., 2019). Moreover, similar to the results obtained in this study, Xu et al. (2015) observed higher pretransplant levels of LPCs (LPC 16:0, LPC 18:0) and LPEs (LPE 16:0, LPE 18:0) in donors after circulatory death compared to donors after brain death. Conversely, Rao et al. found higher levels of LPC 18:0, LPC 26:6, LPE 16:0, and LPC 18:0, along with a corresponding reduction in LPC 20:0, LPC 20:4, LPE 22:0, and LPE 24:6, 24 h after IR-induced acute kidney injury (Rao et al., 2016). The inconclusive results obtained in recent studies may be related to the complexity of

the enzymatic cascade involved in LPC metabolism (Law et al., 2019).

Chemometric analysis revealed significant differences between the SCS, HMP, and NEVKP preservation methods, with further in-depth analysis demonstrating that the method's preservation temperature has a greater impact on the lipidomic profile than its mechanical character. Higher levels of CARs, PCs, ether-linked PCs, ether-linked PEs, phosphatidylinositols (PIs), TGs, most LPCs and LPEs, and longer-chain PEs were observed in the hypothermic group, while higher levels of ceramides (Cer), PSs, and shorter-chain PEs were observed in the normothermic group. Numerous SMs



differentiated the preservation methods, but no dominant trend was observed. As mentioned above, increased levels of long-chain CARs may be related to mitochondria dysfunction and increased production of ROS (Liepinsh et al., 2016; Andrianova et al., 2020), and higher levels of LPCs may be associated with

oxidative stress and pro-inflammatory effects (Kordalewska et al., 2019). Moreover, higher levels of LPEs were observed in DCD livers compared to livers from donors after brain death (Xu et al., 2015), and increased LPE levels were observed in CKD progression (Kordalewska et al., 2019). Rao et al. (2016) and Solati et al.

(2018) have reported elevated levels of PCs in mice and rat ischemia/reperfusion (I/R) models. Similar to our results, they observed increases in PC 34:1, PC 34:2, PC 36:1, PC 36:2, PC 36:3, PC 36:4, PC 38:3, PC 38:4, PC 38:5, PC 38:6, PC 40:4 and PC 40:5. Additionally, Solati et al. reported increased levels of PIs 6 h and 12 h after I/R, while in this study higher levels of PI 36:2 and PI 38:4 were observed in the hypothermic preservation group (Solati et al., 2018). Ether-linked PCs and ether-linked PE were present at higher levels in the hypothermic group compared to the normothermic group. In Rao et al.'s study, significantly elevated levels of a small number of ether-linked phospholipids were observed 6 h after renal I/R (vs. control animals); notably, levels of these ether phospholipids were correlated with plasma creatinine. However, 24 h after I/R, only PC O-38:1 was still elevated, while ether-linked PEs were reduced at this later time point (Rao et al., 2016). Ether lipids differ from their diacyl counterparts, allowing them to contribute unique structural characteristics to biological membranes. Moreover, previous findings suggest that ether lipids play a role in various biological processes, including cell differentiation, cellular signalling, and oxidative-stress reduction (Dean and Lodhi, 2018). While alterations of ether lipids have been reported in several disorders, including neurodegenerative disease, cancer, and metabolic disorders (Rao et al., 2016; Dean and Lodhi, 2018), the molecular mechanism underlying their role in these pathologies remains unclear. Higher levels of three TGs (TG 44:1, TG 56:6, TG 56:7) and three longer-chain PEs (PE 38:4, PE 38:5, PE 40:4) were also observed in the hypothermic group. Similar elevations were reported by Afshinnia et al. (2018) in their study of lipid profiles in CKD. Their results indicated that higher quantities of long polyunsaturated lipids are related to CKD progression. Elsewhere, Solati et al. (2018) observed an increase in longer-chain PEs and a reduction in shorter-chain PEs 24 h after I/R, which aligns with the trend observed for the hypothermic group in our study. The alterations described above suggest the NEVKP method's beneficial effects with respect to kidney grafts. The lower accumulation of lipids in NEVKP kidneys, especially those with pro-inflammatory properties, results in improved graft function following NEVKP compared to hypothermic preservation methods. Additionally, the reductions of CAR 12:0 and CAR 14:1 across perfusion time points may also be indicative of NEVKP's beneficial effects.

A much smaller number of compounds differentiating the HMP, NEVKP, and SCS methods were identified post-perfusion (vs. during preservation). However, after reperfusion, the trend in changes was similar to that observed during perfusion, with most of the significant changes differentiating NEVKP from other hypothermic methods, rather than from HMP and SCS.

A comparison of the kidneys during reperfusion and on POD3 revealed more significant changes in the SCS group compared to the NEVKP group. In particular, the SCS group exhibited elevated levels of ether-linked PEs and PC P-38:4 on POD3. As noted above, Rao et al. reported higher levels of PC O-38:1, PE O-42:3, and PE O-40:4 6 h after I/R, but only PC O-38:1 remained elevated in I/R at 24 h. However, more research is required to investigate the molecular mechanisms underlying the role of ether lipids in kidney disease. Additionally, in the SCS group, lower levels of SMs were identified on POD3. Previous findings have shown an increase in SMs 24 h after I/R in animal models (Rao et al.,

2016; Solati et al., 2018). In contrast, Zhao et al. (2014) observed lower SMs levels in an acute graft rejection group after transplantation, while Tofte et al. (2019) demonstrated that higher levels of specific SMs were associated with a lower risk of end-stage renal disease and all-cause mortality in type 1 diabetes. These findings indicate that lower levels of SMs may be related to impaired graft function. The results of this comparison (donor vs. POD3) provide further evidence that NEVKP enables improved graft function compared to SCS.

The last step of untargeted analysis entailed a comparison of the lipidomic profiles at baseline (donation) and reperfusion and at baseline and POD3. The largest number of statistically significant compounds was identified in the donor-POD3 comparison for the SCS group. While the trends in changes were similar for the SCS and NEVKP groups, the alterations were usually more noticeable in the SCS group. The observed alterations mainly concerned lipids described previously in this study. Higher levels of CARs, a few LPCs and LPEs, several PCs and PEs, and ether-linked PCs on POD3 were observed for both the SCS and NEVKP groups. However, more compounds among these lipid classes were statistically significant for the SCS group. As discussed above, the elevated levels of these lipids may be related to I/R injury, mitochondrial dysfunction, pro-inflammatory effect, and/or oxidative stress. Significant reductions in SM levels on POD3 were observed only for the SCS group. As previously noted, prior findings have shown a connection between reduced SM levels and acute graft rejection (Zhao et al., 2014).

Despite these promising results, this study has several limitations. The first limitation is the small sample sizes. However, since SPME enables multiple analyses over time, it is possible to acquire a large number of samples without requiring more animals. Another limitation was that the obtained results were not compared with routinely assessed clinical parameters; as such, the analysis was not as comprehensive as it might have otherwise been. A final limitation of this study design is the relatively short follow-up period of 3 days post-transplantation. Unfortunately, this interval was necessary, as the porcine experimental setup makes it difficult to investigate over a longer follow-up period of months, or even years.

## 5 Conclusion

SPME chemical biopsy followed by LC-MS/MS analysis enables the minimally invasive and repeated sampling of the same tissue. As such, this method was successfully applied to track alterations in a graft throughout the entire transplantation procedure, and to compare kidney lipidomic profiles during storage with different preservation methods. As a result, we observed that the preservation temperature has a more significant impact on the lipidomic profile of the kidney than the preservation method's mechanical characteristics. Higher levels of CARs, PCs, ether-linked PCs, ether-linked PEs, PIs, TGs, most LPC and LPE, and longer-chain PEs were observed in the hypothermic preservation group, which may be related to I/R injury, mitochondrial dysfunction, pro-inflammatory effect, and oxidative stress. Hence, the obtained results suggest that the use of NEVKP can have a beneficial effect on graft function.

## Data availability statement

The original contributions presented in the study are publicly available. This data can be found here: <https://repositorio.icm.edu.pl/dataset.xhtml?persistentId=doi:10.18150/ATK9DA>

## Ethics statement

The animal study was approved by Animal Care Committee at the Toronto General Research Institute, Ontario, Canada. The study was conducted in accordance with the local legislation and institutional requirements.

## Author contributions

NW: Methodology, Formal analysis, Investigation, Data curation, Writing—original draft, Writing—review and editing, Visualization. KL: Investigation, Formal analysis, Writing—review and editing. IS: Investigation, Writing—review and editing. HR-S: Methodology, Investigation, Writing—review and editing. PU: Methodology, Investigation, Writing—review and editing. JP: Methodology, Supervision, Resources, Writing—review and editing. MS: Conceptualization, Methodology, Investigation, Resources, Writing—review and editing. BB: Conceptualization, Methodology, Supervision, Resources, Investigation, Writing—review and editing. Funding acquisition.

## Funding

The authors declare that financial support was received for the research, authorship, and/or publication of this article. This study

was funded by National Science Centre, grant Opus No. 2017/27/B/NZ5/01013.

## Acknowledgments

The authors would like to acknowledge Supelco/MilliporeSigma for kindly supplying the SPME probes and Thermo Fisher Scientific for granting us access to a Q-Exactive Focus mass spectrometer.

## Conflict of interest

The authors declare that the research was conducted in the absence of any commercial or financial relationships that could be construed as a potential conflict of interest.

## Publisher's note

All claims expressed in this article are solely those of the authors and do not necessarily represent those of their affiliated organizations, or those of the publisher, the editors and the reviewers. Any product that may be evaluated in this article, or claim that may be made by its manufacturer, is not guaranteed or endorsed by the publisher.

## Supplementary material

The Supplementary Material for this article can be found online at: <https://www.frontiersin.org/articles/10.3389/fmolb.2024.1341108/full#supplementary-material>

## References

- Afshinnia, F., Rajendiran, T. M., Soni, T., Byun, J., Wernisch, S., Sas, K. M., et al. (2018). Impaired  $\beta$ -oxidation and altered complex lipid fatty acid partitioning with advancing CKD. *J. Am. Soc. Nephrol.* 29, 295–306. doi:10.1681/ASN.2017030350
- Andrianova, N. V., Popkov, V. A., Klimenko, N. S., Tyakht, A. V., Baydakova, G. V., Frolova, O. Y., et al. (2020). Microbiome-metabolome signature of acute kidney injury. *Metabolites* 10, 142. doi:10.3390/metabo10040142
- Azancot, M. A., Moreso, F., Salcedo, M., Cantarell, C., Perello, M., Torres, I. B., et al. (2014). The reproducibility and predictive value on outcome of renal biopsies from expanded criteria donors. *Kidney Int.* 85, 1161–1168. doi:10.1038/ki.2013.461
- Bojko, B. (2022). Solid-phase microextraction: a fit-for-purpose technique in biomedical analysis. *Anal. Bioanal. Chem.* 414, 7005–7013. doi:10.1007/s00216-022-04138-9
- Breit, M., and Weinberger, K. M. (2016). Metabolic biomarkers for chronic kidney disease. *Arch. Biochem. Biophys.* 589, 62–80. doi:10.1016/j.ab.2015.07.018
- Dare, A. J., Pettigrew, G. J., and Saeb-Parsy, K. (2014). Preoperative assessment of the deceased-donor kidney: from macroscopic appearance to molecular biomarkers. *Transplantation* 97, 797–807. doi:10.1097/01.TP.0000441361.34103.53
- Dean, J. M., and Lodhi, I. J. (2018). Structural and functional roles of ether lipids. *Protein Cell* 9, 196–206. doi:10.1007/s13238-017-0423-5
- Hoher, B., and Adamski, J. (2017). Metabolomics for clinical use and research in chronic kidney disease. *Nat. Rev. Nephrol.* 13, 269–284. doi:10.1038/nrneph.2017.30
- Hosgood, S. A., Hoff, M., and Nicholson, M. L. (2021). Treatment of transplant kidneys during machine perfusion. *Transpl. Int.* 34, 224–232. doi:10.1111/tri.13751
- Kaths, J. M., Echeverri, J., Chun, Y. M., Cen, J. Y., Goldaracena, N., Linares, I., et al. (2017). Continuous normothermic *ex vivo* kidney perfusion improves graft function in donation after circulatory death pig kidney transplantation. *Transplantation* 101, 754–763. doi:10.1097/TP.0000000000001343
- Kaths, J. M., Echeverri, J., Goldaracena, N., Louis, K. S., Yip, P., John, R., et al. (2016). Heterotopic renal autotransplantation in a porcine model: a step-by-step protocol. *J. Vis. Exp.* 2016, 53765–53769. doi:10.3791/53765-v
- Kaths, J. M., Hamar, M., Echeverri, J., Linares, I., Urbanellis, P., Cen, J. Y., et al. (2018). Normothermic *ex vivo* kidney perfusion for graft quality assessment prior to transplantation. *Am. J. Transpl.* 18, 580–589. doi:10.1111/ajt.14491
- Kaths, J. M., Spetzler, V. N., Goldaracena, N., Echeverri, J., Louis, K. S., Foltys, D. B., et al. (2015). Normothermic *ex vivo* kidney perfusion for the preservation of kidney grafts prior to transplantation. *J. Vis. Exp.* 2015, e52909–e52913. doi:10.3791/52909
- Kordalewska, M., Macioszek, S., Wawrzyniak, R., Sikorska-Wisniewska, M., Śledziński, T., Chmielewski, M., et al. (2019). Multiplatform metabolomics provides insight into the molecular basis of chronic kidney disease. *J. Chromatogr. B Anal. Technol. Biomed. Life Sci.* 1117, 49–57. doi:10.1016/j.jchromb.2019.04.003
- Law, S., Chan, M., Marathe, G. K., Parveen, F., Chen, C., and Ke, L. (2019). An updated review of lysophosphatidylcholine metabolism in human diseases. *Int. J. Mol. Sci.* 20, 1149. doi:10.3390/ijms20051149
- Liepinsh, E., Makrecka-Kuka, M., Volska, K., Kuka, J., Makarova, E., Antone, U., et al. (2016). Long-chain acylcarnitines determine ischaemia/reperfusion-induced damage in heart mitochondria. *Biochem. J.* 473, 1191–1202. doi:10.1042/BCJ20160164
- Lindell, S. L., Muir, H., Brassil, J., and Mangino, M. J. (2013). Hypothermic machine perfusion preservation of the DCD kidney: machine effects. *J. Transpl.* 2013, 802618. doi:10.1155/2013/802618

- Łuczykowski, K., Warmużińska, N., and Bojko, B. (2023). Solid phase microextraction—a promising tool for graft quality monitoring in solid organ transplantation. *Separations* 10, 153. doi:10.3390/separations10030153
- McCann, M. R., De la Rosa, M. V. G., Rosania, G. R., and Stringer, K. A. (2021). L-carnitine and acylcarnitines: mitochondrial biomarkers for precision medicine. *Metabolites* 11, 1–21. doi:10.3390/metabo11010051
- Moeckli, B., Sun, P., Lazeyras, F., Morel, P., Moll, S., Pascual, M., et al. (2019). Evaluation of donor kidneys prior to transplantation: an update of current and emerging methods. *Transpl. Int.* 32, 459–469. doi:10.1111/tri.13430
- Rao, S., Walters, K. B., Wilson, L., Chen, B., Bolisetty, S., Graves, D., et al. (2016). Early lipid changes in acute kidney injury using SWATH lipidomics coupled with MALDI tissue imaging. *Am. J. Physiol. - Ren. Physiol.* 310, F1136–F1147. doi:10.1152/ajprenal.00100.2016
- Resch, T., Cardini, B., Oberhuber, R., Weissenbacher, A., Dumfarth, J., Krapf, C., et al. (2020). Transplanting marginal organs in the era of modern machine perfusion and advanced organ monitoring. *Front. Immunol.* 11, 631. doi:10.3389/fimmu.2020.00631
- Solati, Z., Edel, A. L., Shang, Y., Karmin, O., and Ravandi, A. (2018). Oxidized phosphatidylcholines are produced in renal ischemia reperfusion injury. *PLoS One* 13, e0195172. doi:10.1371/journal.pone.0195172
- Stryjak, I., Warmużińska, N., Łuczykowski, K., Hamar, M., Urbanellis, P., Wojtal, E., et al. (2020). Using a chemical biopsy for graft quality assessment. *J. Vis. Exp.*, e60946. doi:10.3791/60946-v
- Swanson, K. J., Aziz, F., Garg, N., Mohamed, M., Mandelbrot, D., Djamali, A., et al. (2020). Role of novel biomarkers in kidney transplantation. *World J. Transpl.* 10, 230–255. doi:10.5500/wjt.v10.i9.230
- Tofte, N., Suvitaival, T., Ahonen, L., Winther, S. A., Theilade, S., Frimodt-Møller, M., et al. (2019). Lipidomic analysis reveals sphingomyelin and phosphatidylcholine species associated with renal impairment and all-cause mortality in type 1 diabetes. *Sci. Rep.* 9, 16398. doi:10.1038/s41598-019-52916-w
- Urbanellis, P., Hamar, M., Kath, J. M., Kollmann, D., Linares, I., Mazilescu, L., et al. (2020). Normothermic *ex vivo* kidney perfusion improves early DCD graft function compared with hypothermic machine perfusion and static cold storage. *Transplantation* 104, 947–955. doi:10.1097/TP.0000000000003066
- Warmużińska, N., Łuczykowski, K., and Bojko, B. (2022). A review of current and emerging trends in donor graft-quality assessment techniques. *J. Clin. Med.* 11, 487. doi:10.3390/jcm11030487
- Xu, J., Casas-Ferreira, A. M., Ma, Y., Sen, A., Kim, M., Proitsi, P., et al. (2015). Lipidomics comparing DCD and DBD liver allografts uncovers lysophospholipids elevated in recipients undergoing early allograft dysfunction. *Sci. Rep.* 5, 17737. doi:10.1038/srep17737
- Zhao, X., Chen, J., Ye, L., and Xu, G. (2014). Serum metabolomics study of the acute graft rejection in human renal transplantation based on liquid chromatography-mass spectrometry. *J. Proteome Res.* 13, 2659–2667. doi:10.1021/pr5001048

## Supplementary Material

### The impact of normothermic and hypothermic preservation methods on kidney lipidome – comparative study using chemical biopsy with microextraction probes

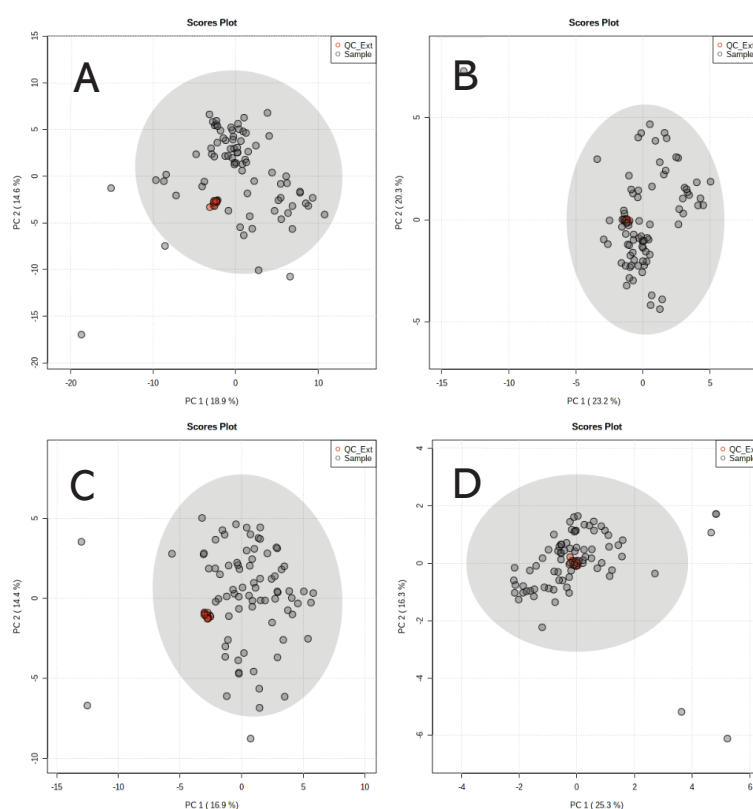
Natalia Warmuzińska<sup>1</sup>, Kamil Łuczykowski<sup>1</sup>, Iga Stryjak<sup>1</sup>, Hernando Rosales-Solano<sup>2</sup>, Peter Urbanellis<sup>3</sup>, Janusz Pawliszyn<sup>2</sup>, Markus Selzner<sup>3,4</sup>, Barbara Bojko<sup>1\*</sup>

<sup>1</sup>Department of Pharmacodynamics and Molecular Pharmacology, Faculty of Pharmacy, Nicolaus Copernicus University in Torun, Collegium Medicum in Bydgoszcz, Bydgoszcz, Poland

<sup>2</sup>Department of Chemistry, University of Waterloo, Waterloo, Ontario N2L 3G1, Canada

<sup>3</sup>Ajmera Transplant Center, Department of Surgery, Toronto General Hospital, University Health Network, Toronto, ON, Canada

<sup>4</sup>Department of Medicine, Toronto General Hospital, Toronto, ON, Canada

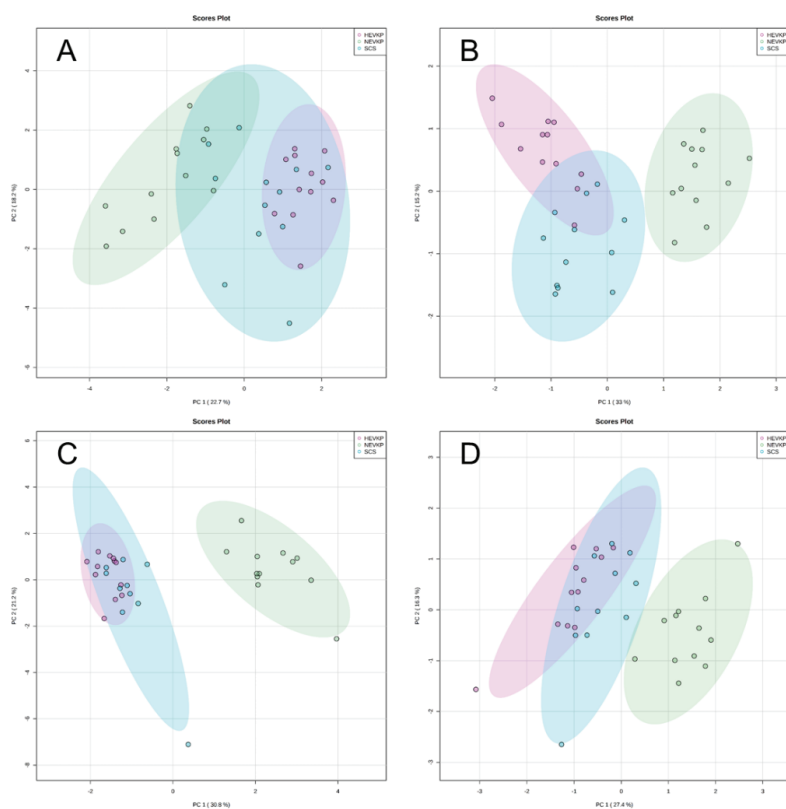


**Fig. S1** Principal component analysis (PCA) plots of all analyzed samples and extraction quality control (QC\_ext) samples. A- RP. positive ionization mode; B – RP. negative ionization mode; C- HILIC. positive ionization mode. D- HILIC. negative ionization mode.

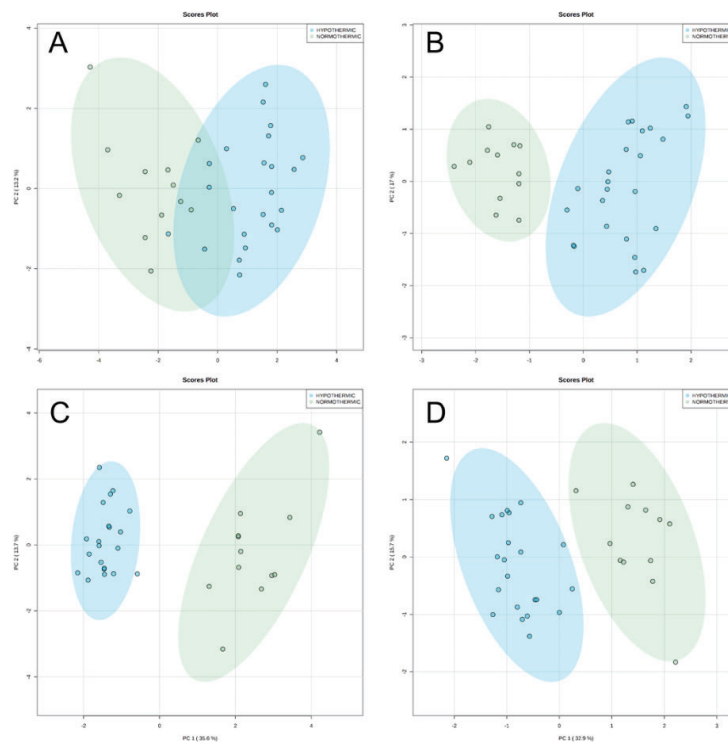
**Table S1.** The list of lipid species identified using MS/MS mode.

Type of LC-HRMS analysis	number of compounds	Identified lipid species
HILIC neg HILIC pos RP neg RP pos	4	PE P-36:4; PE 34:2; PE 36:2; PC 34:1
HILIC pos RP neg RP pos	5	PC 38:5; PC 36:2; PC 36:4; PE 36:3; PC 36:3
HILIC neg RP neg RP pos	8	PE P-38:5; PE 38:4; PE 34:1; PE P-38:4; SM 34:1;O2; PE P-34:1; PC 34:2; PI 36:2
HILIC neg HILIC pos RP neg	3	LPE 20:4; PE 36:4; PE 38:5
RP neg RP pos	15	SM 42:3;O2; LPC 18:1; SM 42:1;O2; SM 42:2;O2; PC 36:1; PE P-36:1; SM 38:1;O2; LPC 18:0; LPC 16:0; PS 36:2; SM 40:1;O2; PS 36:1; LPC 18:2; PC 38:4; PE 36:1
HILIC pos RP pos	12	PC P-38:4; PC O-38:4; PC 36:5; SM 40:4;O2; PC 38:6; LPC 20:4; SM 44:5;O2; SM 36:4;O2; PC 40:5; LPC 18:3; SM 43:4;O2; PC 38:7
HILIC neg RP pos	5	PE P-40:4; PE P-34:2; PE P-34:4; PE P-38:6; PE P-40:5
HILIC neg RP neg	1	PI 38:4
RP pos	34	PE P-38:7; PC 35:1; PC P-34:2; SM 41:2;O2; PC O-36:4; Cer 42:1;O2; DG 38:4; TG 56:6; PC O-32:0; PC 33:1; PC 40:4; CE 18:2; PC 35:3; SM 37:1;O2; PC P-36:4; PC O-34:2; PE O-38:6; CE 20:4; PC O-34:0; SM 34:0;O2; PE 40:4; SM 36:1;O2; DG 38:5; SM 35:1;O2; Cer 42:2;O2; PC 38:3; Cer 41:1;O2; PC 32:1; Cer 40:1;O2; TG 56:7; Cer 38:1;O2; SM 39:1;O2; TG 44:1; MG 18:2
RP neg	4	Cer 34:1;O2; PC 32:0; PC 34:0; PS 38:4

HILIC pos	28	PC 37:4; SM 39:4;O2; PC 40:6; PE O-18:2; PC 21:4; LPE P-16:0; SM 42:5;O2; SM 42:4;O2; PC P-40:7; SM 35:4;O2; CAR 14:0; DG 28:2; PC 32:3; CAR 14:1; SM 36:3;O2; PC 40:8; CAR 14:2; PC 42:9; PS 38:5; SM 41:4;O2; CAR 12:0; SM 38:5;O2; SM 44:4;O2; CAR 18:2; PC P-38:7; SPB 17:0;O3; LPC 15:0; PC 35:6
HILIC neg	9	PE 38:6; PE P-40:6; PE 35:2; LPE 18:0; PI 34:1; LPE 18:2; LPE 18:1; PE P-36:5; LPE 22:4



**Fig. S2** Score plots (PCA) showing separation between different types of kidney preservation. HILIC analyses in positive (A) and negative (B) ionization modes and RP analyses in positive (C) and negative (D) ionization modes.



**Fig. S3** Score plots (PCA) showing separation between normothermic and hypothermic preservation methods. HILIC analyses in positive (A) and negative (B) ionization modes and RP analyses in positive (C) and negative (D) ionization modes.

**Table S2.** The list of compounds that differentiated NEVKP, HMP, and SCS group during perfusion.

Name	Molecular Weight	RT [min]	FDR adjusted p-value	VIP
CAR 12:0	343.2723	8.19 (H)	0.0166	1.0978
CAR 14:1	369.2879	8.00 (H)	0.0023	1.2482
CAR 14:2	367.2723	8.07 (H)	0.00007	1.4621
CAR 18:2	423.3349	7.83 (H)	0.017	<1.0
CE 18:2	648.5845	13.96	0.00002	2.2419

CE 20:4	672.5845	13.88	0.004	<1.0
Cer 34:1;O2	537.5121	9.21	0.00001	1.5089
Cer 38:1;O2	593.5747	10.86	0.00004	<1.0
Cer 40:1;O2	621.606	11.44	0.00002	<1.0
Cer 41:1;O2	635.6216	11.70	0.0004	<1.0
Cer 42:1;O2	649.6373	11.91	0.00002	<1.0
Cer 42:2;O2	647.6216	11.48	0.00002	<1.0
DG 28:2	508.4128	1.40 (H)	>0.05	1.8271
DG 38:4	644.5379	11.20	0.0004	<1.0
DG 38:5	642.5223	10.70	>0.05	1.4463
LPC 15:0	481.3168	9.01 (H)	0.0532	1.0966
LPC 18:0	523.3638	4.65	0.007	<1.0
LPC 18:1	521.3481	4.00	0.0016	<1.0
LPC 18:2	519.3325	3.76	0.0446	<1.0
LPC 20:4	543.3325	8.47 (H)	0.00007	1.32
LPE 18:1	479.3012	9.89 (H)	0.0062	<1.0
LPE 20:4	501.2855	9.71 (H)	0.0002	1.0298
LPE 22:4	529.3168	9.37 (H)	0.00001	1.3161
LPE P-16:0	437.2906	9.44 (H)	0.0069	1.3714
PC 21:4	571.3274	7.73 (H)	0.00002	1.9972
PC 32:0	733.5622	9.09	0.0012	1.2178
PC 32:1	731.5465	8.68	>0.05	1.0028
PC 33:1	745.5622	9.06	0.0001	<1.0
PC 34:0	761.5935	9.87	>0.05	1.1281
PC 34:1	759.5778	9.49	0.00001	<1.0
PC 34:2	757.5622	8.96	0.00001	<1.0
PC 36:1	787.6091	10.23	0.00007	<1.0
PC 36:2	785.5935	9.78	0	<1.0
PC 36:3	783.5778	8.95	0.0004	<1.0
PC 36:4	781.5622	6.8 (H)	0.0008	<1.0
PC 38:3	811.6091	10.06	0.0001	<1.0
PC 38:4	809.5935	9.44	0.0002	<1.0
PC 38:5	807.5778	8.98	0.00001	1.0578

## Supplementary Material

PC 38:6	805.5622	6.74 (H)	0.0045	<1.0
PC 40:4	837.6248	10.33	0.00003	1.5863
PC 40:5	835.6091	6.74 (H)	0.0012	1.1539
PC 40:6	833.5935	6.72 (H)	0.0419	<1.0
PC 40:8	829.5622	6.74 (H)	0.0049	1.2917
PC 42:9	855.5778	6.68 (H)	0.0003	1.2953
PC O-38:4	795.6142	10.25	>0.05	1.5866
PC P-36:4	765.5672	9.39	0.0001	<1.0
PC P-38:4	793.5985	9.65	0.001	1.929
PC P-38:7	787.5516	6.70 (H)	0.0103	<1.0
PE 34:1	717.5309	9.45	0	1.6464
PE 34:2	715.5152	9.11	0	1.3767
PE 35:2	729.5309	7.24 (H)	0.011	1.3977
PE 36:1	745.5622	10.16	0.0001	<1.0
PE 36:2	743.5465	9.73	0.00001	<1.0
PE 36:3	741.5309	9.10	0.0004	1.4669
PE 36:4	739.5152	8.93	0.0003	1.325
PE 38:4	767.5465	7.07 (H)	0.0044	<1.0
PE 38:5	765.5309	9.12	0.0003	1.3479
PE 40:4	795.5778	10.42	0.0011	1.3142
PE O-18:2	477.2855	9.52 (H)	0.0028	1.0759
PE O-38:6	749.5359	9.71	0.0003	2.0622
PE P-34:1	701.5359	10.03	0.0162	<1.0
PE P-34:2	699.5203	9.57	0.0146	1.81
PE P-34:4	695.489	7.08 (H)	0.00001	1.0198
PE P-36:1	729.5672	10.70	>0.05	1.4895
PE P-36:4	723.5203	9.37	0.0002	1.4724
PE P-36:5	721.5046	7.04 (H)	0.0009	<1.0
PE P-38:4	751.5516	6.95 (H)	0.0006	1.2651
PE P-38:5	749.5359	6.96 (H)	0.00001	2.1539
PE P-38:6	747.5203	9.49	0.0002	1.357
PE P-38:7	745.5046	9.54	0.0003	<1.0
PE P-40:4	779.5829	6.93 (H)	0.0002	1.9236

PE P-40:5	777.5672	6.98 (H)	0.00003	2.2587
PE P-40:6	775.5516	6.91 (H)	0.0002	1.8385
PI 36:2	862.5571	8.19	0.0008	1.6546
PI 38:4	886.5571	7.03 (H)	0.0046	<1.0
PS 36:1	789.552	8.60	0.014	1.351
PS 36:2	787.5363	8.31	0.0353	<1.0
PS 38:5	809.5207	8.39 (H)	0.0229	1.0124
SM 34:0;O2	704.5832	8.62	0.0021	<1.0
SM 34:1;O2	702.5676	8.09	0.0006	1.6464
SM 35:1;O2	716.5832	8.74	0.0226	<1.0
SM 35:4;O2	710.5363	8.23 (H)	0.0196	<1.0
SM 36:3;O2	726.5676	7.94 (H)	0.0005	<1.0
SM 36:4;O2	724.5519	8.17 (H)	0.0097	<1.0
SM 38:1;O2	758.6302	10.00	0.00005	<1.0
SM 38:5;O2	750.5676	8.04 (H)	0.04	1.0147
SM 39:1;O2	772.6458	10.35	0.0003	<1.0
SM 39:4;O2	766.5989	8.07 (H)	0.0027	1.0214
SM 40:1;O2	786.6615	10.66	0.016	<1.0
SM 40:4;O2	780.6145	9.99	0.00009	<1.0
SM 41:2;O2	798.6615	10.41	0.00006	1.1097
SM 41:4;O2	794.6302	7.99 (H)	0.00003	<1.0
SM 42:1;O2	814.6928	11.09	0.049	<1.0
SM 42:2;O2	810.6615	10.72	0.0034	<1.0
SM 42:3;O2	810.6615	10.12	0.0256	1.4516
SM 42:4;O2	808.6458	7.98 (H)	0.0002	1.4343
SM 44:5;O2	834.6615	7.94 (H)	0.0334	<1.0
SPB 17:0;O3	303.2773	3.76 (H)	0.0142	1.0497
TG 44:1	748.6581	5.42	0.0036	<1.0
TG 56:6	906.7676	13.84	0.003	1.6641
TG 56:7	904.752	13.63	0.0007	1.6817

(H) indicates that the compound was identified with the use of the HILIC separation method; otherwise compound was identified with the use of the RP separation method

**Table S3.** The list of compounds that differentiated normothermic and hypothermic preservation methods during perfusion.

<b>Name</b>	<b>Molecular Weight</b>	<b>RT [min]</b>	<b>FDR adjusted p-value</b>	<b>VIP</b>
<b>CAR 12:0</b>	<b>343.2723</b>	<b>8.19 (H)</b>	<b>0.012998</b>	<b>1.5032</b>
<b>CAR 14:1</b>	<b>367.2723</b>	<b>8.00 (H)</b>	<b>0.0013804</b>	<b>1.922</b>
<b>CAR 14:2</b>	<b>369.2879</b>	<b>8.07 (H)</b>	<b>0.000016643</b>	<b>2.4572</b>
<b>CE 18:2</b>	<b>648.5845</b>	<b>13.96</b>	<b>0.00036187</b>	<b>1.4812</b>
CE 20:4	672.5845	13.88	0.0017392	1.7246
Cer 34:1;O2	537.5121	9.21	0.00000004863	2.2529
Cer 38:1;O2	593.5747	10.86	0.0000017624	1.5236
Cer 40:1;O2	621.6060	11.44	0.00000030131	1.4366
Cer 41:1;O2	635.6216	11.7	0.000038106	1.1275
Cer 42:1;O2	649.6373	11.91	0.000000094697	1.3617
Cer 42:2;O2	647.6216	11.48	0.0000012533	1.4212
DG 38:4	644.5379	11.2	0.00012417	1.6011
<b>LPC 18:0</b>	<b>523.3638</b>	<b>4.65</b>	<b>0.0066634</b>	<b>&lt;1.0</b>
<b>LPC 18:1</b>	<b>521.3481</b>	<b>4.00</b>	<b>0.00098038</b>	<b>1.1696</b>
LPC 18:2	519.3325	3.76	0.017806	1.0582
<b>LPC 20:4</b>	<b>543.3325</b>	<b>8.47 (H)</b>	<b>0.00028469</b>	<b>1.5064</b>
LPE 18:1	479.3012	9.89 (H)	0.00088297	<1.0
<b>LPE 18:2</b>	<b>477.2855</b>	<b>9.98 (H)</b>	<b>0.043876</b>	<b>&lt;1.0</b>
<b>LPE 20:4</b>	<b>501.2855</b>	<b>9.71 (H)</b>	<b>0.00085391</b>	<b>1.2297</b>
<b>LPE 22:4</b>	<b>529.3168</b>	<b>9.37 (H)</b>	<b>0.00000047936</b>	<b>3.3425</b>
<b>PC 21:4</b>	<b>571.3274</b>	<b>7.73 (H)</b>	<b>0.0000061078</b>	<b>2.8498</b>
PC 33:1	745.5622	9.06	0.0000024173	1.1984
<b>PC 34:1</b>	<b>759.5778</b>	<b>9.49</b>	<b>0.000000094697</b>	<b>1.0634</b>
<b>PC 34:2</b>	<b>757.5622</b>	<b>8.96</b>	<b>0.00000043706</b>	<b>&lt;1.0</b>
<b>PC 36:1</b>	<b>787.6091</b>	<b>10.23</b>	<b>0.000066651</b>	<b>&lt;1.0</b>
<b>PC 36:2</b>	<b>785.5935</b>	<b>9.78</b>	<b>0.00000021044</b>	<b>1.3105</b>
<b>PC 36:3</b>	<b>783.5778</b>	<b>8.95</b>	<b>0.000077031</b>	<b>1.0044</b>
<b>PC 36:4</b>	<b>781.5622</b>	<b>8.97</b>	<b>0.000000094697</b>	<b>1.0376</b>
<b>PC 36:5</b>	<b>779.5465</b>	<b>6.84 (H)</b>	<b>0.037041</b>	<b>&lt;1.0</b>

PC 38:3	811.6091	10.06	0.0000080062	1.1074
PC 38:4	809.5935	9.44	0.00022188	<1.0
PC 38:5	807.5778	8.98	0.000016461	1.1869
PC 38:6	805.5622	8.62	0.00000021044	1.4147
PC 38:7	803.5465	6.76 (H)	0.04374	<1.0
PC 40:4	837.6248	10.33	0.004057	<1.0
PC 40:5	835.6091	9.93	0.0000032907	1.3286
PC 40:8	829.5622	6.74 (H)	0.037529	<1.0
PC P-36:4	765.5672	9.39	0.000054189	1.0278
PC P-38:4	793.5985	9.65	0.012435	1.0888
PC P-38:7	787.5516	6.70 (H)	0.04374	<1.0
PE 34:1	717.5309	9.45	0.00000004863	2.8384
PE 34:2	715.5152	9.11	0.00000004863	2.2595
PE 35:2	729.5309	7.24 (H)	0.010817	1.3899
PE 36:1	745.5622	10.16	0.000000072946	1.6152
PE 36:2	743.5465	7.23 (H)	0.00092477	<1.0
PE 36:4	739.5152	7.12 (H)	0.00017714	1.0423
PE 38:4	767.5465	9.92	0.00000059975	<1.0
PE 38:5	765.5309	7.07 (H)	0.033085	1.942
PE 40:4	795.5778	10.42	0.0060529	<1.0
PE O-18:2	477.2855	9.52 (H)	0.025049	<1.0
PE O-38:6	749.5359	9.71	0.0035824	<1.0
PE P-34:4	695.4890	7.08 (H)	0.00015334	1.0254
PE P-36:1	729.5672	10.7	>0.05	1.1297
PE P-36:4	723.5203	7.00 (H)	0.00041293	<1.0
PE P-38:5	749.5359	9.71	0.00049051	1.0787
PE P-38:6	747.5203	9.49	0.00030555	1.0599
PE P-38:7	745.5046	9.54	0.000045489	<1.0
PE P-40:5	777.5672	10.41	0.019295	<1.0
PI 36:2	862.5571	8.19	0.000045489	1.2293
PI 38:4	886.5571	8.04	0.018924	0.008516
PS 36:1	789.5520	8.6	0.0042238	1.0546
PS 36:2	787.5363	8.31	0.0095296	0.0035736

SM 34:0;O2	704.5832	8.62	0.0013125	<1.0
SM 34:1;O2	702.5676	8.28 (H)	0.01054	<1.0
<b>SM 36:1;O2</b>	<b>730.5989</b>	9.19	<b>0.047821</b>	<b>&lt;1.0</b>
SM 36:3;O2	726.5676	7.94 (H)	0.00096509	1.3935
SM 36:4;O2	724.5519	8.17 (H)	0.010047	2.5622
<b>SM 38:1;O2</b>	<b>758.6302</b>	<b>10.00</b>	<b>0.000000094697</b>	<b>1.1772</b>
<b>SM 39:1;O2</b>	<b>772.6458</b>	<b>10.35</b>	<b>0.000013937</b>	<b>1.1867</b>
<b>SM 39:4;O2</b>	<b>766.5989</b>	<b>8.07 (H)</b>	<b>0.009437</b>	<b>2.6194</b>
<b>SM 40:1;O2</b>	<b>786.6615</b>	<b>10.66</b>	<b>0.0035824</b>	<b>&lt;1.0</b>
<b>SM 40:4;O2</b>	<b>780.6145</b>	<b>9.99</b>	<b>0.00000043706</b>	<b>1.2831</b>
<b>SM 41:2;O2</b>	<b>798.6615</b>	<b>10.41</b>	<b>0.00042726</b>	<b>1.0297</b>
SM 41:4;O2	794.6302	7.99 (H)	0.0000061078	1.9875
<b>SM 42:2;O2</b>	<b>810.6615</b>	<b>10.72</b>	<b>0.00049051</b>	<b>&lt;1.0</b>
SM 42:4;O2	808.6458	7.98 (H)	>0.05	1.0229
SM 44:5;O2	834.6615	7.94 (H)	0.037041	1.8495
SPB 17:0;O3	303.2773	3.76 (H)	0.012998	1.9689
<b>TG 44:1</b>	<b>748.6581</b>	<b>5.42</b>	<b>0.0013125</b>	<b>1.673</b>
<b>TG 56:6</b>	<b>906.7676</b>	<b>13.84</b>	<b>0.0017392</b>	<b>1.7051</b>
<b>TG 56:7</b>	<b>904.7519</b>	<b>13.634</b>	<b>0.00030555</b>	<b>2.1605</b>

Compounds with a higher level in hypothermic preservation methods are highlighted in bold. (H) indicates that the compound was identified with the use of the HILIC separation method; otherwise compound was identified with the use of the RP separation method

**Table S4.** The list of compounds that changed between time points throughout kidney perfusion.

Name	Molecular weight	RT [min]	FDR adjusted p-value
<b>HMP</b>			
LPE P-16:0	437.2906	9.44 (H)	0.04206
LPC 18:3	517.3168	8.66 (H)	0.02929
PC 36:5	779.5465	6.84 (H)	0.04206
PC 36:2	785.5935	6.82 (H)	0.04206
PE P-38:6	747.5203	6.99 (H)	0.04206
PC 34:1	759.5778	6.84 (H)	0.02929
PE 34:1	717.5309	9.45	0.04206

PE P-38:7	745.5046	9.54	0.04206
PC 38:7	803.5465	8.97	0.04206
PC 38:6	805.5622	8.62	0.02929
SM 43:4;O2	822.6615	10.96	0.04206
PE 36:2	743.5465	9.73	0.04206
PE 36:1	745.5622	10.16	0.04206
SM 40:1;O2	786.6615	10.51	0.02929
PI 36:2	862.5571	7.98	0.04206
SM 42:1;O2	814.6928	11.09	0.04206
<b>NEVKP</b>			
CAR 12:0	343.2723	8.19 (H)	0.04206
CAR 14:1	369.2879	8.00 (H)	0.04206
TG 56:7	904.7519	13.63	0.04206

(H) indicates that the compound was identified with the use of the HILIC separation method; otherwise compound was identified with the use of the RP separation method

**Table S5** The list of compounds that differentiate reperfusion and POD3 time points for SCS and NEVKP groups.

Name	Molecular weight	RT [min]	FDR adjusted p-value
<b>SCS</b>			
<b>PC 32:0</b>	<b>733.5622</b>	9.09	<b>0.02524</b>
<b>PC 32:1</b>	<b>731.5465</b>	8.68	<b>0.0136</b>
PC 35:6	763.5152	7.13 (H)	0.01885
PC 38:5	807.5778	6.78 (H)	0.01396
<b>PC P-38:4</b>	<b>793.5985</b>	9.65	<b>0.03351</b>
PE 36:3	741.5309	7.13 (H)	0.01885
PE 36:4	739.5152	7.12 (H)	0.02524
<b>PE P-38:4</b>	<b>751.5516</b>	10.16	<b>0.00537</b>
<b>PE P-40:4</b>	<b>779.5829</b>	6.93 (H)	<b>0.01885</b>
<b>PE P-40:5</b>	<b>777.5672</b>	10.41	<b>0.03351</b>
PS 36:2	785.5935	8.31	0.02524
SM 36:4;O2	724.5519	8.17 (H)	0.04409
SM 38:1;O2	758.6302	10.00	0.03351
SM 38:5;O2	750.5676	8.04 (H)	0.04409
SM 39:4;O2	766.5989	8.07 (H)	0.04409

SM 40:1;O2	786.6615	10.66	0.01885
SM 41:4;O2	794.6302	7.99 (H)	0.01396
SM 42:1;O2	814.6928	11.09	0.00745
SM 42:5;O2	806.6302	7.98 (H)	0.02524
SM 44:4;O2	836.6771	7.93 (H)	0.01395
SM 44:5;O2	834.6615	7.94 (H)	0.01396
<b>NEVKP</b>			
<b>Cer 42:1;O2</b>	<b>649.6373</b>	11.91	<b>0.04409</b>
<b>PC 32:1</b>	<b>731.5465</b>	8.681	<b>0.02524</b>
<b>PC 36:1</b>	<b>787.6091</b>	10.23	<b>0.03351</b>

Compounds with a higher level on POD3 are highlighted in bold. (H) indicates that the compound was identified with the use of the HILIC separation method; otherwise compound was identified with the use of the RP separation method

**Table S6** The list of statistically significant compounds in comparisons donor versus reperfusion for NEVKP, SCS, and HMP groups and donor versus POD3 for NEVKP and SCS groups.

Name	Molecular weight	RT [min]	SCS		NEVKP		HEVKP
			<u>donor</u> reperf	<u>donor</u> POD3	<u>donor</u> reperf	<u>donor</u> POD3	<u>donor</u> reperf
CAR 12:0	343.2723	8.19 (H)	-1.0269	-2.3863*	-0.75457	-1.9376	-0.72092*
CAR 14:0	371.3036	8.02 (H)	-0.99743	-1.4458*	-0.14411	-1.4335	-0.53976
CAR 14:1	369.2879	8.00 (H)	-1.8512	-3.2537*	-1.4426	-2.6111*	-1.579*
CAR 14:2	367.2723	8.07 (H)	-1.9052	-3.8205*	-1.5529	-2.6519*	-1.843
Cer 34:1;O2	537.5121	9.21	-0.40997	-3.032	-0.10856	-1.0166*	-0.51166
Cer 38:1;O2	593.5747	10.86	-0.99705	-2.5056*	0.15087	-0.8167	-0.1308
DG 38:4	644.5379	11.2	0.80067	0.85205	1.203*	0.82122	0.66206
LPC 18:0	523.3638	4.65	1.4609	-0.52977	2.0926*	1.2109	1.1624
LPE 18:1	479.3012	9.89 (H)	-0.63591	-1.9022	-0.013194	-0.70323*	-0.2593
LPE 18:2	477.2855	9.98 (H)	-1.5412	-2.2378*	-0.15548	-1.7369*	-0.37405
LPE 20:4	501.2855	3.76	-0.27498	-3.10097*	1.1081	-1.187	-0.55835
LPE 22:4	529.3168	9.37 (H)	1.5896	0.69982	2.8471*	1.0904	1.3292
PC 21:4	529.2805	7.73 (H)	-1.2417	-2.895*	2.2114	-1.4275	-0.58296

PC 33:1	745.5622	9.06	-0.40149	-0.84172*	-0.30252	-0.81399*	-0.16674
PC 34:1	759.5778	6.84 (H)	0.01432	0.58265*	-0.15719	0.27859	-0.1077
PC 34:1	759.5778	9.49	0.45528	0.46389	0.38095	0.69702*	0.16379
PC 34:2	759.5778	6.95 (H)	0.2117	1.2472*	0.59748*	0.35358	0.20555
PC 36:1	787.6091	10.23	0.84198*	0.69536	0.84269*	0.80845*	0.41556
PC 36:2	785.5935	9.78	0.4727*	0.16546	0.68802*	-0.059386	-0.17535
PC 36:3	783.5778	8.95	0.34175	0.38267	0.63001*	0.26322	0.012774
PC 36:4	781.5622	6.80 (H)	0.37439	1.1162*	0.10911	0.88437*	0.017423
PC 36:5	779.5465	6.84 (H)	-0.072387	0.972*	-0.056695	0.50315	-0.14297
PC 38:4	809.5935	9.44	0.84313*	0.68637	0.81954*	0.8057*	0.40188
PC 38:5	807.5778	8.98	0.61825	0.91831*	0.21079	0.59955	-0.12913
PC 38:6	805.5622	8.62	0.25825	1.2624*	0.79813	0.96236*	-0.33124
PC 38:7	803.5465	6.76 (H)	0.077109	0.82746*	0.23124	0.64013*	-0.16289
PC 40:5	835.6091	6.74 (H)	0.73801	0.73708	0.61389	0.86268*	0.32582
PC 40:5	835.6091	9.93	0.96415*	0.67956	1.0829*	0.75059	0.25282
PC 40:6	833.5935	6.72 (H)	0.27463	0.89181*	0.13454	0.47191	0.29794
PC 42:9	855.5778	6.68 (H)	0.90879	0.92674	0.80355	0.9963*	0.5287
PC O-34:0	747.6142	10.48	-1.5735	-2.7817*	-1.5612	-3.3872*	-1.1642
PC O-34:2	743.5829	9.47	-0.46445	-1.2475*	-0.16527	-1.269	-0.50044
PC O-38:4	795.6142	10.25	-0.31996	-2.6007*	-0.38926	-2.9146*	-0.50296
PC P-38:7	787.5516	6.70 (H)	0.18991	0.65357*	0.15964	0.78866	-0.44508
PC P-40:7	815.5829	6.72 (H)	0.37719	2.0072*	0.22381	1.3804*	0.43299
PE 34:1	717.5309	9.45	-0.96572	-0.20002	-0.66938*	-0.67849	0.046835
PE 36:1	745.5622	10.16	-0.51095	-1.2379*	-0.3879	-1.1418*	-0.34438
PE 36:2	743.5465	9.73	-0.36957	-0.4227	-0.31647	-0.53943*	-0.20688
PE 38:5	765.5309	7.07 (H)	0.059547	0.90129*	0.15016	0.42284	0.098406
PE 38:6	763.5152	7.09 (H)	-0.17372	1.4787*	0.12979	0.44272	0.10214
PE O-18:2	477.2855	9.52 (H)	-1.0905	-1.932	-0.56747	-1.1151*	-0.83822
PE P-36:1	729.5672	10.7	-0.7646	-1.9321*	-0.76332	-1.9386*	-0.59635
PE P-36:4	723.5203	9.37	0.26296	0.35409	0.51307*	0.52871	-0.044015
PE P-38:5	749.5359	9.71	0.82991*	0.58902	-0.056433	0.6526	-0.20911
PI 38:4	886.5571	7.03 (H)	0.64879	0.80067	0.01842	0.17178	0.59439*
PS 36:1	789.552	8.6	0.060431	1.3737*	-0.64782	0.6261	-0.19287

## Supplementary Material

PS 38:4	811.5363	8.12	0.011394	1.3719*	-0.71544	0.37107	-0.082197
SM 35:1;O2	716.5832	8.74	-0.11284	1.1341*	0.51365	0.46723	0.076761
SM 36:1;O2	730.5989	9.19	0.40029	1.037*	0.3062	0.52821	0.36417
SM 38:1;O2	758.6302	10.00	0.026363	1.0932*	0.39029	0.62661	-0.17324
SM 39:1;O2	772.6458	10.35	0.02087	1.8054*	0.66539	1.074	-0.11889
SM 40:1;O2	786.6615	10.66	0.020008	0.86254*	-0.0097978	0.21608	0.13182
SM 40:4;O2	780.6145	9.99	0.069289	1.3723*	0.42525	0.56387*	-0.14442
SM 42:1;O2	814.6928	11.09	-0.69296	0.36006	0.034172	-0.1674	-0.36465*
SM 42:4;O2	808.6458	7.98 (H)	0.49007	1.3599*	0.096101	0.7516	-0.57964
SM 42:5;O2	806.6302	7.98 (H)	-0.27168	1.2378	-1.1471*	-0.30861	-0.21303
SM 43:4;O2	822.6615	7.96 (H)	0.6791	1.1387*	0.31265	0.58048	0.16728
SM 44:4;O2	836.6771	7.93 (H)	-0.79871	1.2099*	-0.18159	-0.59287	0.12269
SM 44:5;O2	834.6615	7.94 (H)	-0.54956	0.90684*	-0.18159	-0.11173	-0.04964

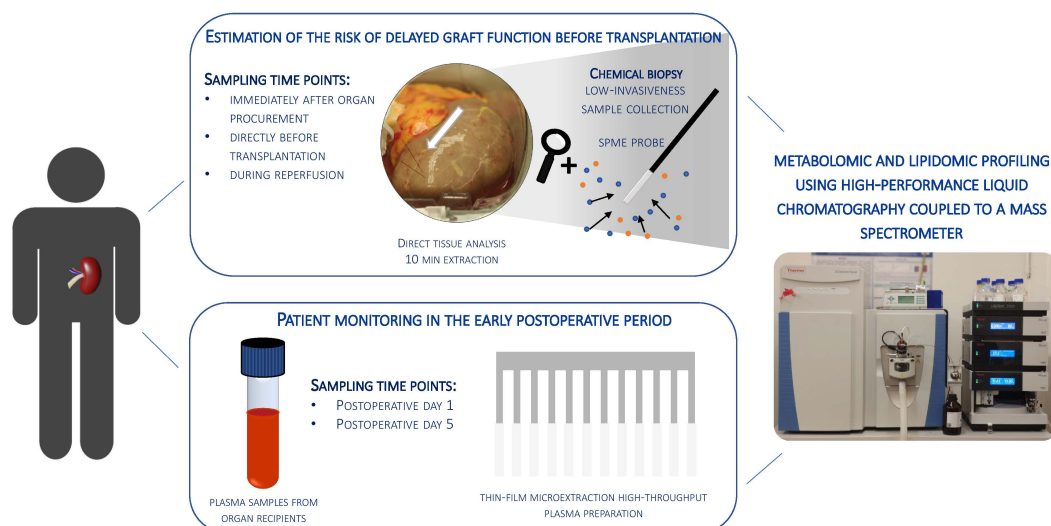
Values are reported as a log<sub>2</sub>(FC); FC- fold change. FCs are calculated as the ratios between two group means. (H) indicates that the compound was identified with the use of the HILIC separation method; otherwise compound was identified with the use of the RP separation method. \* is p value < 0.05

### 7.3. Profilowanie metabolomiczne i lipidomiczne w predykcji ryzyka opóźnionej funkcji przeszczepu z wykorzystaniem mikroekstrakcji do fazy stałej – P.6.

**Opis dotyczy pracy:** N. Warmuzińska, K. Łuczykowski, I. Stryjak, E. Wojtal, A. Woderska-Jasińska, M. Masztalerz, Z. Włodarczyk, B. Bojko: ***Metabolomic and lipidomic profiling for pre-transplant assessment of delayed graft function risk using chemical biopsy with microextraction probes***. Int. J. Mol. Sci., 2024, 25, 13502;

Opóźniona funkcja przeszczepu jest objawem ostrego uszkodzenia nerki i jednym z najczęstszych wczesnych powikłań po przeszczepieniu. DGF wiąże się z gorszymi wynikami przeszczepu, obniżonym przeżyciem długoterminowym, przedłużonym pobytem w szpitalu oraz koniecznością dodatkowego leczenia dializami. Do jego rozwoju przyczyniają się zarówno czynniki związane z dawcą, jak i czynniki przednerkowe, nerkowe lub zanerkowe u biorcy. Przewiduje się, że częstość występowania DGF będzie rosła w związku ze zwiększonym wykorzystaniem nerek od dawców ECD oraz DCD. Trend ten pogłębia zmieniająca się demografia starzejącego się społeczeństwa, skutkująca rosnącym odsetkiem starszych dawców i biorców, co może dodatkowo zwiększać ryzyko pogorszenia jakości przeszczepów i wyników leczenia. W związku z tym istnieje pilna potrzeba opracowania nowych strategii oceny jakości narządów, umożliwiających wczesną predykcję wystąpienia DGF i optymalizację postępowania u pacjentów wysokiego ryzyka.

W niniejszym badaniu przeprowadzono analizy metabolomiczne i lipidomiczne w wielu punktach czasowych, obejmujących zarówno tkankę nerkową od dawców, jak i osocze biorców, w celu wykrycia zmian związanych z DGF. Połączenie analizy tkanki nerki i osocza biorców miało na celu identyfikację związków o potencjale predykcyjnym w ocenie ryzyka DGF oraz ocenę wartości translacyjnej SPME jako narzędzia do oceny jakości przeszczepu i wczesnego wykrywania powikłań. Schemat badania został przedstawiony na Rycinie 3.



**Rycina 3.** Schemat badania - badanie obejmowało próbki pobrane z nerek pozyskanych od dawców zmarłych oraz próbki osocza od biorców narządów.

Po analizie z zastosowaniem wysokosprawnej chromatografii cieczowej sprzężonej ze spektrometrią mas, wykorzystano algorytm random forest do identyfikacji związków o potencjale predykcyjnym w ocenie ryzyka DGF przed przeszczepieniem. Dodatkowo, porównanie profili metabolomicznych i lipidomicznych osocza biorców w pierwszych dniach po operacji pozwoliło na wyodrębnienie metabolitów różnicujących pacjentów z DGF i bez DGF. Zidentyfikowane związki obejmowały głównie aminokwasy i ich pochodne, nukleotydy, kwasy organiczne, peptydy oraz lipidy, w szczególności fosfolipidy i trójglicerydy. Pole pod krzywą ROC (AUC, ang. Area Under the Receiver Operating Characteristic Curve) dla wszystkich opracowanych modeli przekroczyło 0,85, co wskazuje na ich wysoką wartość predykcyjną.

Otrzymane wyniki wskazują na duży potencjał translacyjny metody, który warto podkreślić. Bezpośrednia analiza tkanki dostarcza specyficznych informacji o organie, co ma szczególne znaczenie przy ocenie jakości nerek przeznaczonych do przeszczepienia. Nerki od tego samego dawcy mogą różnić się swoimi właściwościami i wykazywać różne ryzyko rozwoju DGF lub innych powikłań u biorcy. Chociaż translacyjny potencjał biopsji chemicznej był wcześniej podkreślany, to według naszej wiedzy, niniejsze badanie jest pierwszym zastosowaniem biopsji chemicznej do oceny jakości przeszczepu nerkowego w warunkach

klinicznych. Niewątpliwie wyniki uzyskane w tym badaniu są obiecujące i sugerują możliwość włączenia w przyszłości biopsji chemicznej do rutynowej procedury diagnostycznej. Z praktycznego punktu widzenia, pobieranie próbek przeprowadzane bezpośrednio po pobraniu organu i po jego przechowaniu, ale przed przeszczepieniem, może mieć największe zastosowanie. Takie podejście pozwoliłoby na ocenę ryzyka związanego z dawcą i, w przypadku wątpliwości lub wydłużonego czasu zimnego niedokrwienia, na ponowną ocenę ryzyka powikłań. Ponadto, czas ekstrakcji wynoszący 10 minut, użyty w tym badaniu, nie wydłużył czasu niedokrwienia organu oraz nie zaburzał procedury przeszczepienia, ponieważ mały rozmiar sond umożliwił jednoczesne przygotowanie przeszczepu do zabiegu chirurgicznego.

Podsumowując, badanie to podkreśla znaczący potencjał translacyjny biopsji chemicznej oraz analizy metabolitów osoczowych w ocenie ryzyka i nieinwazyjnym monitorowaniu DGF. Zidentyfikowane metabolity stanowią podstawę do opracowania kompleksowej metody oceny i monitorowania DGF, z możliwością jej integracji z rutynową praktyką kliniczną.

Article

# Metabolomic and Lipidomic Profiling for Pre-Transplant Assessment of Delayed Graft Function Risk Using Chemical Biopsy with Microextraction Probes

Natalia Warmużńska <sup>1</sup>, Kamil Łuczykowski <sup>1</sup>, Iga Stryjak <sup>1</sup>, Emilia Wojtal <sup>2</sup>, Aleksandra Woderska-Jasińska <sup>2</sup>, Marek Masztalerz <sup>2</sup>, Zbigniew Włodarczyk <sup>2</sup> and Barbara Bojko <sup>1,\*</sup>

<sup>1</sup> Department of Pharmacodynamics and Molecular Pharmacology, Faculty of Pharmacy, Collegium Medicum in Bydgoszcz, Nicolaus Copernicus University in Toruń, 85-089 Bydgoszcz, Poland

<sup>2</sup> Department of Transplantology and General Surgery, Faculty of Medicine, Collegium Medicum in Bydgoszcz, Antoni Jurasz University Hospital No. 1 in Bydgoszcz, Nicolaus Copernicus University in Toruń, 85-094 Bydgoszcz, Poland

\* Correspondence: bbojko@cm.umk.pl; Tel.: +48-52-585-35-64



**Citation:** Warmużńska, N.; Łuczykowski, K.; Stryjak, I.; Wojtal, E.; Woderska-Jasińska, A.; Masztalerz, M.; Włodarczyk, Z.; Bojko, B. Metabolomic and Lipidomic Profiling for Pre-Transplant Assessment of Delayed Graft Function Risk Using Chemical Biopsy with Microextraction Probes. *Int. J. Mol. Sci.* **2024**, *25*, 13502. <https://doi.org/10.3390/ijms252413502>

Academic Editor: Chiara Riganti

Received: 27 November 2024

Revised: 13 December 2024

Accepted: 15 December 2024

Published: 17 December 2024



**Copyright:** © 2024 by the authors. Licensee MDPI, Basel, Switzerland. This article is an open access article distributed under the terms and conditions of the Creative Commons Attribution (CC BY) license (<https://creativecommons.org/licenses/by/4.0/>).

**Abstract:** Organ shortage remains a significant challenge in transplantology, prompting efforts to maximize the use of available organs and expand the donor pool, including through extended criteria donors (ECDs). However, ECD kidney recipients often face poorer outcomes, including a higher incidence of delayed graft function (DGF), which is linked to worse graft performance, reduced long-term survival, and an increased need for interventions like dialysis. This underscores the urgent need for strategies to improve early DGF risk assessment and optimize post-transplant management for high-risk patients. This study conducted multi-time point metabolomic and lipidomic analyses of donor kidney tissue and recipient plasma to identify compounds predicting DGF risk and assess the translational potential of solid-phase microextraction (SPME) for graft evaluation and early complication detection. The SPME-based chemical biopsy enabled a direct kidney analysis, while thin-film microextraction facilitated high-throughput plasma preparation. Following high-performance liquid chromatography coupled with a mass spectrometry analysis, the random forest algorithm was applied to identify compounds with predictive potential for assessing DGF risk before transplantation. Additionally, a comparison of metabolomic and lipidomic profiles of recipient plasma during the early post-operative days identified metabolites that distinguish between DGF and non-DGF patients. The selected compounds primarily included amino acids and their derivatives, nucleotides, organic acids, peptides, and lipids, particularly phospholipids and triacylglycerols. In conclusion, this study highlights the significant translational potential of chemical biopsies and plasma metabolite analyses for risk assessments and the non-invasive monitoring of DGF. The identified metabolites provide a foundation for developing a comprehensive DGF assessment and monitoring method, with potential integration into routine clinical practice.

**Keywords:** solid-phase microextraction; LC-MS; kidney transplantation; metabolomics; lipidomics; graft quality assessment; DGF

## 1. Introduction

Kidney transplantation is a life-saving procedure for patients with end-stage renal disease, offering improved survival rates and quality of life compared to dialysis. However, the persistent shortage of available organs has resulted in a significant increase in the number of patients on kidney transplant waiting lists [1,2]. This growing imbalance between supply and demand has prompted clinicians to consider kidneys from extended criteria donors (ECDs) and donation after circulatory death (DCD) as alternatives. Unfortunately, recipients of ECD kidneys often experience poorer outcomes than those receiving organs from standard criteria donors, with a higher incidence of delayed graft function

(DGF) and primary nonfunction [3]. DGF is a form of acute renal failure and one of the most frequent early complications in kidney transplant recipients. It is characterized by post-transplantation oliguria, increased allograft immunogenicity, and a higher risk of acute rejection episodes. DGF is associated with poor graft outcomes, decreased long-term survival, prolonged hospitalization, and the need for additional treatments such as dialysis. Both donor-related factors and prerenal, renal, or postrenal transplant factors in the recipient can contribute to the development of this condition [4,5]. The incidence of DGF is anticipated to rise in the coming years due to the increasing use of kidneys from ECDs and DCDs [4]. This trend is further influenced by the changing demographics of aging in human society, leading to a growing proportion of older donors and recipients, which may compound the risks associated with graft quality and post-transplant outcomes. Consequently, there is an urgent need for new strategies to enable early DGF risk assessment and optimize the management of high-risk recipients after transplantation [2,4]. Conventional methods for evaluating renal allografts, including donor medical history, visual inspection, and laboratory tests, often lack the specificity needed to predict the risk of DGF and make accurate diagnoses. While renal biopsy can provide valuable insights into pre-existing donor conditions and vascular changes, as well as help differentiate acute tubular necrosis (ATN)—the main cause of DGF in kidney transplant recipients—from other graft dysfunctions, it remains an invasive procedure [2,4].

In this study, metabolomic and lipidomic analyses were performed at multiple time points on donor kidney tissue and plasma samples from organ recipients to detect changes related to DGF. Metabolomics and lipidomics provide valuable insights into the organism's immediate biochemical responses to various changes, helping to identify compounds associated with conditions such as ischemia, oxidative stress, inflammation, and other metabolic alterations that may contribute to graft dysfunction and complications in transplant recipients [6,7]. Solid-phase microextraction (SPME) chemical biopsy was employed for direct kidney analysis. The probe's small diameter (~200 µm) ensures minimal invasiveness and allows for multiple samplings from the same organ without causing tissue damage. Additionally, thin-film microextraction (TFME) was used as a high-throughput plasma sample preparation method. SPME is a versatile and highly sensitive sample preparation technique that integrates sampling, extraction, and analyte concentration into a single step [7,8]. The combination of kidney graft and recipient plasma analysis aimed to identify compounds with predictive potential for assessing DGF risk and to evaluate the translational applicability of SPME for graft quality assessments and the early detection of complications.

## 2. Results

### 2.1. Demographic Characteristics and Clinical Data

The donors' and recipients' demographic characteristics and clinical parameters are presented in Tables 1 and 2, respectively. Donors were grouped based on the donor type (extended criteria donor (ECD) or standard criteria donor (SCD)), while recipients were classified based on the occurrence of DGF. The last available data were collected for donors prior to organ procurement and for recipients from the final tests conducted before hospital discharge following transplantation.

A statistically significant age difference was observed among donors, as age is one of the primary criteria for categorizing a donor as an ECD. Additionally, SCD donors had significantly lower platelet (PLT) counts compared to ECD donors.

Among recipients, significantly higher creatinine and blood urea nitrogen (BUN) levels and significantly lower glomerular filtration rate (GFR) values were observed in those who developed DGF, indicating that these patients still exhibited poorer kidney function just before their discharge from the hospital.

**Table 1.** Deceased donor characteristics, stratified by donor type.

Characteristic	Total (n = 24)	SCD (n = 19)	ECD (n = 5)	p-Value
Age, year	44.5 [41.5–47.5]	44 [41–46]	60 [60–66]	0.02980
Sex				
Male	17 (71%)	12 (63%)	5 (100%)	>0.05
Hypertension	3 (13%)	3 (16%)	0	>0.05
Cause of death				
Trauma	9 (38%)	7 (37%)	2 (40%)	>0.05
Vascular	12 (50%)	9 (47%)	3 (60%)	>0.05
Others	3 (13%)	3 (16%)	0	
Creatinine, mg/dL	1.27 [0.98–2.13]	1.40 [1.05–2.39]	1.20 [0.60–1.24]	>0.05
Urea, mg/dL	45.64 [37.20–62.00]	44.00 [34.10–51.80]	62.00 [48.00–100.00]	>0.05
Procalcitonin, ng/mL	1.37 [0.57–8.18]	1.11 [0.57–7.96]	2.05 [1.37–13.35]	>0.05
CRP, mg/L	246.60 (135.13)	226.29 (126.44)	323.81 (153.78)	>0.05
WBC, 10 <sup>3</sup> /μL	12.98 [11.05–17.40]	13.00 [11.78–16.70]	10.40 [10.20–18.70]	>0.05
HGB, g/dL	11.11 (2.64)	11.54 (2.64)	9.46 (2.11)	>0.05
PLT, 10 <sup>3</sup> /μL	142.88 (57.46)	130.37 (46.54)	190.40 (75.31)	0.03436
AST, IU/L	52.00 [29.00–95.00]	37.00 [26.00–98.00]	74.50 [52.00–88.00]	>0.05
ALT, IU/L	50.00 [23.00–90.00]	46.00 [23.00–90.00]	55.50 [45.5–81.50]	>0.05
K, mmol/L	4.40 [3.70–4.68]	4.40 [3.80–4.66]	4.07 [3.00–4.90]	>0.05
Na, mmol/L	155.91 (11.04)	157.26 (11.23)	150.78 (9.59)	>0.05
Cl, mmol/L	117.17 (10.91)	119.60 (10.35)	109.38 (9.72)	>0.05

SCD: standard criteria donor, ECD: extended criteria donor.

**Table 2.** Kidney transplant recipient characteristics, stratified by DGF occurrence.

Characteristic	Total (n = 32)	Non DGF (n = 22)	DGF (n = 10)	p-Value
Age, year	57.5 [43.5–64]	57.50 [48–64]	55 [41–63]	>0.05
Sex				
Male	25 (78%)	17 (77%)	8 (80%)	>0.05
Hypertension	27 (84%)	18 (82%)	9 (90%)	>0.05
Donor criteria				>0.05
SCD	26 (81%)	20 (91%)	6 (60%)	>0.05
ECD	6 (19%)	2 (9%)	4 (40%)	>0.05
Preservation method				
HMP	11 (34%)	8 (36%)	3 (30%)	>0.05
SCS	21 (66%)	14 (64%)	7 (70%)	>0.05
Recipients requiring dialysis	13 (40%)	5 (23%)	8 (80%)	0.00506
Bacteria in preservative fluid	12 (37.5%)	9 (41%)	3 (30%)	>0.05
Ischemia time	17 h 26 min (7 h 16 min)	16 h 03 min (7 h 06 min)	20 h 47 min (6 h 54 min)	>0.05
Creatinine, mg/dL	1.59 (0.58)	1.34 (0.41)	2.14 (0.54)	0.00006
GFR, mL/min/1.73 m <sup>2</sup>	50.49 (15.96)	57.77 (13.13)	34.46 (7.72)	0.00001
BUN, mg/dL	31.80 [21.80–38.40]	24.70 [21.40–33.80]	45.00 [35.60–56.50]	0.00098
CRP, mg/L	3.62 [2.48–6.06]	4.98 [3.02–6.23]	2.43 [0.68–3.48]	>0.05
WBC, 10 <sup>3</sup> /μL	8.32 (3.05)	8.62 (3.38)	7.66 (2.15)	>0.05
HGB, g/dL	10.37 (0.91)	10.27 (0.83)	10.60 (1.07)	>0.05
PLT, 10 <sup>3</sup> /μL	229.97 (77.25)	228.41 (76.74)	233.40 (82.41)	>0.05
AST, IU/L	14.00 [11.00–17.00]	14.50 [11.00–19.50]	13.00 [10.50–15.00]	>0.05
ALT, IU/L	15.50 [13.00–29.50]	16.50 [13.00–32.00]	14.50 [11.00–27.00]	>0.05
K, mmol/L	4.42 (0.46)	4.41 (0.52)	4.44 (0.31)	>0.05
Na, mmol/L	141.87 (2.95)	141.78 (3.21)	142.06 (2.41)	>0.05
Cl, mmol/L	110.10 [107.00–112.10]	110.60 [107.30–112.20]	109.90 [107.00–111.00]	>0.05
Ca, mmol/L	2.23 (0.22)	2.26 (0.21)	2.18 (0.25)	>0.05

SCD: standard criteria donor, ECD: extended criteria donor, HMP: hypothermic machine perfusion, SCS: static cold storage.

Furthermore, an additional analysis was conducted to determine whether differences existed in the laboratory test results of donors whose kidneys were associated with DGF in recipients (Table S1); however, no statistically significant differences were observed.

## 2.2. Metabolomic and Lipidomic Analyses

Metabolomic and lipidomic analyses were conducted on the donor's kidney tissue and plasma samples from organ recipients to identify compounds with predictive potential in assessing DGF risk and to evaluate the translational applicability of SPME for graft quality assessments and the early detection of complications. A PCA was employed to confirm the quality of the instrumental analysis for all combinations of chromatographic separation and ionization mode. As shown in Supplementary Figure S1, the pooled quality control (QC) samples formed a tight cluster, confirming the high quality of the analytical performance. For clarity, the results section is divided into two parts: the first part focuses on the assessment of graft quality using a chemical biopsy, while the second part presents the analysis of plasma samples collected from recipients on days 1 and 5 post-operation.

## 2.3. Assessment of Graft Quality Using Chemical Biopsy

To identify compounds with potential predictive value for the early detection of DGF risk, kidney cortex samples were collected using a minimally invasive chemical biopsy at three time points: after organ procurement, prior to transplantation, and during reperfusion. Due to the imbalanced distribution of DGF complication occurrences in the study group, a light oversampling process was applied to the minority cases (DGF) to improve the stability and quality of the modelling results. This process was carried out separately for each of the three time points to maintain the temporal characteristics of the sample and minimize the risk of overfitting the model to the artificially augmented data. The Random Over-Sampling Examples (ROSE) algorithm was used, allowing for the generation of additional observations in the minority group by creating synthetic examples based on the classification variable. For each time point, the sample size of the DGF group was increased to 15, achieving a DGF to non-DGF ratio of 15:22.

An initial selection of metabolites was conducted using the random forest algorithm with 500 decision trees, separately for each time point. Compounds with the highest mean decrease accuracy (MDA) and mean decrease Gini (MDG) values were identified. A list of the 10 metabolites with the highest MDA and MDG values for each analytical block is presented in Table S2. Subsequently, compounds with both high MDA and MDG values were chosen from the preselected set for further model development and included in Table 3. Among the selected compounds were mainly amino acids and their derivatives, organic acids, and lipids, particularly phospholipids and triacylglycerols (TGs).

**Table 3.** Compounds selected for further model development based on MDA and MDG values.

Name	MW	RT	Mean Decrease Accuracy	Mean Decrease Gini	p-Value	AUC	Fold Change
<b>Metabolomics</b>							
Time point 1							
Pyroglutamic acid	129.04	1.75	8.752	1.551	0.002	0.803	4.478
4-oxo-2-nonenal	154.10	10.09	6.484	0.917	0.053	0.692	0.471
N-Butyryl-L-homoserine lactone	171.09	1.74	5.937	0.859	0.013	0.746	0.419
Ornithine	132.09	1.88	5.731	0.889	0.003	0.787	2.735
Glutaric acid	132.04	1.32	4.705	0.474	0.026	0.721	0.375

Table 3. Cont.

Name	MW	RT	Mean Decrease Accuracy	Mean Decrease Gini	p-Value	AUC	Fold Change
<b>Metabolomics</b>							
Time point 1							
Tetramethylpyrazine	136.10	8.95	3.819	0.601	0.039	0.704	1.613
Heptylic acid	130.10	1.69	3.305	0.506	>0.05	0.651	0.983
Time point 2							
Phosphoethanolamine	141.01	11.70	5.746	0.613	0.029	0.715	0.385
Glutamic acid	147.05	1.53	5.577	0.683	0.011	0.748	0.219
Glyceraldehyde 3-phosphate	170.00	2.11	5.243	0.913	0.005	0.779	2.387
Histidine	155.07	1.90	5.065	0.644	>0.05	0.624	1.677
1-Nitronaphthalene-5,6-oxide	189.04	24.76	4.992	0.581	0.019	0.73	1.843
Adenosine	267.10	7.28	4.805	0.643	>0.05	0.645	0.776
Carnitine	161.11	3.35	4.369	0.852	0.006	0.767	0.201
Time point 3							
Phosphoethanolamine	141.01	11.70	9.547	1.966	0.0003	0.852	0.029
3-Indolebutyric acid	203.10	13.52	6.979	1.343	0.0009	0.824	3.763
NA-Val 18:0	383.34	22.19	6.040	0.896	0.026	0.718	1.596
4-Hydroxynonenal	156.12	11.86	5.431	0.606	>0.05	0.552	1.533
Creatine	131.07	1.98	4.971	0.735	0.011	0.748	0.016
Adenosine	267.10	7.28	4.912	0.806	>0.05	0.561	15.12
Arginine	174.11	2.012	4.456	0.636	>0.05	0.679	0.34
<b>Lipidomics HILIC</b>							
Time point 1							
SM 42:1;O2	814.69	7.78	6.180	1.053	0.003	0.79	2.326
PC 38:5	807.58	6.48	5.532	0.638	0.028	0.717	0.091
PC 34:1	759.58	6.53	5.511	0.813	0.001	0.784	0.07
SM 40:2;O2	784.65	7.94	5.046	0.536	>0.05	0.66	0.616
PC 38:6	805.56	6.49	4.820	0.459	>0.05	0.663	4.379
LPC 18:0	523.36	8.84	4.474	0.467	>0.05	0.657	0.621
SM 34:1;O2	702.57	8.16	4.317	0.483	>0.05	0.625	0.954
PE 38:5	765.53	7.42	4.289	0.549	>0.05	0.673	1.471
Time point 2							
PE 38:5	765.53	7.56	7.547	0.981	>0.05	0.578	1.371
PC 34:1	759.58	6.62	6.284	0.636	>0.05	0.681	2.574
PC P-34:2	741.57	6.58	4.900	0.514	0.02	0.727	4.991
PE 38:6	763.52	7.45	4.734	0.673	>0.05	0.654	1.912
SM 40:1;O2	786.66	7.91	4.687	0.567	>0.05	0.678	0.434
PE 36:3	741.53	7.45	4.670	0.495	>0.05	0.596	1.823
PC 38:5	807.58	6.48	4.280	0.468	>0.05	0.668	0.28
LPE 18:0	481.32	10.34	4.040	0.519	>0.05	0.681	0.644
Time point 3							
PE 38:6	763.52	7.45	6.126	0.854	>0.05	0.591	1.313
PE 36:3	741.53	7.45	5.718	0.716	>0.05	0.591	1.231
PC 36:4	781.56	6.52	5.468	0.756	>0.05	0.652	1.029
PE 36:2	743.55	7.56	5.324	0.660	0.024	0.721	2.392
PE 36:4	739.52	7.46	4.985	0.655	>0.05	0.657	0.982
PC 36:3	783.58	6.49	4.715	0.589	>0.05	0.506	0.887
PC 34:2	757.56	6.69	4.289	0.493	>0.05	0.648	0.29

Table 3. Cont.

Name	MW	RT	Mean Decrease Accuracy	Mean Decrease Gini	p-Value	AUC	Fold Change
Lipidomics RP							
Time point 1							
TG 56:0	918.86	14.63	4.684	0.500	0.003	0.79	2.087
TG 48:5	796.66	12.52	4.027	0.456	0.014	0.743	1.401
TG P-52:1	846.80	14.11	3.750	0.295	>0.05	0.502	1.486
Cer 34:0;O2	539.53	10.70	3.701	0.249	>0.05	0.575	0.537
TG 50:1	832.75	13.77	3.282	0.247	>0.05	0.571	0.704
Cer 32:0;O2	511.50	9.99	3.247	0.293	>0.05	0.581	0.653
Time point 2							
TG 56:0	918.86	14.63	5.891	0.650	0.0007	0.833	3.7405
DG 36:4	616.51	10.03	5.395	0.654	>0.05	0.606	1.6009
DG 36:3	618.52	10.46	4.257	0.376	>0.05	0.627	1.201
TG O-52:1	846.80	14.35	4.099	0.274	>0.05	0.603	3.0758
TG 44:3	744.63	12.81	3.955	0.252	>0.05	0.675	1.993
TG 42:0	722.64	12.81	3.807	0.269	0.0268	0.718	2.675
TG 50:0	834.77	13.99	3.676	0.266	>0.05	0.518	2.397
TG 54:2	886.80	14.08	3.258	0.287	>0.05	0.666	3.003
Time point 3							
DG 34:1	594.52	10.73	5.148	0.642	>0.05	0.645	0.5487
TG 56:2	914.83	14.30	4.383	0.378	>0.05	0.645	1.334
TG 54:1	888.81	14.24	4.256	0.404	>0.05	0.524	0.2857
TG 52:0	862.80	14.23	4.221	0.388	>0.05	0.603	0.0913
TG 55:2	900.81	14.13	4.041	0.326	0.042	0.7	0.4624
TG 54:6	878.74	13.94	3.921	0.261	>0.05	0.615	0.7927
TG 50:2	830.74	13.57	3.615	0.236	>0.05	0.533	2.1772
TG 56:3	912.81	14.08	3.608	0.238	>0.05	0.612	0.8343

MW: molecular weight, RT: retention time (min), AUC: area under curve, SM: sphingomyelin, PC: phosphatidylcholine, LPC: lysophosphocholine, PE: phosphatidylethanolamine, LPE: lysophosphatidylethanolamine, TG: triacylglycerol, Cer: ceramide, DG: diglyceride.

Random forest models based on the selected metabolites were evaluated using 10-fold cross-validation to identify the optimal *mtry* value. After determining the optimal *mtry*, the model was retrained with this value, using 10-fold cross-validation, to assess its predictive performance. The model evaluation metrics are presented in Table 4. To visualize the performance of the obtained models, receiver operating characteristic (ROC) curves were generated using the Biomarker Analysis module in MetaboAnalyst 6.0 (Figure 1). The nine predictive models demonstrated a consistent performance across several key metrics. The accuracy ranged from 0.79 to 0.91, indicating a high rate of correct predictions across the models. Cohen's kappa values varied between 0.55 and 0.82, reflecting a strong level of agreement beyond chance. Sensitivity values ranged from 0.73 to 0.93, highlighting the models' ability to reliably detect true positive cases. Specificity values were between 0.77 and 1, indicating a strong performance in correctly classifying true negatives. The precision ranged from 0.73 to 1, and F1-scores varied from 0.73 to 0.88, suggesting a balanced model performance with a good trade-off between precision and recall. Additionally, the area under the ROC curve (AUC) for all models exceeded 0.85, further confirming their strong predictive capabilities. Based on the consistent performance of the models across various metrics, it can be inferred that the selected compounds may have predictive potential for assessing the risk of DGF development.

Table 4. Random forest models’ evaluation metrics.

Metabolomics			
	Time Point 1	Time Point 2	Time Point 3
Accuracy	0.83	0.86	0.78
Kappa	0.66	0.72	0.55
Sensitivity	0.80	0.87	0.73
Specificity	0.86	0.86	0.82
Precision	0.80	0.81	0.73
F1-Score	0.80	0.84	0.73
Lipidomics HILIC			
	Time Point 1	Time Point 2	Time Point 3
Accuracy	0.89	0.89	0.89
Kappa	0.77	0.78	0.78
Sensitivity	0.87	0.93	0.87
Specificity	0.90	0.86	0.91
Precision	0.87	0.82	0.87
F1-Score	0.87	0.88	0.87
Lipidomics RP			
	Time Point 1	Time Point 2	Time Point 3
Accuracy	0.92	0.84	0.86
Kappa	0.82	0.68	0.72
Sensitivity	0.80	0.93	0.87
Specificity	1.00	0.77	0.86
Precision	1.00	0.74	0.81
F1-Score	0.89	0.82	0.84

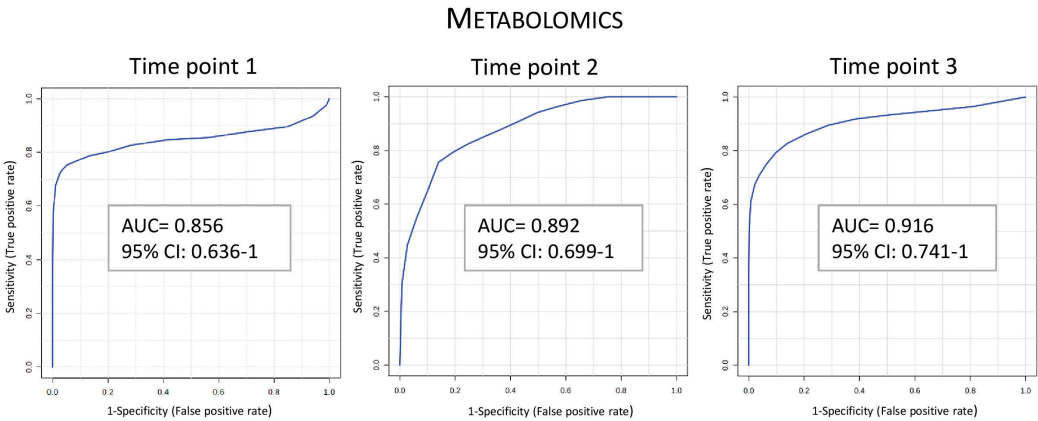
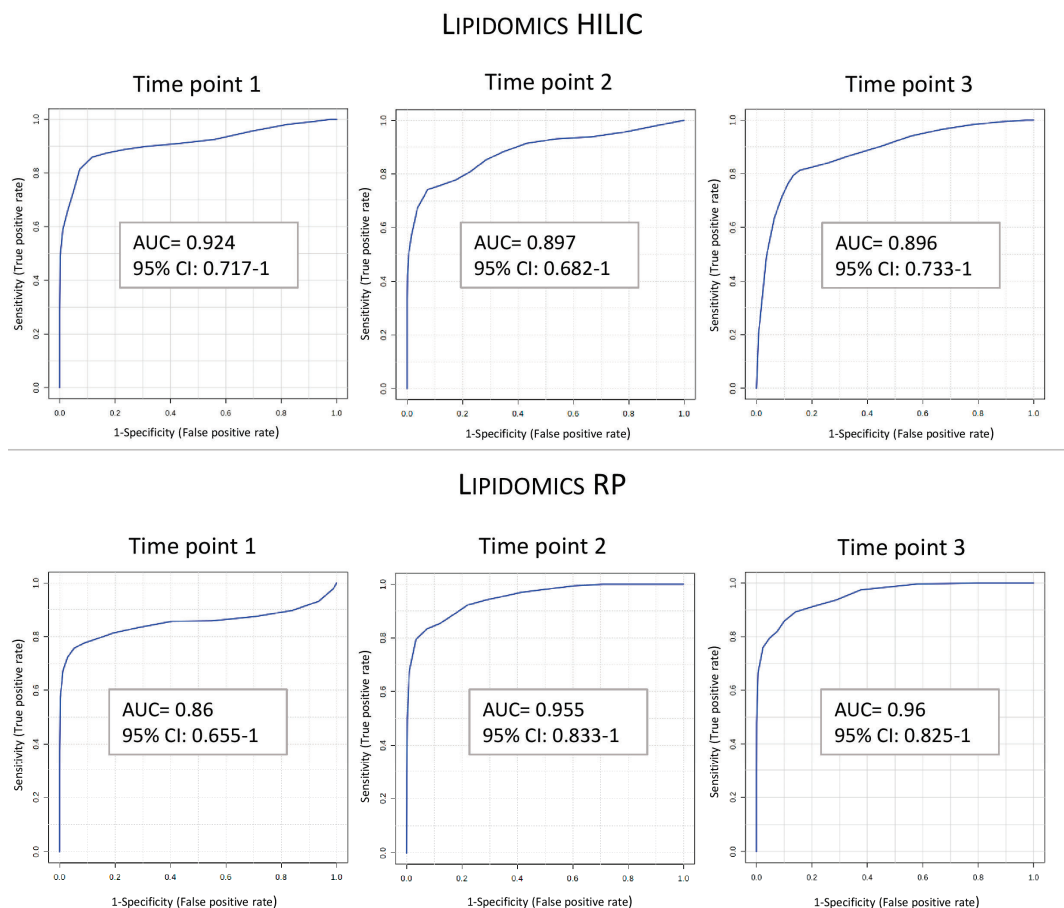
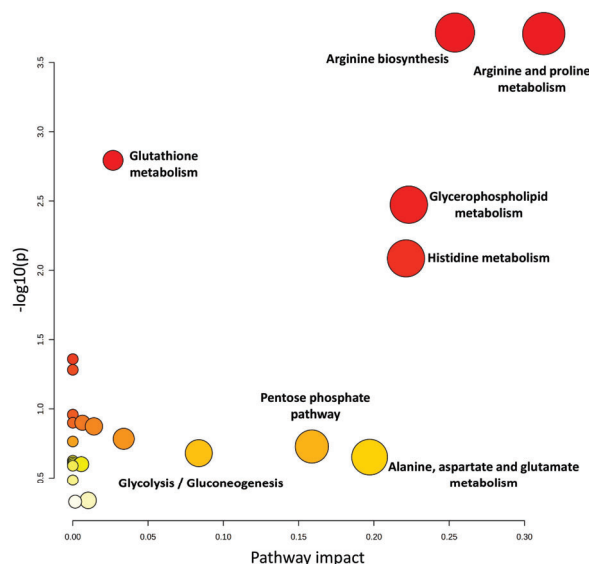


Figure 1. Cont.



**Figure 1.** Receiver operating characteristic (ROC) curves of random forest models for selected compound sets distinguishing between DGF and non-DGF groups. AUC: area under curve.

Furthermore, a pathway analysis was conducted to explore the biological context of the results. This analysis was performed using the list of selected metabolites, with the results presented in Figure 2. The complete list of identified pathways is provided in Table S3.



**Figure 2.** Pathway analysis of metabolites selected for random forest models from metabolomic and lipidomic analyses.

#### 2.4. Analysis of Plasma Samples Collected from Recipients on Days 1 and 5 Post-Operation

A plasma analysis was performed to identify metabolites that differentiate samples from non-DGF and DGF patients. Differential metabolites were selected through a Volcano plot, combining the fold change ( $FC > 2$ ) and a nonparametric Mann–Whitney U test ( $p < 0.05$ ) to ensure selection based on both biological and statistical significance. Analyses were conducted separately for samples collected on post-operative days 1 and 5 (POD1 and POD5, respectively), and the results are summarized in Table 5 and Figure S2. Boxplots of selected statistically significant metabolites are shown in Figure 3. Of the 49 identified compounds, 42 showed elevated levels in the DGF patient group. A greater number of differentiating compounds were observed on POD5. Additionally, metabolites that distinguished the study groups on both sampling days exhibited significantly higher levels on POD5. The identified metabolites are classified into various groups based on their chemical structure, including amino acids, peptides, phenolic acids, lipids, nucleotides, and their derivatives. These molecules play a crucial role in various biological functions, ranging from energy metabolism and fatty acid transport to hormonal regulation and the elimination of toxic metabolic byproducts. A pathway analysis was performed using the list of significantly different compounds identified in the metabolomic and lipidomic analyses. The results are presented in Figure S3 and Table S4.

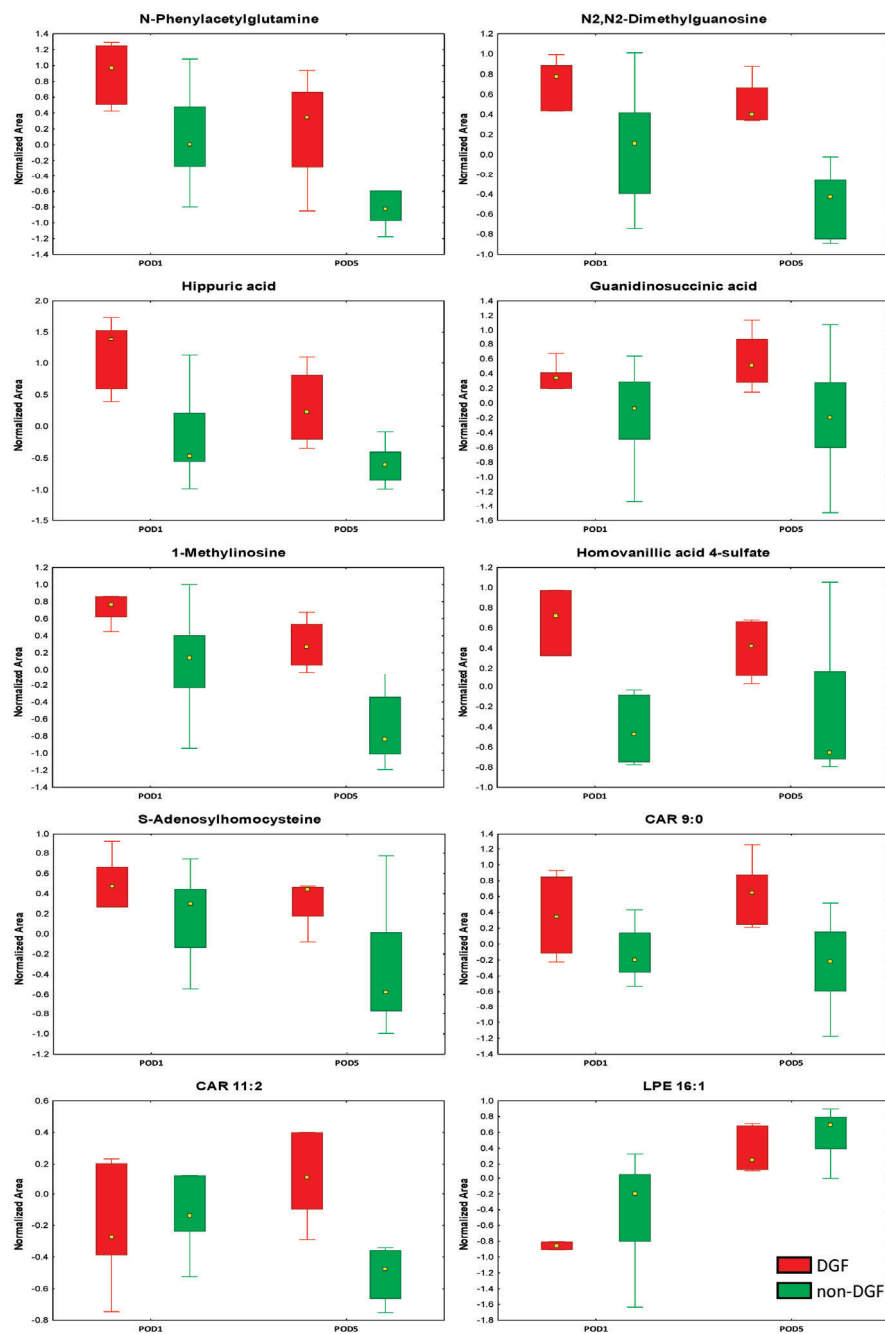
**Table 5.** The list of statistically significant compounds in comparisons of DGF and non-DGF patients on POD1 and POD5.

Name	MW	RT	DGF vs. Non-DGF Patients			
			POD1		POD5	
			FC	<i>p</i> -Value	FC	<i>p</i> -Value
Metabolomics—RP positive ionization mode						
Indole-3-acryloylglycine	244.08	11.70	8.20	0.001	19.32	0.040
4-Hydroxyprolylisoleucine	244.14	9.09	2.92	0.001	n.a	n.a
N-Phenylacetylglutamic acid	265.09	9.90	6.40	0.003	12.94	0.010

Table 5. Cont.

Name	MW	RT	DGF vs. Non-DGF Patients			
			POD1		POD5	
			FC	p-Value	FC	p-Value
Metabolomics—RP positive ionization mode						
3-hydroxydecanoyl carnitine	331.24	18.08	3.22	0.003	2.13	0.026
N-Nonanoylglycine	215.15	9.29	2.98	0.003	4.92	0.018
1-Methylinosine	282.10	6.94	2.97	0.003	2.66	0.018
1-Methylhypoxanthine	150.05	6.94	2.62	0.003	2.95	0.018
Hippuric acid	179.06	8.96	3.95	0.005	9.22	0.006
5-Hydroxyindole	133.05	9.72	3.84	0.005	n.a	n.a
Phenylacetamide	135.07	8.84	3.73	0.005	4.63	0.022
N-Phenylacetylglutamine	264.11	8.85	3.05	0.007	5.72	0.022
Tyramine	137.08	2.13	2.02	0.007	n.a	n.a
Indoleacetyl glutamine	303.12	9.74	2.94	0.013	11.95	0.003
Cinnamoylglycine	205.07	11.48	2.79	0.018	14.38	0.040
N-Phenylacetylaspartic acid	251.08	9.77	2.70	0.018	2.61	0.040
L-Urobilin	590.31	15.71	3.82	0.024	n.a	n.a
alpha-Aminoadipic acid	161.07	1.58	n.a	n.a	2.77	0.010
3-Methylxanthine	166.05	6.66	n.a	n.a	8.09	0.006
1-Methyluric acid	182.04	6.68	n.a	n.a	4.96	0.010
2-Keto-glutaric acid	145.04	1.56	n.a	n.a	2.95	0.010
N2,N2-Dimethylguanosine	311.12	7.31	n.a	n.a	3.12	0.010
Leu-Leu	244.18	14.54	n.a	n.a	0.28	0.018
Pro-Leu	228.15	8.54	n.a	n.a	3.06	0.018
Ala-Leu	202.13	7.32	n.a	n.a	3.33	0.018
9,11alpha-epoxypregn-4-ene-3,20-dione	328.20	11.31	n.a	n.a	2.51	0.018
Cys-Trp	307.10	11.42	n.a	n.a	2.43	0.018
Formiminoglutamic acid	174.06	2.019	n.a	n.a	2.09	0.026
Trp-Phe	351.16	19.58	n.a	n.a	0.43	0.040
Guanidinosuccinic acid	175.06	1.65	n.a	n.a	2.21	0.040
Metabolomics—RP negative ionization mode						
Indole-3-acryloylglycine	244.08	11.70	5.21	0.002	17.05	0.006
N-Phenylacetylglutamic acid	265.09	9.90	4.54	0.007	13.14	0.040
4-Hydroxyprolylleucine	244.14	9.18	2.82	0.009	n.a	n.a
Homovanillic acid 4-sulfate	262.01	7.85	4.09	0.046	n.a	n.a
Gluconic acid	196.06	7.76	2.78	0.046	n.a	n.a
Indoleacetyl glutamine	303.12	9.74	2.77	0.046	10.16	0.003
3-indole carboxylic acid glucuronide	337.08	10.00	n.a	n.a	4.95	0.003
Indoxyl glucuronide	309.08	8.97	n.a	n.a	6.90	0.010
Trp-Phe	351.16	19.58	n.a	n.a	0.43	0.010
11beta-Hydroxyandrostosterone-3-glucuronide	482.25	12.12	n.a	n.a	5.97	0.018
Tetrahydroaldosterone-3-glucuronide	540.26	11.42	n.a	n.a	3.00	0.018
Asp-Phe	280.11	9.88	n.a	n.a	7.12	0.026
Deoxycholic Acid	392.29	16.47	n.a	n.a	0.16	0.026
3,17-Androstenediol glucuronide	468.27	14.35	n.a	n.a	3.90	0.040
LPE 18:0	481.32	18.60	n.a	n.a	0.39	0.040
S-Adenosylhomocysteine	384.12	7.52	n.a	n.a	2.22	0.040
Lipidomics—RP positive ionization mode						
CAR 9:0	301.23	1.53	2.20	0.019	3.05	0.001
Lipidomics—HILIC positive ionization mode						
CAR 17:1	411.33	7.45	0.38	0.019	n.a	n.a
LPE 16:1	451.27	10.50	0.38	0.035	n.a	n.a
CAR 9:0	301.23	8.07	n.a	n.a	3.11	0.001
CAR 11:2	325.23	8.22	n.a	n.a	4.45	0.004
CAR 16:0	399.33	7.50	n.a	n.a	2.54	0.037
SPB 18:0;O2	301.3	10.23	n.a	n.a	2.65	0.048
CAR 14:0	371.30	7.65	n.a	n.a	2.13	0.048

MW: molecular weight, RT: retention time (min), FC: fold change, Leu: leucine, Pro: proline, Ala: alanine, Cys: cysteine, Trp: tryptophan, Phe: phenylalanine, Asp: aspartic acid, LPE: lysophosphatidylethanolamine, CAR: acylcarnitine, SPB: sphinganine, n.a.: not applicable.



**Figure 3.** Selected metabolites differentiating the DGF and non-DGF groups on post-operative days 1 and 5. The rectangle's height represents the normalized peak areas in the interquartile range (Q1 and Q3). The upper whisker denotes the largest data point (excluding any outliers), while the lower whisker denotes the lowest data point (excluding any outliers). The median normalized peak area of each group is indicated with a yellow square.

### 3. Discussion

DGF is one of the most common early complications in kidney transplant recipients, associated with poor graft outcomes, an increased risk of acute rejection, prolonged hospitalization, and the need for additional medical interventions, such as dialysis [4]. Recent research highlights that, beyond its mere occurrence, the duration of DGF may exert the most profound impact on graft outcomes [9,10]. Consequently, there is a pressing need to develop novel methods for early DGF risk assessment and the effective management of high-risk recipients post-transplantation. In recent years, significant efforts have been made to identify potential biomarkers for the early and minimally invasive detection of DGF, as well as to evaluate donor-, recipient-, and surgery-related risk factors [4]. However, conventional diagnostic approaches, such as serum creatinine or GFR measurements, lack specificity, while organ biopsy remains highly invasive [2,4]. To maintain a minimally invasive approach, most studies focus on identifying biomarkers in urine, plasma, or perfusion fluid [4]. Direct tissue analysis is rarely pursued due to the invasive nature of traditional sample preparation techniques, which require the excision of tissue fragments.

The method proposed in this study—chemical biopsy—represents a minimally invasive technique that avoids tissue damage and allows for repeated direct tissue analyses. This approach, combined with a random forest algorithm, allowed for the selection of compounds with potential predictive value for DGF occurrence, which can be evaluated prior to organ transplantation. Furthermore, metabolomic and lipidomic analyses of recipient plasma enabled the identification of compounds differentiating DGF patients during the initial post-operative days.

Among the metabolites forming the basis of the predictive models developed in this study are those previously described in the context of kidney function and peri-transplantation graft performance assessment. In recent years, many studies have attempted to define the role of specific amino acids and their derivatives in kidney function and damage. This work demonstrated that, among this group of compounds, arginine, ornithine, glutamic acid, and histidine may exhibit potential predictive roles in the occurrence of DGF. Ansermet et al. revealed that a possible explanation for the worsening of mitochondrial function in the ischemic kidney may be provided by the metabolic role of arginase 2 (ARG2)-generated ornithine in the proximal tubule [11]. ARG2 in the kidney co-localizes with ornithine aminotransferase, an enzyme catalyzing the conversion of ornithine to glutamate, which can be deaminated to  $\alpha$ -ketoglutarate. The latter may improve the energy deficit in ischemia–reperfusion injury (IRI) by serving as a substrate in the anaerobic adenosine triphosphate (ATP) synthesis pathway in the proximal tubule. This highlights the protective role of ornithine in renal pathology and its potential therapeutic implications in renal transplantation [11,12]. Similarly, arginine and ornithine have been implicated as key amino acids in understanding the mechanisms involved in IRI following liver transplantation [13]. Histidine has also been shown to be an amino acid whose levels in body fluids are correlated with kidney status and was more sensitive to any short-term changes in renal activity than creatinine [14]. A reduced urinary histidine level indicated impaired kidney function, while a low serum histidine level was characteristic for chronic kidney disease (CKD) patients [15,16].

The next metabolites identified in this study were 4-Hydroxynonenal (4-HNE) and 4-oxononenal, two of the most thoroughly studied lipid peroxidation products [17]. The presence of these compounds may indicate oxidative stress as an important factor in kidney damage and dysfunction. Increased lipid peroxidation, measured by an elevation in 4-HNE, was observed in the kidneys for ischemia- or drug-induced acute kidney injury (AKI) [18,19]. In another study, Wang et al. showed that the disruption of mitochondrial energy production by the inhibition of the mitochondrial respiratory chain resulted in increased oxidative stress, leading to glomerular filtration barrier damage [20].

In recent years, adenosine has also been widely studied in the context of renal function and kidney damage. Its role as a signaling molecule in various physiological processes, including renal blood flow regulation and cellular protection during IRI, makes it a critical

factor in kidney transplantation outcomes. Crikis et al. showed that CD39 expression on either endothelial cells or circulating immune cells enhances adenosine generation and follows adenosine A<sub>2A</sub> receptor signaling, contributing to reduced apoptosis under warm ischemia injury and extended cold preservation [21]. However, the role of the ectoenzyme CD73 remains unclear, as research findings suggest both adenosine and adenosine monophosphate as mediators of protection against IRI [22,23]. In a recent paper, Wang et al. reviewed the adenosinergic metabolism pathway as an emerging target for enhancing outcomes in solid organ transplantation [24].

The selected lipids with potential predictive value were primarily TGs, phosphatidylcholine (PC), phosphatidylethanolamine (PE), and sphingomyelin (SM). Lipids belonging to these groups have been previously reported in the literature in relation to graft quality assessment and kidney diseases [25–27]. Changes in TG levels have been associated with the progression of CKD and impaired mitochondrial  $\beta$ -oxidation [27], which is the preferred source of ATP in the kidneys [28]. Furthermore, in our previous studies evaluating different donor types in an animal model, changes in TG levels were also observed [25]. The accumulation of neutral lipids in cells is typically associated with lipotoxicity; however, the renal toxicity of TGs depends on their acyl chain length and the number of double bonds [29,30]. TGs may act as a reservoir for excess free fatty acids that have been removed from cells, thereby preventing fatty-acid-induced lipotoxicity [31].

PCs, PEs, and SMs are essential for cellular structure and function. PCs and PEs are the most abundant phospholipids found in mammalian cells and their subcellular organelles, playing a critical role in membrane integrity and signaling pathways [32]. Changes in the levels of PCs, PEs, and SMs have previously been reported in animal models of IRI [33,34], chronic kidney disease [27,35], acute graft rejection [36], and diabetic nephropathy [37], as well as in studies comparing different kidney preservation strategies [26]. Changes in the levels of PCs and/or PEs may alter the overall PC/PE ratio, which can, in turn, influence processes in various organelles. For instance, a lower PC/PE ratio has been shown to impair liver regeneration, disrupt energy metabolism, increase cell membrane permeability, and induce endoplasmic reticulum stress [32,37].

TFME has already been used for the analysis of body fluids to identify low-molecular-weight metabolites that may serve as potential biomarkers of diseases or pathophysiological conditions [38,39]. In this study, a number of compounds were identified in the plasma that differentiate non-DGF patients from those with DGF. The metabolomic profiles of non-DGF and DGF patients differed already on the first day after transplantation. Furthermore, on POD5, more significant differences in profiles were observed, through the detection of additional metabolites and an increase in the fold changes of those previously identified.

Many of the metabolites identified in this study are considered uremic toxins—organic or inorganic substances that accumulate in the body fluids of individuals with impaired renal function, including acute or chronic renal disease. Sato et al., conducting a metabolomic analysis of plasma from hemodialysis patients, demonstrated that toxins such as 1-methylinosine, N<sub>2</sub>,N<sub>2</sub>-dimethylguanosine, phenylacetylglutamine, and hippuric acid can be used as alternatives to urea and creatinine in assessing organ function [40]. In another study, Grams et al. also identified N<sub>2</sub>,N<sub>2</sub>-dimethylguanosine, hippuric acid, and homovanillic acid 4-sulfate as molecules associated with CKD [41]. Hippuric acid is one of the most well-characterized uremic toxins, shown to be elevated in hemodialysis patients with chronic renal failure compared to both healthy controls and hospitalized patients without renal disease [42]. Sun et al. revealed that hippuric acid promotes the progression of renal fibrosis by disrupting redox homeostasis, which is maintained by the nuclear factor erythroid 2-related factor 2 (NRF2) antioxidant network [43].

Another uremic toxin, guanidinosuccinic acid (GSA), is primarily derived from the metabolism of arginine and plays a role in the urea cycle. In patients with kidney dysfunction, GSA levels can rise significantly due to impaired renal clearance. Zhang et al. demonstrated that GSA levels were markedly elevated in rats exposed to chronic low-dose cadmium, suggesting that GSA could serve as a biomarker for kidney damage [44]. Further-

more, Gu et al. reported a significant increase in GSA concentrations in a rat model of renal failure, indicating that this metabolite may serve as an early biomarker for nephrotoxicity, potentially preceding traditional markers such as creatinine and uric acid [45].

In this work, one of the differentiating metabolites was S-Adenosylhomocysteine (SAH), a direct precursor of all homocysteine produced in the body, formed through the demethylation of S-adenosyl-L-methionine. The correlation between elevated SAH levels in serum or urine and renal dysfunction or insufficiency in patients with end-stage renal disease and CKD has been frequently reported in previous studies [46–49]. SAH is a potent inhibitor of the trans-methylation enzymes, and the accumulation of SAH in plasma might affect the trans-methylation pathway in CKD patients [47,50]. Given that SAH is a potential marker of cardiovascular and renal dysfunction, Klepacki et al. developed and validated an LC-MS method for determining SAH in plasma as an early marker of acute rejection and nephrotoxicity in kidney transplant recipients. Their study showed that samples collected during or prior to clinical events affecting the kidney graft, such as biopsy-proven acute allo-immune reactions and immunosuppressive drug nephrotoxicity, showed significantly higher concentrations of SAH compared to samples from transplant patients during periods of stable kidney graft function [51].

Among the compounds showing higher levels in the DGF recipient group, acylcarnitines (CARs) were also identified. Changes in acylcarnitine levels have been previously associated with various kidney conditions, including AKI, the progression of CKD, and diabetic nephropathy, as documented in several studies [15,26,27,52,53]. CARs play a critical role in transporting long-chain fatty acids into mitochondria, facilitating the  $\beta$ -oxidation process [52,54]. Elevated plasma levels of acylcarnitines indicate mitochondrial damage, while under non-pathological conditions, their concentrations remain low [54,55]. Moreover, elevated CARs levels have been previously observed in patients with reduced GFR, highlighting their association with impaired kidney function [15,56].

The obtained results demonstrate significant translational potential, which is worth emphasizing. Due to the small diameter of the probe and the lack of a need for physical tissue collection, chemical biopsy enables multiple direct analyses of kidney tissue. This capability, which is challenging to achieve with other methods, is coupled with the preservation of the procedure's minimally invasive nature. Direct tissue analysis provides organ-specific insights, which are particularly significant when assessing the quality of kidneys intended for transplantation. Notably, kidneys from the same donor may vary in their characteristics and exhibit different levels of risk for the development of DGF or other complications in the recipient. Biomarker evaluation in recipients' urine or blood presents a promising alternative to current laboratory tests for diagnosing and monitoring post-transplant complications, offering potentially greater levels of sensitivity and specificity. However, for the early identification of complication risks and better management of high-risk patients, it is crucial to develop methods capable of assessing these risks at the stage of graft quality evaluation. The use of a needle biopsy for organ quality assessments varies across medical facilities and countries. For example, while up to 85% of high-risk kidneys undergo biopsies in the United States, pre-transplant biopsies are rarely performed in European centers [2,57]. Furthermore, existing studies assessing the predictive value of renal biopsies concerning graft outcomes have yielded predominantly inconclusive results [58–61]. Another challenge is the low reproducibility of biopsy evaluations between on-call and renal pathologists, as highlighted in previous studies [62]. Additionally, the invasive nature of the procedure often limits biopsies to a single sampling plan. Although the translational potential of chemical biopsy has been previously highlighted [25,26], to the best of our knowledge, this study is the first to apply a chemical biopsy for kidney graft quality assessments in a clinical setting. Undoubtedly, the results obtained in this study are highly promising and suggest the potential for incorporating chemical biopsy into routine diagnostic practices. From a practical standpoint, sampling performed immediately after organ procurement and after preservation but before transplantation may have the greatest utility. This approach would allow for the assessment of donor-related risk factors and,

in cases of doubt or prolonged cold ischemia time, the opportunity to re-evaluate the risk of complications. Moreover, the 10-min extraction used in this study did not prolong the ischemic time of the organ, as the small size of the probes allowed for the simultaneous surgical preparation of the graft (Figure 4). Furthermore, we assume that by applying a targeted analysis on a validated biomarker panel, it will be possible in the future to further shorten the extraction time. Combined with the monitoring of plasma metabolites, this could lead to the development of a comprehensive method for assessing risk and monitoring complications in kidney transplant recipients.



**Figure 4.** Chemical biopsy sampling during simultaneous surgical preparation of the graft.

However, despite these promising results, this study has several limitations that should be considered. The primary limitation is the relatively small sample size and the imbalanced groups. Given the complexity of DGF's underlying causes, further studies with larger sample sizes are needed to validate the results obtained in this study. Moreover, studies conducted on a larger patient cohort should consider the impact of the organ preservation method and other clinical parameters on the assessment of DGF risk, which was not achievable in this study due to the small sample size. Additionally, the lack of metabolomic and lipidomic profiling of recipients' blood before transplantation is a limitation, along with the relatively short follow-up period of 5 days post-transplant. Future research should aim to verify the predictive models developed in this study in the context of long-term outcomes.

#### 4. Materials and Methods

##### 4.1. Chemicals

Reagents, including water (LC/MS Optima grade), ammonium acetate, formic acid, and acetic acid, were sourced from Merck (Poznan, Poland), while acetonitrile, methanol, and isopropanol (all LC/MS Optima grade) were supplied by Alchem (Torun, Poland). Pierce LTQ Velos ESI Positive External Calibrant Solution and Negative Ion Calibration Solution were purchased from Anchem (Anchem, Warsaw, Poland). Prototypes of bio-compatible SPME mixed-mode (MM) probes (C18 and benzenesulfonic acid) were kindly provided by Supelco (Bellefonte, PA, USA).

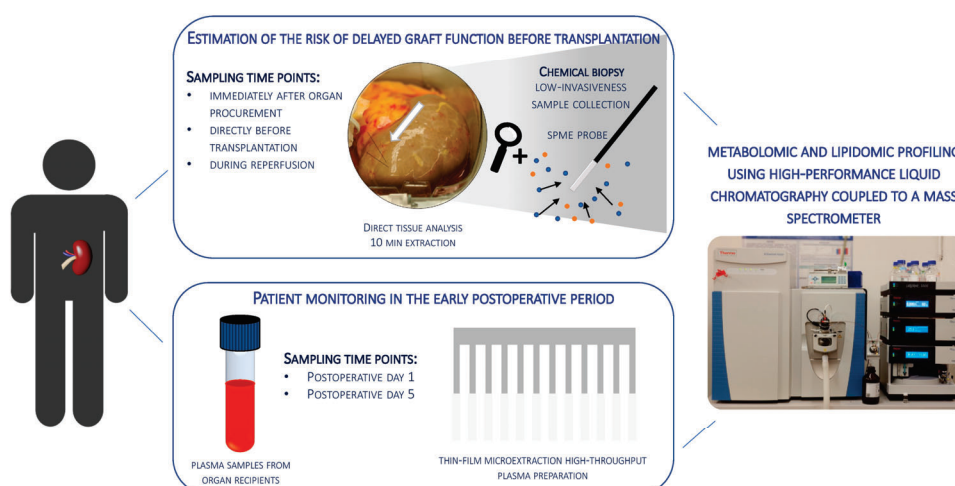
##### 4.2. Patients

This study received prior approval from the Bioethics Committee in Bydgoszcz (KB 636/2017), and informed consent was obtained from all subjects. The study involved samples collected from kidneys recovered from deceased donors ( $n = 24$ ) and plasma samples from organ recipients. The study protocol is illustrated in Figure 5. A total of

32 kidneys were sampled at multiple time points, while plasma samples were obtained from 20 recipients. The condition for including an organ in the study cohort was its qualification for transplantation at Antoni Jurasz University Hospital No. 1 in Bydgoszcz. Decisions were made by the transplant team based on the donor's medical history, laboratory parameters, and, in doubtful cases, kidney biopsy results. The study group included SCD and ECD. The kidneys were preserved using static cold storage or hypothermic machine perfusion. The patient cohort was divided into two groups based on the occurrence of DGF in the organ recipient. The DGF patient group consisted of patients in whom ATN was confirmed by biopsy ( $n = 7$ ) and those diagnosed with DGF based on clinical data ( $n = 3$ ). These two types of DGF patients were combined to allow for a dichotomous definition of DGF. Clinical parameters were collected from donors before organ procurement and from recipients during final tests conducted prior to hospital discharge following transplantation. Donors' laboratory tests were performed at the centers where the kidneys were procured, while recipients' tests were conducted at Antoni Jurasz University Hospital No. 1 in Bydgoszcz. Hematological tests were carried out using the Sysmex XN system, and biochemical parameters were measured with dedicated assays on the Alinity c Abbott system.

#### 4.3. Sample Collection

Kidney tissue sampling was performed using an SPME probe with a 4 mm coating of MM sorbent as the extraction phase. Before use, the probes were conditioned in a 50:50 methanol:water solution at 850 rpm for 30 min to pre-activate the sorbent, ensuring optimal extraction efficiency, followed by steam sterilization in accordance with standard procedures for medical tools and equipment sterilization. Metabolite extraction, referred to as chemical biopsy, was carried out by carefully inserting the probe into the renal cortex for 10 min at three specific time points: immediately after organ procurement (time point 1), directly before transplantation (time point 2), and during reperfusion (time point 3). Following extraction, the probes were rinsed with distilled water to remove residual blood, placed into empty glass vials, transported on ice, and stored at  $-80^{\circ}\text{C}$  until instrumental analysis. Blood samples from recipients were collected in sodium citrate tubes on POD1 and POD5. After centrifugation, the resulting plasma was aliquoted and stored in Eppendorf tubes at  $-80^{\circ}\text{C}$  until instrumental analysis.



**Figure 5.** Study design. The study involved samples collected from kidneys recovered from deceased donors and plasma samples from organ recipients.

#### 4.4. Sample Preparation

Two distinct desorption solutions were employed to desorb analytes from SPME probes and tailored to the specific analytical requirements of the study. For metabolomic analysis, a solution composed of acetonitrile and water (50:50, *v/v*) was utilized. Conversely, for lipidomic analysis, a mixture of isopropanol and methanol (50:50, *v/v*) was applied. In both analytical approaches, desorption was conducted in a total volume of 200  $\mu$ L of the respective desorption solution. The desorption process was carried out for 2 h under agitation at 850 rpm using a BenchMixer™ MultiTube Vortexer (Benchmark Scientific, Edison, NJ, USA). To control for potential contamination, extraction blanks were prepared. These blanks consisted of fibers processed according to the same protocol as the sampling fibers (including preconditioning and desorption), but they were not exposed to kidney samples.

Plasma sample preparation was conducted using SPME, with each step of the process performed on a high-throughput 96-manual TFME system (Professional Analytical System (PAS) Technology, Magdala, Germany). This system enabled the simultaneous analysis of all samples [38]. For metabolomic analyses, extractions were performed using stainless blades coated with hydrophilic-lipophilic balanced (HLB) sorbent, specifically N-vinylpyrrolidone-divinylbenzene copolymer (Alchem, Toruń, Poland). In contrast, for lipidomic studies, blades coated with C18 sorbent (Alchem, Toruń, Poland) were utilized. In both cases, the coating length was 5 mm. The coating preparation procedure followed the spray method described by Mirnaghi et al. [63]. Steel blades were procured from PAS Technology (Magdala, Germany), while polypropylene Nunc 96-well DeepWell plates were obtained from Merck (Poznań, Poland).

Before initiating the extraction, the SPME blades were conditioned for 30 min in 0.5 mL of a methanol:water (50:50, *v/v*) solution in 96-well plates, with agitation at 850 rpm. Following conditioning, a 10-s wash step was performed. Extractions were performed from 0.5 mL of plasma spiked with acetylcarnitine- $d_4$  (Merck, Poland) for metabolomics and SPLASH (Merck, Poland) for lipidomics, respectively, with agitation at 850 rpm for 1 h. After extraction, the blades were placed in 0.5 mL of nanopure water for 10 s. Following the wash step, desorption was conducted in 0.5 mL organic solutions identical to those used for the desorption of SPME probes with agitation (850 rpm) for 2 h.

#### 4.5. LC-MS Analysis

Samples were analyzed using an LC-HRMS procedure involving the coupling of an ultra-high performance liquid chromatograph (Dionex UHPLC system) and a Q-Exactive Focus Orbitrap mass spectrometer (Thermo Fisher Scientific, Bremen, Germany). Data acquisition was performed using dedicated Thermo Scientific software, namely, Xcalibur 4.2 and Free Style 1.4 (Thermo Fisher Scientific, San Jose, CA, USA). The instrument was externally calibrated every 72 h, achieving a mass accuracy of <2 ppm. To ensure consistent performance, within-sequence samples were randomized, and pooled QC samples (comprising 10  $\mu$ L of each sample) were analyzed every 8–10 injections.

#### 4.6. Metabolomics Analysis

Chromatographic separation was carried out in reversed-phase (RP) mode using a pentafluorophenyl column (Supelco Discovery HS F5, 2.1 mm  $\times$  100 mm, 3  $\mu$ m). Samples collected via chemical biopsy were analyzed in positive ionization mode, while plasma samples were analyzed in both positive and negative ionization modes. Detailed parameters of the method, including the mobile phases and gradient employed, have been previously described in [25]. The mass spectrometer parameters in positive ionization mode were as follows: a sheath gas flow rate of 40 a.u.; an aux gas flow rate of 15 a.u.; a spray voltage of 3.5 kV; a capillary temp of 300  $^{\circ}$ C; an aux gas heater temp of 300  $^{\circ}$ C; an S-lens radio frequency level of 55%; an S-lens voltage of 25 V; and a skimmer voltage of 15 V. In negative ionization mode, the mass spectrometer parameters were as follows: a sheath gas flow rate of 48 a.u.; an aux gas flow rate of 11 a.u.; a spray voltage of 2.5 kV; a capillary temp of 256  $^{\circ}$ C;

an aux gas heater temp of 413 °C; an S-lens radio frequency level of 55%; an S-lens voltage of −25 V; and a skimmer voltage of −15 V. The scan range was set to 80–1000 m/z with a resolution of 70,000 full width at half maximum (FWHM). Acquisition was performed using an automatic gain control (AGC) target of 1E6, with the C-trap injection time set to auto. The putative identification of compounds was confirmed based on full MS/dd-MS2 mode. The fragmentation parameters were set as follows: mass resolution—35,000 FWHM; AGC target—2E4; minimum AGC—8E3; intensity threshold—auto; maximum IT—auto; isolation window—3.0 m/z; stepped collision energy—10 V, 20 V, and 40 V; loop count—2; and dynamic exclusion—auto. Fragmentation spectra were verified using online databases including LIPID MAPS, Human Metabolome Database, METLIN, and mzCloud.

#### 4.7. Lipidomics Analysis

Chromatographic separation was carried out on a hydrophilic stationary-phase (HILIC) column (SeQuant ZIC-cHILIC, 3 µm, 100 × 2.1 mm) and in RP using a C18 column (Waters, XSelect CSH C18, 3.5 µm, 2.1 × 75 mm). The analyses were performed in positive electrospray ionization mode. Detailed information on the chromatographic separation and mass spectrometer parameters has been previously described in [26]. The putative identification of compounds was confirmed in full MS/dd-MS2 mode using the following fragmentation parameters: mass resolution—35,000 FWHM; AGC target—2E4; minimum AGC—8E3; intensity threshold—auto; maximum IT—auto; isolation window—3.0 m/z; stepped collision energy—20 V, 30 V, and 50 V; loop count—2; and dynamic exclusion—auto.

#### 4.8. Data Processing and Statistical Analysis

The raw metabolomics data were processed using Compound Discoverer 3.1 (Thermo Fisher Scientific, San Jose, CA, USA) software to identify metabolites present in the samples. Detected metabolites with a signal-to-noise ratio > 3 and a peak intensity > 100,000 were subjected to further analysis. The intensity tolerance was set at 30%, and the RT tolerance was set at 0.2 min. The QC-based area was used for correction (min 80% coverage and max 30% RSD in QC). After peak alignment, gap filling was performed to fill in the missing values via a very small peak at the level of spectrum noise for the compound.

Raw lipidomics data were processed separately using LipidSearch 4.1.30 (Thermo Fisher Scientific, San Jose, CA, United States) software with the following parameters: peak intensity >100,000; a precursor tolerance of 5 ppm; a product tolerance of 10 ppm; an m-score threshold of 2; a Quan m/z tolerance of ±5 ppm; a Quan RT (retention time) range of 0.5 min; and the use of a main isomer filter. H<sup>+</sup>, NH<sub>4</sub><sup>+</sup>, and Na<sup>+</sup> adducts were considered in positive ionization mode. After lipid identification, the alignment process was conducted using LipidSearch with the following parameters: an m-score threshold of 10; a retention time tolerance of 0.25 min; a QC-to-extraction-blank ratio of >5; and a max 30% RSD in the QC. The search mode function of the software sought matches of parent peaks (full scan MS) and product peaks (fragments, MS/MS) with the lipid database entries. The software's search mode matched parent peaks (full scan MS) and product peaks (fragments, MS/MS) with the lipid database entries. Each feature was assigned a grade (A–D) based on its quality, with grade filtering applied to eliminate false positives. During alignment, only lipids identified with grades A to C were retained.

The results from each LC-HRMS block constituted separate datasets and were analyzed independently. Peak areas for the identified compounds were processed using MetaboAnalyst 6.0, Statistica 13.3 PL (StatSoft, Inc., Tulsa, OK, USA) and RStudio (version 2024.9.0+375, Posit Team, 2024) with R version 4.4.1 (R Core Team, 2024). All missing values were replaced with small values assumed to represent the detection limit. Data obtained from chemical biopsy were normalized using the probabilistic quotient normalization (PQN) method, followed by log transformation and Pareto scaling. Plasma data were normalized using an internal standard, followed by log transformation and Pareto scaling. Principal component analysis (PCA) was conducted to visually confirm the quality of the analytical performance.

To evaluate the significance of changes, the Student's *t*-test was used for parametric data, while the Mann–Whitney U test was applied to nonparametric data. Homogeneity was assessed using Levene's test, and normality was checked with the Shapiro–Wilk test. Additionally, Fisher's exact test was used to examine associations between categorical variables. A *p*-value of <0.05 was considered statistically significant.

For metabolomic and lipidomic data obtained from chemical biopsy sampling, the following R packages were used for data preprocessing and model development: ROSE, to address class imbalance; RandomForest, to construct the random forest model; and caret, for model training and cross-validation. To visualize the performance of the resulting models, ROC curves were generated using the Biomarker Analysis module in MetaboAnalyst 6.0. The same platform was also used for pathway analysis, employing the Homo sapiens Kyoto Encyclopedia of Genes and Genomes (KEGG) metabolic pathway database.

## 5. Conclusions

In conclusion, the findings of this study highlight the significant translational potential of chemical biopsy and plasma metabolite analysis for assessing the risk and the non-invasive monitoring of DGF. The compounds identified in this research provide a basis for future studies aimed at validating their predictive value in a larger cohort. Upon the completion of studies involving a broader patient population, it is anticipated that a comprehensive method for assessing and monitoring DGF will be developed, with the potential for integration into routine clinical practice.

**Supplementary Materials:** The following supporting information can be downloaded at: <https://www.mdpi.com/article/10.3390/ijms252413502/s1>.

**Author Contributions:** N.W.: Writing—original draft, Writing—review and editing, Conceptualization, Methodology, Formal analysis, Investigation, Data curation, Visualization; K.L.: Writing—original draft, Writing—review and editing, Investigation; Formal analysis; I.S.: Conceptualization, Methodology, Investigation; E.W.: Conceptualization, Investigation; A.W.-J.: Investigation, Data curation; M.M.: Investigation; Z.W.: Writing—review and editing, Investigation, Resources; B.B.: Writing—review and editing, Conceptualization, Methodology, Resources, Supervision, Funding acquisition. All authors have read and agreed to the published version of the manuscript.

**Funding:** This research was funded by the National Science Centre grant Opus number 2017/27/B/NZ5/01013.

**Institutional Review Board Statement:** The study was conducted in accordance with the Declaration of Helsinki, and approved by Bioethics Committee of Collegium Medicum in Bydgoszcz at Nicolaus Copernicus University in Toruń (KB 636/2017).

**Informed Consent Statement:** Informed consent was obtained from all subjects involved in the study.

**Data Availability Statement:** The datasets generated during and/or analyzed during the current study are available from the corresponding author on reasonable request.

**Acknowledgments:** The authors would like to acknowledge Supelco/MilliporeSigma for kindly supplying the SPME probes and Thermo Fisher Scientific for granting us access to a Q Exactive Focus mass spectrometer. The authors would like to thank the personnel of the Department of Transplantology and General Surgery in Bydgoszcz for their kind assistance in the project.

**Conflicts of Interest:** The authors declare no conflicts of interest.

## Abbreviations

4-HNE 4-Hydroxynonenal; AGC automatic gain control; AKI acute kidney injury; Ala alanine; ARG2 arginase 2; Asp aspartic acid; ATN acute tubular necrosis; ATP adenosine triphosphate; AUC area under curve; BUN blood urea nitrogen; CAR acylcarnitine; Cer ceramide; CKD chronic kidney disease; Cys cysteine; DCD donation after circulatory death; DG diglyceride; DGF delayed graft function; ECD extended criteria donor; FC fold change; FWHM full width at half maximum; GFR glomerular filtration rate; GSA guanidinosuccinic acid; HILIC hydrophilic stationary phase; HLB hydrophilic–lipophilic balanced; HMP hypothermic machine perfusion; IRI ischemia-reperfusion

injury; Leu leucine; LPC lysophosphocholine; LPE lysophosphatidylethanolamine; MDA mean decrease accuracy; MDG mean decrease Gini; MM mixed mode; NRF2 nuclear factor erythroid 2-related factor 2; PAS Professional Analytical System; PC phosphatidylcholine; PCA principal component analysis; PE phosphatidylethanolamine; Phe phenylalanine; PLT platelet; POD post-operative day; PQN probabilistic quotient normalization; Pro proline; QC quality control; ROC Receiver operating characteristic; ROSE Random Over-Sampling Examples; RP reversed-phase; SAH S-Adenosylhomocysteine; SCS static cold storage; SM sphingomyelin; SPB sphinganine; SPME solid-phase microextraction; TFME thin-film microextraction; TG triacylglycerol; Trp tryptophan.

## References

- Swanson, K.J.; Aziz, F.; Garg, N.; Mohamed, M.; Mandelbrot, D.; Djamali, A.; Parajuli, S. Role of Novel Biomarkers in Kidney Transplantation. *World J. Transplant.* **2020**, *10*, 230–255. [\[CrossRef\]](#) [\[PubMed\]](#)
- Warmuzińska, N.; Łuczykowski, K.; Bojko, B. A Review of Current and Emerging Trends in Donor Graft-Quality Assessment Techniques. *J. Clin. Med.* **2022**, *11*, 487. [\[CrossRef\]](#) [\[PubMed\]](#)
- McGuinness, D.; Mohammed, S.; Monaghan, L.; Wilson, P.A.; Kingsmore, D.B.; Shapter, O.; Stevenson, K.S.; Coley, S.M.; Devey, L.; Kirkpatrick, R.B.; et al. A Molecular Signature for Delayed Graft Function. *Aging Cell* **2018**, *17*, e12825. [\[CrossRef\]](#) [\[PubMed\]](#)
- Mezzolla, V.; Pontrelli, P.; Fiorentino, M.; Stasi, A.; Franzin, R.; Rascio, F.; Grandaliano, G.; Stallone, G.; Infante, B.; Gesualdo, L.; et al. Emerging Biomarkers of Delayed Graft Function in Kidney Transplantation. *Transplant. Rev.* **2021**, *35*, 100629. [\[CrossRef\]](#)
- Perico, N.; Cattaneo, D.; Sayegh, M.H.; Remuzzi, G. Delayed Graft Function in Kidney Transplantation. *Lancet* **2004**, *364*, 1814–1827. [\[CrossRef\]](#)
- Belhaj, M.R.; Lawler, N.G.; Hoffman, N.J. Metabolomics and Lipidomics: Expanding the Molecular Landscape of Exercise Biology. *Metabolites* **2021**, *11*, 151. [\[CrossRef\]](#)
- Łuczykowski, K.; Warmuzińska, N.; Bojko, B. Solid Phase Microextraction—A Promising Tool for Graft Quality Monitoring in Solid Organ Transplantation. *Separations* **2023**, *10*, 153. [\[CrossRef\]](#)
- Roszkowska, A.; Miękus, N.; Bączek, T. Application of Solid-Phase Microextraction in Current Biomedical Research. *J. Sep. Sci.* **2019**, *42*, 285–302. [\[CrossRef\]](#)
- Budhiraja, P.; Reddy, K.S.; Butterfield, R.J.; Jadlowiec, C.C.; Moss, A.A.; Khamash, H.A.; Kodali, L.; Misra, S.S.; Heilman, R.L. Duration of Delayed Graft Function and Its Impact on Graft Outcomes in Deceased Donor Kidney Transplantation. *BMC Nephrol.* **2022**, *23*, 154. [\[CrossRef\]](#)
- Phillips, B.L.; Ibrahim, M.; Greenhall, G.H.B.; Mumford, L.; Dorling, A.; Callaghan, C.J. Effect of Delayed Graft Function on Longer-Term Outcomes after Kidney Transplantation from Donation after Circulatory Death Donors in the United Kingdom: A National Cohort Study. *Am. J. Transplant.* **2021**, *21*, 3346–3355. [\[CrossRef\]](#)
- Ansermet, C.; Centeno, G.; Lagarrigue, S.; Nikolaeva, S.; Yoshihara, H.A.; Pradervand, S.; Barras, J.L.; Dattner, N.; Rotman, S.; Amati, F.; et al. Renal Tubular Arginase-2 Participates in the Formation of the Corticomedullary Urea Gradient and Attenuates Kidney Damage in Ischemia-Reperfusion Injury in Mice. *Acta Physiol.* **2020**, *229*, e13457. [\[CrossRef\]](#) [\[PubMed\]](#)
- Weinberg, J.M.; Venkstachalam, M.A.; Roeser, N.F.; Saikumar, P.; Dong, Z.; Senter, R.A.; Nissim, I. Anaerobic and Aerobic Pathways for Salvage of Proximal Tubules from Hypoxia-Induced Mitochondrial Injury. *Am. J. Physiol. Ren. Physiol.* **2000**, *279*, F927–F943. [\[CrossRef\]](#) [\[PubMed\]](#)
- Shah, J.A.; Patel, M.S.; Louras, N.; Sachs, D.H.; Vagefi, P.A. Amino Acid and Lipid Profiles Following Pig-to-Primate Liver Xenotransplantation. *Xenotransplantation* **2019**, *26*, e12473. [\[CrossRef\]](#) [\[PubMed\]](#)
- Stanimirova, I.; Banasik, M.; Ząbek, A.; Dawiskiba, T.; Kościelska-Kasprzak, K.; Wojtowicz, W.; Krajewska, M.; Janczak, D.; Młynarz, P. Serum Metabolomics Approach to Monitor the Changes in Metabolite Profiles Following Renal Transplantation. *Sci. Rep.* **2020**, *10*, 17223. [\[CrossRef\]](#)
- Bassi, R.; Niewczas, M.A.; Biancone, L.; Bussolino, S.; Merugumala, S.; Tezza, S.; D’Addio, F.; Nasr, M.B.; Valderrama-Vasquez, A.; Uselli, V.; et al. Metabolomic Profiling in Individuals with a Failing Kidney Allograft. *PLoS ONE* **2017**, *12*, e0169077. [\[CrossRef\]](#)
- Watanabe, M.; Suliman, M.E.; Qureshi, A.R.; Garcia-Lopez, E.; Bárány, P.; Heimbürger, O.; Stenvinkel, P.; Lindholm, B. Consequences of Low Plasma Histidine in Chronic Kidney Disease Patients: Associations with Inflammation, Oxidative Stress, and Mortality. *Am. J. Clin. Nutr.* **2008**, *87*, 1860–1866. [\[CrossRef\]](#)
- Kuiper, H.C.; Langsdorf, B.L.; Miranda, C.L.; Joss, J.; Jubert, C.; Mata, J.E.; Stevens, J.F. Quantitation of Mercapturic Acid Conjugates of 4-Hydroxy-2-Nonenal and 4-Oxo-2-Nonenal Metabolites in a Smoking Cessation Study. *Free Radic. Biol. Med.* **2010**, *48*, 65–72. [\[CrossRef\]](#)
- Kovacevic, S.; Ivanov, M.; Zivotic, M.; Brkic, P.; Miloradovic, Z.; Jeremic, R.; Mihailovic-Stanojevic, N.; Vajic, U.J.; Karanovic, D.; Jovovic, D.; et al. Immunohistochemical Analysis of 4-Hne, Ngal, and Ho-1 Tissue Expression after Apocynin Treatment and Hbo Preconditioning in Postischemic Acute Kidney Injury Induced in Spontaneously Hypertensive Rats. *Antioxidants* **2021**, *10*, 1163. [\[CrossRef\]](#)

19. Kim, J.Y.; Jo, J.; Kim, K.; An, H.J.; Gwon, M.G.; Gu, H.; Kim, H.J.; Yang, A.Y.; Kim, S.W.; Jeon, E.J.; et al. Pharmacological Activation of Sirt1 Ameliorates Cisplatin-Induced Acute Kidney Injury by Suppressing Apoptosis, Oxidative Stress, and Inflammation in Mice. *Antioxidants* **2019**, *8*, 322. [\[CrossRef\]](#)
20. Wang, S.X.; Solin, M.L.; Ahola, H.; Luimula, P.; Holthöfer, H. Interactions between Mitochondrial Proteins and Lipid Peroxidation Products in the Maintenance of the Glomerular Filtration Barrier in the in Vitro Perfused Kidney. *Exp. Nephrol.* **2001**, *9*, 14–20. [\[CrossRef\]](#)
21. Crikis, S.; Lu, B.; Murray-Segal, L.M.; Selan, C.; Robson, S.C.; D'Apice, A.J.F.; Nandurkar, H.H.; Cowan, P.J.; Dwyer, K.M. Transgenic Overexpression of CD39 Protects against Renal Ischemia-Reperfusion and Transplant Vascular Injury. *Am. J. Transplant.* **2010**, *10*, 2586–2595. [\[CrossRef\]](#) [\[PubMed\]](#)
22. Itabashi, Y.; Ravichandran, R.; Bansal, S.; Chin, C.; Poulson, C.; Sureshbabu, A.; Nair, S.S.; Perincheri, S.; Mohanakumar, T. Role for Exosomes with Self-Antigens and Immune Regulatory Molecules in Allo- and Auto-Immunity Leading to Chronic Immune Injury Following Murine Kidney Transplantation. *Transpl. Immunol.* **2022**, *75*, 101702. [\[CrossRef\]](#) [\[PubMed\]](#)
23. Rajakumar, S.V.; Lu, B.; Crikis, S.; Robson, S.C.; D'Apice, A.J.F.; Cowan, P.J.; Dwyer, K.M. Deficiency or Inhibition of CD73 Protects in Mild Kidney Ischemia-Reperfusion Injury. *Transplantation* **2010**, *90*, 1260–1264. [\[CrossRef\]](#) [\[PubMed\]](#)
24. Wang, B.; Zhou, A.; Pan, Q.; Li, Y.; Xi, Z.; He, K.; Li, D.; Li, B.; Liu, Y.; Liu, Y.; et al. Adenosinergic Metabolism Pathway: An Emerging Target for Improving Outcomes of Solid Organ Transplantation. *Transl. Res.* **2024**, *263*, 93–101. [\[CrossRef\]](#) [\[PubMed\]](#)
25. Stryjak, I.; Warmuzińska, N.; Łuczykowski, K.; Jaroch, K.; Urbanellis, P.; Selzner, M.; Bojko, B. Metabolomic and Lipidomic Landscape of Porcine Kidney Associated with Kidney Perfusion in Heart Beating Donors and Donors after Cardiac Death. *Transl. Res.* **2024**, *267*, 79–90. [\[CrossRef\]](#)
26. Warmuzińska, N.; Łuczykowski, K.; Stryjak, I.; Rosales-Solano, H.; Urbanellis, P.; Pawliszyn, J.; Selzner, M.; Bojko, B. The Impact of Normothermic and Hypothermic Preservation Methods on Kidney Lipidome—Comparative Study Using Chemical Biopsy with Microextraction Probes. *Front. Mol. Biosci.* **2024**, *11*, 1341108. [\[CrossRef\]](#)
27. Afshinnia, F.; Rajendiran, T.M.; Soni, T.; Byun, J.; Wernisch, S.; Sas, K.M.; Hawkins, J.; Bellovich, K.; Gipson, D. Impaired  $\beta$ -Oxidation and Altered Complex Lipid Fatty Acid Partitioning with Advancing CKD. *J. Am. Soc. Nephrol.* **2018**, *29*, 295–306. [\[CrossRef\]](#)
28. Jang, H.S.; Noh, M.R.; Kim, J.; Padanilam, B.J. Defective Mitochondrial Fatty Acid Oxidation and Lipotoxicity in Kidney Diseases. *Front. Med.* **2020**, *7*, 65. [\[CrossRef\]](#)
29. Afshinnia, F.; Kretzler, M.; Afshinnia, F.; Nair, V.; Lin, J.; Rajendiran, T.M.; Soni, T.; Byun, J.; Sharma, K.; Fort, P.E.; et al. Increased Lipogenesis and Impaired  $\beta$ -Oxidation Predict Type 2 Diabetic Kidney Disease Progression in American Indians. *JCI Insight* **2019**, *4*, e130317. [\[CrossRef\]](#)
30. Weinberg, J.M. Lipotoxicity. *Kidney Int.* **2006**, *70*, 1560–1566. [\[CrossRef\]](#)
31. Erpicum, P.; Rowart, P.; Defraigne, J.O.; Krzesinski, J.M.; Jouret, F. What We Need to Know about Lipid-Associated Injury in Case of Renal Ischemia-Reperfusion. *Am. J. Physiol.-Ren. Physiol.* **2018**, *315*, F1714–F1719. [\[CrossRef\]](#) [\[PubMed\]](#)
32. van der Veen, J.N.; Kennelly, J.P.; Wan, S.; Vance, J.E.; Vance, D.E.; Jacobs, R.L. The Critical Role of Phosphatidylcholine and Phosphatidylethanolamine Metabolism in Health and Disease. *Biochim. Biophys. Acta-Biomembr.* **2017**, *1859*, 1558–1572. [\[CrossRef\]](#) [\[PubMed\]](#)
33. Rao, S.; Walters, K.B.; Wilson, L.; Chen, B.; Bolisetty, S.; Graves, D.; Barnes, S.; Agarwal, A.; Kabarowski, J.H. Early Lipid Changes in Acute Kidney Injury Using SWATH Lipidomics Coupled with MALDI Tissue Imaging. *Am. J. Physiol.-Ren. Physiol.* **2016**, *310*, F1136–F1147. [\[CrossRef\]](#) [\[PubMed\]](#)
34. Solati, Z.; Edell, A.L.; Shang, Y.; Karmin, O.; Ravandi, A. Oxidized Phosphatidylcholines Are Produced in Renal Ischemia Reperfusion Injury. *PLoS ONE* **2018**, *13*, e0195172. [\[CrossRef\]](#)
35. Tofte, N.; Suvitaival, T.; Ahonen, L.; Winther, S.A.; Theilade, S.; Frimodt-Møller, M.; Ahluwalia, T.S.; Rossing, P. Lipidomic Analysis Reveals Sphingomyelin and Phosphatidylcholine Species Associated with Renal Impairment and All-Cause Mortality in Type 1 Diabetes. *Sci. Rep.* **2019**, *9*, 16398. [\[CrossRef\]](#)
36. Zhao, X.; Chen, J.; Ye, L.; Xu, G. Serum Metabolomics Study of the Acute Graft Rejection in Human Renal Transplantation Based on Liquid Chromatography-Mass Spectrometry. *J. Proteome Res.* **2014**, *13*, 2659–2667. [\[CrossRef\]](#)
37. Hou, B.; He, P.; Ma, P.; Yang, X.; Xu, C.; Lam, S.M.; Shui, G.; Yang, X.; Zhang, L.; Qiang, G.; et al. Comprehensive Lipidome Profiling of the Kidney in Early-Stage Diabetic Nephropathy. *Front. Endocrinol.* **2020**, *11*, 359. [\[CrossRef\]](#)
38. Łuczykowski, K.; Warmuzińska, N.; Operacz, S.; Stryjak, I.; Bogusiewicz, J.; Jacyna, J.; Wawrzyniak, R.; Struck-Lewicka, W.; Markuszewski, M.J.; Bojko, B. Metabolic Evaluation of Urine from Patients Diagnosed with High Grade (Hg) Bladder Cancer by Spme-Lc-Ms Method. *Molecules* **2021**, *26*, 2194. [\[CrossRef\]](#)
39. Łuczykowski, K.; Warmuzińska, N.; Kollmann, D.; Selzner, M.; Bojko, B. Biliary Metabolome Profiling for Evaluation of Liver Metabolism and Biliary Tract Function Related to Organ Preservation Method and Degree of Ischemia in a Porcine Model. *Int. J. Mol. Sci.* **2023**, *24*, 2127. [\[CrossRef\]](#)
40. Sato, E.; Kohno, M.; Yamamoto, M.; Fujisawa, T.; Fujiwara, K.; Tanaka, N. Metabolomic Analysis of Human Plasma from Haemodialysis Patients. *Eur. J. Clin. Investig.* **2011**, *41*, 241–255. [\[CrossRef\]](#)
41. Grams, M.E.; Tin, A.; Rebholz, C.M.; Shafi, T.; Köttgen, A.; Perrone, R.D.; Sarnak, M.J.; Inker, L.A.; Levey, A.S.; Coresh, J. Metabolomic Alterations Associated with Cause of CKD. *Clin. J. Am. Soc. Nephrol.* **2017**, *12*, 1787–1794. [\[CrossRef\]](#) [\[PubMed\]](#)
42. Pieniazek, A.; Bernasinska-slomczewska, J.; Gwozdziński, L. Uremic Toxins and Their Relation with Oxidative Stress Induced in Patients with Ckd. *Int. J. Mol. Sci.* **2021**, *22*, 6196. [\[CrossRef\]](#) [\[PubMed\]](#)

43. Sun, B.; Wang, X.; Liu, X.; Wang, L.; Ren, F.; Wang, X.; Leng, X. Hippuric Acid Promotes Renal Fibrosis by Disrupting Redox Homeostasis via Facilitation of NRF2–KEAP1–CUL3 Interactions in Chronic Kidney Disease. *Antioxidants* **2020**, *9*, 783. [\[CrossRef\]](#) [\[PubMed\]](#)
44. Zhang, M.; Jia, S.; Liu, Y.; Liu, Y.; Li, S.; Bo, L.; Zhao, X.; Sun, C. Metabonomics Analysis of Kidneys in Rats Administered with Chronic Low-Dose Cadmium by Ultra-Performance Liquid Chromatography–Mass Spectrometry. *J. Appl. Toxicol.* **2019**, *39*, 441–450. [\[CrossRef\]](#) [\[PubMed\]](#)
45. Gu, L.; Wang, X.; Zhang, Y.; Jiang, Y.; Lu, H.; Bi, K.; Chen, X. Determination of 12 Potential Nephrotoxicity Biomarkers in Rat Serum and Urine by Liquid Chromatography with Mass Spectrometry and Its Application to Renal Failure Induced by Semen Strychni. *J. Sep. Sci.* **2014**, *37*, 1058–1066. [\[CrossRef\]](#)
46. Herrmann, W.; Schorr, H.; Obeid, R.; Makowski, J.; Fowler, B.; Kuhlmann, M.K. Disturbed Homocysteine and Methionine Cycle Intermediates S-Adenosylhomocysteine and S-Adenosylmethionine Are Related to Degree of Renal Insufficiency in Type 2 Diabetes. *Clin. Chem.* **2005**, *51*, 891–897. [\[CrossRef\]](#)
47. Valli, A.; Carrero, J.J.; Qureshi, A.R.; Garibotto, G.; Bárány, P.; Axelsson, J.; Lindholm, B.; Stenvinkel, P.; Anderstam, B.; Suliman, M.E. Elevated Serum Levels of S-Adenosylhomocysteine, but Not Homocysteine, Are Associated with Cardiovascular Disease in Stage 5 Chronic Kidney Disease Patients. *Clin. Chim. Acta* **2008**, *395*, 106–110. [\[CrossRef\]](#)
48. Zhu, S.; Zhang, F.; Shen, A.W.; Sun, B.; Xia, T.Y.; Chen, W.S.; Tao, X.; Yu, S.Q. Metabolomics Evaluation of Patients With Stage 5 Chronic Kidney Disease Before Dialysis, Maintenance Hemodialysis, and Peritoneal Dialysis. *Front. Physiol.* **2021**, *11*, 630646. [\[CrossRef\]](#)
49. Chen, T.H.; Liu, C.W.; Ho, Y.H.; Huang, C.K.; Hung, C.S.; Smith, B.H.; Lin, J.C. Gut Microbiota Composition and Its Metabolites in Different Stages of Chronic Kidney Disease. *J. Clin. Med.* **2021**, *10*, 3881. [\[CrossRef\]](#)
50. Yang, J.; Fang, P.; Yu, D.; Zhang, L.; Zhang, D.; Jiang, X.; Yang, W.Y.; Bottiglieri, T.; Kunapuli, S.P.; Yu, J.; et al. Chronic Kidney Disease Induces Inflammatory CD40+ Monocyte Differentiation via Homocysteine Elevation and DNA Hypomethylation. *Circ. Res.* **2016**, *119*, 1226–1241. [\[CrossRef\]](#)
51. Klepacki, J.; Brunner, N.; Schmitz, V.; Klawitter, J.; Christians, U.; Klawitter, J. Development and Validation of an LC-MS/MS Assay for the Quantification of the Trans-Methylation Pathway Intermediates S-Adenosylmethionine and S-Adenosylhomocysteine in Human Plasma. *Clin. Chim. Acta* **2013**, *421*, 91–97. [\[CrossRef\]](#) [\[PubMed\]](#)
52. Kordalewska, M.; Macioszek, S.; Wawrzyniak, R.; Sikorska-Wisniewska, M.; Śledziński, T.; Chmielewski, M.; Mika, A.; Markuszewski, M.J. Multiplatform Metabolomics Provides Insight into the Molecular Basis of Chronic Kidney Disease. *J. Chromatogr. B Anal. Technol. Biomed. Life Sci.* **2019**, *1117*, 49–57. [\[CrossRef\]](#) [\[PubMed\]](#)
53. Andrianova, N.V.; Popkov, V.A.; Klimenko, N.S.; Tyakht, A.V.; Baydakova, G.V.; Frolova, O.Y.; Zorova, L.D.; Pevzner, I.B.; Zorov, D.B.; Plotnikov, E.Y. Microbiome-Metabolome Signature of Acute Kidney Injury. *Metabolites* **2020**, *10*, 142. [\[CrossRef\]](#)
54. Breit, M.; Weinberger, K.M. Metabolic Biomarkers for Chronic Kidney Disease. *Arch. Biochem. Biophys.* **2016**, *589*, 62–80. [\[CrossRef\]](#) [\[PubMed\]](#)
55. Hoher, B.; Adamski, J. Metabolomics for Clinical Use and Research in Chronic Kidney Disease. *Nat. Rev. Nephrol.* **2017**, *13*, 269–284. [\[CrossRef\]](#) [\[PubMed\]](#)
56. Goek, O.N.; Döring, A.; Gieger, C.; Heier, M.; Koenig, W.; Prehn, C.; Römisch-Margl, W.; Wang-Sattler, R.; Illig, T.; Suhre, K.; et al. Serum Metabolite Concentrations and Decreased GFR in the General Population. *Am. J. Kidney Dis.* **2012**, *60*, 197–206. [\[CrossRef\]](#)
57. Dare, A.J.; Pettigrew, G.J.; Saeb-Parsy, K. Preoperative Assessment of the Deceased-Donor Kidney: From Macroscopic Appearance to Molecular Biomarkers. *Transplantation* **2014**, *97*, 797–807. [\[CrossRef\]](#)
58. Traynor, C.; Saeed, A.; O’Ceallaigh, E.; Elbadri, A.; O’Kelly, P.; de Freitas, D.G.; Dorman, A.M.; Conlon, P.J.; O’Seaghdha, C.M. Pre-Transplant Histology Does Not Improve Prediction of 5-Year Kidney Allograft Outcomes above and beyond Clinical Parameters. *Ren. Fail.* **2017**, *39*, 671–677. [\[CrossRef\]](#)
59. Yap, Y.T.; Ho, Q.Y.; Kee, T.; Ng, C.Y.; Chionh, C.Y. Impact of Pre-Transplant Biopsy on 5-Year Outcomes of Expanded Criteria Donor Kidney Transplantation. *Nephrology* **2021**, *26*, 70–77. [\[CrossRef\]](#)
60. De Vusser, K.; Lerut, E.; Kuypers, D.; Vanrenterghem, Y.; Jochmans, I.; Monbaliu, D.; Pirenne, J.; Naesens, M. The Predictive Value of Kidney Allograft Baseline Biopsies for Long-Term Graft Survival. *J. Am. Soc. Nephrol.* **2013**, *24*, 1913–1923. [\[CrossRef\]](#)
61. Phillips, B.L.; Kassimatis, T.; Atalar, K.; Wilkinson, H.; Kessaris, N.; Simmonds, N.; Hilton, R.; Horsfield, C.; Callaghan, C.J. Chronic Histological Changes in Deceased Donor Kidneys at Implantation Do Not Predict Graft Survival: A Single-Centre Retrospective Analysis. *Transpl. Int.* **2019**, *32*, 523–534. [\[CrossRef\]](#) [\[PubMed\]](#)
62. Azancot, M.A.; Moreso, F.; Salcedo, M.; Cantarell, C.; Perello, M.; Torres, I.B.; Montero, A.; Trilla, E.; Sellarés, J.; Morote, J.; et al. The Reproducibility and Predictive Value on Outcome of Renal Biopsies from Expanded Criteria Donors. *Kidney Int.* **2014**, *85*, 1161–1168. [\[CrossRef\]](#) [\[PubMed\]](#)
63. Mirnaghi, F.S.; Chen, Y.; Sidisky, L.M.; Pawliszyn, J. Optimization of the Coating Procedure for a High-Throughput 96-Blade Solid Phase Microextraction System Coupled with LC-MS/MS for Analysis of Complex Samples. *Anal. Chem.* **2011**, *83*, 6018–6025. [\[CrossRef\]](#) [\[PubMed\]](#)

**Disclaimer/Publisher’s Note:** The statements, opinions and data contained in all publications are solely those of the individual author(s) and contributor(s) and not of MDPI and/or the editor(s). MDPI and/or the editor(s) disclaim responsibility for any injury to people or property resulting from any ideas, methods, instructions or products referred to in the content.

# Supplementary Information

## Metabolomic and lipidomic profiling for pre-transplant risk assessment of delayed graft function using chemical biopsy with microextraction probes

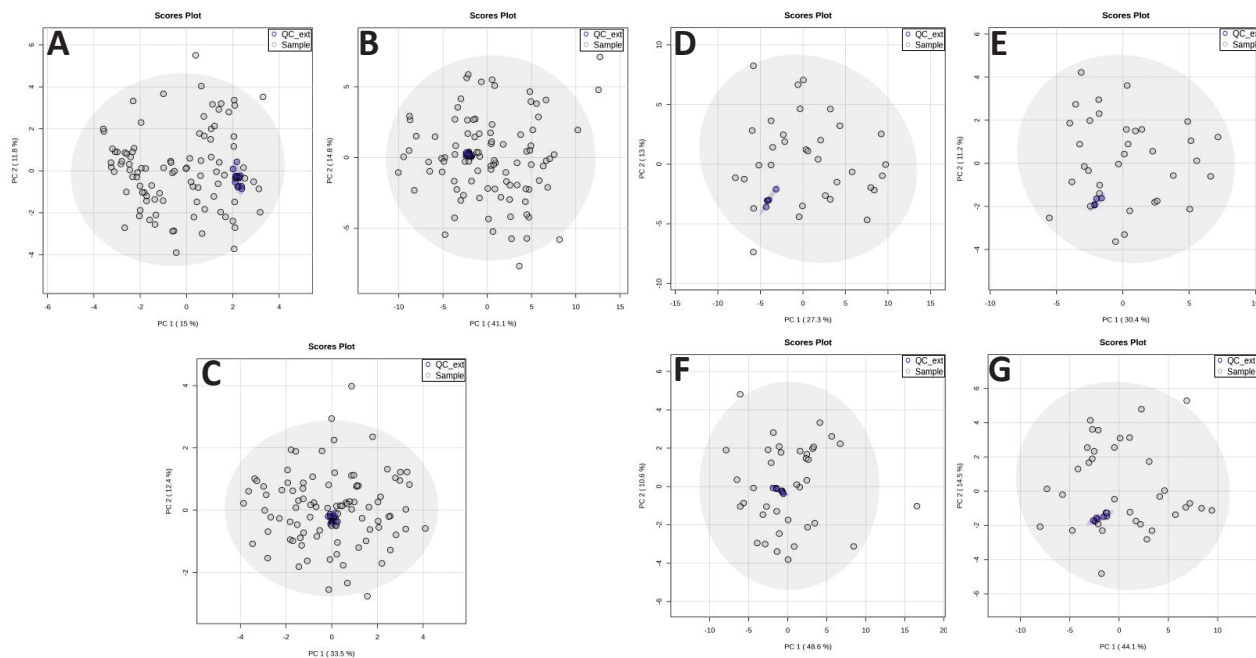
Natalia Warmużńska<sup>1</sup>, Kamil Łuczykowski<sup>1</sup>, Iga Stryjak<sup>1</sup>, Emilia Wojtal<sup>2</sup>, Aleksandra Woderska-Jasińska<sup>2</sup>, Marek Masztalerz<sup>2</sup>, Zbigniew Włodarczyk<sup>2</sup>, Barbara Bojko<sup>1</sup>

<sup>1</sup>Department of Pharmacodynamics and Molecular Pharmacology, Faculty of Pharmacy, Collegium Medicum in Bydgoszcz, Nicolaus Copernicus University in Torun, Bydgoszcz, Poland

<sup>2</sup>Department of Transplantology and General Surgery, Collegium Medicum in Bydgoszcz, Antoni Jurasz University Hospital No. 1 in Bydgoszcz, Nicolaus Copernicus University in Torun, Bydgoszcz, Poland

**Table S1.** Donors laboratory test results whose kidneys were associated with delayed graft function (DGF) in recipients.

Characteristic	Total (n=32)	non DGF (n=22 )	DGF (n=10)	p-value
Ischemia time	17h26min (7h09min)	16h03min (7h06min)	20h27min (6h35min)	>0.05
Creatinine, mg/dL	1.27 [0.98-2.13]	1.35 [1.05-2.13]	1.15 [0.90-1.50]	>0.05
Urea, mg/dL	45.00 [37.20-62.00]	47.00 [37.20-90.00]	39.30 [24.70-48.00]	>0.05
CRP, mg/L	256.09 (127.38)	242.85 (134.01)	285.21 (112.29)	>0.05
Procalcitonin, ng/mL	1.37 [0.57-9.12]	5.35 [0.57-9.12]	1.07 [0.44-2.05]	>0.05
WBC, 10 <sup>3</sup> /uL	12.98 [11.75-18.40]	12.96 [11.70-16.70]	13.52 [11.78-20.10]	>0.05
HGB, g/dL	10.50 [8.80-13.75]	9.90 [8.50-14.00]	11.40 [10.20-12.60]	>0.05
PLT, 10 <sup>3</sup> /uL	145.50 [92.00-169.50]	146.00 [92.00-171.00]	139.00 [127.00-168.00]	>0.05
AST, IU/L	68.00 [31.00-98.00]	54.00 [29.00-95.00]	68.00 [52.00-132.00]	>0.05
ALT, IU/L	51.00 [26.00-103.00]	62.00 [26.00-109.00]	46.00 [45.00-60.00]	>0.05
K, mmol/L	4.21 (0.74)	4.22 (0.63)	4.20 (0.99)	>0.05
Na, mmol/L	156.59 (11.82)	154.24 (9.89)	161.77 (14.47)	>0.05
Cl, mmol/L	117.62 (11.63)	115.62 (10.06)	121.43 (13.93)	>0.05



**Figure S1.** Principal component analysis (PCA) plots of all analyzed samples and extraction quality control (QC) samples for chemical biopsy analysis: (A) metabolomics, (B) Lipidomics RP, (C) Lipidomics HILIC, and plasma samples analysis: (D) Metabolomics – RP Positive ionization mode, (E) Metabolomics – RP Negative ionization mode, (F) Lipidomics - RP Positive ionization mode, (G) Lipidomics - HILIC Positive ionization mode.

**Table S2.** Metabolites with the highest MDA and MDG values for each analytical block.

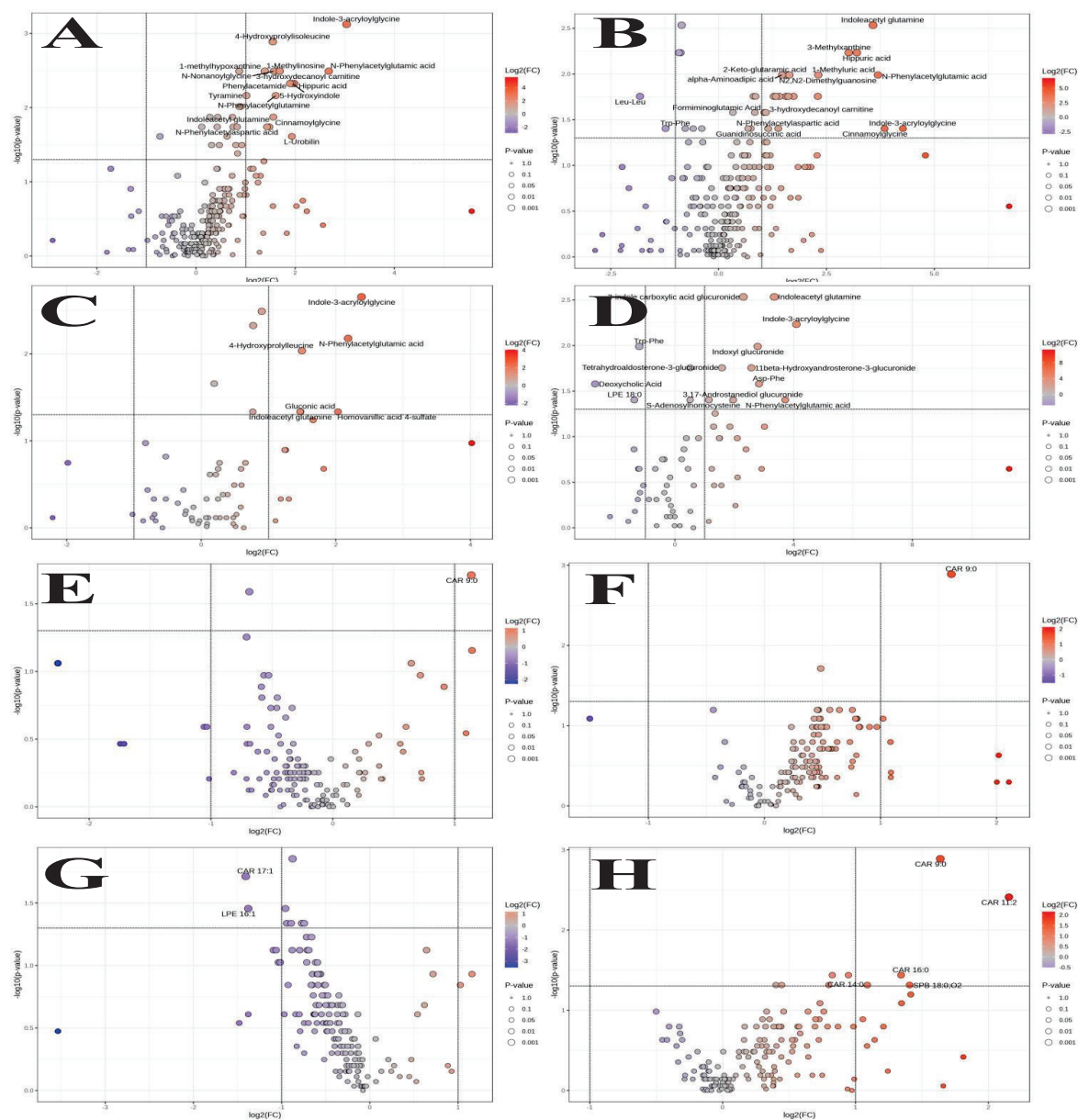
Name	MW	RT	Mean Decrease Accuracy	Mean Decrease Gini
<b>Metabolomics</b>				
Time point 1				
Pyroglutamic acid	129.04	1.75	8.752	1.551
4-oxo-2-nonenal	154.10	10.09	6.484	0.917
N-Butyryl-L-homoserine lactone	171.09	1.74	5.937	0.859
Ornithine	132.09	1.88	5.731	0.889
Glutaric acid	132.04	1.32	4.705	0.474
Tetramethylpyrazine	136.10	8.95	3.819	0.601
Heptylic acid	130.10	1.69	3.305	0.506
Glyceraldehyde 3-phosphate	169.99	2.11	3.870	0.433
Carnitine	161.11	3.35	3.570	0.226
Dopamine	153.08	9.93	3.371	0.452
4-Nitroaniline	138.04	6.84	2.658	0.602
Leucine	131.09	9.14	1.558	0.533
Nicotine glucuronide	338.15	16.46	0.056	0.456
Time point 2				
Phosphoethanolamine	141.01	11.70	5.746	0.613
Glutamic acid	147.05	1.53	5.577	0.683
Glyceraldehyde 3-phosphate	169.99	2.11	5.243	0.913
Histidine	155.07	1.90	5.065	0.644
1-Nitronaphthalene-5,6-oxide	189.04	24.76	4.992	0.581
Adenosine	267.10	7.28	4.805	0.643
Carnitine	161.11	3.35	4.369	0.852
Homocycloleucine	143.09	1.75	5.215	0.553
3,5-Dihydroxypentanoic acid	134.06	1.73	4.545	0.296
7-Methyl-2,6,9,12-tetraoxahexadecane	248.20	14.09	4.523	0.358
NA-Val 18:0	383.34	22.19	4.090	0.607
5-Aminopentanoic acid	117.08	1.70	3.851	0.601
Tetramethylpyrazine	136.10	8.95	4.251	0.564
Time point 3				
Phosphoethanolamine	141.01	11.70	9.547	1.966
3-Indolebutyric acid	203.10	13.52	6.979	1.343
NA-Val 18:0	383.34	22.19	6.040	0.896
4-Hydroxynonenal	156.12	11.86	5.431	0.606
Creatine	131.07	1.98	4.971	0.735
Adenosine	267.10	7.28	4.912	0.806
Arginine	174.11	2.01	4.456	0.636
Dopamine	153.08	9.93	3.553	0.383
Taurine	125.01	1.26	3.092	0.261
3,5-Dihydroxypentanoic acid	134.06	1.73	3.006	0.251
Glyceraldehyde 3-phosphate	169.99	2.11	1.335	0.510
Heptylic acid	130.10	1.69	2.699	0.438
Pyroglutamic acid	129.04	1.75	2.747	0.389

Lipidomics HILIC				
Time point 1				
SM 42:1;O2	814.69	7.78	6.180	1.053
PC 38:5	807.58	6.48	5.532	0.638
PC 34:1	759.58	6.53	5.511	0.813
SM 40:2;O2	784.65	7.94	5.046	0.536
PC 38:6	805.56	6.49	4.820	0.459
LPC 18:0	523.36	8.84	4.474	0.467
SM 34:1;O2	702.57	8.16	4.317	0.483
PE 38:5	765.53	7.42	4.289	0.549
PE O-38:5	751.55	7.26	4.591	0.408
PE 34:1	717.53	7.46	4.248	0.399
PC O-34:2	743.58	6.59	2.375	0.547
PC 38:4	809.59	6.46	3.967	0.422
Time point 2				
PE 38:5	765.53	7.56	7.547	0.981
PC 34:1	759.58	6.62	6.284	0.636
PC P-34:2	741.57	6.58	4.900	0.514
PE 38:6	763.52	7.45	4.734	0.673
SM 40:1;O2	786.66	7.91	4.687	0.567
PE 36:3	741.53	7.45	4.670	0.495
PC 38:5	807.58	6.48	4.280	0.468
LPE 18:0	481.32	10.34	4.040	0.519
LPC P-16:0	479.34	8.58	4.035	0.363
PC 36:3	783.58	6.49	3.274	0.554
Time point 3				
PE 38:6	763.52	7.45	6.126	0.854
PE 36:3	741.53	7.45	5.718	0.716
PC 36:4	781.56	6.52	5.468	0.756
PE 36:2	743.55	7.56	5.324	0.660
PE 36:4	739.52	7.46	4.985	0.655
PC 36:3	783.58	6.49	4.715	0.589
PC 34:2	757.56	6.69	4.289	0.493
SM 40:2;O2	784.65	7.94	4.819	0.356
SM 36:1;O2	730.6	8.03	4.441	0.350
SM 40:1;O2	786.66	7.91	4.368	0.400
PE 40:7	789.53	7.42	3.929	0.841
PE P-36:1	729.57	7.38	4.188	0.528
PC 33:4	739.52	7.47	3.712	0.520
Lipidomics RP				
Time point 1				
TG 56:0	918.86	14.63	4.684	0.500
TG 48:5	796.66	12.52	4.027	0.456
TG P-52:1	846.80	14.11	3.750	0.295
Cer 34:0;O2	539.53	10.70	3.701	0.249
TG 50:1	832.75	13.77	3.282	0.247
Cer 32:0;O2	511.50	9.99	3.247	0.293

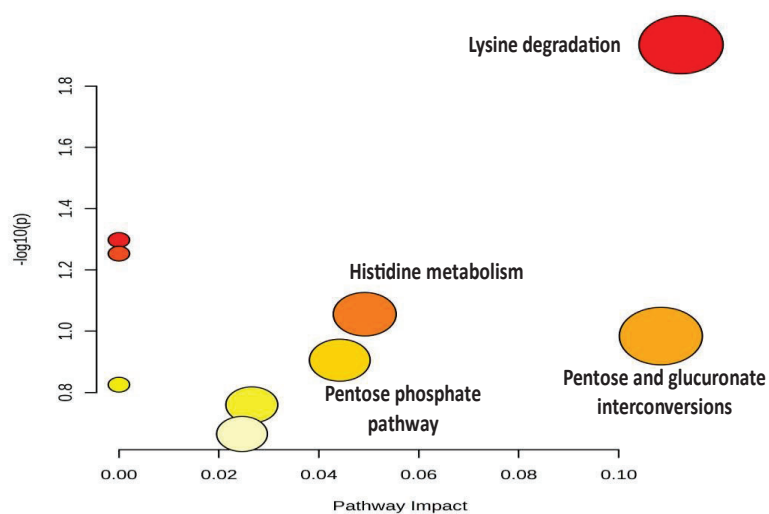
DG 36:3	618.52	10.46	3.361	0.186
TG 54:1	888.81	14.27	3.225	0.178
TG 53:3	870.77	13.75	3.085	0.157
TG 50:0	834.77	13.99	3.052	0.146
DG 36:2	620.54	10.88	3.029	0.375
TG 34:0	610.52	11.14	2.175	0.275
TG 46:5	768.63	12.63	2.497	0.244
DG 35:1	608.54	11.02	2.953	0.235
Time point 2				
TG 56:0	918.86	14.63	5.891	0.650
DG 36:4	616.51	10.03	5.395	0.654
DG 36:3	618.52	10.46	4.257	0.376
TG O-52:1	846.80	14.35	4.099	0.274
TG 44:3	744.63	12.81	3.955	0.252
TG 42:0	722.64	12.81	3.807	0.269
TG 50:0	834.77	13.99	3.676	0.266
TG 54:2	886.80	14.08	3.258	0.287
TG 54:1	888.81	14.27	3.348	0.138
TG 50:4	826.71	13.13	3.237	0.144
DG 36:2	620.54	10.88	2.556	0.287
DG 32:2	564.48	9.55	2.943	0.275
Time point 3				
DG 34:1	594.52	10.73	5.148	0.642
TG 56:2	914.83	14.30	4.383	0.378
TG 54:1	888.81	14.24	4.256	0.404
TG 52:0	862.80	14.23	4.221	0.388
TG 55:2	900.81	14.13	4.041	0.326
TG 54:6	878.74	13.94	3.921	0.261
TG 50:2	830.74	13.57	3.615	0.236
TG 56:3	912.81	14.08	3.608	0.238
TG 56:6	906.77	13.71	4.061	0.229
DG 55:2	886.84	13.61	3.700	0.191
TG 50:0	834.77	13.99	3.004	0.289
TG 55:4	896.78	14.16	3.379	0.288

**Table S3.** Results of pathway analysis of metabolites selected for Random Forest models from metabolomic and lipidomic analyses

Pathway name	Match status	p	FDR
Arginine biosynthesis	3/14	0.000192	0.007836
Arginine and proline metabolism	4/36	0.000196	0.007836
Glutathione metabolism	3/28	0.001608	0.042886
Glycerophospholipid metabolism	3/36	0.00336	0.067201
Histidine metabolism	2/16	0.008204	0.13126
Linoleic acid metabolism	1/5	0.043716	0.58288
Nitrogen metabolism	1/6	0.052243	0.59707
alpha-Linolenic acid metabolism	1/13	0.10999	0.93626
Butanoate metabolism	1/15	0.12587	0.93626
Glycosylphosphatidylinositol (GPI)-anchor biosynthesis	1/15	0.12587	0.93626
Glycerolipid metabolism	1/16	0.13372	0.93626
Fructose and mannose metabolism	1/20	0.16445	0.93626
beta-Alanine metabolism	1/21	0.17197	0.93626
Pentose phosphate pathway	1/23	0.18683	0.93626
Glycolysis / Gluconeogenesis	1/26	0.20865	0.93626
Alanine, aspartate and glutamate metabolism	1/28	0.22289	0.93626
Lysine degradation	1/30	0.2369	0.93626
Inositol phosphate metabolism	1/30	0.2369	0.93626
Porphyrin metabolism	1/31	0.24382	0.93626
Glyoxylate and dicarboxylate metabolism	1/32	0.25067	0.93626
Sphingolipid metabolism	1/32	0.25067	0.93626
Glycine, serine and threonine metabolism	1/33	0.25747	0.93626
Arachidonic acid metabolism	1/44	0.32857	1
Metabolism of xenobiotics by cytochrome P450	1/68	0.46233	1
Purine metabolism	1/70	0.47227	1



**Figure S2.** Volcano plots showing differences between DGF and non-DCD DGF groups: (A) metabolomic analysis in positive ionization mode on POD1, (B) metabolomic analysis in positive ionization mode on POD5, (C) metabolomic analysis in negative ionization mode on POD1, (D) metabolomic analysis in negative ionization mode on POD5, (E) lipidomics analysis - RP positive ionization mode on POD1, (F) lipidomics analysis - RP positive ionization mode on POD5, (G) lipidomics analysis - HILIC positive ionization mode on POD1, (H) lipidomics analysis - HILIC positive ionization mode on POD5.



**Figure S3.** Pathway analysis of significantly differential features from plasma metabolomic and lipidomic analyses.

**Table S4.** Results of pathway analysis of significantly differential features from plasma metabolomic and lipidomic analyses.

Pathway name	Match status	p	FDR
Lysine degradation	2/30	0.011624	0.92993
Ascorbate and aldarate metabolism	1/9	0.050394	1
Caffeine metabolism	1/10	0.055851	1
Histidine metabolism	1/16	0.088015	1
Pentose and glucuronate interconversions	1/19	0.10373	1
Pentose phosphate pathway	1/23	0.12431	1
Alanine, aspartate and glutamate metabolism	1/28	0.14944	1
Cysteine and methionine metabolism	1/33	0.17392	1
Tyrosine metabolism	1/42	0.21642	1

## 8. Wnioski

- Mikroekstrakcja do fazy stałej pozwala na monitorowanie zmian zachodzących w narządzie podczas całej procedury przeszczepienia- od pobrania narządu, przez jego przechowywanie, aż po reperfuzję, a w połączeniu z analizą UHPLC-MS umożliwia identyfikację licznych związków o zróżnicowanej polarności.
- Temperatura przechowywania narządu ma większy wpływ na profil lipidomiczny nerki niż mechaniczny charakter metody konserwacji.
- Zastosowanie perfuzji normotermicznej powodowało mniejszą kumulację lipidów związanych z uszkodzeniem niedokrwienno-reperfuzyjnym, dysfunkcją mitochondrialną, działaniem prozapalnym i stresem oksydacyjnym, co wskazuje, że jej zastosowanie może korzystnie wpływać na funkcję narządu.
- Wśród zidentyfikowanych związków najbardziej obiecującymi do stworzenia panelu oceniającego ryzyko wystąpienia powikłań oraz funkcję narządu są głównie aminokwasy i ich pochodne, nukleotydy, kwasy organiczne, peptydy oraz lipidy z grup LPC, LPE, CAR, TG, PE i PC.
- Zastosowanie biopsji chemicznej w warunkach klinicznych nie wydłuża czasu zimnego niedokrwienia ani nie zaburza przebiegu procedury przeszczepienia, co znacząco zwiększa jej potencjał translacyjny oraz może ułatwić wdrożenie do rutynowej diagnostyki.
- Potencjalna wartość predykcyjna zidentyfikowanych związków musi zostać potwierdzona w przyszłych badaniach z udziałem większej grupy pacjentów.

## 9. Bibliografia

1. Swanson, K.J.; Aziz, F.; Garg, N.; Mohamed, M.; Mandelbrot, D.; Djamali, A.; Parajuli, S. Role of novel biomarkers in kidney transplantation. *World J. Transplant.* **2020**, *10*, 230–255, doi:<https://dx.doi.org/10.5500/wjt.v10.i9.230>.
2. Eurotransplant: Statistics Report Library. Dostęp online na: <https://statistics.eurotransplant.org/>. Data ostatniego wejścia: 20.04.2025.
3. Do Nguyen, H.; Yong, K.; Croke, R.; Lim, W.H. The Impact of Donor Type and Quality on Renal Transplant Outcomes. In *Understanding the Complexities of Kidney Transplantation*; 2011; pp. 189–214 ISBN 0000957720.
4. Moeckli, B.; Sun, P.; Lazeyras, F.; Morel, P.; Moll, S.; Pascual, M.; Bühler, H. Evaluation of donor kidneys prior to transplantation: an update of current and emerging methods. *Transpl. Int.* **2019**, *32*, 459–469, doi:10.1111/tri.13430.
5. Rege, A.; Irish, B.; Castleberry, A.; Vikraman, D.; Sanoff, S.; Ravindra, K.; Collins, B.; Sudan, D. Trends in Usage and Outcomes for Expanded Criteria Donor Kidney Transplantation in the United States Characterized by Kidney Donor Profile Index. *Cureus* **2016**, *8*, e887, doi:10.7759/cureus.887.
6. McGuinness, D.; Mohammed, S.; Monaghan, L.; Wilson, P.A.; Kingsmore, D.B.; Shapter, O.; Stevenson, K.S.; Coley, S.M.; Devey, L.; Kirkpatrick, R.B.; et al. A molecular signature for delayed graft function. *Aging Cell* **2018**, *17*, e12825, doi:10.1111/accel.12825.
7. Mezzolla, V.; Pontrelli, P.; Fiorentino, M.; Stasi, A.; Franzin, R.; Rascio, F.; Grandaliano, G.; Stallone, G.; Infante, B.; Gesualdo, L.; et al. Emerging biomarkers of delayed graft function in kidney transplantation. *Transplant. Rev.* **2021**, *35*, 100629, doi:10.1016/j.trre.2021.100629.
8. Bojko, B. Solid-phase microextraction: a fit-for-purpose technique in biomedical analysis. *Anal. Bioanal. Chem.* **2022**, *414*, 7005–7013, doi:10.1007/s00216-022-04138-9.
9. Reyes-Garcés, N.; Boyacı, E.; Gómez-Ríos, G.A.; Olkiewicz, M.; Monnin, C.; Bojko, B;

- Vuckovic, D.; Pawliszyn, J. Assessment of solid phase microextraction as a sample preparation tool for untargeted analysis of brain tissue using liquid chromatography-mass spectrometry. *J. Chromatogr. A* **2021**, *1638*, 11–13, doi:10.1016/j.chroma.2020.461862.
10. Cuevas-Delgado, P.; Warmuzińska, N.; Łuczykowski, K.; Bojko, B.; Barbas, C. Exploring sample treatment strategies for untargeted metabolomics: A comparative study of solid phase microextraction (SPME) and homogenization with solid-liquid extraction (SLE) in renal tissue. *Anal. Chim. Acta* **2024**, *1312*, doi:10.1016/j.aca.2024.342758.
  11. Ramani Venkata, A.; Ramesh, M. A Concise Review on Lipidomics Analysis in Biological Samples. *ADMET DMPK* **2021**, *9*, 1–22, doi:10.5599/admet.913.
  12. Han, X.; Gross, R.W. The foundations and development of lipidomics. *J. Lipid Res.* **2022**, *63*, 100164, doi:10.1016/j.jlr.2021.100164.
  13. Zhao, Y.Y.; Vaziri, N.D.; Lin, R.C. Lipidomics: New insight into kidney disease. *Adv. Clin. Chem.* **2015**, *68*, 153–175, doi:10.1016/bs.acc.2014.11.002.

## 10. Spis rycin

<b>Rycina 1.</b> Wykresy punktowe PLS-DA przedstawiające rozdział między perfuzjami HBD i DCD. Analizy lipidomiczne z użyciem rozdziału (A) HILIC i (B) RP.....	70
<b>Rycina 2.</b> Wykresy analizy PCA przedstawiające rozdzielanie pomiędzy różnymi typami konserwacji nerek. Analiza HILIC w trybie jonizacji dodatniej (A) i ujemnej (B) oraz analiza RP w trybie jonizacji dodatniej (C) i ujemnej (D). ....	111
<b>Rycina 3.</b> Schemat badania - badanie obejmowało próbki pobrane z nerek pozyskanych od dawców zmarłych oraz próbki osocza od biorców narządów.....	141

## 11. Wykaz osiągnięć

### 11.1. Publikacje naukowe

- N. Warmuzińska, K. Łuczykowski, I. Stryjak, E. Wojtal, A. Woderska-Jasińska, M. Masztalerz, Z. Włodarczyk, B. Bojko: ***Metabolomic and lipidomic profiling for pre-transplant assessment of delayed graft function risk using chemical biopsy with microextraction probes***. Int. J. Mol. Sci., 2024, 25, 13502; punktacja MNiSW: 140, IF: 4,900
- K. Łuczykowski, N. Warmuzińska, K. Jaroch, D. Kollmann, M. Selzner, B. Bojko: ***Recent solid-phase microextraction-based analytical approaches for the profiling of biliary bile acids in pre-transplant assessments of liver grafts subjected to normothermic ex vivo liver perfusion***. Anal. Chim. Acta, 2024, 1318, 342954; punktacja MNiSW: 100, IF: 5,700
- P. Cuevas-Delgado, N. Warmuzińska, K. Łuczykowski, B. Bojko, C. Barbas: ***Exploring sample treatment strategies for untargeted metabolomics : a comparative study of solid phase microextraction (SPME) and homogenization with solid-liquid extraction (SLE) in renal tissue***. Anal. Chim. Acta, 2024, 1312, 342758; punktacja MNiSW: 100, IF: 5,700
- N. Warmuzińska, K. Łuczykowski, I. Stryjak, H. Rosales-Solano, P. Urbanellis, J. Pawliszyn, M. Selzner, B. Bojko: ***The impact of normothermic and hypothermic preservation methods on kidney lipidome—comparative study using chemical biopsy with microextraction probes***. Front. Mol. Biosci., 2024, 11, 1341108; punktacja MNiSW: 140, IF: 3,900
- I. Stryjak, N. Warmuzińska, K. Łuczykowski, K. Jaroch, P. Urbanellis, M. Selzner, B. Bojko: ***Metabolomic and lipidomic landscape of porcine kidney associated with kidney perfusion in heart beating donors and donors after cardiac death***. Transl Res., 2024, 267:79-90; punktacja MNiSW: 140, IF: 6,400
- K. Łuczykowski, N. Warmuzińska, D. Kollmann, M. Selzner, B. Bojko: ***Biliary Metabolome Profiling for Evaluation of Liver Metabolism and Biliary Tract Function Related to Organ Preservation Method and Degree of Ischemia in a Porcine Model***. Int. J. Mol. Sci., 2023, 24, 2127; punktacja MNiSW: 140, IF: 4,900

- K. Łuczykowski, N. Warmuzińska, B. Bojko: ***Solid phase microextraction – a promising tool for graft quality monitoring in solid organ transplantation.*** Separations, 2023, 10, 153; punktacja MNiSW: 20, IF: 2,500
- N. Warmuzińska, K. Łuczykowski, B. Bojko: ***A review of current and emerging trends in donor graft-quality assessment techniques.*** J. Clin. Med., 2022, 11, 487; punktacja MNiSW:140, IF: 3,900
- W. Filipiak, K. Żuchowska, M. Marszałek, D. Depka, T. Bogiel, N. Warmuzińska, B. Bojko: GC-MS profiling of volatile metabolites produced by Klebsiella pneumoniae. Front Mol Biosci., 2022, 9, 1019290; punktacja MNiSW:140, IF: 5,000
- K. Łuczykowski, N. Warmuzińska, B. Bojko: ***Current approaches to the analysis of bile and the determination of bile acids in various biological matrices as supportive tools to traditional diagnostic testing for liver dysfunction and biliary diseases.*** Trac-Trends Anal. Chem., 2021, 142, 116307; punktacja MNiSW: 140, IF: 14,908
- K. Łuczykowski, N. Warmuzińska, S. Operacz, I. Stryjak, J. Bogusiewicz, J. Jacyna, R. Wawrzyniak, W. Struck-Lewicka, M.J. Markuszewski, B. Bojko: ***Metabolic evaluation of urine from patients diagnosed with high grade (HG) bladder cancer by SPME-LC-MS method.*** Molecules, 2021, 26, 2194; punktacja MNiSW: 140, IF: 4,927
- I. Stryjak, N. Warmuzińska, J. Bogusiewicz, K. Łuczykowski, B. Bojko: ***Monitoring of the influence of long-term oxidative stress and ischemia on the condition of kidneys using solid-phase microextraction chemical biopsy coupled with liquid chromatography-high-resolution mass spectrometry.*** J. Sep. Sci., 2020, 43, 9-10; punktacja MNiSW: 70, IF: 3,645
- I. Stryjak, N. Warmuzińska, K. Łuczykowski, M. Hamar, P. Urbanellis, E. Wojtal, M. Masztalerz, M. Selzner, Z. Włodarczyk, B. Bojko: ***Using a chemical biopsy for graft quality assessment.*** Jove-J. Vis. Exp, 2020, 160, e60946; punktacja MNiSW: 70, IF: 1,355

Łączna punktacja MNiSW: 1480, IF: 67,735

### 11.2. Rozdziały w monografii naukowej

- A. Roszkowska, N. Warmuzińska, K. Łuczykowski, B. Bojko, **Chapter 17: SPME in Lipid Analysis w książce *Evolution of Solid Phase Microextraction Technology***; The Royal Society of Chemistry 2023, ISBN 9781839166808 punktacja MNiSW dla wydawnictw publikujących recenzowane monografie naukowe: 20
- A. Roszkowska, K. Łuczykowski, N. Warmuzińska, B. Bojko, **Chapter 13: SPME and Related Techniques in Biomedical Research w książce *Evolution of Solid Phase Microextraction Technology***; The Royal Society of Chemistry 2023, ISBN 9781839166808; punktacja MNiSW dla wydawnictw publikujących recenzowane monografie naukowe: 20

### 11.3. Wystąpienia konferencyjne

- N. Warmuzińska, K. Łuczykowski, I. Stryjak, D. Kollmann, P. Urbanellis, M. Selzner, B. Bojko: ***Mikroekstrakcja do fazy stałej jako nowa alternatywa diagnostyczna w transplantologii. 65. Zjazd Naukowy Polskiego Towarzystwa Chemicznego, 18.09.2023-22.09.2023, Toruń, Polska***
- P. Cuevas-Delgado, N. Warmuzińska, K. Łuczykowski, B. Bojko, C. Barbas: ***Untargeted metabolomics sample treatment strategies for renal tissue: a comparative study of solid phase microextraction (SPME) and homogenization-solid liquid extraction (Homo-SLE)***. 3rd Nordic Metabolomics Conference, October 18.10.2023-20.10.2023, Trondheim, Norwegia
- N. Warmuzińska, K. Łuczykowski, I. Stryjak, P. Urbanellis, M. Selzner, B.Bojko: ***Comparison of the impact of normothermic and hypothermic preservation methods on kidney lipidomic profile using spme chemical biopsy***. 21st Congress of the European Society for Organ Transplantation, 17.09.2023-20.09.2023, Ateny, Grecja
- K. Łuczykowski, N. Warmuzińska, D. Kollmann, M. Selzner, B. Bojko: ***Analysis of the bile metabolome to search for potential biomarkers of quality of the liver with particular emphasis on bile acids***. 21st Congress of the European Society for Organ Transplantation, 17.09.2023-20.09.2023, Ateny, Grecja
- N. Warmuzińska, K. Łuczykowski, I. Stryjak, D. Kollmann, P. Urbanellis, M. Selzner, B. Bojko: ***Solid phase microextraction: new diagnostic tool in transplant surgery***.

33rd International Symposium on Pharmaceutical and Biomedical Analysis (PBA 2023), 02.07.2023-06.07.2023, Ankara, Turcja

- K. Łuczykowski, N. Warmuzińska, I. Stryjak, D. Kollmann, M. Selzner, B. Bojko: ***Application of thin-film solid-phase microextraction to bile analysis: bile fingerprint as a prognostic marker during liver transplantation.*** 20th Biennial European Society for Organ Transplantation (ESOT) Congress, 29.08.2021-01.09.2021, Mediolan, Włochy
- N. Warmuzińska, I. Stryjak, K. Łuczykowski, M. Hamar, P. Urbanellis, M. Selzner, B. Bojko: ***Low invasive SPME tissue sampling as a new tool, for graft quality assessment.*** 20th Biennial European Society for Organ Transplantation (ESOT) Congress, 29.08.2021-01.09.2021, Mediolan, Włochy
- N. Warmuzińska, I. Stryjak, K. Łuczykowski, M. Hamar, P. Urbanellis, M. Selzner, B. Bojko: ***Identification of lipidomic changes by SPME-LC-MS as a graft quality assessment in kidney transplantation.*** 9th International Singapore Lipid Symposium "Lipidomic technologies and applications", 01.03.2021-05.03.2021, Singapur, Republika Singapuru
- K. Łuczykowski, N. Warmuzińska, I. Stryjak, D. Kollmann, M. Selzner, B. Bojko: ***Analysis of changes in bile acids concentration in bile in response to the degree of liver ischemia and the method of organ preservation.*** MSACL 2019 EU. The 6th European Congress & Exhibits : Mass Spectrometry: Applications to the Clinical Lab., 22.09.2019-26.09.2019, Salzburg, Austria
- I. Stryjak, N. Warmuzińska, K. Łuczykowski, M. Hamar, M. Selzner, B. Bojko: ***Solid phase microextraction (SPME) in kidney examination : LC-MS/MS-based identification of potentially significant metabolites in graft quality assessment.*** MSACL 2019 EU. The 6th European Congress & Exhibits : Mass Spectrometry: Applications to the Clinical Lab., 22.09.2019-26.09.2019, Salzburg, Austria
- N. Warmuzińska, I. Stryjak, K. Łuczykowski, J. Bogusiewicz, M. Hamar, M. Selzner B. Bojko: ***Graft quality assessment in kidney transplantation by monitoring lipidomic changes in the organ during transplantation using solid phase microextraction (SPME).*** MSACL 2019 EU. The 6th European Congress & Exhibits : Mass Spectrometry: Applications to the Clinical Lab., 22.09.2019-26.09.2019, Salzburg, Austria

- K. Łuczykowski, N. Warmuzińska, I. Stryjak, B. Bojko: ***Profilowanie metabolomiczne żółci z wykorzystaniem mikroekstrakcji do fazy stałej (SPME) : określenie zmian zachodzących w czasie perfuzji wątroby podczas zabiegu transplantacji.*** XI Interdyscyplinarna Konferencja Naukowa TYGIEL 2019 "Interdyscyplinarność kluczem do rozwoju", 23.03.2019-24.03.2019, Lublin, Polska
- I. Stryjak, N. Warmuzińska, K. Łuczykowski, B. Bojko: ***Mikroekstrakcja do fazy stałej (SPME) w badaniach nerek : identyfikacja metabolitów o potencjalnym znaczeniu diagnostycznym.*** XI Interdyscyplinarna Konferencja Naukowa TYGIEL 2019 "Interdyscyplinarność kluczem do rozwoju", 23.03.2019-24.03.2019, Lublin, Polska
- N. Warmuzińska, K. Łuczykowski, J. Bogusiewicz, B.Bojko: ***Lipidomika w badaniach in vivo: jak przygotować włókna SPME?.*** XI Interdyscyplinarna Konferencja Naukowa TYGIEL 2019 "Interdyscyplinarność kluczem do rozwoju", 23.03.2019-24.03.2019, Lublin, Polska

#### **11.4. Projekty naukowe**

- „Nowe narzędzia analityczne oparte na mikroekstrakcji do fazy stałej do poszukiwania i oznaczania biomarkerów jakości nerek selekcjonowanych do transplantacji oraz oceny wczesnej funkcji przeszczepu” - NCN Preludium 23 - **kierownik projektu**
- „Szybka i nieinwazyjna ocena okołotransplantacyjna ludzkich graftów wątroby poddanych perfuzji hipo- i normotermicznej” - NCN OPUS 21 - **wykonawca projektu**
- „Bezbiopsyjna analiza metabolomiczna i lipidomiczna nerek jako krok w kierunku lepszej oceny jakości narządów selekcjonowanych do transplantacji i uszkodzenia poreperfuzyjnego” - NCN OPUS 14 - **wykonawca projektu**

## 12. Opinia Komisji Bioetycznej

4/2017

Uniwersytet Mikołaja Kopernika w Toruniu  
Collegium Medicum im L. Rydygiera w Bydgoszczy

KOMISJA BIOETYCZNA

Ul. M. Skłodowskiej-Curie 9, 85-094 Bydgoszcz, tel.(052) 585-35-63, fax.(052) 585-38-11

KB 636/2017

Bydgoszcz, 24.10.2017r.

Działając na podstawie art.29 Ustawy z dnia 5 grudnia 1996 roku o zawodzie lekarza (Dz.U. z 1997 r. Nr 28 poz. 152 (wraz z późniejszymi zmianami), zarządzenia Ministra Zdrowia i Opieki Społecznej z dnia 11 maja 1999 r. w sprawie szczegółowych zasad powoływania i finansowania oraz trybu działania komisji bioetycznych (Dz.U.Nr 47 poz.480) oraz Zarządzeniem Nr 21 Rektora UMK z dnia 4 marca 2009 r. z późn. zm. w sprawie powołania oraz zasad działania Komisji Bioetycznej Uniwersytetu Mikołaja Kopernika w Toruniu przy Collegium Medicum im Ludwika Rydygiera w Bydgoszczy oraz zgodnie z zasadami zawartymi w ICH – GCP

**Komisja Bioetyczna przy UMK w Toruniu, Collegium Medicum w Bydgoszczy**

(skład podano w załączeniu), na posiedzeniu w dniu **24.10.2017r.** przeanalizowała wniosek, który złożyła kierownik badania:

**dr hab. n. farm. Barbara Bojko**  
**Katedra Farmakodynamiki i Farmakologii Molekularnej**  
**Collegium Medicum w Bydgoszczy**

z zespołem w składzie:

- prof. dr hab. n. med. Zbigniew Włodarczyk, dr hab. n. farm. Barbara Bojko,  
mgr farm. Iga Stryjak, mgr Joanna Bogusiewicz, mgr Natalia Warmuzińska,  
lek. med. Emilia Wojtal,

w sprawie badania:

**„Ocena jakości nerek selekcionowanych do transplantacji oraz badanie uszkodzenia poreperfuzyjnego za pomocą bezbiopsyjnej analizy metabolomicznej i lipidomicznej narządów.”**

Po zapoznaniu się ze złożonym wnioskiem i w wyniku przeprowadzonej dyskusji oraz głosowania Komisja podjęła

### **Uchwałę o pozytywnym zaopiniowaniu wniosku**

w sprawie przeprowadzenia badań, w zakresie określonym we wniosku pod warunkiem:

- poinformowania uczestników badania o celu oraz zakresie badań i uzyskania od każdego z nich osobnej, pisemnej, świadomej zgody na udział w badaniu, zgodnie z obowiązującymi przepisami, datowanej najpóźniej na moment rozpoczęcia badania a nie wcześniej niż data uzyskania z Komisji Bioetycznej zgody na takie badanie;
- zachowania tajemnicy wszystkich danych, w tym danych osobowych pacjentów, umożliwiających ich identyfikację w ewentualnych publikacjach;
- zapewnienia, że osoby uczestniczące w eksperymencie badawczym nie są ubezwłasnowolnione, nie są żołnierzami służby zasadniczej, nie są osobami pozbawionymi wolności, nie pozostają w zależności służbowej, dydaktycznej lub innej z prowadzącym badanie;
- sugerujemy uzyskanie podpisu uczestnika badania pod informacją o badaniu, lub sporządzenie formularza informacji i świadomej zgody na udział w badaniu na jednej kartce.

Jednocześnie informujemy, iż „Zgoda na udział w badaniu” winna zawierać m.in.: imię i nazwisko badanej osoby; Nr historii choroby pacjenta (L.ks.gl. Oddziału/Poradni) oraz datę i podpis badanej osoby, a także klauzulę, że uczestnik badania wyraża zgodę na przetwarzanie danych osobowych dotyczących realizacji tematu badawczego, z wyjątkiem publikacji danych osobowych.

Kierownik badania zobowiązany jest do przechowywania wszystkich dokumentów dotyczących badania przez okres dwudziestu lat.

***Zgoda obowiązuje od daty posiedzenia (24.10.2017 r.) do końca 2020 r.***

*Wydana opinia dotyczy tylko rozpatrywanego wniosku z uwzględnieniem przedstawionego projektu; każda zmiana i modyfikacja wymaga uzyskania odrębnej opinii. Wnioskodawca zobowiązany jest do informowania o wszelkich poprawkach, które mogłyby mieć wpływ na opinię Komisji oraz poinformowania o zakończeniu badania.*

*Od niniejszej uchwały podmiot zamierzający przeprowadzić eksperyment medyczny, kierownik zakładu opieki zdrowotnej, w której eksperyment medyczny ma być przeprowadzony, mogą wnieść odwołanie do Odwoławczej Komisji Bioetycznej przy Ministrze Zdrowia, za pośrednictwem Komisji Bioetycznej przy Collegium Medicum im. L. Rydygiera w Bydgoszczy, w terminie 14 dni od daty otrzymania niniejszej Uchwały.*

Prof. dr hab. med. Karol Śliwka

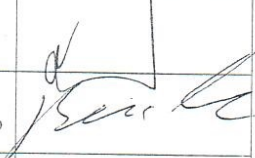
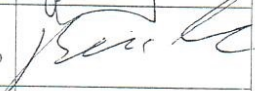
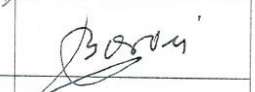
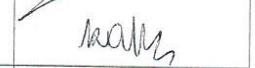
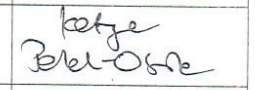
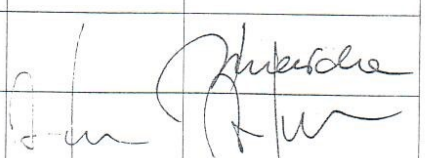

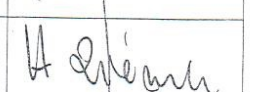
Przewodniczący Komisji Bioetycznej



Otrzymuje:

dr hab. n. farm. Barbara Bojko  
Katedra Farmakodynamiki i Farmakologii Molekularnej  
Collegium Medicum w Bydgoszczy

**Lista obecności**  
**na posiedzeniu Komisji Bioetycznej**  
**w dniu 14.11.2017 r.**

Lp.	Imię i nazwisko	Funkcja	Podpis
1.	Prof. dr hab. med. Karol Śliwka	przewodniczący	
2.	Prof. dr hab. Adam Buciński	z-ca przewodniczącego	
3.	Prof. dr hab. med. Anna Balcar-Boroń		
4.	Prof. dr hab. med. Mieczysława Czerwionka-Szaflarska		
5.	Prof. dr hab. med. Marek Grabiec		
6.	Prof. dr hab. med. Zbigniew Włodarczyk		
7.	Dr hab. n. med. Katarzyna Pawlak-Osińska, prof. UMK		
8.	Ks. dr hab. Wojciech Szukalski, prof. UAM		
9.	Dr n. med. Radosława Staszak-Kowalska		
10.	Dr hab. n. med. Maria Kłopocka		
11.	Mgr prawa Patrycja Brzezicka		
12.	Mgr prawa Joanna Połetek-Żygas		
13.	Mgr piel. Hanna Ziemińska		

**Uniwersytet Mikołaja Kopernika w Toruniu**  
**Collegium Medicum im L. Rydygiera w Bydgoszczy**  
**KOMISJA BIOETYCZNA**

Ul. M. Skłodowskiej-Curie 9, 85-094 Bydgoszcz, tel.(052) 585-35-63, fax.(052) 585-38-11

---

**KB 636/2017**

Bydgoszcz, 24.11.2020 r.

Działając na podstawie art.29 Ustawy z dnia 5 grudnia 1996 roku o zawodzie lekarza (Dz. U. z 1997 r. Nr 28 poz. 152 (wraz z późniejszymi zmianami), zarządzenia Ministra Zdrowia i Opieki Społecznej z dnia 11 maja 1999 r. w sprawie szczegółowych zasad powoływania i finansowania oraz trybu działania komisji bioetycznych (Dz. U. Nr 47 poz.480) oraz Zarządzeniem Nr 21 Rektora UMK z dnia 4 marca 2009 r. z późn. zm. w sprawie powołania oraz zasad działania Komisji Bioetycznej Uniwersytetu Mikołaja Kopernika w Toruniu przy Collegium Medicum im Ludwika Rydygiera w Bydgoszczy oraz zgodnie z zasadami zawartymi w ICH – GCP

**Komisja Bioetyczna przy UMK w Toruniu, Collegium Medicum w Bydgoszczy**

(której skład podano w załączeniu) na posiedzeniu w dniu **24.11.2020 r.** przeanalizowała prośbę o wyrażenie zgody na:

- wydłużenie okresu prowadzenia badań do końca 2022 roku

którą złożyła:

**dr hab. n. farm. Barbara Bojko, prof. UMK**  
**Katedra Farmakodynamiki i Farmakologii Molekularnej**  
**Collegium Medicum w Bydgoszczy**

w sprawie badania:

**„Ocena jakości nerek selekcionowanych do transplantacji oraz badanie uszkodzenia poreperfuzyjnego za pomocą bezbiopsyjnej analizy metabolomicznej i lipidomicznej narządów.”**

Po zapoznaniu się ze złożonym dokumentem i w wyniku przeprowadzonej dyskusji oraz głosowania jawnego Komisja przyjęła do wiadomości podane informacje i wyraża zgodę na powyższe pod warunkami określonymi w uchwale Komisji podjętej w dniu 24.10.2017 r.

Zgoda na kontynuowanie przedmiotowego badania obowiązuje do końca 2022 r.


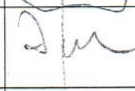
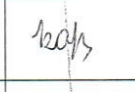

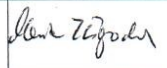
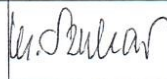


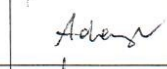
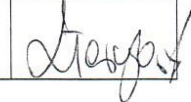
Prof. dr hab. med. Karol Śliwka

Przewodniczący Komisji Bioetycznej

Otrzymuje:

dr hab. n. farm. Barbara Bojko, prof. UMK  
Katedra Farmakodynamiki i Farmakologii Molekularnej  
Collegium Medicum w Bydgoszczy

**Lista obecności**  
**na posiedzeniu Komisji Bioetycznej**  
**w dniu 24.11.2020 r.**

Lp.	Imię i nazwisko	Funkcja/ Specjalizacja	Podpis
1.	Prof. dr hab. med. Karol Śliwka	Przewodniczący <i>medycyna sądowa</i>	
2.	Mgr prawa Joanna Połetek-Żygas	Z – ca przewodniczącego <i>prawniczka</i>	
3.	Prof. dr hab. med. Mieczysława Czerwionka-Szaflarska	<i>pediatra, alergologia i gastroenterologia dziecięca</i>	
4.	Prof. dr hab. med. Anna Balcar-Boroń	<i>pediatria, nefrologia</i>	
5.	Prof. dr hab. med. Marek Grabiec	<i>położnictwo, ginekologia onkologiczna</i>	
6.	Prof. dr hab. med. Zbigniew Włodarczyk	<i>chirurgia ogólna, transplantologia kliniczna</i>	
7.	Dr hab. n. med. Katarzyna Pawlak-Osińska, prof. UMK	<i>organizacja ochrony zdrowia, otolaryngologia</i>	
8.	Prof. dr hab. n. med. Maria Kłopotcka	<i>choroby wewnętrzne, gastroenterologia</i>	
9.	Ks. dr hab. Wojciech Szukalski, prof. UAM	<i>duchowny</i>	
10.	Dr n. med. Radosława Staszak-Kowalska	<i>pediatria, choroby płuc</i>	
11.	Mgr prawa Patrycja Brzezicka	<i>prawniczka</i>	
12.	Mgr farm. Aleksandra Adamczyk	<i>farmaceutka</i>	
13.	Mgr Lidia Iwińska-Tarczykowska	<i>pielęgniarka</i>	

## 13. Oświadczenie autora rozprawy doktorskiej

*Załącznik nr 5 do uchwały Nr 38 Senatu UMK z dnia 26 września 2023 r.  
w sprawie postępowania o nadanie stopnia doktora  
na Uniwersytecie Mikołaja Kopernika w Toruniu*

Bydgoszcz, dnia 14.04.2025 r.

mgr Natalia Warmuzińska  
Katedra Farmakodynamiki i Farmakologii Molekularnej  
Collegium Medicum w Bydgoszczy  
Uniwersytet Mikołaja Kopernika  
Bydgoszcz, Polska

**Rada Dyscypliny Nauki Medyczne  
Uniwersytetu Mikołaja Kopernika  
w Toruniu**

### Oświadczenie o współautorstwie

Niniejszym oświadczam, że mój udział w poniższych pracach polegał na:

Stryjak, N. Warmuzińska, K. Łuczykowski, M. Hamar, P. Urbanellis, E. Wojtał, M. Masztalerz, M. Selzner, Z. Włodarczyk, B. Bojko: Using a chemical biopsy for graft quality assessment. Jove-J. Vis. Exp, 2020, 160, e60946:

- Przygotowaniu i optymalizacji części lipidomicznej protokołu
- Przeprowadzeniu analizy instrumentalnej, analizie uzyskanych wyników części lipidomicznej
- Przygotowaniu pierwotnej wersji manuskryptu, wprowadzaniu poprawek, odpowiadaniu na recenzję

N. Warmuzińska, K. Łuczykowski, B. Bojko: A review of current and emerging trends in donor graft-quality assessment techniques. J. Clin. Med., 2022, 11, 487;

- Dokonaniu przeglądu literatury
- Przygotowaniu pierwotnej wersji manuskryptu, wprowadzaniu poprawek, odpowiedzi na recenzje
- Zaakceptowaniu końcowej wersji manuskryptu

K. Łuczykowski, N. Warmuzińska, B. Bojko: Solid phase microextraction – a promising tool for graft quality monitoring in solid organ transplantation. Separations, 2023, 10, 153

- Dokonaniu przeglądu literatury
- Przygotowaniu pierwotnej wersji manuskryptu, wprowadzaniu poprawek, odpowiedzi na recenzje
- Zaakceptowaniu końcowej wersji manuskryptu

Stryjak, N. Warmuzińska, K. Łuczykowski, K. Jaroch, P. Urbanellis, M. Selzner, B. Bojko: Metabolomic and lipidomic landscape of porcine kidney associated with kidney perfusion in heart beating donors and donors after cardiac death. *Transl Res.*, 2024, 267:79-90

- Przeprowadzeniu analizy instrumentalnej, analizy statystycznej oraz interpretacji wyników części lipidomicznej, wizualizacja danych
- Przygotowaniu pierwotnej wersji manuskryptu, wprowadzaniu poprawek, odpowiedzi na recenzję
- Zaakceptowaniu końcowej wersji manuskryptu

N. Warmuzińska, K. Łuczykowski, I. Stryjak, H. Rosales-Solano, P. Urbanellis, J. Pawliszyn, M. Selzner, B. Bojko, 2024, The impact of normothermic and hypothermic preservation methods on kidney lipidome—comparative study using chemical biopsy with microextraction probes. *Front. Mol. Biosci.*, 11, 1341108:

- Przeprowadzeniu analizy instrumentalnej, analizy statystycznej oraz interpretacji wyników, wizualizacja danych
- Przygotowaniu pierwotnej wersji manuskryptu, wprowadzaniu poprawek, odpowiedzi na recenzję
- Zaakceptowaniu końcowej wersji manuskryptu

N. Warmuzińska, K. Łuczykowski, I. Stryjak, E. Wojtal, A. Woderska-Jasińska, M. Masztalerz, Z. Włodarczyk, B. Bojko: Metabolomic and lipidomic profiling for pre-transplant assessment of delayed graft function risk using chemical biopsy with microextraction probes. *Int. J. Mol. Sci.*, 2024, 25, 13502

- Planowaniu eksperymentu i stosowanej metodyki
- Pobieraniu próbek z wykorzystaniem sond mikroekstrakcyjnych
- Przeprowadzeniu analizy instrumentalnej, analizy statystycznej oraz interpretacji wyników, wizualizacja danych
- Przygotowaniu pierwotnej wersji manuskryptu, wprowadzaniu poprawek, odpowiedzi na recenzję
- Zaakceptowaniu końcowej wersji manuskryptu

  
(podpis)

## 14. Oświadczenia współautorów

*Załącznik nr 5 do uchwały Nr 38 Senatu UMK z dnia 26 września 2023 r.  
w sprawie postępowania o nadanie stopnia doktora  
na Uniwersytecie Mikołaja Kopernika w Toruniu*

Bydgoszcz, dnia 14.04.2025 r.

mgr Kamil Łuczykowski  
Katedra Farmakodynamiki i Farmakologii Molekularnej  
Collegium Medicum w Bydgoszczy  
Uniwersytet Mikołaja Kopernika  
Bydgoszcz, Polska

**Rada Dyscypliny Nauki Medyczne  
Uniwersytetu Mikołaja Kopernika  
w Toruniu**

### Oświadczenie o współautorstwie

Niniejszym oświadczam, że mój udział w poniższych pracach polegał na:

Stryjak, N. Warmuzińska, K. Łuczykowski, M. Hamar, P. Urbanellis, E. Wojtal, M. Masztalerz, M. Selzner, Z. Włodarczyk, B. Bojko: Using a chemical biopsy for graft quality assessment. Jove-J. Vis. Exp. 2020, 160, e60946:

- Pomocy w analizie instrumentalnej oraz analizie uzyskanych wyników
- Zaakceptowaniu końcowej wersji manuskryptu

N. Warmuzińska, K. Łuczykowski, B. Bojko: A review of current and emerging trends in donor graft-quality assessment techniques. J. Clin. Med., 2022, 11, 487;

- Pomocy w redagowaniu pracy
- Zaakceptowaniu końcowej wersji manuskryptu

K. Łuczykowski, N. Warmuzińska, B. Bojko: Solid phase microextraction – a promising tool for graft quality monitoring in solid organ transplantation. Separations, 2023, 10, 153

- Dokonaniu przeglądu literatury
- Przygotowaniu pierwotnej wersji manuskryptu, wprowadzaniu poprawek, odpowiedzi na recenzje
- Zaakceptowaniu końcowej wersji manuskryptu

Stryjak, N. Warmuzińska, K. Łuczykowski, K. Jaroń, P. Urbanellis, M. Selzner, B. Bojko: Metabolomic and lipidomic landscape of porcine kidney associated with kidney perfusion in heart beating donors and donors after cardiac death. *Transl Res.*, 2024, 267:79-90

- Pomocy w analizie instrumentalnej oraz analizie uzyskanych wyników
- Zaakceptowaniu końcowej wersji manuskryptu

N. Warmuzińska, K. Łuczykowski, I. Stryjak, H. Rosales-Solano, P. Urbanellis, J. Pawliszyn, M. Selzner, B. Bojko, 2024, The impact of normothermic and hypothermic preservation methods on kidney lipidome—comparative study using chemical biopsy with microextraction probes. *Front. Mol. Biosci.*, 11, 1341108:

- Pomocy w analizie instrumentalnej oraz analizie uzyskanych wyników
- Zaakceptowaniu końcowej wersji manuskryptu

N. Warmuzińska, K. Łuczykowski, I. Stryjak, E. Wojtal, A. Woderska-Jasińska, M. Masztalerz, Z. Włodarczyk, B. Bojko: Metabolomic and lipidomic profiling for pre-transplant assessment of delayed graft function risk using chemical biopsy with microextraction probes. *Int. J. Mol. Sci.*, 2024, 25, 13502

- Pomocy w analizie instrumentalnej oraz analizie uzyskanych wyników
- Pomocy w redagowaniu pracy i odpowiedzi na recenzje
- Zaakceptowaniu końcowej wersji manuskryptu

  
(podpis)

Bydgoszcz, dnia 14.04.2025 r.

prof. dr hab. Barbara Bojko  
Katedra Farmakodynamiki i Farmakologii Molekularnej  
Collegium Medicum w Bydgoszczy  
Uniwersytet Mikołaja Kopernika  
Bydgoszcz, Polska

**Rada Dyscypliny Nauki Medyczne  
Uniwersytetu Mikołaja Kopernika  
w Toruniu**

## **Oświadczenie o współautorstwie**

Niniejszym oświadczam, że mój udział w poniższych pracach polegał na:

Stryjak, N. Warmuzińska, K. Łuczykowski, M. Hamar, P. Urbanellis, E. Wojtal, M. Masztalerz, M. Selzner, Z. Włodarczyk, B. Bojko: Using a chemical biopsy for graft quality assessment. Jove-J. Vis. Exp, 2020, 160, e60946:

- Zapewnieniu finansowania badań
- Planowaniu eksperymentu i stosowanej metodyki
- Nadzorowaniu prowadzenia badań i analizie wyników
- Pomocy w redagowaniu pracy i odpowiedzi na recenzje
- Zaakceptowaniu końcowej wersji manuskryptu

N. Warmuzińska, K. Łuczykowski, B. Bojko: A review of current and emerging trends in donor graft-quality assessment techniques. J. Clin. Med., 2022, 11, 487;

- Pomocy w redagowaniu pracy i odpowiedzi na recenzje
- Zaakceptowaniu końcowej wersji manuskryptu

K. Łuczykowski, N. Warmuzińska, B. Bojko: Solid phase microextraction – a promising tool for graft quality monitoring in solid organ transplantation. Separations, 2023, 10, 153

- Dokonaniu przeglądu literatury
- Przygotowaniu pierwotnej wersji manuskryptu, wprowadzaniu poprawek, odpowiedzi na recenzje
- Zaakceptowaniu końcowej wersji manuskryptu

Stryjak, N. Warmużyńska, K. Łuczykowski, K. Jaroch, P. Urbanellis, M. Selzner, B. Bojko: Metabolomic and lipidomic landscape of porcine kidney associated with kidney perfusion in heart beating donors and donors after cardiac death. *Transl Res.*, 2024, 267:79-90

- Zapewnieniu finansowania badań
- Planowaniu eksperymentu i stosowanej metodyki
- Nadzorowaniu prowadzenia badań i analizie wyników
- Pomocy w redagowaniu pracy i odpowiedzi na recenzje
- Zaakceptowaniu końcowej wersji manuskryptu

N. Warmużyńska, K. Łuczykowski, I. Stryjak, H. Rosales-Solano, P. Urbanellis, J. Pawliszyn, M. Selzner, B. Bojko, 2024, The impact of normothermic and hypothermic preservation methods on kidney lipidome—comparative study using chemical biopsy with microextraction probes. *Front. Mol. Biosci.*, 11, 1341108:

- Zapewnieniu finansowania badań
- Planowaniu eksperymentu i stosowanej metodyki
- Nadzorowaniu prowadzenia badań i analizie wyników
- Pomocy w redagowaniu pracy i odpowiedzi na recenzje
- Zaakceptowaniu końcowej wersji manuskryptu

N. Warmużyńska, K. Łuczykowski, I. Stryjak, E. Wojtal, A. Woderska-Jasińska, M. Masztalerz, Z. Włodarczyk, B. Bojko: Metabolomic and lipidomic profiling for pre-transplant assessment of delayed graft function risk using chemical biopsy with microextraction probes. *Int. J. Mol. Sci.*, 2024, 25, 13502

- Zapewnieniu finansowania badań
- Planowaniu eksperymentu i stosowanej metodyki
- Nadzorowaniu prowadzenia badań i analizie wyników
- Pomocy w redagowaniu pracy i odpowiedzi na recenzje
- Zaakceptowaniu końcowej wersji manuskryptu

Kierownik  
Instytutu Farmakodynamiki i Farmakologii Molekularnej  
prof. dr hab. Barbara Bojko  
.....  
(podpis)

Bydgoszcz, dnia 14.04.2025 r.

mgr Iga Stryjak-Kwiatkowska  
Katedra Farmakodynamiki i Farmakologii Molekularnej  
Collegium Medicum w Bydgoszczy  
Uniwersytet Mikołaja Kopernika

**Rada Dyscypliny Nauki Medyczne  
Uniwersytetu Mikołaja Kopernika  
w Toruniu**

### **Oświadczenie o współautorstwie**

Niniejszym oświadczam, że mój udział w poniższych pracach polegał na:

Stryjak, N. Warmuzińska, K. Łuczykowski, M. Hamar, P. Urbanellis, E. Wojtal, M. Masztalerz, M. Selzner, Z. Włodarczyk, B. Bojko: Using a chemical biopsy for graft quality assessment. Jove-J. Vis. Exp, 2020, 160, e60946:

- Przygotowaniu i optymalizacji części metabolomicznej protokołu
- Przeprowadzeniu analizy instrumentalnej, analizie uzyskanych wyników części metabolomicznej
- Przygotowaniu pierwotnej wersji manuskryptu, wprowadzaniu poprawek, odpowiadaniu na recenzję

Stryjak, N. Warmuzińska, K. Łuczykowski, K. Jaroch, P. Urbanellis, M. Selzner, B. Bojko: Metabolomic and lipidomic landscape of porcine kidney associated with kidney perfusion in heart beating donors and donors after cardiac death. Transl Res., 2024, 267:79-90

- Przeprowadzeniu analizy instrumentalnej, analizie statystycznej oraz interpretacji wyników części metabolomicznej,
- Przygotowanie pierwotnej wersji manuskryptu
- Zaakceptowaniu końcowej wersji manuskryptu

N. Warmuzińska, K. Łuczykowski, I. Stryjak, H. Rosales-Solano, P. Urbanellis, J. Pawliszyn, M. Selzner, B. Bojko, 2024, The impact of normothermic and hypothermic preservation methods on kidney lipidome—comparative study using chemical biopsy with microextraction probes. Front. Mol. Biosci., 11, 1341108:

- Pomocy w analizie instrumentalnej
- Zaakceptowaniu końcowej wersji manuskryptu

N. Warmuzińska, K. Łuczykowski, I. Stryjak, E. Wojtal, A. Woderska-Jasińska, M. Masztalerz, Z. Włodarczyk, B. Bojko: Metabolomic and lipidomic profiling for pre-transplant assessment of delayed graft function risk using chemical biopsy with microextraction probes. *Int. J. Mol. Sci.*, 2024, 25, 13502

- Planowaniu eksperymentu i stosowanej metodyki
- Pobieraniu próbek z wykorzystaniem sond mikroekstrakcyjnych
- Pomocy w analizie instrumentalnej
- Zaakceptowaniu końcowej wersji manuskryptu

*Stryjak-Kwiatkowska*  
.....  
(podpis)

Bydgoszcz, dnia 14.04.2025 r.

dr hab. Karol Jaroch, prof. UMK  
Katedra Farmakodynamiki i Farmakologii Molekularnej  
Collegium Medicum w Bydgoszczy  
Uniwersytet Mikołaja Kopernika

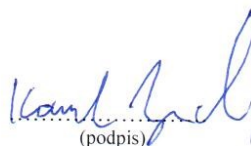
**Rada Dyscypliny Nauki Medyczne  
Uniwersytetu Mikołaja Kopernika  
w Toruniu**

### **Oświadczenie o współautorstwie**

Niniejszym oświadczam, że mój udział w poniższej pracy polegał na:

Stryjak, N. Warmuzińska, K. Łuczykowski, K. Jaroch, P. Urbanellis, M. Selzner, B. Bojko:  
Metabolomic and lipidomic landscape of porcine kidney associated with kidney perfusion in heart  
beating donors and donors after cardiac death. Transl Res., 2024, 267:79-90

- Pobieraniu próbek z wykorzystaniem sond mikroekstrakcyjnych
- Zaakceptowanie końcowej wersji manuskryptu

  
(podpis)

Bydgoszcz, dnia 14.04.2025 r.

prof. dr hab. Zbigniew Włodarczyk  
Katedra Transplantologii i Chirurgii Ogólnej  
Collegium Medicum w Bydgoszczy  
Uniwersytet Mikołaja Kopernika  
Bydgoszcz, Polska

**Rada Dyscypliny Nauki Medyczne  
Uniwersytetu Mikołaja Kopernika  
w Toruniu**

### **Oświadczenie o współautorstwie**


Niniejszym oświadczam, że mój udział w poniższych pracach polegał na:

Stryjak, N. Warmuzińska, K. Łuczykowski, M. Hamar, P. Urbanellis, E. Wojtal, M. Masztalerz, M. Selzner, Z. Włodarczyk, B. Bojko: Using a chemical biopsy for graft quality assessment. Jove-J. Vis. Exp, 2020, 160, e60946:

- Udziale w planowaniu eksperymentu od strony klinicznej
- Nadzorowaniu pobierania próbek, rekrutacji pacjentów i pobieraniu próbek za pomocą sond mikroekstrakcyjnych
- Sprawdzeniu i akceptacji końcowej wersji manuskryptu

N. Warmuzińska, K. Łuczykowski, I. Stryjak, E. Wojtal, A. Woderska-Jasińska, M. Masztalerz, Z. Włodarczyk, B. Bojko: Metabolomic and lipidomic profiling for pre-transplant assessment of delayed graft function risk using chemical biopsy with microextraction probes. Int. J. Mol. Sci., 2024, 25, 13502:

- Udziale w planowaniu eksperymentu od strony klinicznej
- Nadzorowaniu pobierania próbek, rekrutacji pacjentów i pobieraniu próbek za pomocą sond mikroekstrakcyjnych
- Sprawdzeniu i akceptacji końcowej wersji manuskryptu

  
(podpis)

Bydgoszcz, dnia 14.04.2025 r.

dr Marek Masztalerz  
Katedra Transplantologii i Chirurgii Ogólnej  
Collegium Medicum w Bydgoszczy  
Uniwersytet Mikołaja Kopernika  
Bydgoszcz, Polska

**Rada Dyscypliny Nauki Medyczne  
Uniwersytetu Mikołaja Kopernika  
w Toruniu**

### **Oświadczenie o współautorstwie**

Niniejszym oświadczam, że mój udział w poniższych pracach polegał na:

Stryjak, N. Warmuzińska, K. Łuczykowski, M. Hamar, P. Urbanellis, E. Wojtal, M. Masztalerz, M. Selzner, Z. Włodarczyk, B. Bojko: Using a chemical biopsy for graft quality assessment. Jove-J. Vis. Exp, 2020, 160, e60946:

- Rekrutacji pacjentów i pobieraniu próbek za pomocą sond mikroekstrakcyjnych
- Zaakceptowaniu końcowej wersji manuskryptu

N. Warmuzińska, K. Łuczykowski, I. Stryjak, E. Wojtal, A. Woderska-Jasińska, M. Masztalerz, Z. Włodarczyk, B. Bojko: Metabolomic and lipidomic profiling for pre-transplant assessment of delayed graft function risk using chemical biopsy with microextraction probes. Int. J. Mol. Sci., 2024, 25, 13502:

- Rekrutacji pacjentów i pobieraniu próbek za pomocą sond mikroekstrakcyjnych
- Zaakceptowaniu końcowej wersji manuskryptu

   
.....  
(podpis)

Bydgoszcz, dnia 14.04.2025 r.

Lek. Emilia Wojtal  
Katedra Transplantologii i Chirurgii Ogólnej  
Collegium Medicum w Bydgoszczy  
Uniwersytet Mikołaja Kopernika  
Bydgoszcz, Polska

**Rada Dyscypliny Nauki Medyczne  
Uniwersytetu Mikołaja Kopernika  
w Toruniu**

### Oświadczenie o współautorstwie

Niniejszym oświadczam, że mój udział w poniższych pracach polegał na:

Stryjak, N. Warmuzińska, K. Łuczykowski, M. Hamar, P. Urbanellis, E. Wojtal, M. Masztalerz, M. Selzner, Z. Włodarczyk, B. Bojko: Using a chemical biopsy for graft quality assessment. Jove-J. Vis. Exp, 2020, 160, e60946:

- Udziale w planowaniu eksperymentu od strony klinicznej
- Rekrutacji pacjentów i pobieraniu próbek za pomocą sond mikroekstrakcyjnych
- Zaakceptowaniu końcowej wersji manuskryptu

N. Warmuzińska, K. Łuczykowski, I. Stryjak, E. Wojtal, A. Woderska-Jasińska, M. Masztalerz, Z. Włodarczyk, B. Bojko: Metabolomic and lipidomic profiling for pre-transplant assessment of delayed graft function risk using chemical biopsy with microextraction probes. Int. J. Mol. Sci., 2024, 25, 13502:

- Udziale w planowaniu eksperymentu od strony klinicznej
- Rekrutacji pacjentów i pobieraniu próbek za pomocą sond mikroekstrakcyjnych
- Zaakceptowaniu końcowej wersji manuskryptu

Emilia Wojtal  
Specjalista chirurgii ogólnej  
Transplantologii klinicznej  
33225  
  
(podpis)

Bydgoszcz, dnia 14.04.2025 r.

dr Aleksandra Woderska-Jasińska  
Katedra Transplantologii i Chirurgii Ogólnej  
Collegium Medicum w Bydgoszczy  
Uniwersytet Mikołaja Kopernika  
Bydgoszcz, Polska

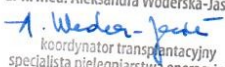
**Rada Dyscypliny Nauki Medyczne  
Uniwersytetu Mikołaja Kopernika  
w Toruniu**

### **Oświadczenie o współautorstwie**

Niniejszym oświadczam, że mój udział w poniższej pracy polegał na:

N. Warmuzińska, K. Łuczykowski, I. Stryjak, E. Wojtal, A. Woderska-Jasińska, M. Masztalerz, Z. Włodarczyk, B. Bojko: Metabolomic and lipidomic profiling for pre-transplant assessment of delayed graft function risk using chemical biopsy with microextraction probes. Int. J. Mol. Sci., 2024, 25, 13502

- Udziale w planowaniu eksperymentu od strony klinicznej
- Koordynowaniu procesu pobierania próbek za pomocą sond mikroekstrakcyjnych
- Przygotowaniu bazy danych klinicznych
- Zaakceptowaniu końcowej wersji manuskryptu

040/413P dr n. med. Aleksandra Woderska-Jasińska  
  
koordynator transplantacyjny  
specjalista pielęgniarstwa operacyjnego  
.....  
(podpis)

Toronto, 14.04.2025 r.

Matyas Hamar  
Ajmera Transplant Center, Department of Surgery, Toronto  
General Hospital, University Health Network, Toronto, ON,  
Canada

**Council for the Discipline of  
Medical Sciences  
Nicolaus Copernicus University in  
Toruń**

### **Declaration of Contribution**

I declare that my contribution to the following paper was as follows:

Stryjak I., Warmuzińska N., Łuczykowski K., Hamar M., Urbanellis P., Wojtal E., Masztalerz M.,  
Selzner M., Włodarczyk Z., Bojko B. (2020). Using a chemical biopsy for graft quality assessment.  
Jove–J. Vis. Exp., 160, e60946.

- Contributed to the methodological design related to animal procedures and surgical intervention
- Performed animal procedures and sample collection
- Approved the final version of the manuscript



.....  
(signature)

Signed by Markus Selzner, on Behalf of Matyas Hamar

Toronto, 14.04.2025 r.

Hernando Rosales-Solano  
Department of Chemistry,  
University of Waterloo,  
Waterloo, ON, Canada

**Council for the Discipline of  
Medical Sciences  
Nicolaus Copernicus University in  
Toruń**

### **Declaration of Contribution**

I declare that my contribution to the following papers was as follows:

N. Warmuzińska, K. Łuczykowski, I. Stryjak, H. Rosales-Solano, P. Urbanellis, J. Pawliszyn, M. Selzner, B. Bojko, 2024, The impact of normothermic and hypothermic preservation methods on kidney lipidome—comparative study using chemical biopsy with microextraction probes. *Front. Mol. Biosci.*, 11, 1341108:

- Preparation of microextraction probes
- Coordination of and participation in sample collection via microextraction probes
- Approved the final version of the manuscript



Hernando Rosales-Solano

.....  
(signature)

Toronto, 14.04.2025 r.

Peter Urbanellis  
Department of Surgery  
Ajmera Transplant Centre  
Toronto General Hospital, University Health Network  
Toronto, Canada

**Council for the Discipline of  
Medical Sciences  
Nicolaus Copernicus  
University in Toruń**

## **Declaration of Contribution**

I declare that my contribution to the following papers was as follows:

„I. Stryjak, N. Warmuzińska, K. Łuczykowski, M. Hamar, P. Urbanellis, E. Wojtal, M. Masztalerz, M. Selzner, Z. Włodarczyk, B. Bojko, 2020, Using a chemical biopsy for graft quality assessment. Jove-J. Vis. Exp., 160, e60946”:

- Contributed to the methodological design related to animal procedures and surgical intervention
- Performed animal procedures and sample collection
- Approved the final version of the manuscript

„N. Warmuzińska, K. Łuczykowski, I. Stryjak, H. Rosales-Solano, P. Urbanellis, J. Pawliszyn, M. Selzner, B. Bojko, 2024, The impact of normothermic and hypothermic preservation methods on kidney lipidome—comparative study using chemical biopsy with microextraction probes. Front. Mol. Biosci., 11, 1341108”:

- Contributed to the methodological design related to animal procedures and surgical intervention
- Performed animal procedures and sample collection
- Approved the final version of the manuscript

„I. Stryjak, N. Warmuzińska, K. Łuczykowski, K. Jaroń, P. Urbanellis, M. Selzner, B. Bojko,  
2024, Metabolomic and lipidomic landscape of porcine kidney associated with kidney perfusion  
in heart beating donors and donors after cardiac death. Transl Res., 267:79-90”:

- Contributed to the methodological design related to animal procedures and surgical intervention
- Performed animal procedures and sample collection
- Approved the final version of the manuscript

*prof. dr hab. Barbara Bojko*  
Kierownik  
Katedry Farmakodynamiki i Farmakologii Molekularnej  
prof. dr hab. Barbara Bojko  
(signature)

Toronto, 14.04.2025 r.

Markus Selzner, MD  
Department of Surgery  
Ajmera Transplant Centre  
Toronto General Hospital, University Health Network  
Toronto, Canada

**Council for the Discipline of  
Medical Sciences  
Nicolaus Copernicus University in  
Toruń**

## **Declaration of Contribution**

I declare that my contribution to the following papers was as follows:

Stryjak I., Warmuzińska N., Łuczykowski K., Hamar M., Urbanellis P., Wojtal E., Masztalerz M., Selzner M., Włodarczyk Z., Bojko B. (2020). Using a chemical biopsy for graft quality assessment. *Jove–J. Vis. Exp.*, 160, e60946.


- Conceptualization of the experiment and methodology
- Performed animal procedures and sample collection
- Reviewed and approved the final version of the manuscript

N. Warmuzińska, K. Łuczykowski, I. Stryjak, H. Rosales-Solano, P. Urbanellis, J. Pawliszyn, M. Selzner, B. Bojko, 2024, The impact of normothermic and hypothermic preservation methods on kidney lipidome—comparative study using chemical biopsy with microextraction probes. *Front. Mol. Biosci.*, 11, 1341108:

- Conceptualization of the experiment and methodology
- Performed animal procedures and sample collection
- Reviewed and approved the final version of the manuscript

I. Stryjak, N. Warmuzińska, K. Łuczykowski, K. Jaroch, P. Urbanellis, M. Selzner, B. Bojko, 2024, Metabolomic and lipidomic landscape of porcine kidney associated with kidney perfusion in heart beating donors and donors after cardiac death. *Transl Res.*, 267:79-90:

- Conceptualization of the experiment and methodology
- Performed animal procedures and sample collection
- Reviewed and approved the final version of the manuscript



(signature)

Bydgoszcz, dnia 14.04.2025 r.

prof. dr hab. Janusz Pawliszyn  
Department of Chemistry,  
University of Waterloo,  
Waterloo, ON, Canada

**Rada Dyscypliny Nauki Medyczne  
Uniwersytetu Mikołaja Kopernika  
w Toruniu**

### **Oświadczenie o współautorstwie**

Niniejszym oświadczam, że mój udział w poniżej pracy polegał na:

N. Warmuzińska, K. Łuczykowski, I. Stryjak, H. Rosales-Solano, P. Urbanellis, J. Pawliszyn, M. Selzner, B. Bojko, 2024, The impact of normothermic and hypothermic preservation methods on kidney lipidome—comparative study using chemical biopsy with microextraction probes. *Front. Mol. Biosci.*, 11, 1341108:

- Zapewnieniu materiałów niezbędnych do przygotowania sond mikroekstrakcyjnych
- Nadzorze nad pobieraniem próbek
- Akceptacji finalnej wersji manuskryptu



.....  
(podpis)